



Politechnika
Śląska

WYDZIAŁ CHEMICZNY

KATEDRA FIZYKOCHEMII I TECHNOLOGII POLIMERÓW

mgr inż. Katarzyna Niesyto

Załączniki do

ROZPRAWY DOKTORSKIEJ

Zaprojektowanie szczepionych poli(cieczy jonowych)
jako potencjalnych układów dostarczania leków
w terapii przeciwbakteryjnej

Przewodnik po monotematycznym cyklu publikacji

Promotor: prof. dr hab. inż. Dorota Neugebauer

Gliwice, 2024

STRESZCZENIE ROZPRAWY DOKTORSKIEJ

Zaprojektowanie szczepionych poli(cieczy jonowych) jako potencjalnych układów dostarczania leków w terapii przeciwbakteryjnej

mgr inż. Katarzyna Niesyto

Promotor: prof. dr hab. inż. Dorota Neugebauer

CEL I ZAKRES BADAŃ

Celem badań przedstawionych w niniejszej pracy doktorskiej było opracowanie nowych układów polimerowych jako nanoosiłków leków bazujących na polimerach szczepionych, które zawierały jednostki cholinowej cieczy jonowej (IL), tj. chlorku [2-(metakryloiloxy)etylo]trimetyloamoniowego (TMAMA). W związku z tym za pomocą kontrolowanej polimeryzacji z przeniesieniem atomu (ATRP) otrzymano dobrze zdefiniowane kopolimery, które różniły się liczbą łańcuchów bocznych, czyli stopniem szczepienia, ich długością, czyli stopniem polimeryzacji oraz zawartością TMAMA. Dla porównania zsyntezowano również analogiczne kopolimery liniowe. Obecność anionów chlorkowych, zarówno w kopolimerach szczepionych, jak i liniowych, wykorzystano w reakcji wymiany jonowej, aby wprowadzić leki w formie jonowej (aniony farmaceutyczne). Według tej strategii polimery chlorkowe mogły służyć jako uniwersalne matryce do uzyskania koniugatów jonowych polimer-lek.

Drugim istotnym wątkiem badawczym było wykorzystanie amfifilowego charakteru otrzymanych kopolimerów jako nośniki micelarne w enkapsulacji leków w formie niejonowej. W wyniku połączenia obydwu tych strategii, tj. wymiany anionowej i enkapsulacji, z udziałem polimerów szczepionych zostały otrzymane micelarne układy koniugatów jonowych jako układy podwójne do terapii skojarzonej transportujące dwa leki o działaniu synergistycznym, które w różny sposób są związane z matrycą polimerową (jonowe wiązanie vs. fizyczne oddziaływanie). Badane układy ukierunkowano na transport leków stosowanych w leczeniu chorób dolnych dróg oddechowych, w tym gruźlicy. Obok podstawowej charakterystyki fizykochemicznej polimerów, zbadano wpływ parametrów strukturalnych nośnika na szybkość uwalniania leku, jak również oceniono cytotoksyczność układów.

Z uwagi na zróżnicowany charakter matryc polimerowych oraz wybranych leków modelowych, badane układy pogrupowano w następujący sposób:

- Koniugaty polimerów z anionami farmaceutycznymi: p aminosalicylanu (PAS^-), klawulanianu (CLV^-), piperacyliny (PIP^-), fusydanu (FUS^-),
- Micele polimerów chlorkowych z enkapsulowanym lekiem w formie niejonowej: izoniazyd (ISO), tazobaktam (TAZ), ryfampicyna (RIF),
- Micelarne układy koniugatów polimerowych do transportu pary leków (jonowy/niejonowy): PAS^-/ISO , PIP^-/TAZ , FUS^-/RIF .

WYKAZ PUBLIKACJI NAUKOWYCH STANOWIĄCYCH MONOTEMATYCZNY CYKL

Niniejszą rozprawę stanowi monotematyczny cykl siedmiu artykułów naukowych opublikowanych w latach 2020-2024 w czasopismach rejestrowanych w bazie Journal Citation Records (JCR):

P.1. Synthesis and Characterization of Ionic Graft Copolymers: Introduction and In Vitro Release of Antibacterial Drug by Anion Exchange.

K. Niesyto, D. Neugebauer

Polymers. 2020, 12, 2159. (IF2020= 4.329; MEiN=100 pkt)

P.2. Linear Copolymers Based on Choline Ionic Liquid Carrying Anti-Tuberculosis Drugs: Influence of Anion Type on Physicochemical Properties and Drug Release.

K. Niesyto, D. Neugebauer

International Journal of Molecular Sciences 2021, 22, 284 (IF2021= 6.208; MEiN=140 pkt)

P.3. Dual-Drug Delivery via the Self-Assembled Conjugates of Choline-Functionalized Graft Copolymers.

K. Niesyto, A. Mazur, D. Neugebauer

Materials 2022, 15, 4457 (IF2022= 3.4; MEiN=140 pkt)

P.4. Ionic Liquid-based Polymer Matrices for Single and Dual Drug Delivery: Impact of Structural Topology on Characteristics and In Vitro Delivery Efficiency.

K. Niesyto, S. Keihankhadiv, A. Mazur, Mielańczyk, A., D. Neugebauer

International Journal of Molecular Sciences 2024, 25, 1292 (IF2022=5.6; MEiN=140 pkt)

P.5. Piperacillin/Tazobactam co-delivery by micellar ionic conjugate systems carrying pharmaceutical anions and encapsulated drug

K. Niesyto, A. Mazur, D. Neugebauer

Pharmaceutics 2024, 16, 198 (IF2022= 5.4; MEiN=100 pkt)

P.6. Biological in vitro evaluation of PIL graft conjugates: cytotoxicity characteristics.

K. Niesyto, W. Łyżniak, M. Skonieczna, D. Neugebauer

International Journal of Molecular Sciences 2021, 22, 7741 (IF2021= 6.208; MEiN=140 pkt)

P.7. Toxicity evaluation of choline ionic liquid-based nanocarriers of pharmaceutical agents for lung treatment.

K. Niesyto, M. Skonieczna, M. Adamiec-Organisćioek, D. Neugebauer

Journal of Biomedical Materials Research Part B - Applied Biomaterials 2023, 111(7), 1374-1385 (IF2022= 3.4; MEiN=140 pkt)

PODSUMOWANIE WKŁADU WŁASNEGO DOKTORANTKI

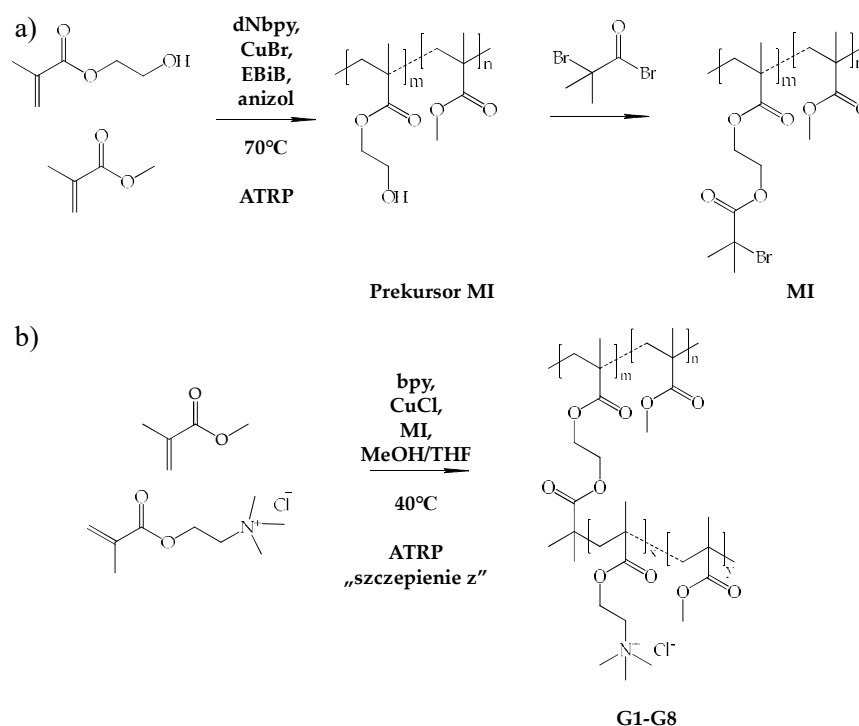
Udział w opracowaniu koncepcji i planu badawczego; przeprowadzenie syntezy prekursorów makroinicjatora, makroinicjatorów oraz polimerów liniowych i szczepionych; otrzymanie koniugatów, miceli oraz koniugatów micelarnych jako nośników leków zawierających jeden bądź dwa rodzaje leków; przeprowadzenie charakterystyki fizykochemicznej otrzymanych polimerów oraz nośników; przeprowadzenie badań uwalniania leków; przeprowadzenie badań biologicznych; opracowanie, analiza i interpretacja wyników; przygotowanie oryginalnych projektów manuskryptów publikacji; Stypendystka - wykonawca badań w ramach programu OPUS (grant nr 2017/27/B/ST5/00960; 2019-2022).

Oświadczenia współautorów publikacji szczegółowo określające ich indywidualny wkład autorski znajdują się w załącznikach do niniejszej rozprawy.

OPIS PRZEDMIOTU BADAŃ, WYNIKI I WNIOSKI

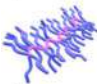
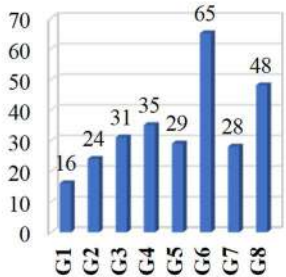
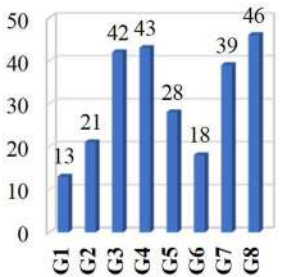
Synteza kopolimerów metodą ATRP (P.1.; P.2.)

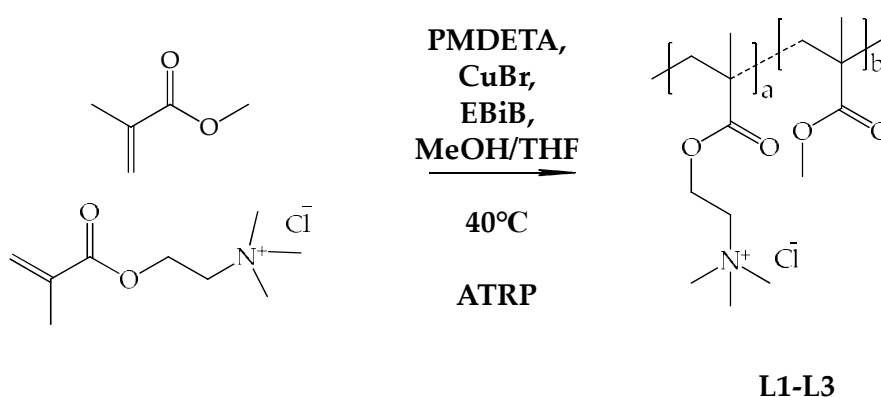
W ramach niniejszej pracy doktorskiej opracowano innowacyjne systemy polimerowe jako nośniki leków do zastosowania w terapii przeciwbakteryjnej chorób dolnych dróg oddechowych, wykorzystujące kopolimery szczepione zawierające jednostki cholinowej cieczy jonowej, tj. chlorku [2-(metakryloiloxy)etylo]trimetyloamoniowego (TMAMA), który jest znany ze swojej aktywności biologicznej. Do otrzymania dobrze zdefiniowanych kopolimerów szczepionych wykorzystano kontrolowaną polimeryzację z przeniesieniem atomu (ATRP). Jonowa struktura TMAMA umożliwiła przeprowadzenie wymiany jonowej anionu chlorkowego na aniony farmaceutyczne zwiększając aktywność biologiczną systemów. Jednocześnie zastosowanie komonomeru TMAMA o charakterze hydrofilowym w różnych proporcjach wyjściowych (TMAMA/MMA=25/75, 50/50, 75/25) pozwoliło na osiągnięcie zróżnicowanego balansu hydrofilowo-hydrofobowego w badanych układach polimerowych. Porównawczo przeprowadzono serię badań z udziałem analogowych polimerów liniowych. Badania nośników obejmowały dobrze zdefiniowane kopolimery o zróżnicowanej topologii, tj. szczepione G1-G8 vs. liniowe L1-L3, które zsyntezowano przy użyciu różnych układów inicjujących (makroinicjator vs. inicjator). Kopolimery szczepione G1-G8 zostały otrzymane w wyniku dwuetapowej reakcji kontrolowanej polimeryzacji rodnikowej z przeniesieniem atomu (ATRP) (rys.1, tab.1). Natomiast kopolimery liniowe L1-L3 o wzorze ogólnym P(MMA-co-TMAMA) otrzymano na drodze jednoetapowej reakcji ATRP (rys.2, tab.2).



Rysunek 1. Schematy reakcji otrzymywania a) P(MMA-co-BIEM) jako MI, oraz b) kopolimeru szczepionego, gdzie EBiB jest inicjatorem.



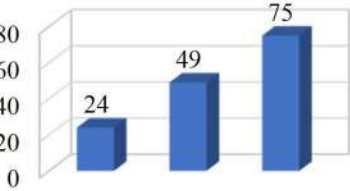
Tabela 1. Podstawowe parametry kopolimerów szczepionych.

	TMAMA/ MMA	DP _n	n _{sc}	DG (mol.%)	DP _{SC}	F _{TMAMA} (mol.%)	M _n × 10 ⁻³ (g/mol)	Đ
G1	25/75						115	1,68
G2	25/75	186	48	26			169	1,90
G3	50/50						244	1,31
G4	50/50						273	1,15
G5	25/75	292	133	46			554	1,24
G6	25/75						1 091	1,11
G7	50/50						584	1,03
G8	50/50						1 007	-



Rysunek 2. Schemat reakcji otrzymywania kopolimeru liniowego.

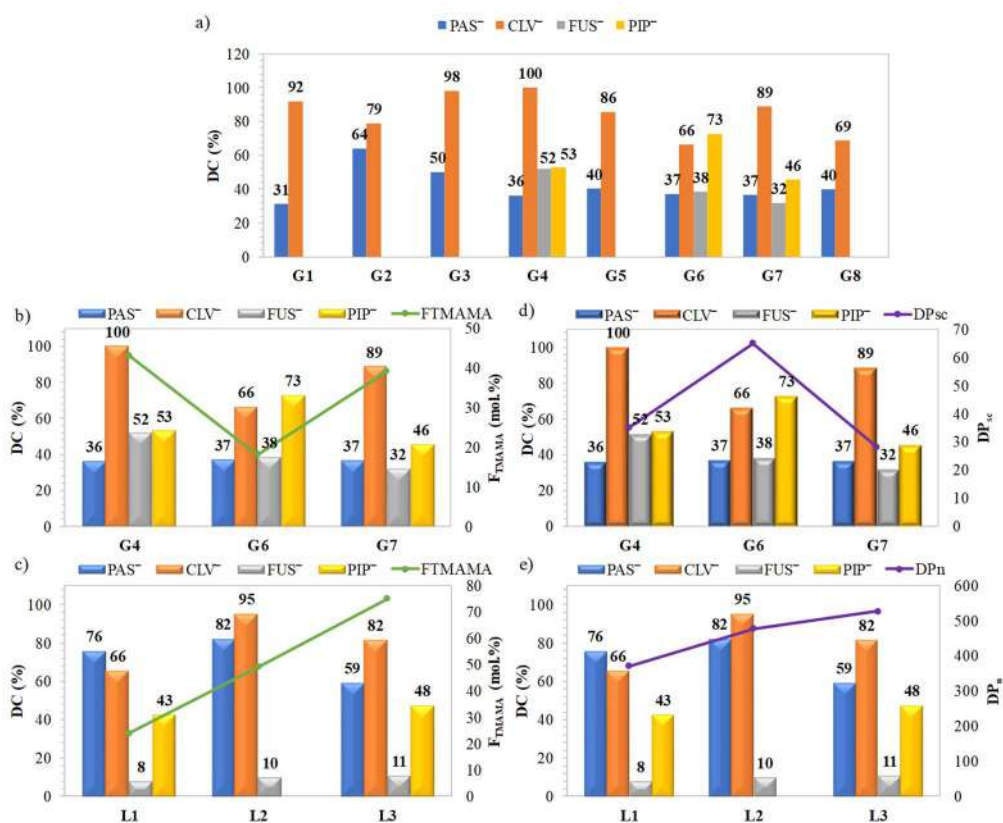
Tabela 2. Podstawowe parametry kopolimerów liniowych.

	TMAMA/MMA	DP _n	F _{TMAMA} (mol.%)	M _n × 10 ⁻³ (g/mol)	Đ
L1	25/75			47	1,74
L2	50/50			73	1,36
L3	75/25			96	1,27

Większość kopolimerów charakteryzowała się wąskim rozrzutem ciężarów cząsteczkowych określonych na drodze chromatografii żelowej GPC (dla kopolimerów szczepionych $\bar{D} = 1,03-1,90$, dla kopolimerów liniowych $\bar{D} = 1,27-1,74$). Analiza ta w większości przypadków potwierdziła kontrolowany przebieg reakcji, a początkowe stosunki komonomerów TMAMA/MMA (25/75, 50/50 dla kopolimerów szczepionych oraz 25/75, 50/50 lub 75/25 dla kopolimerów liniowych).

Wymiana anionów chlorkowych w polimerze na aniony farmaceutyczne – otrzymywanie koniugatów jonowych (P.1.; P.2.; P.3.; P.5.)

W wyniku reakcji wymiany jonowej otrzymano koniugaty jonowe PIL-lek. Do badań wybrano sole sodowe lub potasowe zawierające następujące aniony: *p*-aminosalicylan (PAS⁻), klawulanian (CLV⁻), fusydan (FUS⁻) oraz piperacylina (PIP⁻). Reakcję wymiany oraz ilość wprowadzonego leku do matrycy polimerowej pośrednio analizowano w oparciu o zawartość leku (ang. Drug content, DC), którą określono na podstawie widm UV-Vis. Zarówno topologia i struktura kopolimeru, jak również struktura leku znacząco wpływały na wartości DC, o czym świadczą różnice dla układów o podobnej zawartości frakcji jonowej (rys. 3). Biorąc pod uwagę strukturę kopolimeru - zawartość frakcji hydrofilowej oraz stopień szczeplenia odgrywały kluczową rolę w efektywności reakcji wymiany na lek. Zauważono, że im większy udział frakcji jonowej, przy jednoczesnym luźniejszym rozkładzie łańcuchów bocznych w polimerze, tym osiągnięto lepsze rezultaty DC dla CLV⁻, PAS⁻ i FUS⁻, co w szczególności zaobserwowano dla kopolimeru G4. Odwrotną zależność odnotowano dla układów z PIP⁻, w których większe zagęszczenie łańcuchów bocznych oraz niższe F_{TMAMA} prowadziło do wyższych wartości DC, jak w przypadku kopolimeru G6, zaś dla pozostałych kopolimerów G4 i G7 wartości DC były dwukrotnie mniejsze niż dla CLV.



Rysunek 3. Zestawienie zawartości leku (DC) a) dla wszystkich badanych koniugatów kopolimerów szczeplonych, b-c) DC w korelacji z zawartością frakcji jonowej F_{TMAMA} i d-e) długością łańcucha zawierającego jednostki TMAMA.

W przypadku liniowych kopolimerów (rys. 3c, e) (P.2. – Tab. 2.; Fig. 4) DC CLV⁻ i PAS⁻ były najwyższe dla układu o średniej wartości F_{TMAMA} oraz długości łańcucha (L2). Wyższa zawartość hydrofobowych jednostek ograniczała wprowadzanie leku do matrycy, co skutkowało niższymi wartościami DC. Zauważono, że im większa była zawartość jednostek hydrofobowych w kopolimerach liniowych, a tym samym ich luźniejsze rozmieszczenie w łańcuchu, tym wyższe DC osiągnięto sugerując lepszą dostępność do jonowych ugrupowań.

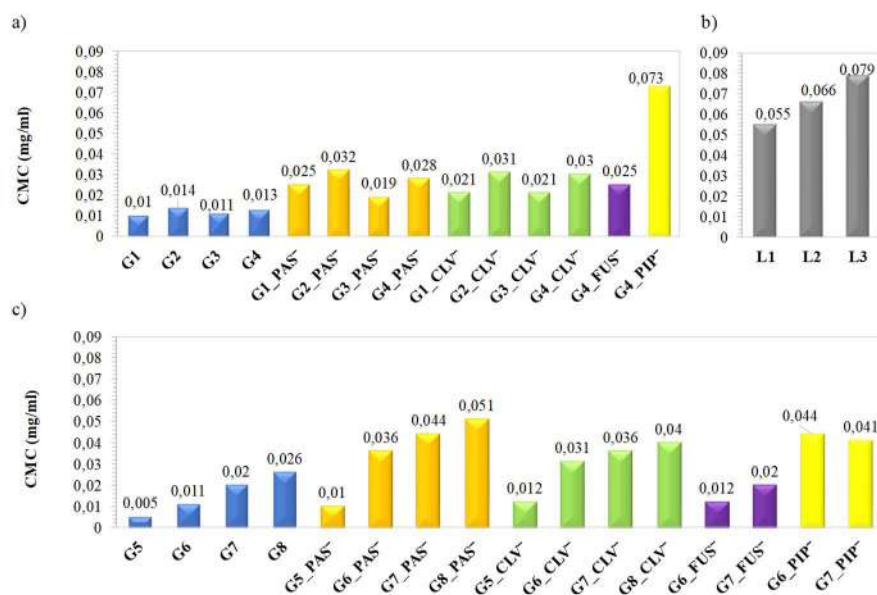
Analogicznie do układów szczepionych, DC PIP⁻ było wyższe dla mniej hydrofilowych układów o większych długościach łańcuchów.

Zachowanie polimerów i ich koniugatów w środowisku wodnym (P.1.; P.2.; P.3.; P.5.)

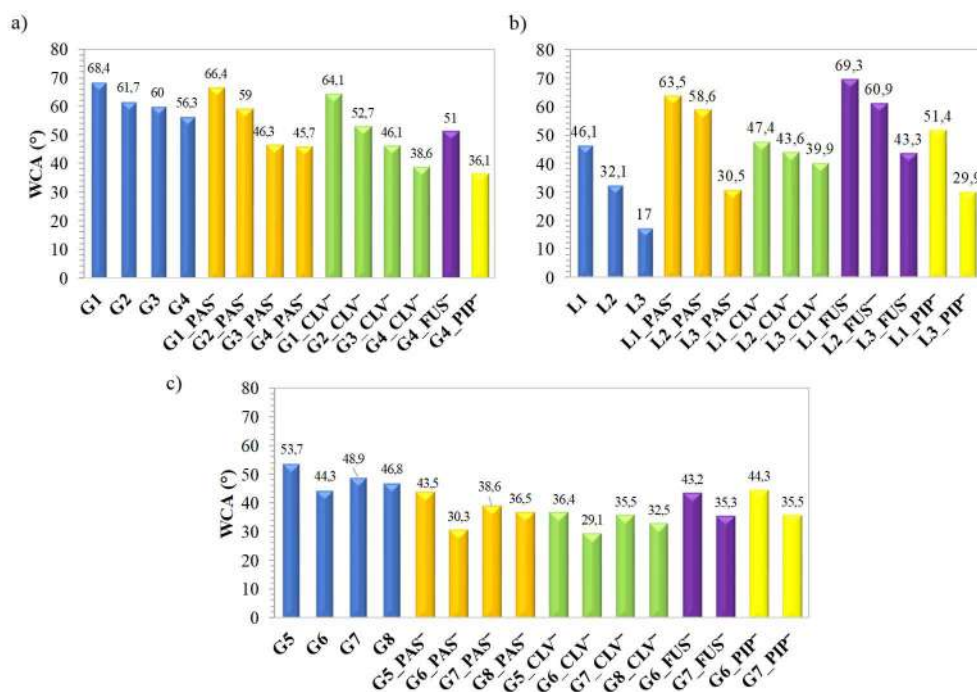
Powstałe koniugaty na bazie kopolimerów liniowych w roztworze wodnym formowały nanocząstki o wielkościach 9–306 nm. Z kolei kopolimery szczepione z przeciwjonem chlorkowym tworzyły struktury osiągające średnice hydrodynamiczne (D_h) o rozmiarach 18-368 nm. Ich koniugaty z PAS⁻ i CLV⁻ posiadały podobne rozmiary, odpowiednio 23-354 nm, 18-357 nm. Koniugaty FUS⁻ tworzyły nieco mniejsze cząstki w zakresie 26-208 nm, a wymiana z PIP⁻ spowodowała wzrost wartości D_h , osiągając rozmiary między 20-451 nm.

Zdolność otrzymanych kopolimerów szczepionych i liniowych do formowania nanocząstek potwierdzono poprzez krytyczne stężenie micelizacji (CMC), które określono zarówno dla kopolimerów z przeciwjonem chlorkowym, jak również wybranych koniugatów z lekami (rys. 4). Wartości CMC wyznaczano na podstawie zmierzonego napięcia międzyfazowego (IFT). Najwyższe wartości CMC odnotowano dla kopolimerów G7 i G8 charakteryzujących się gęściejszym rozmieszczeniem łańcuchów bocznych i wysoką zawartością frakcji TMAMA w łańcuchach bocznych ($DG=46\%$ mol.; $F_{TMAMA}=39$ i 46% mol. odpowiednio dla G7 i G8) oraz kopolimeru L3 o najdłuższym łańcuchu i największej zawartości frakcji jonowej ($DP_n=396$; $F_{TMAMA}=75\%$ mol.). Po wymianie na PAS⁻, CLV⁻ i PIP⁻ w polimerach szczepionych odnotowano wzrost CMC. W przypadku FUS⁻, dla kopolimeru o niższym DG wymiana leku spowodowała wzrost wartości CMC (0,013 vs. 0,025 mg/mL przy $DG = 26\%$ mol.), podczas gdy wartości CMC nie zmieniły się dla kopolimerów o wyższym stopniu szczepienia ($DG = 46\%$ mol.), co spowodowane było bardziej hydrofobowym charakterem leku, jak również wartością DC w koniugacie FUS, która była prawie dwukrotnie wyższa dla G4 w porównaniu z G6 i G7.

Za pomocą goniometru został także wyznaczony kąt zwilżania (WCA) powierzchni warstwy polimerowej, który może zmieniać się ze względu na strukturę matrycy polimerowej, jak i charakter wprowadzonego leku (rys. 5). Zauważono, że wraz ze zwiększeniem się stopnia szczepienia i jednocześnie F_{TMAMA} , wartości WCA zmniejszały się, wskazując na wzrastającą hydrofilowość układów. Podobnie w przypadku kopolimerów liniowych, zwilżalność wzrastała wraz z zawartością frakcji TMAMA. Ponadto, warstwy kopolimerów liniowych w porównaniu ze szczepionymi wykazywały większą hydrofilowość, co może być spowodowane przewagą jednostek o charakterze hydrofobowym, a jednocześnie dużo dłuższymi łańcuchami bocznymi w kopolimerach szczepionych. Wymiana jonowa na aniony farmaceutyczne w kopolimerach szczepionych spowodowała zmniejszenie się wartości WCA, co oznacza, że w tym przypadku koniugowane leki zwiększały solubilizację układów. Odwrotna zależność po wprowadzeniu leków w postaci jonowej do matryc opartych na kopolimerach liniowych, wynika z braku występowania efektu separacji fazowej, która następuje w kopolimerach szczepionych ze względu na hydrofobowy łańcuch główny. Obserwacje te potwierdzają, że topologia, parametry strukturalne, długość łańcuchów a równocześnie charakter chemiczny leku miały znaczący wpływ na zwilżalność warstw kopolimerów.



Rysunek 4. Wartości krytycznego stężenia micelizacji (CMC) a) kopolimerów szczepionych G1-G4 oraz ich koniugatów z lekami, b) kopolimerów liniowych L1-L3 oraz c) kopolimerów szczepionych G5-G8 oraz ich koniugatów z lekami.



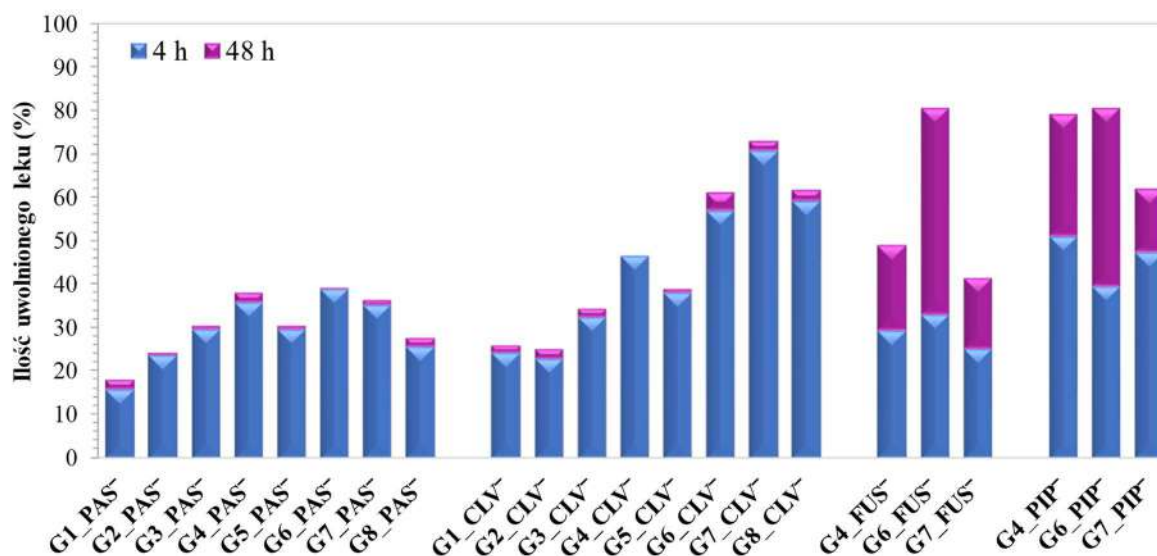
Rysunek 5. Kąty zwilżania (WCA) dla kopolimerów a) G1-G4 o mniejszym stopniu szczepienia i ich koniugatów b) L1-L3 i ich koniugatów oraz c) G5-G8 o większym stopniu szczepienia i ich koniugatów wyznaczone metodą goniometryczną.

Uwalnianie skoniugowanego leku w postaci anionu farmaceutycznego (P.1.; P.2.; P.3.; P.5.)

Proces uwalniania *in vitro* skoniugowanych jonowo leków przeprowadzono w buforze fosforanowym (PBS, pH= 7,4, 37°C). Uwalnianie prowadzono przez 72 h, jednakże efektywny proces można było odnotować do 4 godzin, po czym następowało wolniejsze uwalnianie trwające do 24-48 godzin. Uwalnianie leku, podobnie jak jego wcześniejsze wprowadzenie, silnie zależało od struktury polimeru, w tym topologii i ilości grup jonowych, a w przypadku kopolimerów szczepionych także od stopnia szczepienia. Ponadto, zauważono związek pomiędzy rodzajem skoniugowanego anionu farmaceutycznego a szybkością uwalniania leku.

Z uwagi na większą zawadę steryczną anionów FUS⁻ i PIP⁻ rozmieszczonych w łańcuchach bocznych, uwalnianie tych leków zachodziło z wyraźnie mniejszą szybkością (rys. 6). Spośród badanych układów niniejsze leki uwalniały się w największej ilości dla próbki G6, która posiadała gęsto rozmieszczone łańcuchy boczne, jednocześnie przy najmniejszej zawartości frakcji hydrofilowej. Z kolei, mniejszy stopień szczepienia był bardziej korzystny dla uwalniania leków tworzących mniejszą zawadę steryczną, tj. PAS⁻ i CLV⁻, co warunkowało szybszą dyfuzję leku, gdzie już po 4 godzinach większość substancji aktywnej została uwolniona.

Proces uwalniania z kopolimerów liniowych jako układów do porównania efektywności dostarczania leków jonowych, był najkorzystniejszy dla PAS⁻ pod względem procentowej ilości uwolnionego leku jak również wyjściowej zawartości leku. Podobnie, FUS⁻ okazał się dogodnym lekiem do uwalniania z polimerów liniowych, jednakże mała wartość DC generowała małe stężenie uwolnionego leku. Z kolei, uwalnianie CLV⁻ i PIP⁻ z tych kopolimerów przebiegło ze znacznie mniejszą wydajnością, sugerując silniejsze oddziaływania tych anionów farmaceutycznych z matrycą polimeru tworzące stosunkowo stabilne pary jonowe.

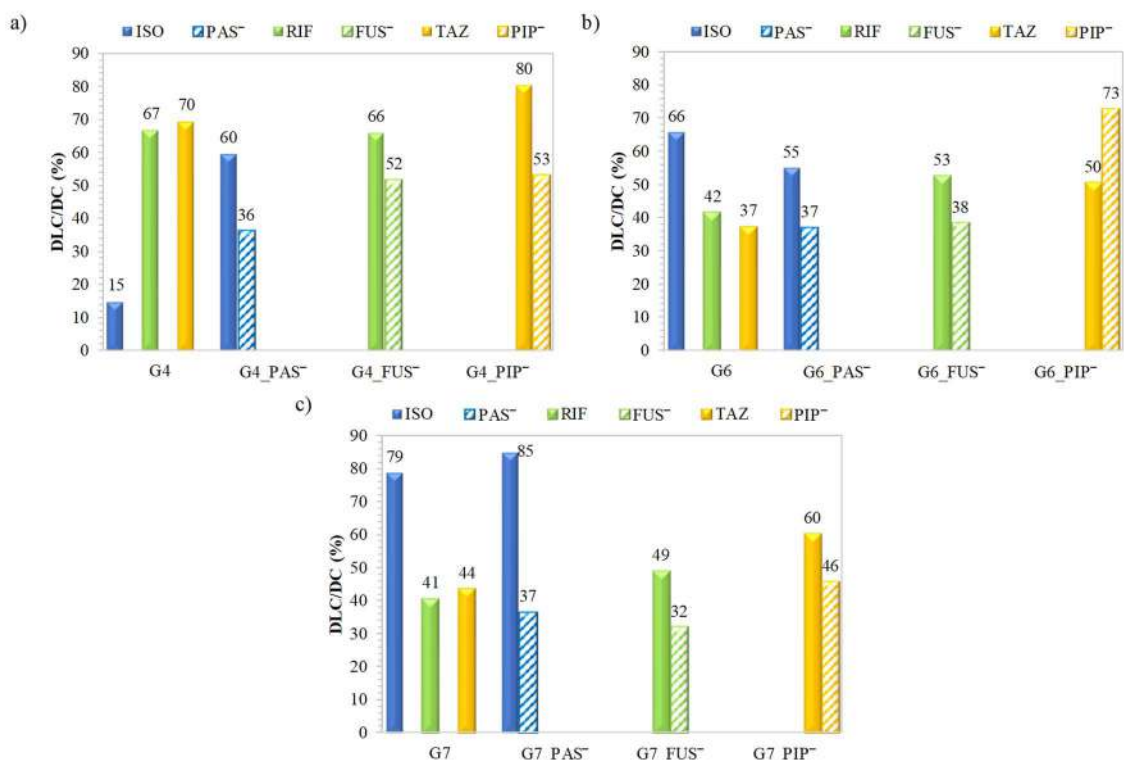


Rysunek 6. Ilości uwolnionych leków jonowych dla układów szczepionych.

Enkapsulacja leków – układy oparte na kopolimerach szczepionych i ich koniugatach (P.3.; P.4.; P.5.)

Z uwagi na wykazane zdolności do samoorganizacji w roztworach wodnych kopolimerów szczepionych wykorzystano je do enkapsulacji leku fizycznie oddziałującego z matrycą polimerową. W przypadku kopolimerów z przeciwjonem chlorkowym załadowanie leku prowadziło do uzyskania układów pojedynczych transportujących jeden rodzaj leku. Szczególnym podejściem była enkapsulacja leków w samoorganizujących się koniugatach z przeciwjonem farmaceutycznym, w wyniku czego uzyskano układy podwójnie aktywne z parą współdziałających leków, tj. jonowego połączonego za pomocą wiązania chemicznego oraz niejonowego oddziałującego w sposób fizyczny z matrycą polimeru.

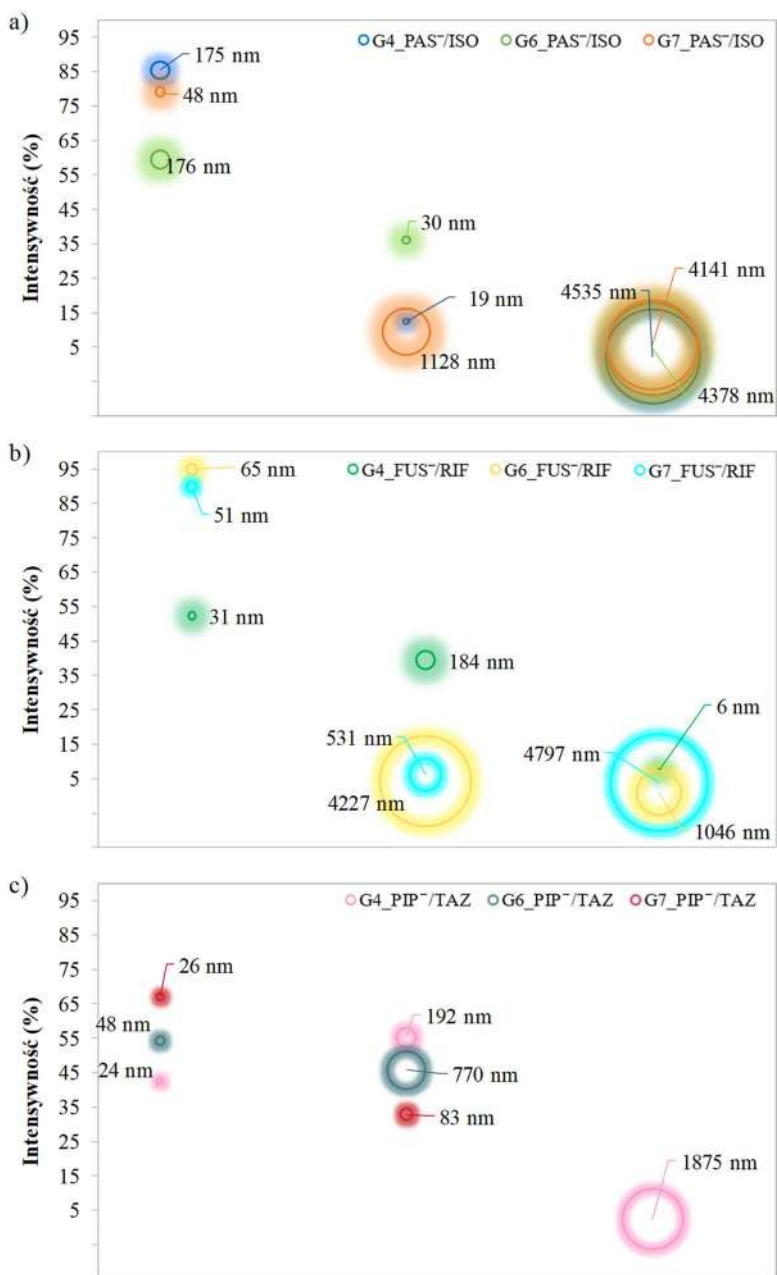
W tym celu wybrano trzy modelowe leki, tj. izoniazyd (ISO), ryfampicyna (RIF) oraz tazobaktam (TAZ). Efektywność procesu enkapsulacji podczas samoorganizacji wybranych kopolimerów szczepionych i ich koniugatów oceniono na podstawie zawartości załadowanego leku (ang. Drug-Loading Content, DLC) (rys. 7). Zanotowano pozytywny wpływ obecności anionu farmaceutycznego na efektywność enkapsulacji. Ponadto zauważono ścisłą zależność stopnia szczepienia oraz charakteru leku na efektywność enkapsulacji. Hydrofilowy lek ISO był znacznie lepiej enkapsulowany przez układy o większym stopniu szczepienia, tj. G6 i G7, w porównaniu z G4. Z kolei, enkapsulacja leków trudno rozpuszczalnych w wodzie, tj. RIF i TAZ okazała się bardziej efektywna w układach G4 o mniejszym stopniu szczepienia. Uzyskane wyniki potwierdzają, że rodzaj leku niejonowego w korelacji z parametrami strukturalnymi matrycy polimerowej wpływa na wartości DLC.



Rysunek 7. Zawartości leków niejonowych w układach pojedynczych oraz zawartość leków niejonowych w układach podwójnych vs. zawartości anionów.

Badania wielkości nanocząstek układów podwójnych utworzonych w roztworze wodnym wykazały, że w porównaniu z układami pojedynczymi (rozd. 3.3) tworzyły mniejsze struktury (rys. 8), tj. 30-175 nm dla układów PAS⁻/ISO i 31-184 nm dla układów FUS⁻/RIF. Podobny efekt uzyskano dla układów PIP⁻/TAZ, których rozmiary cząstek osiągały 24-192 nm,

aczkolwiek wykazywały one większą tendencję do agregacji, na co wskazywała obecność znaczącej frakcji >500 nm (46%), podczas gdy w przypadku pozostałych układów agregaty występowały wyłącznie w małych ilościach (<10%). Przedstawiony komentarz dotyczy przeważających frakcji.



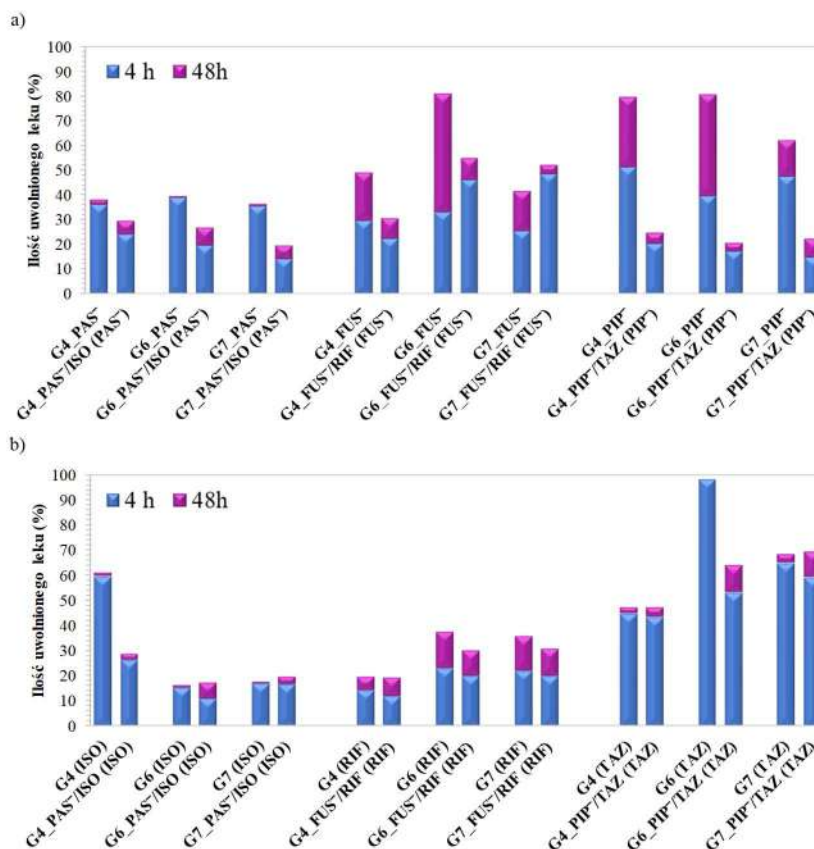
Rysunek 8. Średnice hydrodynamiczne (Dh) nanocząstek polimerowych wyznaczone metodą DLS dla układów podwójnych.

Uwalnianie leków niejonowych oraz współuwalnianie pary leków o synergistycznym działaniu (P.3.; P.4.; P.5.)

Proces uwalniania *in vitro*, podobnie jak w przypadku koniugatów z anionem farmaceutycznym, przeprowadzono w warunkach imitujących środowisko płynów ustrojowych, czyli w roztworze PBS (pH=7.4, 37°C). Otrzymane wyniki wykazały, że obecność enkapsulowanego leku wpłynęła na ograniczenie ilości uwolnionego leku jonowego, w porównaniu z układami pojedynczymi niosącymi aniony farmaceutyczne (rys. 9a).

Największe różnice były odnotowane w przypadku uwalniania PIP⁻, gdzie po enkapsulacji leku w trakcie współuwalniania anion farmaceutyczny został uwolniony w znacznie mniejszej ilości.

Podobnie jak w przypadku leków jonowych uwalnianie leku niejonowego zależało silnie od matrycy jak również od charakteru leku (rys. 9b). Najkorzystniejszą matrycą pod względem ilości uwolnionego ISO był kopolimer G4 o najkrótszych łańcuchach bocznych, mniejszym stopniu szczypania oraz największej zawartości frakcji jonowej spośród badanych układów. Z kolei, leki trudno rozpuszczalne w wodzie, tj. RIF i TAZ, były najlepiej uwalniane z układu kopolimeru G6 o najdłuższych łańcuchach bocznych, większym stopniu szczypania, a przede wszystkim najmniejszej frakcji TMAMA.



Rysunek 9. Procentowe ilości uwolnionych leków w układach pojedynczych vs. skojarzonych dla leków a) jonowych b) niejonowych po 4 i 48 h.

Biologiczna ocena układów dostarczania leków — badania cytotoksyczności (P.6.; P.7.)

Przeprowadzono ewaluację cytotoksyczności układów dostarczających leki, opartą na badaniach kolorymetrycznych z użyciem bromku 3-(4,5-dimetylotiazol-2-ilo)-2,5-difenylo-tetrazoliowego (MTT) oraz analizie metodą cytometrii przepływowej obejmujące test apoptozy i analizy cyklu komórkowego. Z uwagi, że otrzymane nośniki były testowane pod kątem transportu leków stosowanych w leczeniu dolnych dróg oddechowych, w tym gruźlicy, do badania cytotoksyczności użyto model ludzkich komórek nabłonka oskrzeli (BEAS-2B) oraz linii nowotworowych, tj. gruczolaka ludzkiej linii komórek podstawnych nabłonka pęcherzyków płucnych (A549) oraz niedrobnokomórkowego raka płuc (H1299). Dodatkowo dla układów kopolimerów liniowych przeprowadzono pomiary ekspresji genów dla interleukin

IL6 i IL8. Badania cytotoksyczności *in vitro* przeprowadzone z udziałem otrzymanych nośników polimerowych potwierdziły brak efektu cytotoksycznego na linię prawidłowych komórek BEAS-2B, przy czym koniugaty z PAS⁻, CLV⁻, FUS⁻ i PIP⁻ wykazały znikomy wpływ na żywotność komórek. Z kolei, badane układy powodowały proliferację komórek nowotworowych A549 i H1299. Wykazana selektywność działania większości badanych układów warunkowała brak znaczących zmian dla linii komórek prawidłowych oraz negatywny wpływ wobec komórek nowotworowych.

Podsumowanie i wnioski

Zastosowanie układów kopolimerów szczepionych pozwoliło na wolniejszy i bardziej kontrolowany przebieg uwalniania, z uwagi większej trwałości struktury micelarnej, w porównaniu z układami opartymi na splecionych łańcuchach kopolimerów liniowych.

Odpowiednio duża ilość wprowadzonego leku do łańcuchów i jego uwolnienie w zadowalającej ilości procentowej ostatecznie zapewniało względnie wysokie stężenie leku uwolnionego z kopolimerów szczepionych, co może gwarantować skuteczność terapii.

Efektywność koniugacji i enkapsulacji leku, a także szybkość uwalniania leku (jonowego oraz niejonowego) można regulować poprzez strukturę nośnika polimerowego, gdzie szczególną rolę odgrywa gęstość rozmieszczenia łańcuchów bocznych w polimerze, ale równocześnie istotna jest struktura i charakter zastosowanych leków oraz ich współdziałanie w matrycy.

Badania cytotoksyczności *in vitro* przeprowadzone z udziałem otrzymanych nośników polimerowych wykazały znikomy wpływ na normalne linie komórkowe BEAS-2B i proliferację komórek nowotworowych A549. Biorąc pod uwagę, że osłabiony immunologicznie organizm jest podatny na rozwój nowotworów, efekt selektywnego działania systemów dostarczania leków jest niezwykle pożądany. To świadczy o dużym potencjale aplikacyjnym jako nowych alternatywnych układów w leczeniu chorób układu oddechowego ze względu na możliwość ich szerokiego zastosowania przeciwko patogenom lub komórkom nowotworowym.

Obecne jednostki choliny w matrycy polimeru i wprowadzone leki przeciwbakteryjne, sprawiają, że układy te mogą znaleźć potencjalne zastosowanie w leczeniu chorób dróg oddechowych, w tym gruźlicy, z uwzględnieniem terapii skojarzonej dostarczając parę synergistycznie działających leków, przy jednoczesnym zapobieganiu rozwijania się nowotworów.

W przypadku zastosowania w terapii przeciwgruźliczej ich szybkie działanie w efektywnym czterogodzinnym cyklu powinno zapewnić efektywny przebieg leczenia. Jednak ich wykorzystanie wymaga dalszych testów obejmujących szczegółowe badania biologiczne *in vivo*, które w pełni potwierdzą możliwość zastosowania otrzymanych polimerowych układów dostarczania leków w ludzkim organizmie.

Podsumowując, w ramach niniejszych badań zostały zaprojektowane kopolimery szczepione z przeciwciałami farmaceutycznymi, które wydają się być obiecującymi nośnikami z punktu widzenia fizykochemicznego i pod kątem cytotoksyczności.

SUMMARY OF DOCTORAL DISSERTATION

Designing of grafted poly(ionic liquids) as potential drug delivery systems for antibacterial therapy

mgr inż. Katarzyna Niesyto

Promoter: prof. dr hab. inż. Dorota Neugebauer

THE AIM AND SCOPE OF THE RESEARCH

The aim of the research presented in this doctoral thesis was to develop new polymer systems as drug nanocarriers based on graft polymers that contained units of choline ionic liquid (IL), i.e. [2-(methacryloyloxy)ethyl]trimethylammonium chloride (TMAMA). Therefore, using controlled atom transfer polymerization (ATRP), well-defined copolymers were obtained, which differed with the number of side chains, i.e. the degree of grafting, the degree of polymerization, and the TMAMA content. For comparison purpose, analogous linear copolymers were also synthesized. The presence of chloride anions, both in graft and linear copolymers, was used in the ion exchange reaction to introduce drugs in ionic form (pharmaceutical anions). According to this strategy, chloride polymers could serve as universal templates for obtaining ionic polymer-drug conjugates.

The second important research topic was the use of the amphiphilic nature of the obtained copolymers as micellar carriers in the encapsulation of drugs in non-ionic form. As a result of combining both strategies, i.e. anion exchange and encapsulation, with the use of graft polymers, micellar ionic conjugates were obtained as dual systems for combined therapy transporting two drugs with a synergistic effect which are variably linked to the polymer matrix (ionic bond vs. physical impact). The tested systems were designed for transporting drugs used in the treatment of lower respiratory tract diseases, including tuberculosis. In addition to the basic physicochemical characteristics of the polymers, the influence of the structural parameters of the carrier on the drug release rate was examined, and the cytotoxicity of the systems was assessed.

Due to the diverse nature of polymer matrices and selected model drugs, the tested systems were grouped as follows:

- Polymer conjugates with pharmaceutical anions: *p*-aminosalicylate (PAS⁻), clavulanate (CLV⁻), piperacillin (PIP⁻), fusidate (FUS⁻),
- Micelles based on chloride polymers with encapsulated drug in non-ionic form: isoniazid (ISO), tazobactam (TAZ), rifampicin (RIF),
- Micellar ionic conjugate systems for two drugs transporting (ionic/non-ionic): PAS⁻/ISO, PIP⁻/TAZ, FUS⁻/RIF.

LIST OF SCIENTIFIC PUBLICATIONS CONSTITUTING A MONOTIVE CYCLE

This dissertation is a monothematic series of seven scientific articles published in 2020-2024 in journals registered in the Journal Citation Records (JCR) database:

P.1. Synthesis and Characterization of Ionic Graft Copolymers: Introduction and In Vitro Release of Antibacterial Drug by Anion Exchange.

K. Niesyto, D. Neugebauer

Polymers. 2020, 12, 2159. (IF2020= 4.329; MEiN=100 pkt)

P.2. Linear Copolymers Based on Choline Ionic Liquid Carrying Anti-Tuberculosis Drugs: Influence of Anion Type on Physicochemical Properties and Drug Release.

K. Niesyto, D. Neugebauer

International Journal of Molecular Sciences 2021, 22, 284 (IF2021= 6.208; MEiN=140 pkt)

P.3. Dual-Drug Delivery via the Self-Assembled Conjugates of Choline-Functionalized Graft Copolymers.

K. Niesyto, A. Mazur, D. Neugebauer

Materials 2022, 15, 4457 (IF2022= 3.4; MEiN=140 pkt)

P.4. Ionic Liquid-based Polymer Matrices for Single and Dual Drug Delivery: Impact of Structural Topology on Characteristics and In Vitro Delivery Efficiency.

K. Niesyto, S. Keihankhadiv, A. Mazur, Mielańczyk, A., D. Neugebauer

International Journal of Molecular Sciences 2024, 25, 1292 (IF2022=5.6; MEiN=140 pkt)

P.5. Piperacillin/Tazobactam co-delivery by micellar ionic conjugate systems carrying pharmaceutical anions and encapsulated drug

K. Niesyto, A. Mazur, D. Neugebauer

Pharmaceutics 2024, 16, 198 (IF2022= 5.4; MEiN=100 pkt)

P.6. Biological in vitro evaluation of PIL graft conjugates: cytotoxicity characteristics.

K. Niesyto, W. Łyżniak, M. Skonieczna, D. Neugebauer

International Journal of Molecular Sciences 2021, 22, 7741 (IF2021= 6.208; MEiN=140 pkt)

P.7. Toxicity evaluation of choline ionic liquid-based nanocarriers of pharmaceutical agents for lung treatment.

K. Niesyto, M. Skonieczna, M. Adamiec-Organisiciok, D. Neugebauer

Journal of Biomedical Materials Research Part B - Applied Biomaterials 2023, 111(7), 1374-1385 (IF2022= 3.4; MEiN=140 pkt)

SUMMARY OF THE DOCTORAL STUDENT'S OWN CONTRIBUTION

Participation in the development of the concept and research plan; conducting the synthesis of macroinitiator precursors, macroinitiators and linear and graft polymers; obtaining conjugates, micelles and micellar conjugates as drug carriers containing one or two types of drugs; conducting physicochemical characterization of the obtained polymers and carriers; conducting drug release studies; conducting biological research; development, analysis and interpretation of results; preparation of original drafts of publication manuscripts; Scholarship holder - research contractor under the OPUS program (grant no. 2017/27/B/ST5/00960; 2019-2022).

Declarations of the co-authors of the publication detailing their individual authorial contribution are included in the appendices to this dissertation.

DESCRIPTION OF THE SUBJECT OF THE RESEARCH, RESULTS AND CONCLUSIONS

Synthesis of copolymers using the ATRP method (P.1.; P.2.)

During studies, innovative polymer systems were developed as drug carriers for antibacterial therapy of lower respiratory tract diseases, using grafted copolymers containing units of choline ionic liquid, i.e. [2-(methacryloyloxy)ethyl]trimethylammonium chloride (TMAMA), which is known from biological activity. For this purpose, controlled Atom Transfer Radical Polymerization (ATRP) was used to obtain well-defined copolymers. The ionic structure of TMAMA enabled the ion exchange of the chloride anion for pharmaceutical anions, increasing the biological activity of the systems. At the same time, the use of the hydrophilic TMAMA comonomer in various initial proportions (TMAMA/MMA = 25/75, 50/50, 75/25) allowed to achieve a different hydrophilic-hydrophobic balance in the tested polymer systems. Comparatively, a series of tests were carried out using analog linear polymers. Carrier studies included well-defined copolymers with diverse topologies, i.e. grafted G1-G8 vs. linear L1-L3, which were synthesized using different initiator systems (initiator vs. macroinitiator). Grafted copolymers G1-G8 were obtained as a result of a two-stage controlled atom transfer radical polymerization (ATRP) reaction (Fig. 1, Table 1). In turn, linear copolymers L1-L3 were obtained by a one-step ATRP reaction (Fig. 2, Table 2).

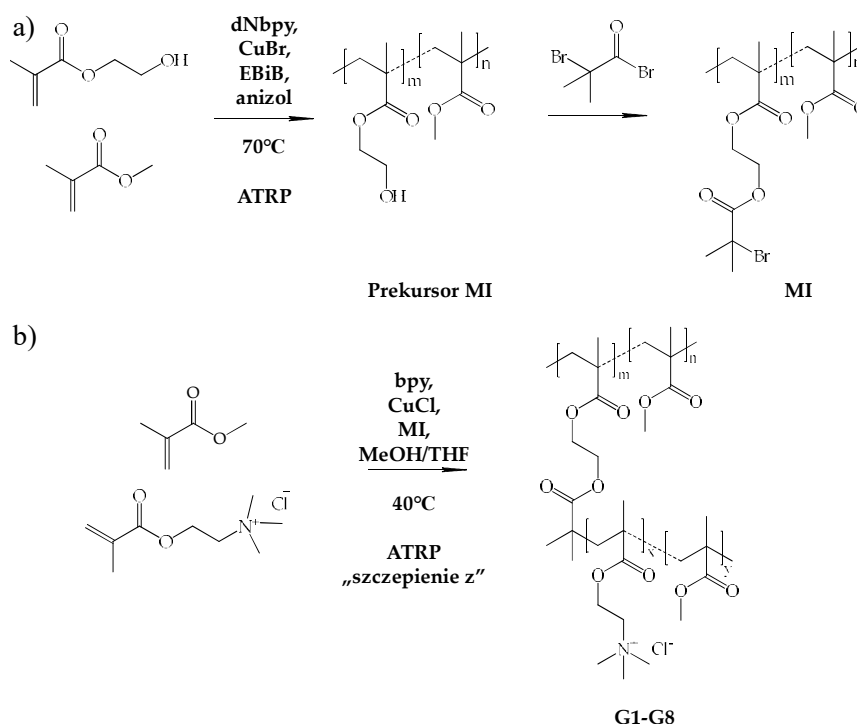
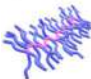
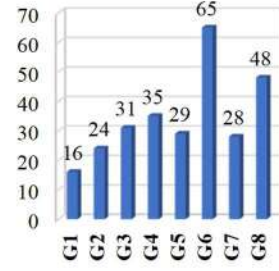
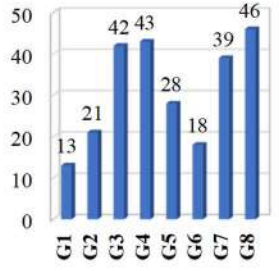
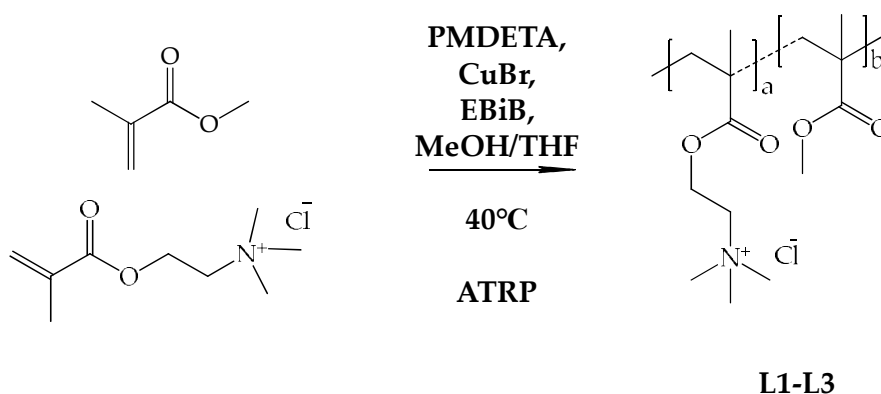





Figure 1. Reaction schemes for preparing a) P(MMA-co-BIEM) as macroinitiator, and b) graft copolymer, where EBiB is the initiator.

Table 1. Characteristics of graft copolymers.

	TMAMA/ MMA	DP _n	n _{sc}	DG (mol.%)	DP _{SC}	F _{TMAMA} (mol.%)	M _n × 10 ⁻³ (g/mol)	Đ
G1	25/75						115	1,68
G2	25/75	186	48	26			169	1,90
G3	50/50						244	1,31
G4	50/50	273	1,15					
G5	25/75	554	1,24					
G6	25/75	1091	1,11					
G7	50/50	292	133	46			584	1,03
G8	50/50						1007	-

**Figure 2.** Reaction scheme for obtaining a linear copolymer.**Table 1.** Characteristics of linear copolymers.

	TMAMA/MMA	DP _n	F _{TMAMA} (mol.%)	M _n × 10 ⁻³ (g/mol)	Đ
L1	25/75			47	1,74
L2	50/50			73	1,36
L3	75/25			96	1,27

Most copolymers were characterized by a low dispersity determined by GPC (for graft copolymers $\bar{D} = 1.03-1.90$, for linear copolymers $\bar{D} = 1.27-1.74$). In most cases, this analysis confirmed the controlled course of the reaction and the initial ratios of TMAMA/MMA comonomers (25/75, 50/50 for graft copolymers and 25/75, 50/50 or 75/25 for linear copolymers).

The ion exchange of chloride anions for pharmaceutical one – ionic conjugates obtaining (P.1.; P.2.; P.3.; P.5.)

PIL-drug ion conjugates were obtained as a result of the ion exchange reaction. For this purpose sodium or potassium salts containing the following anions were selected: *p*-aminosalicylate (PAS⁻), clavulanate (CLV⁻), fusidate (FUS⁻) and piperacillin (PIP⁻). The exchange reaction and the amount of drug introduced into the polymer matrix were indirectly analyzed by the drug content (DC), which was determined with UV-Vis spectra. Both the topology and structure of the copolymer, as well as the structure of the drug, significantly influenced the DC values, as showed by the differences for systems with similar ionic fraction content (Fig. 3). Considering the structure of the copolymer, the content of the hydrophilic fraction and the degree of grafting had a big impact on the exchange reaction effectiveness. It was noticed that the higher ionic fraction, with loosely grafted side chains, affected better DC results were achieved for CLV⁻, PAS⁻ and FUS⁻, which was especially observed for the G4 copolymer. An inverse relationship was noted for systems with PIP⁻, in which a higher density of side chains and lower F_{TMAMA} led to higher DC values, as in the case of the G6 copolymer, while for the remaining graft copolymers G4 and G7, the DC values were twice lower than for CLV⁻.

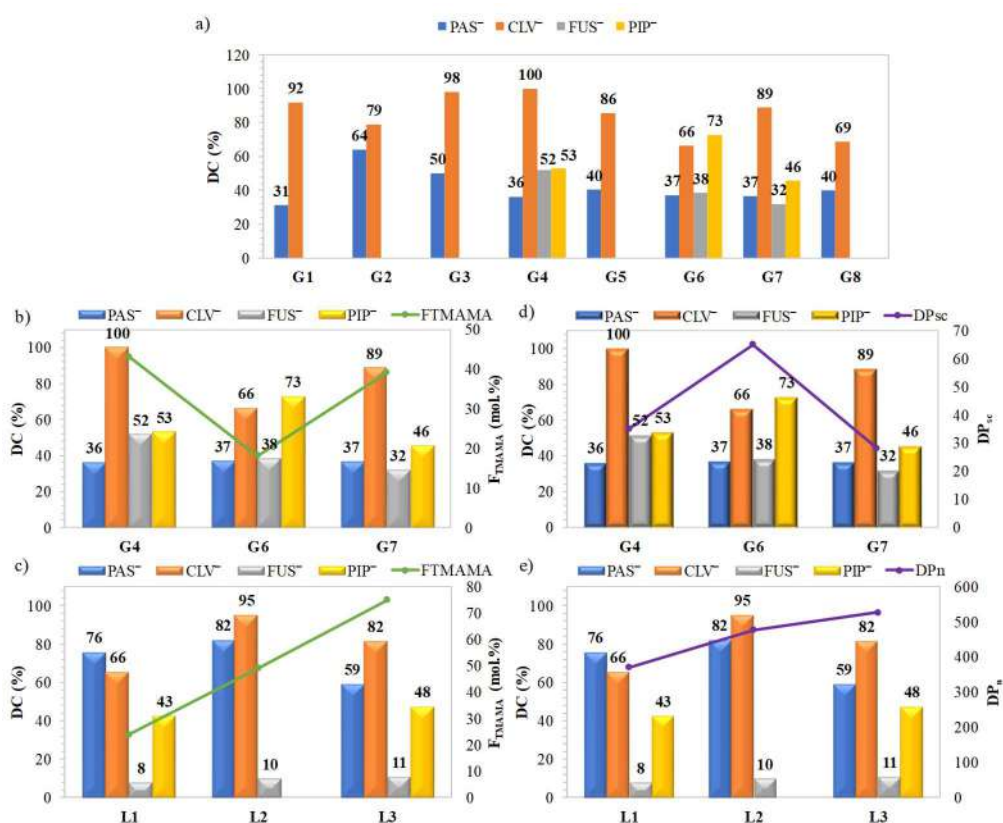


Figure 3. Summary of drug content (DC) for a) all tested conjugates of graft copolymers, b-c) DC in correlation with the content of the ionic fraction F_{TMAMA} and d-e) the length of the chain containing TMAMA units.

In the case of linear copolymers (Fig. 3c, e), DC CLV⁻ and PAS⁻ were the highest for the system with the medium F_{TMAMA} value and chain length (L2). A higher content of hydrophobic units limited drug loading into the matrix, resulting in lower DC values. It was noticed that the higher content of hydrophobic units in the linear copolymers, and thus their looser distribution in the chain, the higher DC was achieved, suggesting better accessibility to ionic moieties. Analogous to grafted systems, DC PIP⁻ was higher for less hydrophilic systems with longer chain lengths.

Behavior of polymers and their conjugates in an aqueous environment (P.1.; P.2.; P.3.; P.5.)

The obtained conjugates based on linear copolymers in aqueous solution formed nanoparticles with sizes of 9–306 nm. In turn, copolymers grafted with a chloride counterion formed structures reaching hydrodynamic diameters (D_h) of 18–368 nm. Their conjugates with PAS^- and CLV^- had similar sizes, 23,354 nm, 18–357 nm, respectively. FUS^- conjugates formed slightly smaller particles in the range of 26–208 nm, and exchange with PIP^- resulted in an increase in D_h values, reaching sizes between 20–451 nm.

The ability of the obtained graft and linear copolymers to form nanoparticles was confirmed by the critical micellization concentration (CMC), which was determined both for copolymers with a chloride counterion, as well as for selected drug conjugates (Fig. 4). CMC values were determined by the measured interfacial tension (IFT). The highest CMC values were recorded for densely grafted copolymers G7 and G8 characterized by a high content of the TMAMA fraction in the side chains ($DG = 46$ mol%; $F_{TMAMA} = 39$ and 46 mol% for G7 and G8, respectively) and the L3 copolymer with the longest chain and the highest ionic fraction content ($DP_n = 396$; $F_{TMAMA} = 75$ mol%). After ionic exchange with PAS^- , CLV^- and PIP^- , an increase in CMC was observed in the grafted polymers. In the case of FUS^- , for the copolymer with lower DG , drug replacement resulted in an increase in CMC values (0.013 vs. 0.025 mg/mL at $DG = 26$ mol%), while CMC values were not changed for copolymers with a higher grafting degree ($DG = 46$ % mol.), due to the more hydrophobic nature of the drug, as well as the DC value in the FUS conjugate, which was almost twice as high for G4 compared to G6 and G7.

The water contact angle (WCA) of the polymer layer surface was also determined using a goniometer. The WCA may change due to the structure of the polymer matrix and the nature of the introduced drug (Fig. 5). It was noticed that as the degree of grafting and F_{TMAMA} increased, the WCA values decreased, indicating the increasing hydrophilicity of the systems. Similarly, in the case of linear copolymers, wettability increased with the TMAMA fraction content. Moreover, the layers of linear copolymers showed greater hydrophilicity as compared to the graft copolymers, which can be caused by the predominance of hydrophobic units and much longer side chains in the graft copolymers. Ion exchange for pharmaceutical anions in graft copolymers resulted in a decrease in the WCA value, which means that in this case the conjugated drugs increased the solubilization of the systems. The inverse relationship after the introduction of drugs in ionic form into matrices based on linear copolymers resulted from the lack of phase separation effect, which occurs in graft copolymers due to the hydrophobic main chain. These observations confirmed that the topology, structural parameters, chain length and at the same time the chemical nature of the drug had a significant impact on the wettability of the copolymer layers.

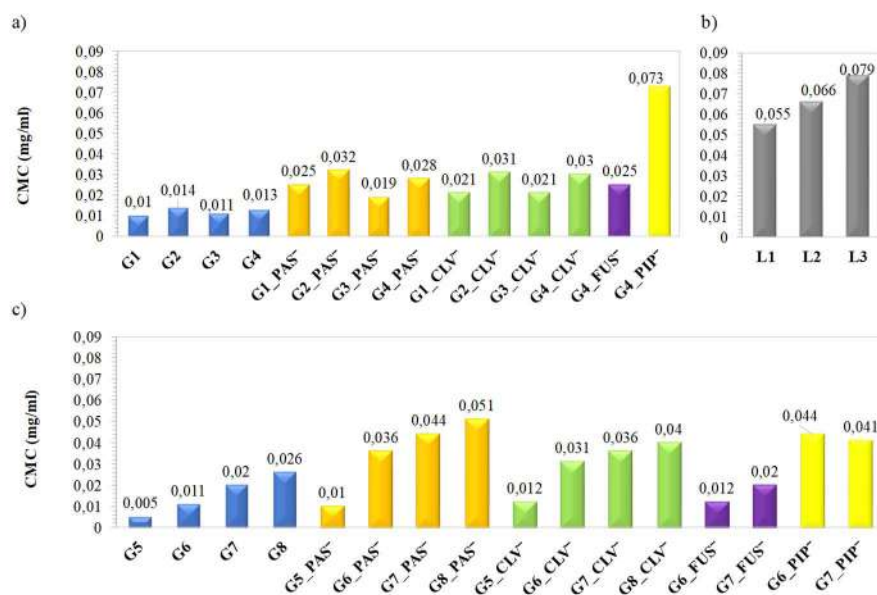


Figure 4. Critical micellization concentration (CMC) values of a) G1-G4 graft copolymers and their drug conjugates, b) L1-L3 linear copolymers, and c) G5-G8 graft copolymers and their drug conjugates.

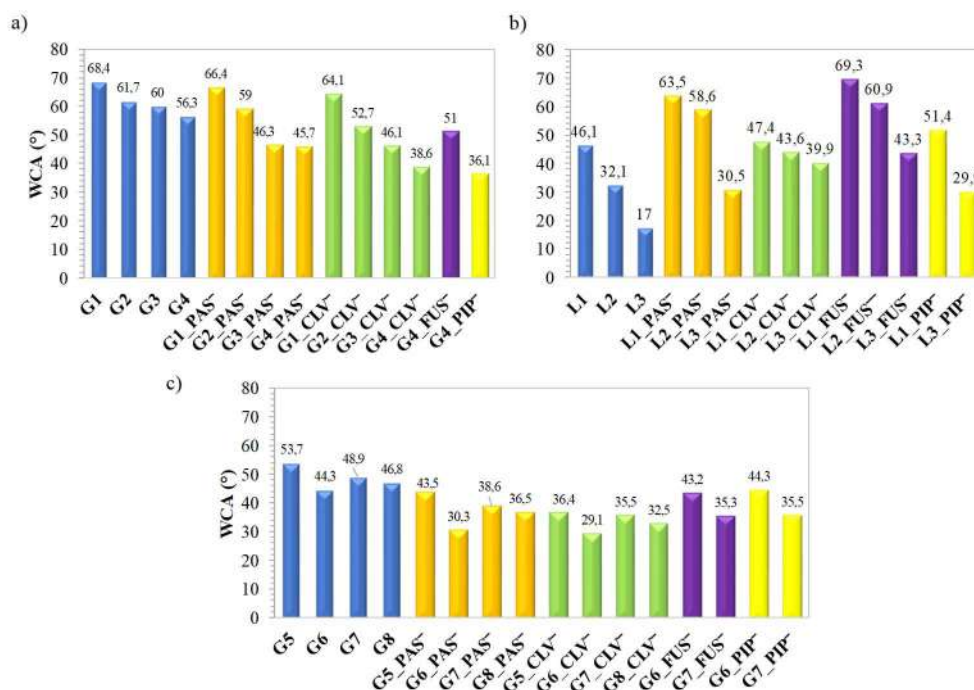


Figure 5. Water contact angles (WCA) for copolymers a) G1-G4 with a lower degree of grafting and their conjugates, b) L1-L3 and their conjugates and c) G5-G8 with a higher degree of grafting and their conjugates determined by the goniometric method.

Release of the conjugated drug in the form of a pharmaceutical anion (P.1.; P.2.; P.3.; P.5.)

The in vitro release process of ionically conjugated drugs was carried out in phosphate buffer saline (PBS, pH = 7.4, 37°C). The release was carried out for 72 hours, however, an effective process could be observed for up to 4 hours, followed by a slower release lasting up

to 24-48 hours. The drug release strongly depended on the structure of the polymer, including its topology and the number of ionic groups. In the case of graft copolymers, the degree of grafting also played a significant role. Moreover, a relationship was noticed between the type of conjugated pharmaceutical anion and the drug release rate.

Due to the greater steric hindrance of the FUS⁻ and PIP⁻ anions distributed in the side chains, the release of these drugs occurred at a significantly lower rate (Fig. 6). Among the tested systems, these drugs were released in the largest amounts for the G6 sample, which had densely spaced side chains, at the same time with the lowest content of the hydrophilic fraction. In turn, a lower grafting degree was more beneficial for the release of drugs creating less steric hindrance, i.e. PAS⁻ and CLV⁻, which resulted in faster drug diffusion, where after 4 hours most of the active substance was released.

The release process from linear copolymers as systems for comparing the efficiency of ionic drug delivery was the most favorable for PAS⁻ in terms of the percentage of drug released as well as the initial drug content. Similarly, FUS⁻ proved to be a convenient drug for release from linear polymers, however, a low DC value generated a low concentration of released drug. In turn, the release of CLV⁻ and PIP⁻ from these copolymers was much less efficient, suggesting stronger interactions of these pharmaceutical anions with the polymer matrix, creating relatively stable ion pairs.

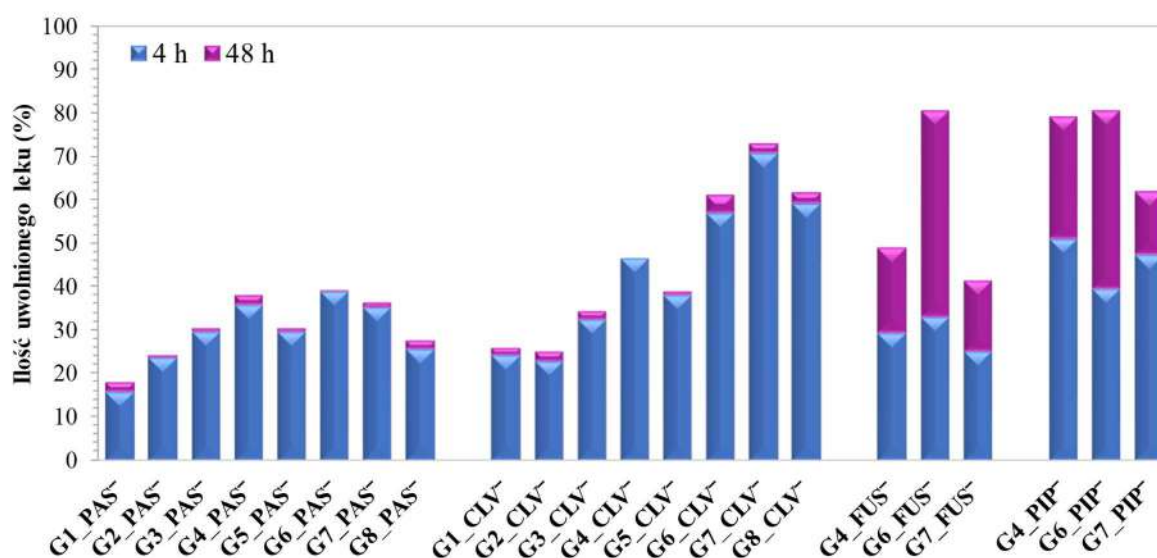


Figure 6. Amounts of released ionic drugs for graft systems.

Encapsulation of drugs - systems based on graft copolymers and their conjugates (P.3.; P.4.; P.5.)

Due to the demonstrated ability to self-organize in aqueous solutions of graft copolymers, they were used for non-ionic drug encapsulation that physically interacts with the polymer matrix. In the case of copolymers with a chloride counterion, drug loading led to obtaining single systems transporting one type of drug. A special approach was the encapsulation of drugs in self-assembled conjugates with a pharmaceutical counterion, which resulted in doubly active systems with a pair of interacting drugs, i.e. an ionic one connected by a chemical bond and a non-ionic one physically interacting with the polymer matrix.

For this purpose, three model drugs were selected, i.e. isoniazid (ISO), rifampicin (RIF) and tazobactam (TAZ). The efficiency of the encapsulation process during self-assembly of selected graft copolymers and their conjugates was assessed based on the Drug-Loading Content (DLC) (Fig. 7). A positive effect of the pharmaceutical anion presence on the encapsulation efficiency was noted. Moreover, a relationship between the grafting degree and the nature of the drug on the encapsulation efficiency was observed. The hydrophilic ISO drug was significantly better encapsulated by systems with a higher DG, i.e. G6 and G7, compared to G4. In turn, encapsulation of drugs that are sparingly soluble in water, i.e. RIF and TAZ, turned out to be more effective in G4 systems with a lower DG. The obtained results confirm that the type of non-ionic drug in correlation with the structural parameters of the polymer matrix affects the DLC values.

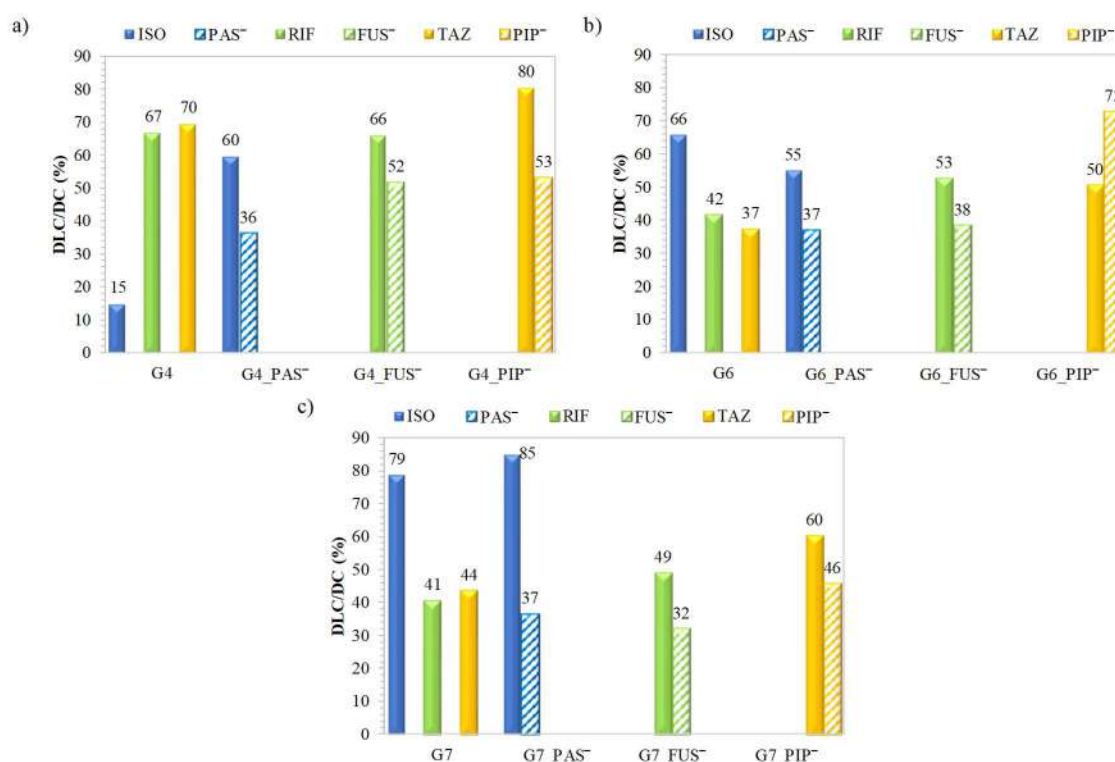


Figure 7. Contents of non-ionic drugs in single systems and contents of non-ionic drugs in dual systems vs. pharmaceutical anion content.

Studies on the size of nanoparticles of dual systems in aqueous solution showed that, as compared to single systems, they formed smaller structures (Fig. 8), i.e. 30-175 nm for PAS⁻/ISO systems and 31-184 nm for FUS⁻/RIF systems. A similar effect was obtained for the PIP⁻/TAZ systems, in which the particle sizes reached 24-192 nm. Although they showed a greater tendency to aggregate, as indicated by the presence of a significant fraction >500 nm (46%), while in the case of the remaining systems, the aggregates occurred only in small amounts (<10%). The presented commentary refers only to the prevailing fractions.

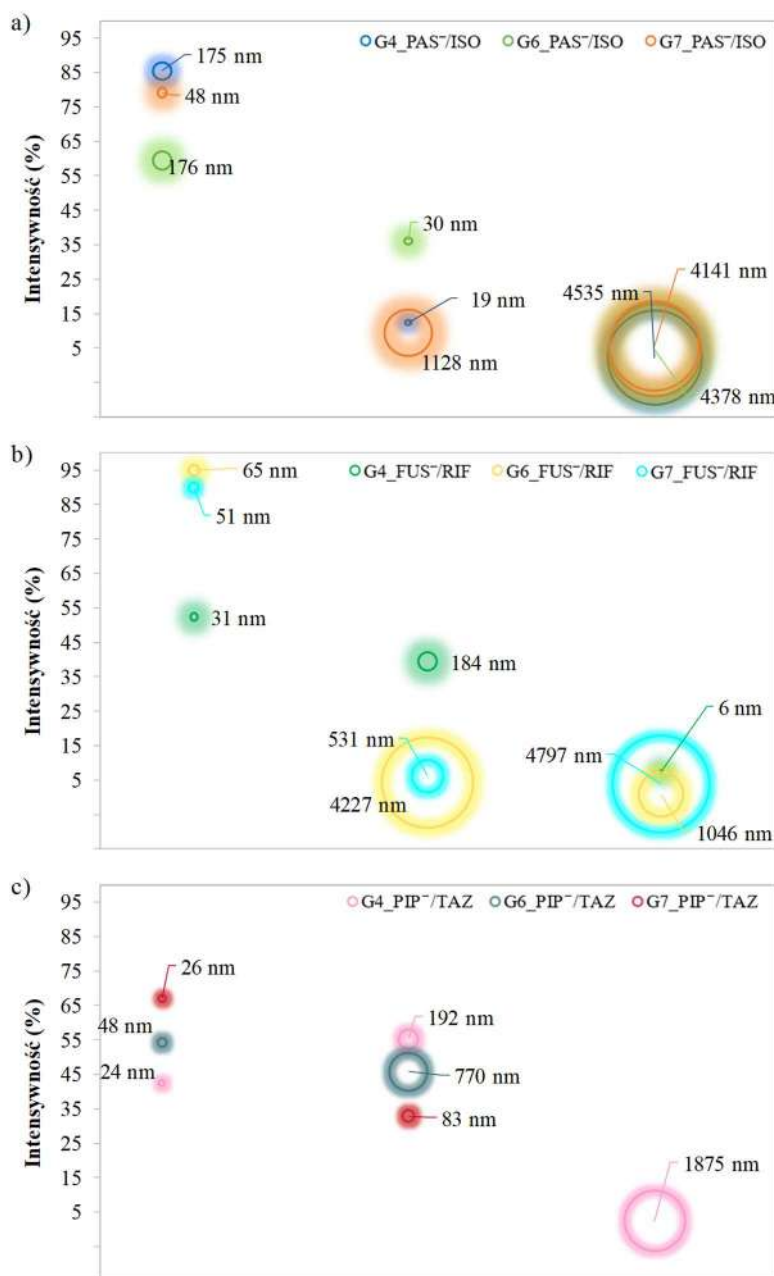


Figure 8. Hydrodynamic diameters (Dh) of polymer nanoparticles determined by DLS for dual systems.

Release of non-ionic drugs and co-release of a pair of drugs with a synergistic effect (P.3.; P.4.; P.5.)

The in vitro release process, in similarity to the conjugates with a pharmaceutical anion, was carried out in conditions imitating the environment of body fluids, i.e. PBS solution (pH = 7.4, 37°C). The obtained results showed that the presence of the encapsulated drug reduced the amount of the released ionic drug, as compared to single systems carrying pharmaceutical anions (Fig. 9a). The largest differences were noted in the case of PIP⁻ release, where after drug encapsulation during co-release, the pharmaceutical anion was released in a much smaller amount.

As in the case of ionic drugs, the release of non-ionic drugs depended strongly on both the polymer matrix and the nature of the drug (Fig. 9b). The most favourable matrix in terms of

the amount of released ISO was the G4 copolymer with the shortest side chains, lower degree of grafting and the highest ionic fraction content among the tested systems. In turn, drugs that were sparingly soluble in water, i.e. RIF and TAZ, were released in the highest rate from the G6-based system with the longest side chains, a higher degree of grafting, and the smallest TMAMA fraction.

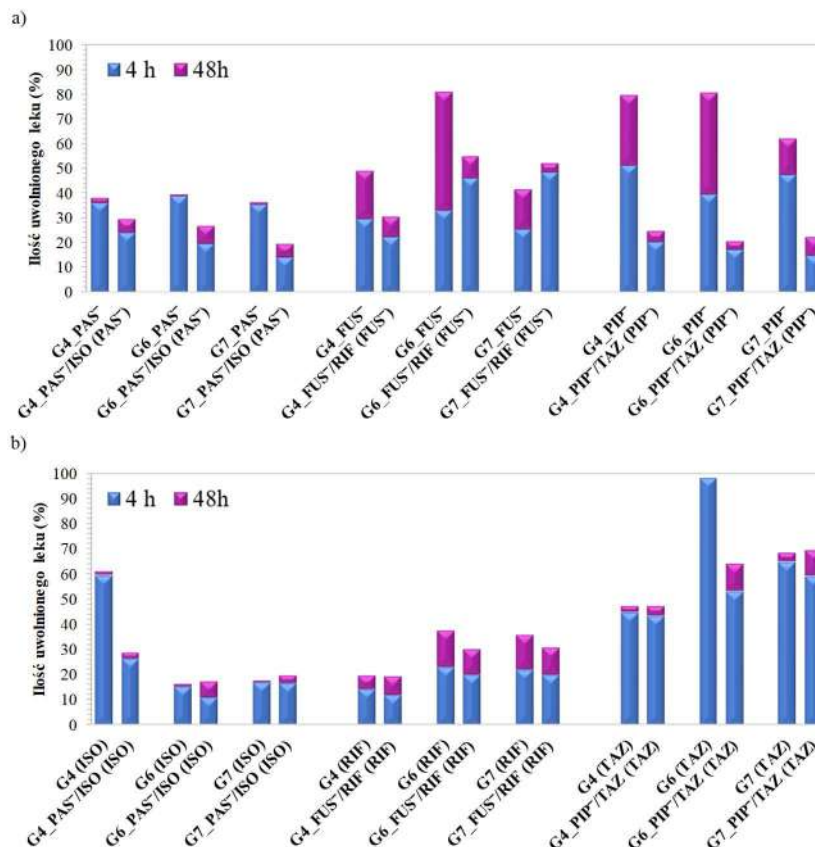


Figure 9. The amounts of released drugs in single vs. dual systems for a) ionic drugs b) non-ionic drugs after 4 and 48 h.

Biological assessment of drug delivery systems - cytotoxicity tests (P.6.; P.7.)

An evaluation of the cytotoxicity of drug delivery systems was carried out, based on colorimetric tests using 3-(4,5-dimethylthiazol-2-yl)-2,5-diphenyltetrazolium bromide (MTT) and flow cytometric analysis, including an apoptosis test and cell cycle analyses. Since the obtained carriers were tested for the transport of drugs used in the treatment of the lower respiratory tract, including tuberculosis, the model of human bronchial epithelial cells (BEAS-2B) and cancer lines, i.e. human basal alveolar epithelial cell adenoma (A549) and non-small cell lung cancer (H1299), were used to test cytotoxicity. Additionally, gene expression measurements for interleukins IL6 and IL8 were performed for linear copolymer systems.

In vitro cytotoxicity tests performed with the obtained polymer carriers confirmed the lack of cytotoxic effect on the normal BEAS-2B cell line, while conjugates with PAS⁻, CLV⁻, FUS⁻ and PIP⁻ showed a negligible effect on cell viability. In turn, the tested systems caused the proliferation of A549 and H1299 cancer cells. The demonstrated selectivity of action of most of the tested systems resulted in no significant changes for normal cell lines and a negative effect on cancer cells.

Summary and conclusions

The use of graft copolymer systems allowed for a slower and more controlled release process due to the greater stability of their micellar structure, compared to systems based on tangled chains of linear copolymers.

An appropriately large amount of drug introduced into the chains and its release in a satisfactory percentage ultimately ensured a relatively high concentration of drug released from the graft copolymers, which may guarantee the effectiveness of the therapy.

The efficiency of drug conjugation and encapsulation, as well as the (ionic and non-ionic) drug release rate can be regulated by the structure of the polymer carrier, where the density of the side chains in the polymer plays a special role, but at the same time the structure and nature of the drugs and their interaction in the matrix are important.

In vitro cytotoxicity studies of the obtained polymer carriers showed a negligible effect on normal BEAS-2B cell lines and cancer A549 cell proliferation. Considering that an immunologically weakened body during disease is susceptible to the cancer, the effect of selective action of drug delivery systems is extremely desirable. This indicated a high application potential as new alternative systems in the treatment of respiratory diseases due to the possibility of their wide use against pathogens or cancer cells.

The presence of choline units in the polymer matrix and the introduced antibacterial drugs make these systems have potential applications in the treatment of respiratory diseases, including combination therapy transporting a pair of synergistic drugs.

In the context of anti-tuberculosis treatment, their rapid action, completing a full cycle of effectiveness within four hours ensure an effective course of treatment. However, their use requires further tests, including detailed *in vivo* biological studies, which will fully confirm the possibility of using the obtained polymer drug delivery systems in the human body.

To sum up, in this research, graft copolymers with pharmaceutical counterions were designed, which seem to be promising drug carriers from the physicochemical point of view and in terms of cytotoxicity.

PUBLIKACJA P.1

Synthesis and Characterization of Ionic Graft Copolymers: Introduction and In Vitro Release of Antibacterial Drug by Anion Exchange

Niesyto, K., Neugebauer, D.

Polymers 2020, 12, 2159

Article

Synthesis and Characterization of Ionic Graft Copolymers: Introduction and In Vitro Release of Antibacterial Drug by Anion Exchange

Katarzyna Niesyto and Dorota Neugebauer * 

Department of Physical Chemistry and Technology of Polymers, Faculty of Chemistry, Silesian University of Technology, 44-100 Gliwice, Poland; katarzyna.niesyto@polsl.pl

* Correspondence: Dorota.Neugebauer@polsl.pl

Received: 1 September 2020; Accepted: 20 September 2020; Published: 22 September 2020



Abstract: Amphiphilic graft copolymers based on [2-(methacryloyloxy)ethyl]trimethylammonium chloride (TMAMA) were obtained for the delivery of pharmaceutical ionic drugs, such as *p*-aminosalicylate (PAS) and clavunate (CLV) anions. The side chains were attached by *grafting from* a multifunctional macroinitiator via atom transfer radical polymerization (ATRP) to get polymers with different grafting degrees and ionic content. The self-assembling ability, confirmed by determining the critical micelle concentration (CMC) through interfacial tension (IFT) with the use of goniometry, was reduced after ion exchange (CMC twice higher than for chloride anions contained copolymers 0.005–0.026 mg/mL). Similarly, the hydrophilicity level (adjusted by the content of ionic fraction) evaluated by the water contact angle (WCA) of the polymer film surfaces was decreased with the increase of trimethylammonium units (68°–44°) and after introduction of pharmaceutical anions. The exchange of Cl[−] onto PAS[−] and CLV[−] in the polymer matrix was yielded at 31%–64% and 79%–100%, respectively. The exchange onto phosphate anions to release the drug was carried out (PAS: 20%–42%, 3.1–8.8 μg/mL; CLV: 25%–73%, 11–31 μg/mL from 1 mg of drug conjugates). Because of the bacteriostatic activity of PAS and the support of the action of the antibiotics by CLV, the designed water-soluble systems could be alternatives for the treatment of bacterial infections, including pneumonia and tuberculosis.

Keywords: pharmaceutical anion; ion exchange; graft copolymers; choline; drug delivery

1. Introduction

Traditional medicine does not use the full potential of therapeutics when the drug dose at destination is reduced by premature decay, or its concentration is too high and damaging for cells. Hence, the pharmaceutical industry is looking for better solutions in the production of medicines. The drug delivery systems (DDS) based on polymer carriers seem to solve the drug distribution problem with conventional medicines [1–5]. These systems are commonly used to improve bioavailability and increase therapeutic efficacy [1,6–8]. Besides, the carrier enables the controlled release of the drug [8–12] by maintaining its constant concentration and avoiding exceeding the toxicity threshold. The polymeric carrier has to be biocompatible and nontoxic to the healthy cells [9,13–16]. Among the nonlinear polymer graft topology, where the side chains are attached to a main chain [17–21], it is convenient to adjust the physico- and biochemical properties by grafting degree, the length of backbone and grafts. The well-defined graft copolymers can be obtained by the *grafting from* reaction with the use of multifunctional macroinitiators [22,23] and direct formation of polymeric ionic liquids (PILs) as the side chains [24,25].

PILs consist of repeating groups containing ionic pairs in the polymer chain [26–28]. They have the unique properties of ionic liquids and exhibit increased mechanical strength and durability [27,29–31]. Ionic liquids (ILs) are mostly defined as green solvents, but nowadays the studies have indicated that some of them can be toxic [32,33]. One of the lowest toxicities has been reported for cholinium-based ionic liquids, which have been applied to prepare biocompatible gels [34]. The choline is a water soluble organic chemical compound that has a quaternary ammonium group, usually it is in the form of a chloride [35,36]. This molecule supports biological functions [34,37,38] as a precursor of acetylcholine [39]. The presence of an ionic group in the cholinium unit gives the opportunity for the ion exchange reaction, which in the case of polymerized ionic liquids can be advantageous for incorporation of pharmaceutical ions, i.e., sulfacetamid, salicylate [40–42]. There are also reports of other types of PILs, based on imidazolium and pyridinium transporting naproxen anions [43] or guanidinium with ampicillin anions [44].

In this work we report on new PIL systems based on the grafted polymers, which are capable of the delivery of ionic drugs introduced by anion exchange in suitable media imitating body fluids in the human body. The main part of the study was focused on designing graft copolymers, in which the polymerizable ionic liquid [2-(methacryloyloxy)ethyl]trimethylammonium chloride in various ratios with methyl methacrylate were contained in the side chains P(MMA-*co*-TMAMA). The *grafting from* strategy required the preparation of multifunctional macroinitiators, that is copolymers of methyl methacrylate and 2-(2-bromoisobutyryloxy)ethyl methacrylate P(MMA-*co*-BIEM) with two different contents of bromoester initiating groups to get in the next step the copolymers with various grafting degrees. The ion exchange reaction was carried out with sodium *p*-aminosalicylate (NaPAS) or potassium clavunate (KCLV), which are a pharmaceuticals used as the second-line antituberculosis drug or in combination with a broad-spectrum activity antibiotic, in the treatment of infections of the respiratory tract. The studies on drug release via anion exchange supported by phosphate anions contained in buffer solution were performed to evaluate the physicochemical effectiveness of systems in the delivery of pharmaceutical anions with antibacterial activity.

2. Materials and Methods

Methyl methacrylate (MMA) and 2-(hydroxyethyl) methacrylate (HEMA) (both Alfa Aesar, Warsaw, Poland), were dried, whereas [2-(methacryloyloxy)ethyl]trimethylammonium chloride (TMAMA, 80% aq. solution, Sigma-Aldrich, Poznan, Poland) was concentrated to a constant weight by water evaporation. Anisole (99%, Alfa Aesar, Warsaw, Poland) was desiccated using 4 Å molecular sieves (Chempure, Piekary Śląskie, Poland). Copper(I) bromide and chloride (CuBr and CuCl; both Fluka, 98%, Steinheim, Germany) were purified by stirring in glacial acetic acid, followed by filtration and washing with ethanol and diethyl ether, then dried under vacuum; 2,2'-Bipyridine (bpy), 4,4'-dinonyl-2,2'-dipyridyl (dNbpy, 97%), tetrahydrofuran (THF), pyridine (99%), α -bromoisobutyrate bromide (BIBB, 98%), ethyl 2-bromoisobutyrate (EBiB), potassium clavunate (KCLV), and sodium *p*-aminosalicylate (NaPAS) were used as received (all Sigma Aldrich, Poznan, Poland).

2.1. Synthesis of Multifunctional Macroinitiators

The synthesis procedure includes ATRP to obtain copolymers of 2-hydroxyethyl methacrylate and methyl methacrylate, and then esterification of the hydroxyl groups to introduce the bromoester initiating group. Details are presented in the Supplementary Materials (Table S1, Figures S1–S2).

2.2. Synthesis of Graft Copolymers Bearing Cl⁻ (Example for G2)

Comonomers TMAMA (1.80 g, 8.66 mmol) and MMA (2.74 mL, 25.90 mmol), methanol (2 mL), THF (1 mL), bpy (54.14 mg, 0.35 mmol) and macroinitiator Ia (196.50 mg, including 0.35 mmol of initiating sites) were placed into a Schlenk flask and degassed by two freeze-pump-thaw cycles. The initial sample was taken and the CuCl catalyst (25.83 mg, 0.17 mmol) was introduced to the mixture. The reaction was carried out for 1 h, then the first part of the mixture (3 mL) was taken

out and then stopped by exposing to air. The reaction with the rest of the mixture was continued for another 1 h, and then stopped. The polymer was twice precipitated in chloroform-diethyl ether mixture, and then dried.

2.3. Ionic Exchange for the Introduction of Pharmaceutical Anions (Example for G2)

The copolymer G2 (20 mg, including 0.03 mmol of TMAMA units) was dissolved in methanol (1 mL). Then the pharmaceutical salt, NaPAS (7.90 mg, 0.03 mmol) or KCLV (5.56 mg, 0.03 mmol) was added to keep the reaction for 48 h. The products containing PAS (26.2 mg) or CLV (19.66 mg) were obtained after drying under reduced pressure. Yields: 92% and 98%, respectively.

2.4. Drug Release of Pharmaceutical Anions

The grafted copolymers with exchanged pharmaceutical anions (1.0 mg) were dissolved in 1 mL of phosphate buffered saline (PBS) solution (pH = 7.4). Then, a dialysis membrane bag (MWCO = 3.5 kDa) filled out by the solution (1 mL) was introduced into a glass vial with 45 mL of PBS and stirred at 37 °C. During the drug release, buffer samples (2.5 mL) were taken at appropriate intervals and analyzed on a UV–Vis spectrophotometer, measuring absorbance at $\lambda = 265$ (PAS⁻) or 257 nm (CLV⁻). The amount of drug in the release medium (d) was calculated with the use of following formulas:

$$x = \frac{y - b}{a} \quad (1)$$

$$d = \frac{x}{c} * 100\% \quad (2)$$

where: a is the value of the slope of the calibration curve, b is the intercept of the calibration curve, x is a value of the concentration on the basis of the calibration curve equation, y is a value of absorbance at the determined wavelength for PAS⁻ ($\lambda = 265$ nm) and CLV⁻ ($\lambda = 257$ nm).

2.5. Characterization

¹H-NMR spectra were registered by a UNITY/NOVA (Varian, Mulgrave, Victoria, Australia) spectrometer operating at 300 MHz. The measurements were performed for the samples in deuterated dimethyl sulfoxide (DMSO) with tetramethylsilane (TMS) as an internal standard. The monomer conversion was determined by gas chromatograph 6850 Network GC System (Agilent Technologies, Santa Clara, CA, USA) using acetone as the solvent. Molecular weight (M_n) and dispersity index (\mathcal{D}) were evaluated by size exclusion chromatography (SEC). The measurements for samples of macroinitiators and their precursors were provided in THF line (1100 Agilent 1260 Infinity with differential refractometer MDS RI detector, Agilent Technologies, Santa Clara, CA, USA) at 40 °C with the flow rate of 0.8 mL/min using precolumn guard (5 mm × 7.5 mm) and column PLGel 5 μ m MIXED-C 300 (7.5 mm × 300 mm). The calculations were based on polystyrene standards (580–300,000 g/mol). In the case of graft copolymers the SEC measurements were performed in DMF with addition of 10 mM LiBr (Chromatograph Ultimate 3000 with differential refractometer RefractoMax 521 detector, Thermo Fisher Scientific, Waltham, MA, USA) at 50 °C with a flow of rate 0.25 mL/min using precolumn TSKgel Guard SuperMPHZ-H 6 μ m (4.6 mm × 2 cm) and two columns TSKgel SuperMultiporeHZ-H 6 μ m (4.6 mm × 15 cm). These calculations were based on poly(ethylene oxide) (PEO) standards (982–969,000 g/mol). Fourier-transform infrared spectroscopy (FT-IR) was conducted with Spectrum Two 1000 FT-IR Infrared Spectrometer with attenuated total reflection (ATR) (Perkin Elmer, Waltham, MA, USA). The critical micelle concentration (CMC) was determined by the measuring interfacial tension (IFT) with the pendant drop method using goniometer (OCA 15EC, DataPhysics, Filderstadt, Germany). The polymer concentration in aqueous solution was ranged in 5×10^{-4} –0.3 mg/mL. SCA20_U software was used for data collecting and processing. This module software also enabled the measurement of water contact angles (WCA) of water dropped on polymer film. The solution of polymer dissolved in methanol (0.3 mg/mL) was applied to properly prepared and degreased glass

plates by spin coating. The sessile drop method was used to drop 4 μL of water. The hydrodynamic diameters (D_h) of particles and polydispersity index (PDI) were measured by dynamic light scattering (DLS) using a Zetasizer Nano-S90 (Malvern Technologies, Malvern, UK). Samples placed in poly(methyl methacrylate) (PMMA) cells after dilution with a solvent (1.0 mg/mL) were put in the thermostatted cell compartment of the instrument at 25 $^\circ\text{C}$. Each measurement was repeated three times, to create an average value. During drug release, samples taken in appropriate times intervals were analyzed by ultraviolet–visible light spectroscopy in PMMA cells (UV–Vis, spectrometer Evolution 300, Thermo Fisher Scientific, Waltham, MA, USA) to determine the drug content (DC) and the amount of released pharmaceutical anions (PAS^- or CLV^-).

3. Results

3.1. Synthesis and Characterization of Grafted Copolymers with PIL Side Chains

The grafted copolymers P(MMA-*co*-(BIEM-*graft*-(TMAMA-*co*-MMA))) varying with content of TMAMA units (25% and 50%) and grafting degree (DG = 26% and 46%) were obtained by ATRP catalyzed with CuCl/bpy complex in THF/MeOH at 40 $^\circ\text{C}$ (Figure 1). The parameter of grafting degree was adjusted by using a multifunctional macroinitiator (MI) Ia or IIa (Table 1) with different contents of initiating units (DP_{BIEM}) in the copolymerization of TMAMA and MMA. The ^1H NMR spectrum of graft copolymer in comparison to that of its macroinitiator (Figure 2) shows a new signal **10** between 3.4 and 3.0 ppm assigned to 9H in trimethylammonium groups. The formation of side chains was also confirmed by the appearance of two signals **8** and **9** coming from the $-\text{CH}_2-\text{O}-$ (3.86–3.66 ppm) and $-\text{CH}_2-\text{N}^+$ (4.63–4.44 ppm) groups in TMAMA units, respectively. Additionally, the signals of methylene and methyl protons (**1** at 1.9 ppm and **2** ranged in 0.6–1.2 ppm) became more intensive because they are also contained in the polymethacrylate side chains. The conversions of TMAMA presented in Table 2 were calculated from the ^1H NMR analysis for the reaction mixture by estimating integration of signals from unreacted comonomers TMAMA (6.19–6.07 ppm) in relation to the constant intensity of pyrene signal (8.26–8.18 ppm) used as the internal standard (Figure S3).

Table 1. Data for precursors (I and II), and multifunctional macroinitiators (MI) (Ia and IIa) synthesized by atom transfer radical polymerization (ATRP) and esterification reaction.

No.	HEMA/MMA	$\text{DP}_{\text{HEMA}}^a$ (DP_{BIEM})	DP_n^a	$M_n^a \times 10^{-3}$ (g/mol)	$M_n^b \times 10^{-3}$ (g/mol)	\bar{D}^b
I	25/75	48	186	20.3	23.4	1.47
Ia		(48)		27.4	22.6	1.37
II	50/50	133	292	33.4	26.5	1.71
IIa		(133)		53.2	33.4	1.63

MMA: Methyl methacrylate, HEMA: 2-(hydroxyethyl) methacrylate; Conditions: I: $[\text{HEMA}]_0:[\text{MMA}]_0:[\text{EBiB}]_0:[\text{CuBr}]_0:[\text{dNbpy}]_0 = 150:450:1:1:2$, 3 h, II: $300:300:1:1:2$, 1 h, anisole 10 vol.% of monomers, 70 $^\circ\text{C}$; bromoesterification of copolymers I, II resulting in Ia and IIa (yield: 100%): pyridine, rt, stirred overnight; ^a calculated with the use of monomer conversion by ^1H NMR, the conversion values in Table S1, DP_n is polymerization degree of chain, wherein HEMA before and BIEM after esterification; ^b determined by SEC (THF, polystyrene calibration).

Table 2. Characteristics of graft copolymers.

No.	MI	Time (h)	n_{sc}^a	DG (mol.%)	X_{TMAMA} (%)	DP_{sc}^a	F_{TMAMA}^a (mol.%)	$M_n^a \times 10^{-3}$ (g/mol)	$M_n^b \times 10^{-3}$ (g/mol)	\bar{D}^b
G1		0.5			9	16	13	114.7	12.5	1.68
G2	Ia	1	48	26	22	24	21	168.6	17.5	1.9
G3		1			26	31	42	243.6	54.7	1.31
G4		2			30	35	43	273.1	36.3	1.15

Table 2. Cont.

No.	MI	Time (h)	n_{sc}^a	DG (mol.%)	X_{TMAMA}^a (%)	DP_{sc}^a	F_{TMAMA}^a (mol.%)	$M_n^a \times 10^{-3}$ (g/mol)	$M_n^b \times 10^{-3}$ (g/mol)	\bar{D}^b
G5		1			30	29	28	553.9	194.0	1.24
G6	IIa	2	133	46	48	65	18	1090.5	391.1	1.11
G7		1			22	28	39	583.5	-	-
G8		2			44	48	46	1007.2	-	-

Conditions: G1, G2, G5, G6: $[TMAMA]_0:[MMA]_0:[MI]_0:[CuCl]_0:[bpy]_0 = 25:75:1:1:2$, G3, G4, G7, G8: $[TMAMA]_0:[MMA]_0:[MI]_0:[CuCl]_0:[bpy]_0 = 50:50:1:1:2$, methanol:THF = 2:1 *v/v*, where methanol:TMAMA = 1:1 *v/wt*, 40 °C; ^a determined with ¹H NMR, where X_{TMAMA} is TMAMA monomer conversion, DP_{sc} is polymerization degree of side chains, F_{TMAMA} is content of TMAMA in side chains, n_{sc} is number of side chains, DG is degree of grafting related to n_{sc} per total DP_n of backbone, ^b determined with SEC (DMF, PEO calibration).

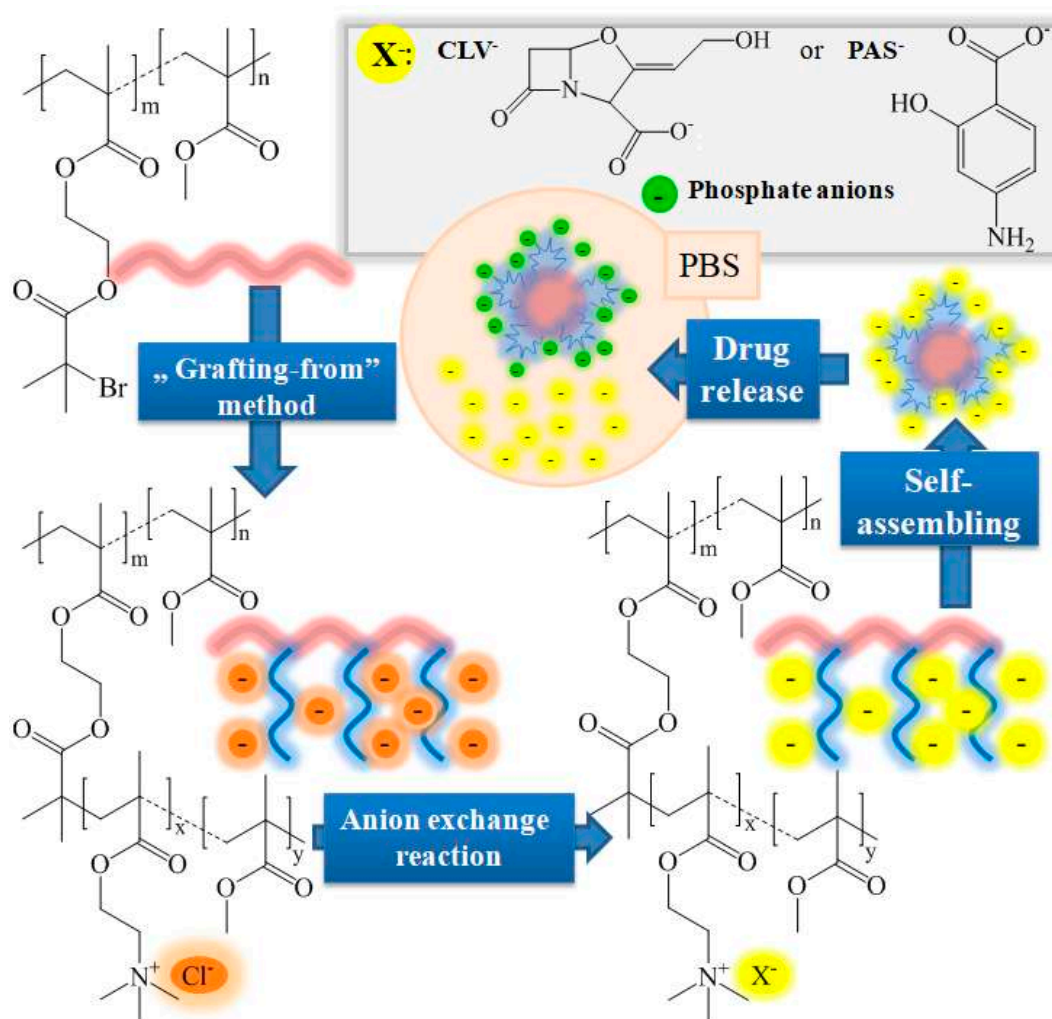


Figure 1. Schematic route for systems based on grafted copolymers with ionic side chains carrying pharmaceutical anions.

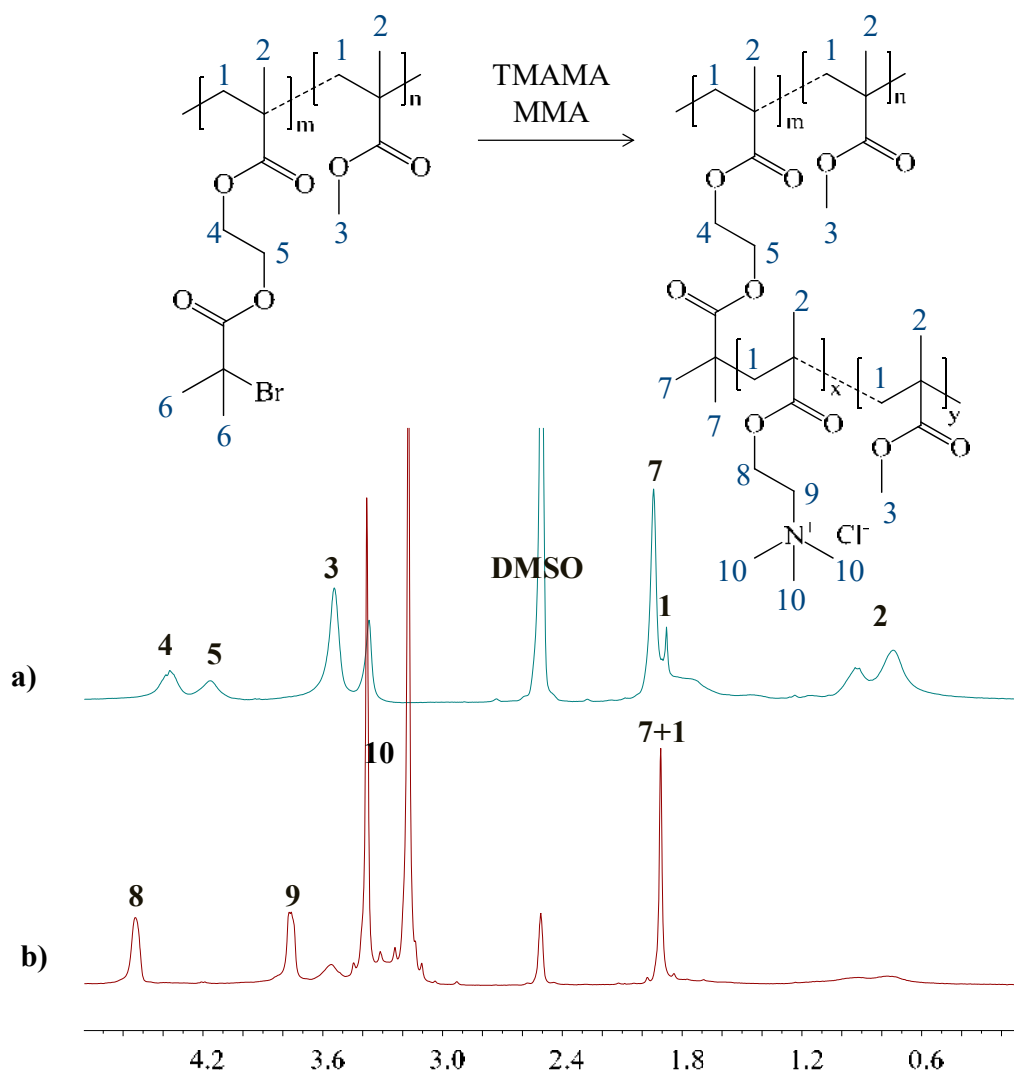


Figure 2. ¹H NMR spectra of (a) macroinitiator Ia, and (b) grafted copolymer G2.

3.2. Ionic Exchange with NaPAS and KCLV

The exchange reaction of chloride anions in TMAMA units distributed statistically along the side chains was applied to introduce pharmaceuticals in the anionic form. This reaction was based on mixing of the appropriate grafted copolymer and the selected bioactive compounds, that is *p*-aminosalicylate sodium salt (NaPAS) or clavunate potassium salt (KCLV), per 48 h at room temperature (Figure 1). PAS as a second-line antituberculosis drug, which belongs to the group of bacteriostatic drugs, is applied as an adjunct to therapy with other antituberculosis drugs, e.g., streptomycin. CLV is β -lactam drug with a penicillin-like structure, which itself does not have clinically significant antibacterial activity, but in combination with an β -lactam antibiotics, e.g., amoxicillin, it inactivates bacterial β -lactamases and thus prevents the breakdown of the antibiotic. The exchange reaction with pharmaceutical salts enables the formation of carrier-drug ionic conjugates as alternative drug delivery systems mostly for the treatment of respiratory tract infections, such as chronic bronchitis, bacterial sinusitis, acute otitis media, community acquired pneumonia and tuberculosis.

The amount of introduced drug in a polymer matrix was verified by drug content (DC, Table 3), which was determined with the use of UV–Vis spectra for systems containing PAS[−] or CLV[−]. Dependently on the chemical nature of the pharmaceutical substance, the DC in the polymer matrix with the same hydrophilic-hydrophobic balance differed, indicating 31%–64% for PAS and twice as high for CLV (66%–100%), which could also be related to lower steric hindrance of the latter.

Table 3. Characteristics of polymer bearing *p*-aminosalicylate (PAS)/clavunate (CLV) and evaluation of release effect determined by UV–Vis.

No.	Hydrophilic Fraction ^a (mol.%)	Drug Content (DC) (%)		Released Drug after 48 h (%)		Concentration of Released Drug (µg/mL)	
		PAS ⁻	CLV ⁻	PAS ⁻	CLV ⁻	PAS ⁻	CLV ⁻
G1	10	31.2	92.0	18.2	26.1	3.1	13.3
G2	18	63.9	78.6	24.5	25.4	8.8	11.1
G3	37	49.9	98.1	30.6	34.5	8.5	18.8
G4	39	36.2	100	42.4	46.8	7.7	26.7
G5	26	40.2	85.7	30.7	39.1	6.2	18.7
G6	18	37.0	66.3	40.0	61.2	7.4	22.5
G7	36	36.5	88.7	36.5	73.0	6.7	31.1
G8	44	39.7	68.5	28.3	61.8	5.6	30.4

^a calculated with the use of ¹H NMR spectra (Figures S4 and S5).

3.3. Amphiphilic Properties and Wettability

Because of the amphiphilic character of the obtained graft copolymers with the ionic nature of the side chains (hydrophilic content 10–44 mol.%) the self-assembling superstructures could be formed in aqueous solution. This ability was determined by the CMC value for each polymer system by interfacial tension (IFT), which was convenient for evaluating amphiphilic properties by separating into the interface due to lower surface tension at critical concentration. The goniometry method was used to measure the IFT of aqueous solutions with various concentrations of the grafted copolymers and both types of drug conjugates ($c = 5 \times 10^{-4}$ –0.3 mg/mL). The IFT of measured samples vs. $\log C$ was plotted, where the cross-over point was determined as the CMC value (Figure 3). The CMC data summarized in Table 4 shows that the arrangement of TMAMA units in the polymer have the crucial impact of creating micellar structures. It was noticed that the increase in the chain length resulted in an increase in the CMC value (G1 vs. G2, G3 vs. G4, G5 vs. G6, G7 vs. G8). The highest CMC was observed for samples G7 and G8 (0.020–0.026 mg/mL), which are characterized with both a dense distribution of the side chains and ionic groups among the side chains. Similar to the basic graft polymers with chloride anions, their modified analogs bearing PAS or CLV anions were also self-assembled in aqueous solution (Table 4). In each case the ion exchange with pharmaceutical anions led to a double increase in the CMC value (i.e., G1: 0.01 mg/mL vs G1_PAS: 0.025 mg/mL and G1_CLV: 0.021 mg/mL) maintaining the same correlations as the above-described. This means that the micelles are formed at higher concentrations than in the case of graft polymers with chloride anions as the effect of the hydrophilic nature of the pharmaceutical anions ($Cl^- < PAS^-, CLV^-$) which shift the hydrophilic–hydrophobic balance improving solubility of the systems in aqueous solution.

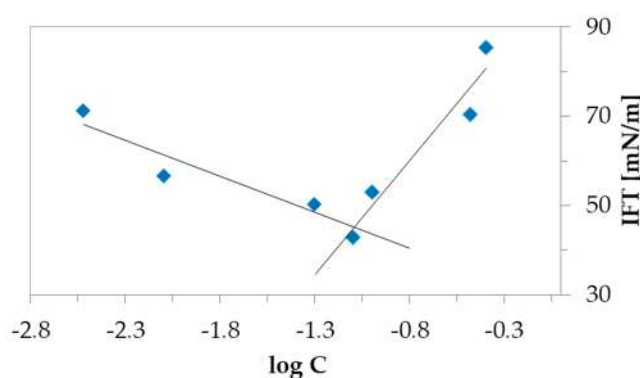


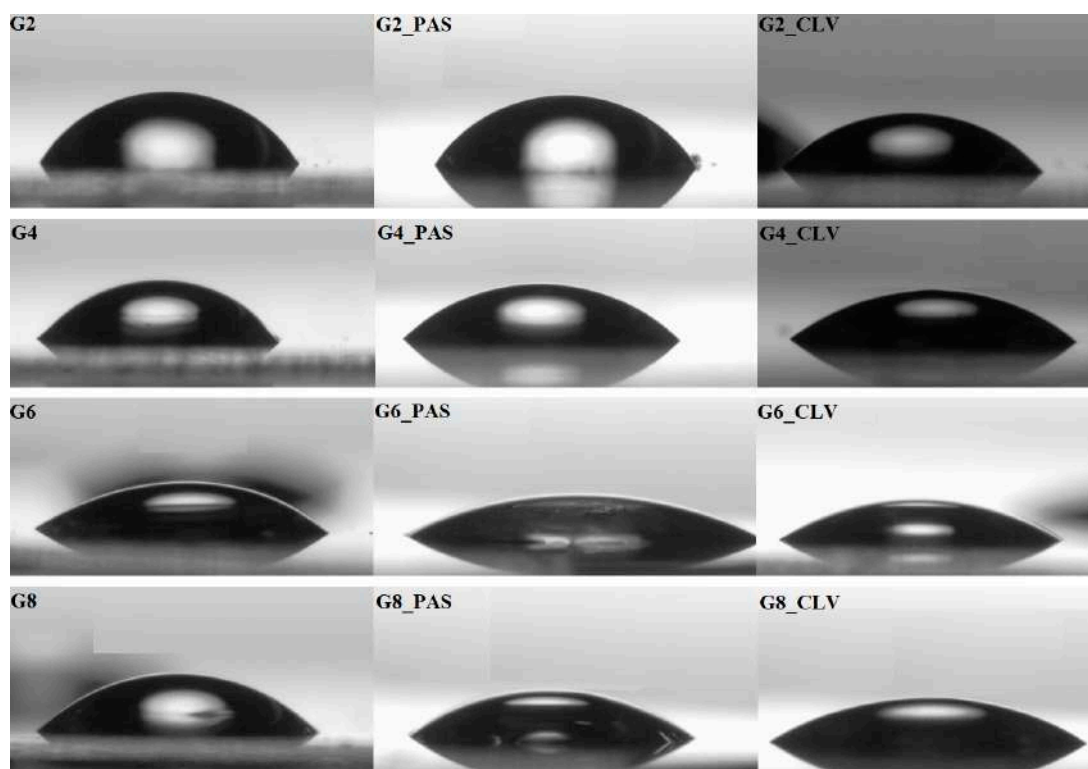
Figure 3. Variation of the surface tension with the logarithm of the concentration of grafted copolymer G2 in aqueous solution at 25 °C.

Table 4. Characteristics of graft copolymers in aqueous solution and surface wettability by goniometer method.

No.	CMC ^a (mg/mL)			WCA ^b (°)		
	Cl ⁻	PAS ⁻	CLV ⁻	Cl ⁻	PAS ⁻	CLV ⁻
G1	0.010	0.025	0.021	68.4	66.4	64.1
G2	0.014	0.032	0.031	61.7	59.0	52.7
G3	0.011	0.019	0.021	60.0	46.3	46.1
G4	0.013	0.028	0.030	56.3	45.7	38.6
G5	0.005	0.010	0.012	53.7	43.5	36.4
G6	0.011	0.036	0.031	44.3	30.3	29.1
G7	0.020	0.044	0.036	48.9	38.6	35.5
G8	0.026	0.051	0.040	46.8	36.5	32.5

CMC: critical micelle concentration, WCA: water contact angle; ^a measured by IFT at a concentration 1 mg/mL, ^b measured by sessile drop method on the polymer film (polymer solution 0.3 mg/mL spin-coated on glass plate).

The use of goniometer was also advantageous for the WCA measurements by sessile water drop method to quantify the wettability of the surface of polymer films made by spin coating. The WCA values presented in Table 4 demonstrate dependence on the grafting density, which supported higher values for low DG (G1–G4) than that for higher grafting density systems (G5–G8). The hydrophobicity of polymers was reduced by the increased chain length and the amount of TMAMA units (Cl: 68°–44°). After exchange with pharmaceutical ions the WCA values were reduced for films of ionic drug polymer conjugates showing the improved hydrophilicity of these systems. The changeable wettability is clearly seen in the attached photos of a water drop on the sample surfaces (Figure 4). Furthermore, a similar relationship between hydrophilicity degree and TMAMA content was also observed for conjugate systems (PAS: 66°–30°; CLV: 64°–29°).

**Figure 4.** Representative screen shots of the goniometry measured samples.

Both the chloride containing polymers and those with pharmaceutical anions were analyzed by DLS to determine the hydrodynamic diameters (D_h) of their particles in water solutions Figures 5 and S6).

The graft copolymers with chloride counterions mostly formed one fraction of the superstructures reaching sizes in the range of 72–203 nm (G3, G5–G8), whereas three or two fractions were distinguished in G1, G2 and G4, where the main fraction accounted for ~60% (18–124 nm).

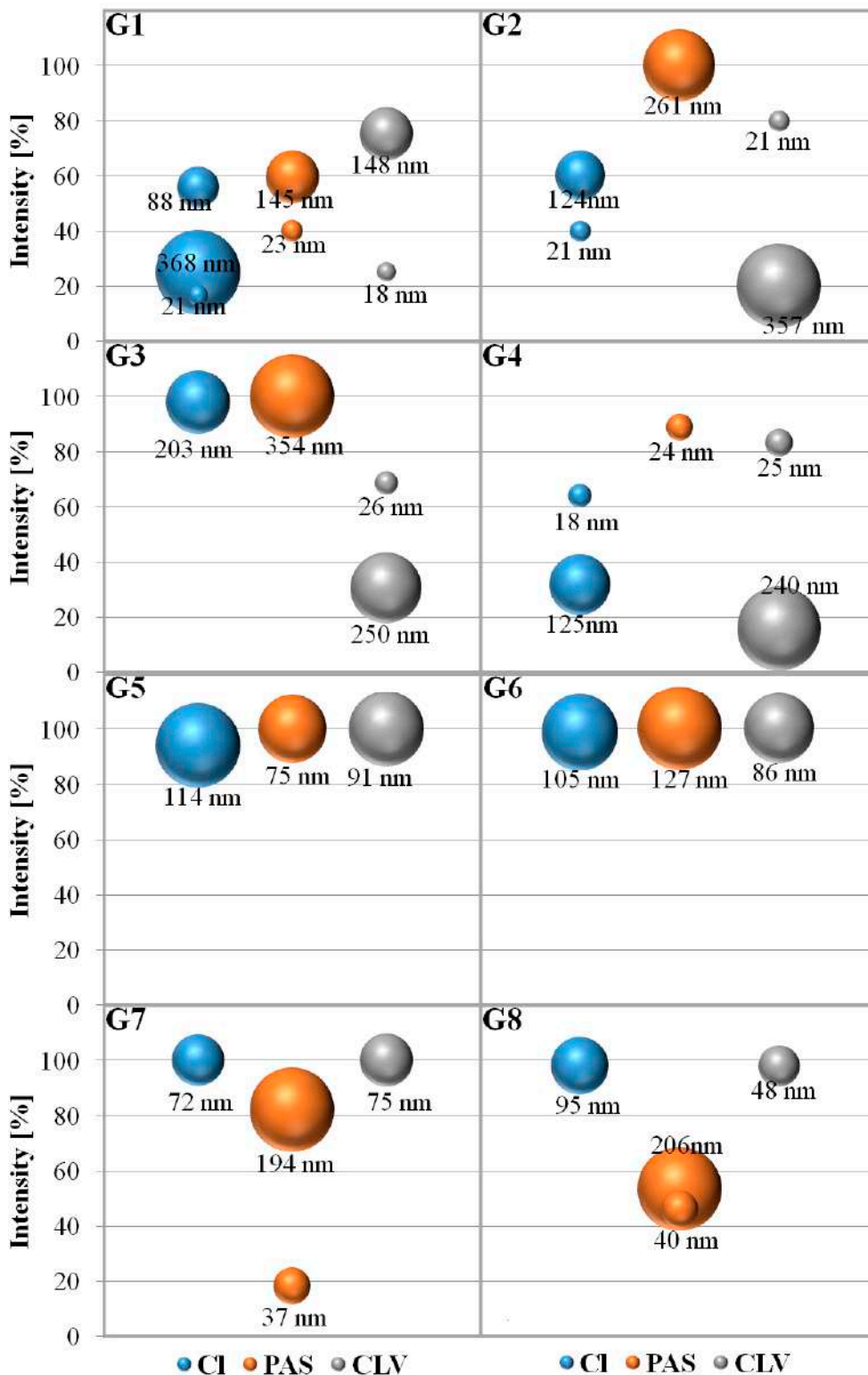


Figure 5. Hydrodynamic diameters (D_h) of polymer nanoparticles determined by dynamic light scattering (DLS).

After PAS introduction, the polymer nanoparticles in the prevailing fraction indicated a tendency to increase in size in the range of 24–354 nm, with the exception of G1 and G5 (almost doubly reduced to 145 nm and 75 nm, respectively). Additionally, they were usually characterized by the presence of one fraction, excluding G1, G7 and G8 systems, which existed in two fractions (~20–40 nm and ~140–200 nm as the dominating one). Another relationship was noticed after exchange to CLV⁻, where the particles mostly became smaller (21–148 nm corresponding to the main fraction as 69%–100%). In this series the systems based on higher density graft copolymers G5–G8 were self-assembled to a homogeneous fraction of particles below 100 nm. Comparing all systems, including those containing drugs, the smallest particles were obtained in the case of sample G4, i.e., 18 nm (Cl⁻), 24 nm (PAS⁻), and 25 nm (CLV⁻) as the dominating fraction (64%–90%). The small particles corresponded to small micelle cores, which were provided by G4 due to the highest content of ionic fraction (43%) and the lowest content of hydrophobic fraction (61%) in the group of copolymers with lower density of ionic side chains grafted from shorter hydrophobic main chain in contrast to the series G5–G8. The detailed data with regard to particular nanoparticle fractions, their sizes, and polydispersity index are given in Table S2.

3.4. Drug Release

The delivery of PAS and CLV in anionic form is possible in PBS media, because the contained phosphate anions are able to replace PAS⁻ and CLV⁻ in the polymer matrix (Figure 1). The release experiments, which were carried out in pH 7.4 in 37 °C per 48 h, demonstrated the increasing intensity of the drug absorption peak in UV–Vis spectra with the release time of PAS/CLV (Figure S7).

The kinetic profiles in Figure 6 represent an increasing rate of PAS⁻ and CLV⁻ release with the increase in the amounts of ionic groups, especially it was demonstrated by PAS systems of loosely grafted copolymers G1–G4. Effective changes in the amount of released drug were observed for up to three hours (16%–40% of PAS⁻ and 22%–63% of CLV⁻), whereas no significant process progress was noticed above that time up to 48 h (Table 3). Although a low percentage of drug was released by G2_PAS (24%) this system seems to be the most efficient in the PAS delivery (8.8 µg/mL), due to the highest DC of the obtained conjugates (~64%). A similar concentration of released drug was detected for G3_PAS (8.50 µg/mL), i.e., the system with the same grafting degree, but a higher content of ionic units in the side chains. In the case of PAS⁻ based copolymers with low DG, the drug release rate could be regulated by an increase in the side chain length and further improved by the content of ionic moieties in the side chain (G1 < G2 < G3 < G4 in the range of 15%–35% after 3 h, Figure 6a). However, the most efficient drug release was proved for the G7_CLV system (31.1 µg/mL). Similarly, G8_CLV was able to exchange a large amount of the drug (30.4 µg/mL), whereas the DC was almost the lowest in the CLV series (68%).

In comparison with PAS⁻, the CLV⁻ is a more beneficial drug to exchange chloride anions and to be exchanged for phosphate anions in PBS media, especially in the case of the densely grafted copolymers G7–G8 demonstrating the highest release rate (Figure 6d). It means that the interaction of trimethylammonium cations and CLV anions is weaker than with PAS, and additionally the larger number of side chains generates steric hindrance, which is helpful to lose the CLV anions. At the same time, the largest content of ionic fraction at the lower grafting density of G4 provides charge repulsion to increase rigidity of ionic side chains supporting a significantly higher rate of CLV release than for other samples in the series G1–G4 (50% vs. 20%–30% after 3 h, Figure 6c). In turn, the release rate of PAS for system G8 (Figure 6b) with a similar kinetics profile to G2, shows that a double higher grafting degree, combined with high ionic content can be a limiting parameter for drug release due to the relatively strong PAS interactions with the polymer matrix.

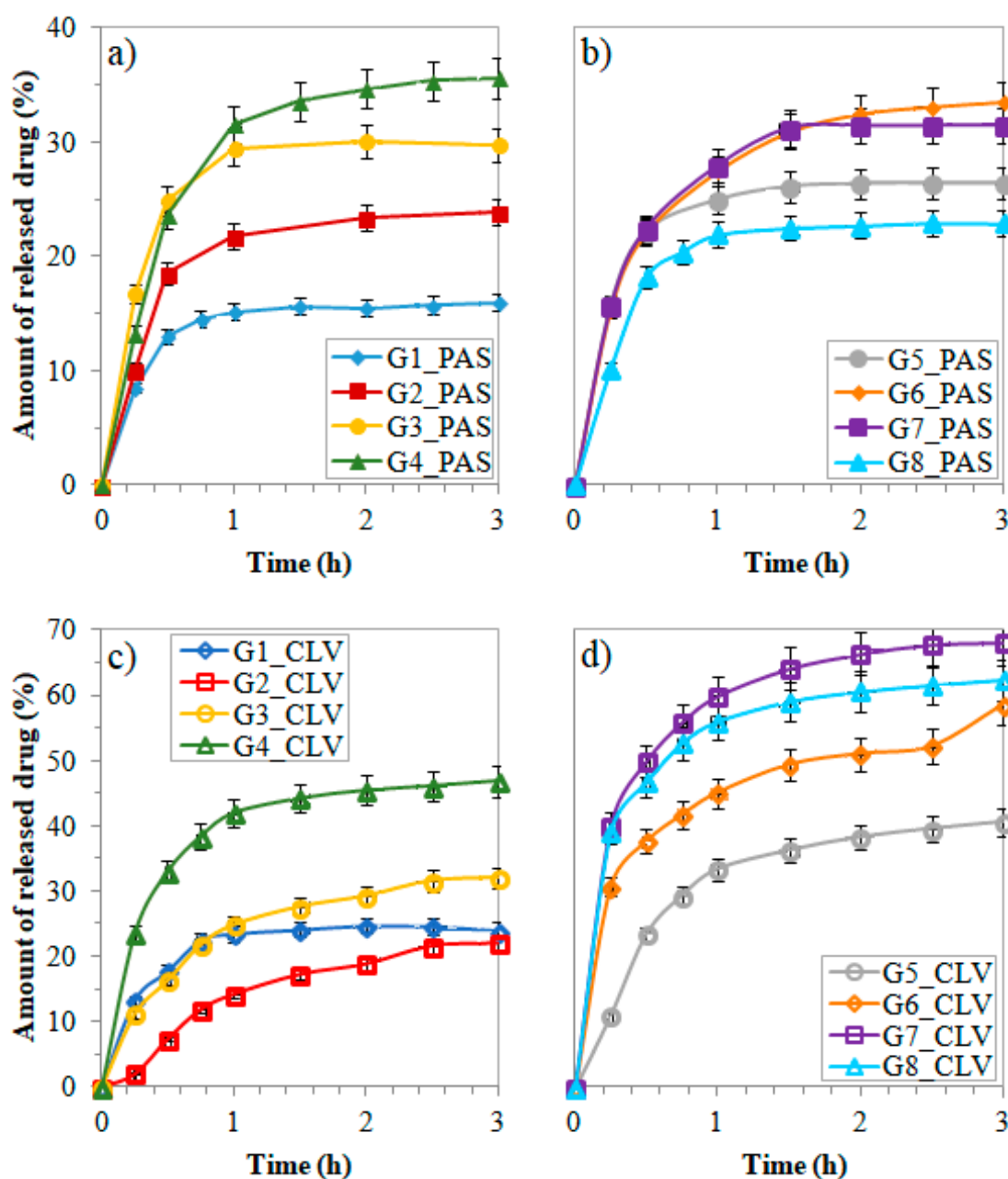


Figure 6. Release profiles of (a) and (b) PAS, (c) and (d) CLV anions from systems based on grafted copolymers.

4. Conclusions

A “grafting from” via ATRP was applied to obtain the ionic graft copolymers based on biocompatible choline, which were modified by exchange with the use of pharmaceutical ions PAS and CLV. These carriers were studied to verify their drug delivery properties by the influence of grafting degree, length and the number of ionic units in the side chains, which can be regulated by proper conditions of reactions. Composition and grafting degree of the copolymers affected the values of CMC to form the self-assembling superstructures at concentrations ranging between 0.005 and 0.026 mg/mL by ionic polymers bearing chloride anions, 0.010 and 0.051 mg/mL for conjugates with PAS ions and 0.012 and 0.040 mg/mL after exchange onto CLV anions. The grafted polymers were beneficial for sufficient drug introduction, but it was more effective for CLV (66%–100%) than in the case of PAS (31%–64%). Similarly, the effect of CLV release by anion exchange in PBS (h) was detected as more

valuable, reaching 40%–75% for densely grafted polymers, whereas in the other cases the maximum of released drug provided was in the lower level up to 40%–50% after 48 h. Additionally, it was also noticed for CLV, that in the case of slightly lower DC values (66–89%), these systems supported higher drug release (39%–73% corresponding to 19–31 µg/mL of released CLV⁻). The concentration of PAS was significantly lower (>8.50 µg/mL), which meant that these systems have to be used on a larger scale to deliver therapeutic doses. Our studies indicated that the designed graft copolymers with pharmaceutical counterions seemed to be promising carriers from the physicochemical aspect. In the case of their applications, their rapid action within the three-hour cycle should be effective in the treatment of bacterial infections.

Supplementary Materials: The following are available online at <http://www.mdpi.com/2073-4360/12/9/2159/s1>, S1: Synthesis of multifunctional macroinitiators, Table S1: Conversion values in synthesis of macroinitiator precursors determined by ¹H NMR, Figure S1: ¹H NMR spectra of precursor and multifunctional macroinitiator, Figure S2: FT-IR spectra for precursor and multifunctional macroinitiator, Figure S3: ¹H NMR spectra of a mixture before starting of reaction, and at the end of copolymerization resulting in grafted copolymer G2, Figure S4: ¹H NMR spectra of grafted copolymers G2 and G2_PAS, Figure S5: ¹H NMR spectra of grafted copolymers G5 and CLV G5_CLV, Table S2: Hydrodynamic diameters of nanoparticles determined with DLS, Figure S6: DLS histograms of particles formed by graft copolymers, Figure S7: UV–Vis spectra of released drugs for G2_PAS and G2_CLV systems.

Author Contributions: K.N.: data curation, formal analysis, investigation, writing—original draft; D.N.: conceptualization, methodology, funding acquisition, project administration, writing—review and editing, supervision. All authors have read and agreed to the published version of the manuscript.

Funding: These studies were financially supported by the National Science Center, grant no. 2017/27/B/ST5/00960.

Conflicts of Interest: The authors declare no conflict of interest.

References

1. Zhang, Y.; Chan, H.F.; Leong, K.W. Advanced Materials and Processing for Drug Delivery: The Past and the Future. *Adv. Drug Deliv. Rev.* **2013**, *65*, 104–120. [[CrossRef](#)]
2. Vega-Vasquez, P.; Mosier, N.S.; Irudayaraj, J. Nanoscale Drug Delivery Systems: From Medicine to Agriculture. *Frint. Bioeng. Biotechnol.* **2020**, *7*, 1–16. [[CrossRef](#)]
3. Pandey, R.; Khuller, G.K. Polymer based drug delivery systems for mycobacterial infections. *Curr. Drug Deliv.* **2004**, *1*, 195–201. [[CrossRef](#)] [[PubMed](#)]
4. Visser, J.G.; Van Staden, A.; Smith, C. Harnessing Macrophages for Controlled-Release Drug Delivery: Lessons From Microbes. *Front. Pharmacol.* **2019**, *10*, 1–18. [[CrossRef](#)] [[PubMed](#)]
5. Chen, K.; Liao, S.; Guo, S.; Zheng, X.; Wang, B.; Duan, Z.; Zhang, H.; Gong, Q.; Luo, K. Multistimuli-Responsive PEGylated Polymeric Bioconjugate-Based Nano-aggregate for Cancer Therapy. *Chem. Eng. J.* **2020**, *391*, 123543. [[CrossRef](#)]
6. Jain, N.; Gupta, B.; Thankur, N.; Jain, R.; Banweer, J.; Jain, D.K.; Jain, S. Phytosome: A Novel Drug Delivery System for Herbal Medicine. *Int. J. Pharm. Sci. Drug Res.* **2010**, *2*, 224–228.
7. Devi, V.K.; Jain, N.; Valli, K.S. Importance of novel drug delivery systems in herbal medicines. *Pharmacogn Rev.* **2010**, *4*, 27–31.
8. Li, D.-C.; Zhong, X.-K.; Zeng, Z.-P.; Jiang, J.-G.; Li, L.; Zhao, M.; Yang, X.-Q.; Chen, J.; Zhang, B.-S.; Zhao, Q.-Z.; et al. Application of targeted drug delivery system in Chinese medicine. *J. Control Release* **2009**, *138*, 103–112. [[CrossRef](#)]
9. Bhowmik, D.; Gopinath, H.; Kumar, B.P.; Duraiavel, S.; Kumar, K.P.S. Controlled Release Drug Delivery Systems. *J. Pharm. Innov.* **2012**, *1*, 24–32.
10. Fleige, E.; Quadir, M.A.; Haag, R. Stimuli-responsive polymeric nanocarriers for the controlled transport of active compounds: Concepts and applications. *Adv. Drug Deliv. Rev.* **2012**, *64*, 866–884. [[CrossRef](#)]
11. Maksym-Bebenek, P.; Neugebauer, D. Self-assembling polyether-b-polymethacrylate graft copolymers loaded with indomethacin. *Int. J. Polym. Mater. PO* **2017**, *66*, 317–325. [[CrossRef](#)]
12. Maksym-Bebenek, P.; Neugebauer, D. Synthesis of amphiphilic semigrafted pseudo-Pluronics for self-assemblies carrying indomethacin. *RSC Adv.* **2016**, *6*, 88444–88452. [[CrossRef](#)]

13. Simone, E.A.; Dziubla, T.D.; Muzykantov, V. Polymeric carriers: Role of geometry in drug delivery. *Expert Opin. Drug Deliv.* **2018**, *5*, 1293–1300. [[CrossRef](#)] [[PubMed](#)]
14. Michalak, G.; Głuszek, K.; Piktel, E.; Deptuła, P.; Puszkarcz, I.; Niemirowicz, K.; Bucki, R. Polymeric nanoparticles—A novel solution for delivery of antimicrobial agents. *Stud. Med.* **2016**, *32*, 56–62. [[CrossRef](#)]
15. Zhang, Y.; Sun, T.; Jiang, C. Biomacromolecules as carriers in drug delivery and tissue engineering. *Acta Pharm. Sin. B* **2018**, *8*, 34–50. [[CrossRef](#)]
16. Mokhtarzadeh, A.; Alibakhshi, A.; Yaghoobi, H.; Hashemi, M.; Hejazi, M.; Ramezani, M. Recent advances on biocompatible and biodegradable nanoparticles as gene carriers. *Expert Opin. Biol. Ther.* **2016**, *16*, 1–43. [[CrossRef](#)]
17. Maksym-Bębenek, P.; Neugebauer, D. Study on Self-Assembled Well-Defined PEG Graft Copolymers as Efficient Drug-Loaded Nanoparticles for Anti-Inflammatory Therapy. *Macromol. Biosci.* **2015**, *15*, 1616–1624. [[CrossRef](#)]
18. Maksym-Bębenek, P.; Biela, T.; Neugebauer, D. Synthesis and investigation of monomodal hydroxy-functionalized PEG methacrylate based copolymers with high polymerization degrees. Modification by “grafting from”. *React. Funct. Polym.* **2014**, *82*, 33–40. [[CrossRef](#)]
19. Ayres, N. Polymer brushes: Applications in biomaterials and nanotechnology. *Polym. Chem.* **2010**, *1*, 769–777. [[CrossRef](#)]
20. Bury, K.; Neugebauer, D.; Biela, T. Methacrylate copolymers with hydroxyl terminated caprolactone chains via ATRP. A route to grafted copolymers. *React. Funct. Polym.* **2011**, *71*, 616–624. [[CrossRef](#)]
21. Maksym-Bębenek, P.; Biela, T.; Neugebauer, D. Water soluble well-defined acidic graft copolymers based on a poly(propylene glycol) macromonomer. *RSC Adv.* **2015**, *5*, 3627–3635. [[CrossRef](#)]
22. Cheng, G.; Boker, A.; Zhang, M.; Krausch, G.; Muller, A. Amphiphilic Cylindrical Core-Shell Brushes via a “Grafting From” Process Using ATRP. *Macromolecules* **2001**, *34*, 6883–6888. [[CrossRef](#)]
23. Janata, M.; Masar, B.; Toman, L.; Vlcek, P.; Policka, P.; Brus, J.; Holler, P. Multifunctional ATRP macroinitiators for the synthesis of graft copolymers. *React. Funct. Polym.* **2001**, *50*, 67–75. [[CrossRef](#)]
24. Bielas, R.; Mielańczyk, A.; Skonieczna, M.; Mielańczyk, L.; Neugebauer, D. Choline supported poly(ionic liquid) graft copolymers as novel delivery systems of anionic pharmaceuticals for anti-inflammatory and anti-coagulant therapy. *Sci. Rep.* **2019**, *9*, 14410. [[CrossRef](#)]
25. Neugebauer, D.; Mielańczyk, A.; Bielas, R.; Odrobińska, J.; Kupczak, M.; Niesyto, K. Ionic Polymethacrylate Based Delivery Systems: Effect of Carrier Topology and Drug Loading. *Pharmaceutics* **2019**, *11*, 337. [[CrossRef](#)]
26. Nie, J.; Xiao, S.; Tan, R.; Wang, T.; Duan, X. New Insights on the Fast Response of Poly(Ionic Liquid)s to Humidity: The Effect of Free-Ion Concentration. *Nanomaterials* **2019**, *9*, 749. [[CrossRef](#)]
27. Yuan, J.; Antonietti, M. Poly(ionic liquid)s: Polymers expanding classical property profiles. *Polymer* **2011**, *52*, 1469–1482. [[CrossRef](#)]
28. Zhang, S.; Zhuang, Q.; Zhang, M.; Wang, H.; Gao, Z.; Sun, J.; Yuan, J. Poly(ionic liquid) composites. *Chem. Soc. Rev.* **2020**, *49*, 1726–1755. [[CrossRef](#)]
29. Biswas, Y.; Banerjee, P.; Mandal, T.K. From Polymerizable Ionic Liquids to Poly(ionic liquid)s: Structure Dependent Thermal, Crystalline, Conductivity, and Solution Thermoresponsive Behaviors. *Macromolecules* **2019**, *52*, 945–958. [[CrossRef](#)]
30. Tan, Z.Q.; Liu, J.F.; Pang, L. Advances in analytical chemistry using the unique properties of ionic liquids. *TrAC Trends. Anal. Chem.* **2012**, *39*, 218–227. [[CrossRef](#)]
31. Yuan, J.; Mecerreyes, D.; Antonietti, M. Poly(ionic liquid)s: An update. *Prog. Polym. Sci.* **2013**, *38*, 1009–1036. [[CrossRef](#)]
32. Zhao, D.; Liao, Y.; Zhang, Z. Toxicity of Ionic Liquids. *Clean* **2007**, *35*, 42–48. [[CrossRef](#)]
33. Frade, R. Ionic Liquids in Green Chemistry—Prediction of Ionic Liquids Toxicity Using Different Models. In *Green Chemistry for Environmental Remediation*; Singh, V., Sanghi, R., Eds.; Wiley: Lisbon, Portugal, 2012; pp. 343–355.
34. Isik, M.; Gracia, R.; Kollnus, L.; Tome, L.; Marrucho, I.; Mecerreyes, D. Cholinium-Based Poly(ionic liquid)s: Synthesis, Characterisation, and Application as Biocompatible Ion Gels and Cellulose Coatings. *ACS Macro. Lett.* **2013**, *2*, 975–979. [[CrossRef](#)]
35. Petkovic, M.; Ferguson, J.L.; Gunaratne, H.Q.N.; Ferreira, R.; Leitão, M.C.; Seddon, K.R.; Rebelo, L.P.N.; Pereira, C.S. Novel biocompatible cholinium-based ionic liquids-toxicity and biodegradability. *Green Chem.* **2010**, *12*, 643–649. [[CrossRef](#)]

36. Ventura, S.P.M.; Silva, F.; Gonçalves, A.M.M.; Pereira, J.L.; Gonçalves, F.; Coutinho, J.A.P. Ecotoxicity analysis of cholinum-based ionic liquids to *Vibrio fischeri* marine bacteria. *Ecotoxicol. Environ. Saf.* **2014**, *102*, 48–54. [[CrossRef](#)] [[PubMed](#)]
37. Shahriari, S.; Tomé, L.C.; Araújo, J.M.M.; Rebelo, L.P.N.; Coutinho, J.A.P.; Marrucho, I.M.; Freire, M.G. Aqueous biphasic systems: A begin route using cholinum-based ionic liquids. *RCS Adv.* **2013**, *3*, 1835–1843. [[CrossRef](#)]
38. Isik, M.; Gracia, R.; Kollnus, L.; Tome, L.; Marrucho, I.; Mecerreyes, D. Cholinium Lactate Methacrylate: Ionic Liquid Monomer for Cellulose Composites and Biocompatible Ion Gels. *Macromol. Symp.* **2014**, *342*, 21–24. [[CrossRef](#)]
39. Lee, H.C.; Fellenz-Maloney, M.P.; Liscovitch, M.; Blusztajn, J.K. Phospholipase D-catalyzed hydrolysis of phosphatidylcholine provides the choline precursor for acetylcholine synthesis in a human neuronal cell line. *Proc. Natl. Acad. Sci. USA* **1993**, *90*, 10086–10090. [[CrossRef](#)]
40. Bielas, R.; Siewniak, A.; Skonieczna, M.; Adamiec, M.; Mielańczyk, Ł.; Neugebauer, D. Choline based polymethacrylate matrix with pharmaceutical cations as co-delivery system for antibacterial and anti-inflammatory combined therapy. *J. Mol. Liq.* **2019**, *285*, 114–122. [[CrossRef](#)]
41. Bielas, R.; Mielańczyk, A.; Siewniak, A.; Neugebauer, D. Trimethylammonium-based polymethacrylate ionic liquids with tunable hydrophilicity and charge distribution as carriers of salicylate anions. *ACS Sustain. Chem. Eng.* **2016**, *4*, 4181–4191. [[CrossRef](#)]
42. Bielas, R.; Łukowiec, D.; Neugebauer, D. Drug delivery via anion exchange of salicylate decorating poly(meth)acrylates based on pharmaceutical ionic liquid. *New J. Chem.* **2017**, *21*, 12801–12807. [[CrossRef](#)]
43. Hosseinzadeh, F.; Mahkam, M.; Galehassadi, M. Synthesis and characterization of ionic liquid functionalized polymers for drug delivery of an anti-inflammatory drug. *Des. Monomers Polym.* **2012**, *15*, 279–388. [[CrossRef](#)]
44. Gorbunova, M.; Lemkina, L.; Borisova, I. New guanidine-containing polyelectrolytes as advanced antibacterial materials. *Eur. Polym. J.* **2018**, *105*, 426–433. [[CrossRef](#)]



© 2020 by the authors. Licensee MDPI, Basel, Switzerland. This article is an open access article distributed under the terms and conditions of the Creative Commons Attribution (CC BY) license (<http://creativecommons.org/licenses/by/4.0/>).

Supplementary Materials

Synthesis and characterization of ionic graft copolymers: introduction and *in-vitro* release of antibacterial drug by anion exchange

Katarzyna Niesyto ¹, Dorota Neugebauer ^{1*}

¹ Department of Physical Chemistry and Technology of Polymers, Faculty of Chemistry, Silesian University of Technology, 44-100 Gliwice, Poland

* Correspondence: Dorota.Neugebauer@polsl.pl

Received: date; Accepted: date; Published: date

Content:

S1. Synthesis of multifunctional macroinitiators P(MMA-*co*-BIEM) (example for Ia).

Table S1. Conversion values in synthesis of macroinitiator precursors determined by ¹H NMR.

Figure S1. ¹H NMR spectra of a) precursor I, and b) multifunctional macroinitiator Ia

Figure S2. FT-IR spectra for (a) precursor I, and (b) multifunctional macroinitiator Ia.

Figure S3. ¹H NMR spectra of a mixture a) before starting of reaction, and b) at the end of copolymerization resulting in grafted copolymer G2.

Figure S4. ¹H NMR spectra of grafted copolymers a) G2, and b) G2_PAS.

Figure S5. ¹H NMR spectra of grafted copolymers a) G5, and b) G5_CLV.

Table S2. Hydrodynamic diameters of nanoparticles determined with DLS.

Figure S6. DLS histograms of particles formed by graft copolymers (1 mg/mL aq. solution).

Figure S7. UV-Vis spectra of released drug for a) G2_PAS, and b) G2_CLV systems.

S1. Synthesis of multifunctional macroinitiators P(MMA-*co*-BIEM) (example for Ia)

Comonomers HEMA (1.40 mL, 11.50 mmol) and MMA (3.70 mL, 34.50 mmol), anisole (0.50 mL), dNbpy (62.66 mg, 15.30×10^{-2} mmol) and CuBr (10.99 mg, 7.67×10^{-2} mmol) were placed into a Schlenk flask and degassed by two freeze-pump-thaw cycles. The initial sample was taken and EBiB initiator (113.77 μ L, 7.67×10^{-2} mmol) was introduced to the mixture. Next, the reaction flask was immersed in an oil bath at 70°C. The reaction was stopped by exposing to air. The reaction mixture diluted in THF was passed through a neutral alumina column to remove copper catalyst, then the polymer was precipitated in diethyl ether and vacuum dried. ¹H NMR of P(MMA-*co*-HEMA) (Figure S1a) (DMSO-*d*₆, δ , ppm): 5.01–4.72 (1H, –CH₂–OH), 3.90–3.82 (2H, –CH₂–OH), 4.17–4.05 (2H, –COO–CH₂–), 3.56–3.48 (3H, –O–CH₃), 1.94–1.57 (2H, –CH₂– backbone), 1.4–0.51 (3H, –CH₃ backbone). FT-IR (Figure S2a) (cm⁻¹): 3600–3100 ν (O–H), 3000–2800 ν (C–H), 1750 ν (C=O), 1150 ν (C–O).

The obtained hydroxyl-functionalized polymer **I** (0.70 g, including 0.90 mmol of HEMA units) was dissolved in pyridine (6 mL). Next, the mixture was placed in an ice bath to cool it down to 0 °C. After cooling α -bromoisobutyrate bromide (BIBB) (166.21 μ L, 1.34 mmol) was added dropwise. The mixture was stirred overnight. Next, the bromoester-functionalized polymer **Ia** was precipitated in cooled water and vacuum dried. ¹H NMR of P(MMA-*co*-BIEM) (Figure S1b) (DMSO-*d*₆, δ , ppm): 4.47–4.28 (2H, –CH₂–OOC–C–(CH₃)₂Br), 4.28–4.08 (2H, –COO–CH₂–), 3.74–3.44 (3H, –O–CH₃), 2.02–1.91 (6H, –(CH₃)₂Br initiating moiety), 1.94–1.57 (2H, –CH₂– backbone), 1.4–0.51 (3H, –CH₃ backbone). FT-IR (Figure S2b) (cm⁻¹): 3000–2800 ν (C–H), 1750 ν (C=O), 1150 ν (C–O).

Table S1. Conversion values in synthesis of macroinitiator precursors determined by ¹H NMR.

	HEMA conversion	MMA conversion	total conversion
I	32	31	31
II	44	53	49

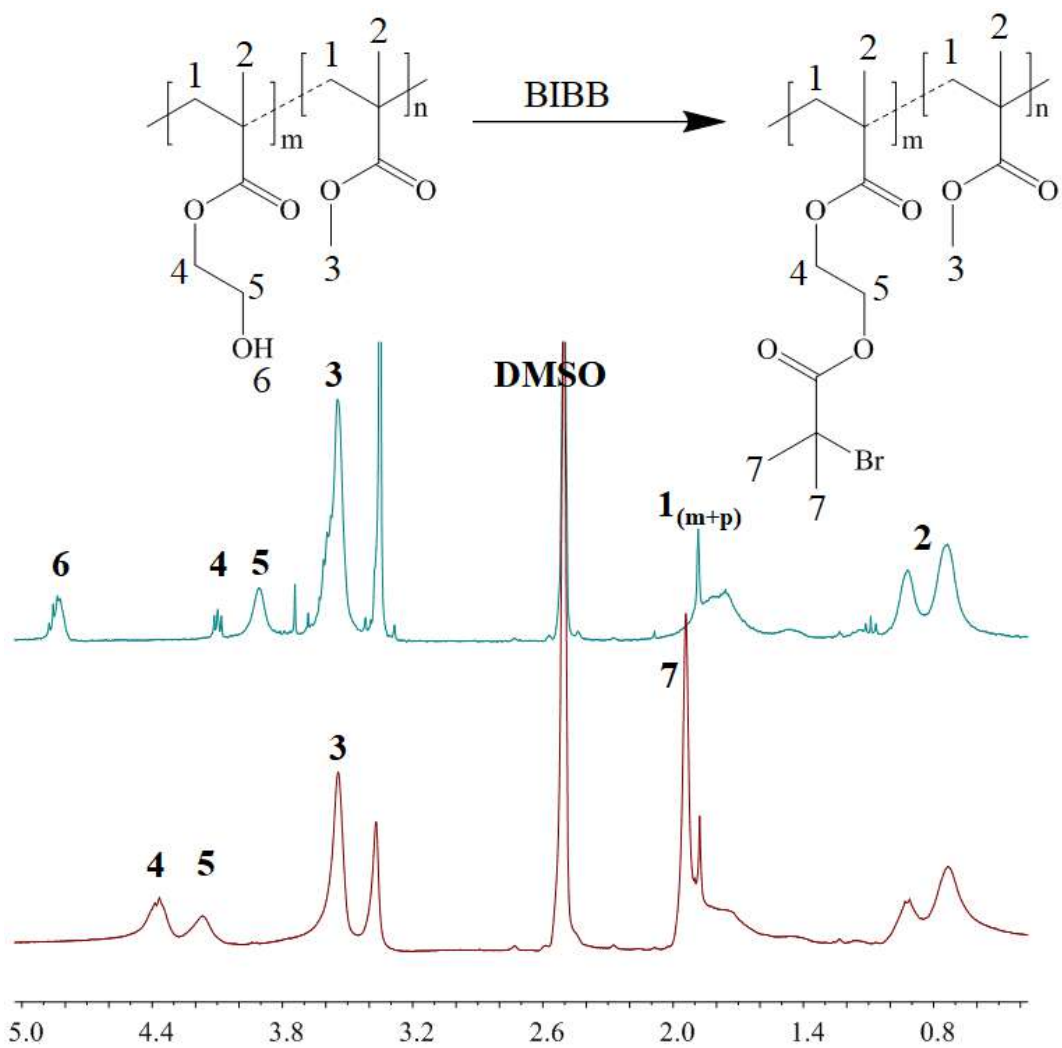


Figure S1. ^1H NMR spectra of a) precursor I, and b) multifunctional macroinitiator Ia.

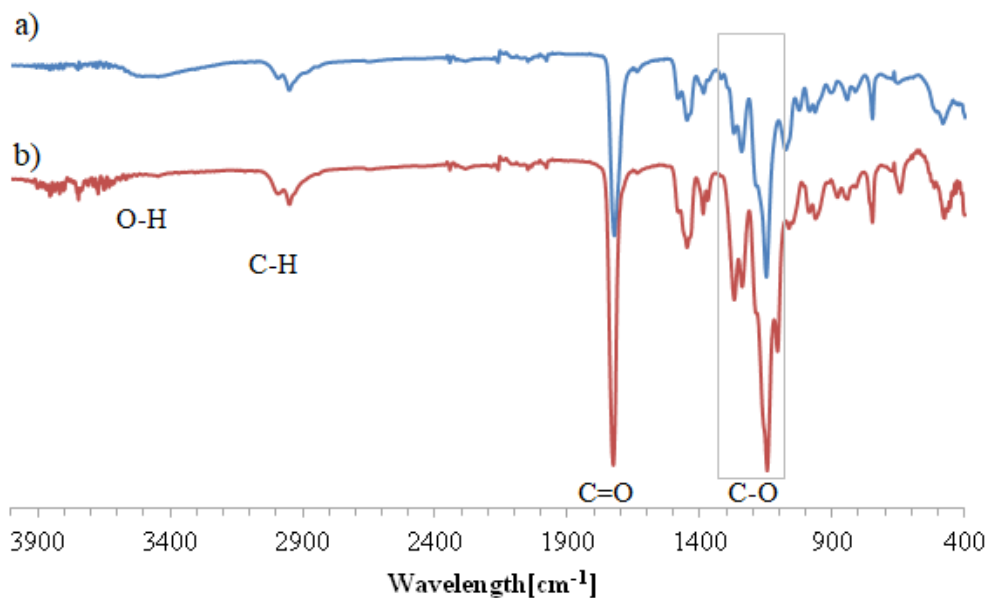


Figure S2. FT-IR spectra for (a) precursor I, and (b) multifunctional macroinitiator Ia.

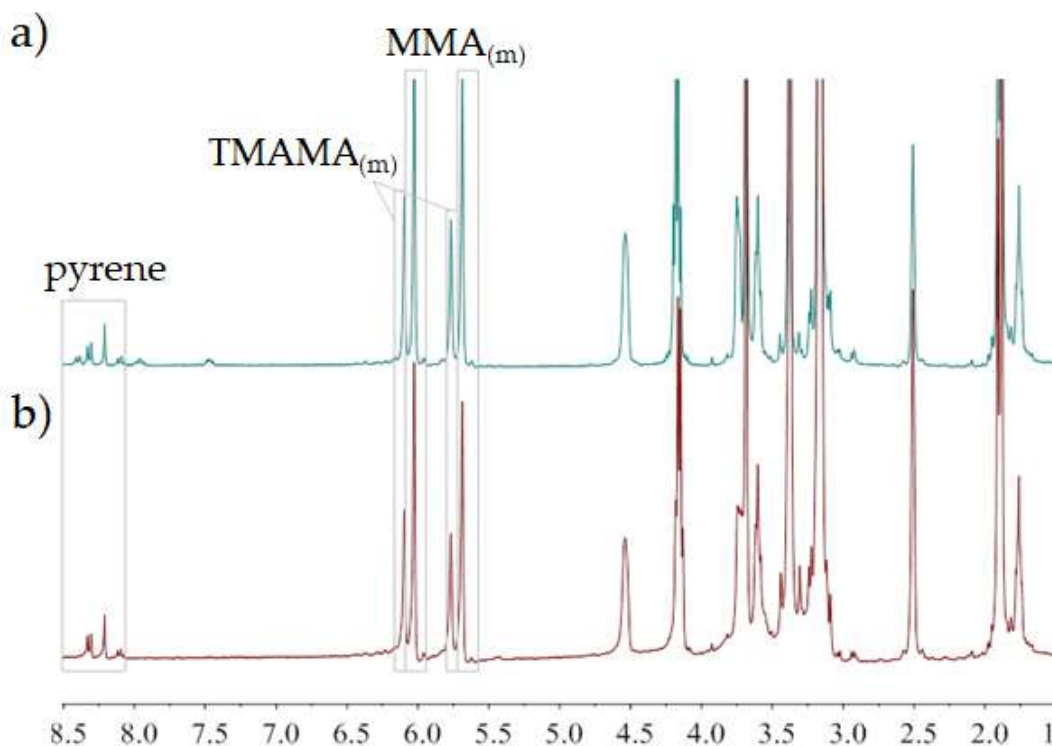


Figure S3. ^1H NMR spectra of a mixture a) before starting of reaction, and b) at the end of copolymerization resulting in grafted copolymer G2.

^1H NMR (DMSO- d_6 , δ , ppm): 4.63-4.43 (2H, $-\text{CH}_2\text{-O}-$), 4.47-4.28 (2H, $-\text{CH}_2\text{-OOC-C}(\text{CH}_3)_2\text{Br}$), 4.28-4.08 (2H, $-\text{COO-CH}_2$), 3.86-3.65 (2H, $-\text{CH}_2\text{-N}^+$), 3.65-3.47 (3H, $-\text{O-CH}_3$), 3.42-3.01 (9H, $-\text{N}^+(\text{CH}_3)_3$), 1.98-1.82 (6H, $-(\text{CH}_3)_2\text{Br}$ initiating moiety), 1.4-0.51 (3H, $-\text{CH}_3$ backbone).

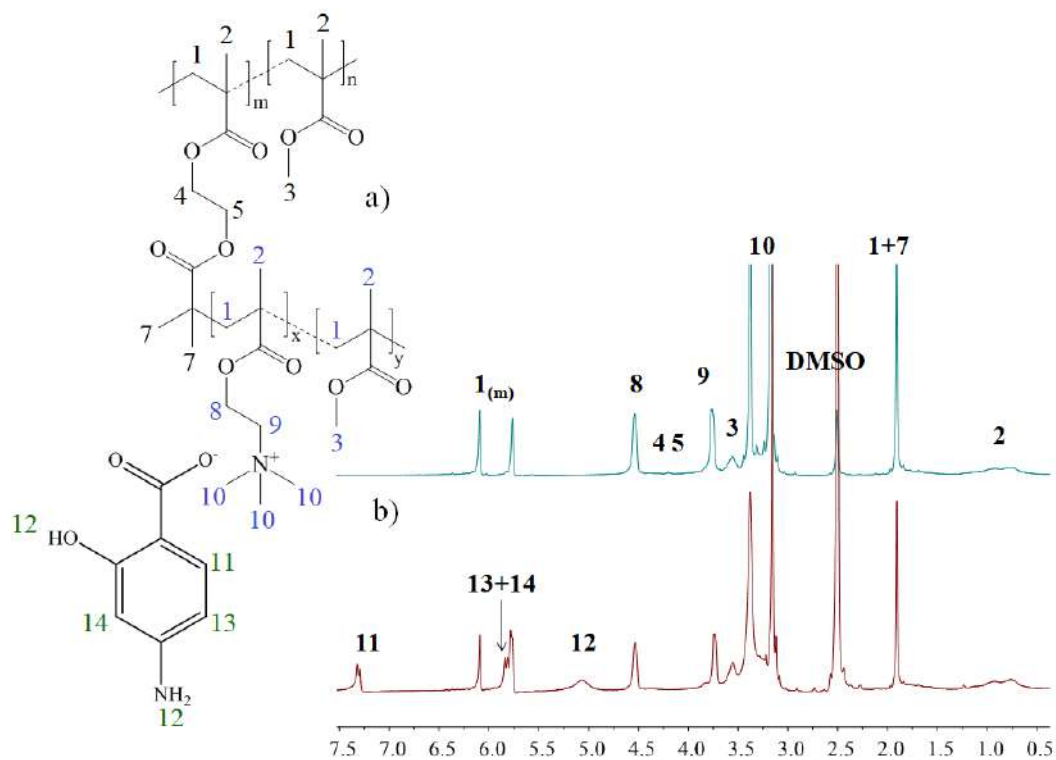


Figure S4. ^1H NMR spectra of grafted copolymers a) G2, and b) G2_PAS, where * $1_{(m)}$ is related to monomer residue.

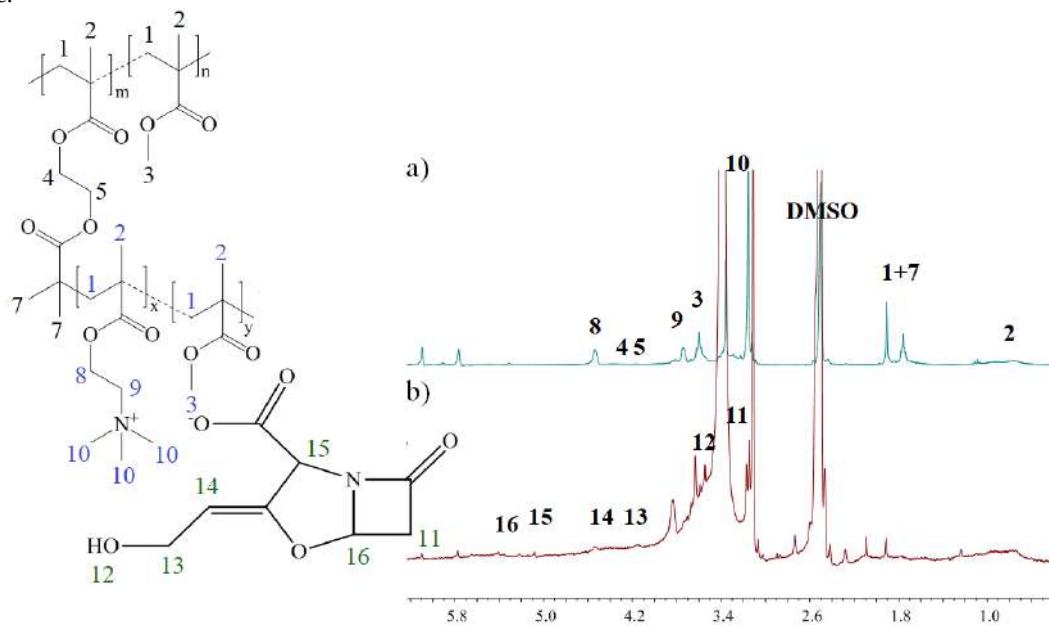


Figure S5. ^1H NMR spectra of grafted copolymers a) G5, and b) G5_CLV, where * $1_{(m)}$ is related to monomer residue.

Table S2. Hydrodynamic diameters of nanoparticles determined with DLS^a.

	Cl ⁻			PAS ⁻			CLV ⁻		
	PDI	Size [nm]	Intensity [%]	PDI	Size [nm]	Intensity	PDI	Size [nm]	Intensity
G1	0.361	88	56	0.503	145	59	0.601	148	75
		368	25		23	40		18	25
		21	17						
G2	0.427	124	60	0.114	261	100	0.365	21	80
		21	40					357	20
G3	0.295	203	98	0.775	354	100	0.442	26	69
								250	31
G4	0.454	18	64	0.264	24	89	0.397	25	83
		125	32					240	11
G5	0.444	114	94	0.265	75	100	0.268	91	100
G6	0.293	105	99	0.291	127	100	0.253	86	100
G7	0.241	72	100	0.443	194	82	0.316	75	98
					37	18			
G8	0.349	95	98	0.459	206	54	0.163	48	98
					40	46			

^aconcentration of copolymer in water: 1mg/mL.

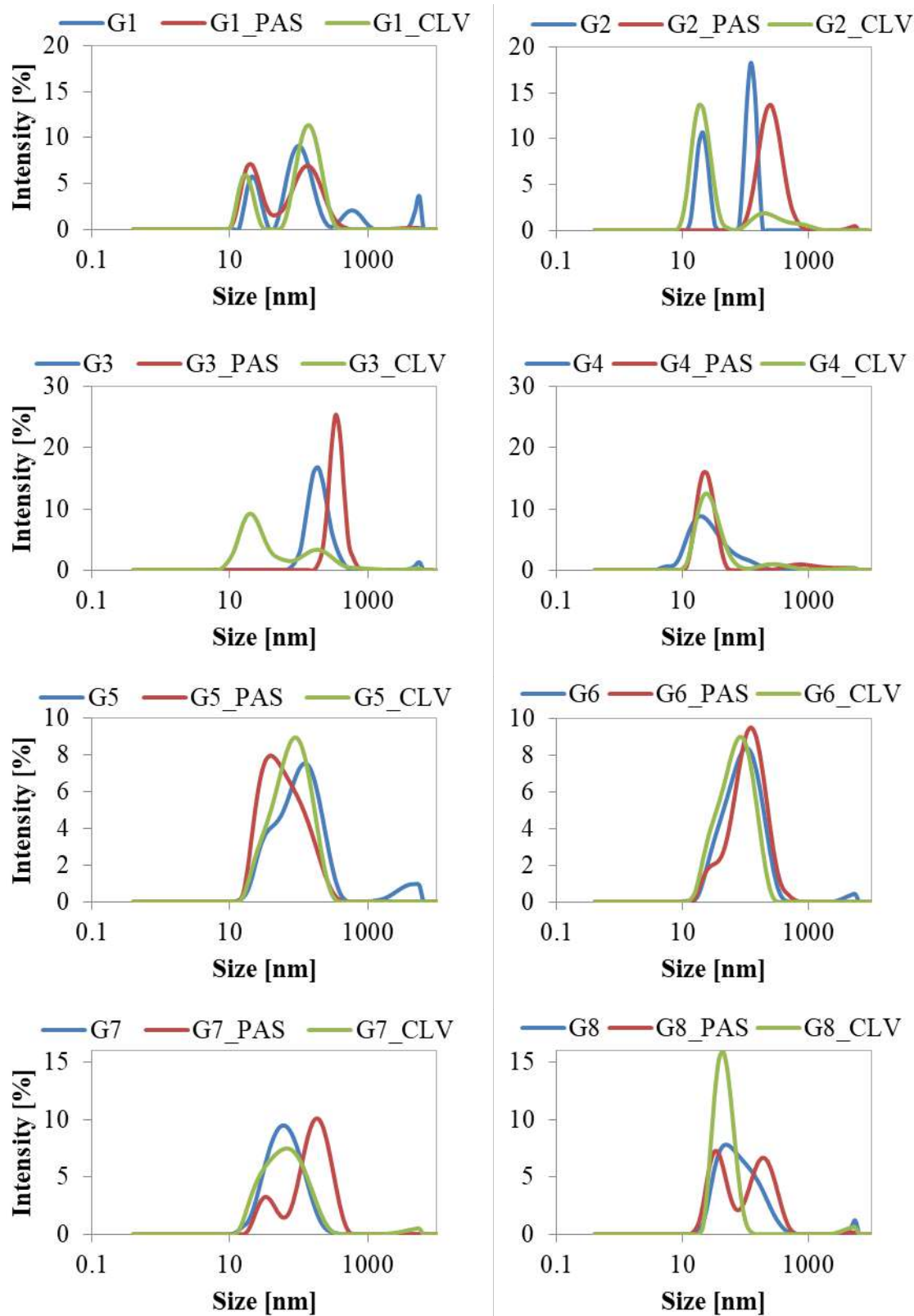


Figure S6. DLS histograms of particles formed by graft copolymers (1 mg/mL aq. solution).

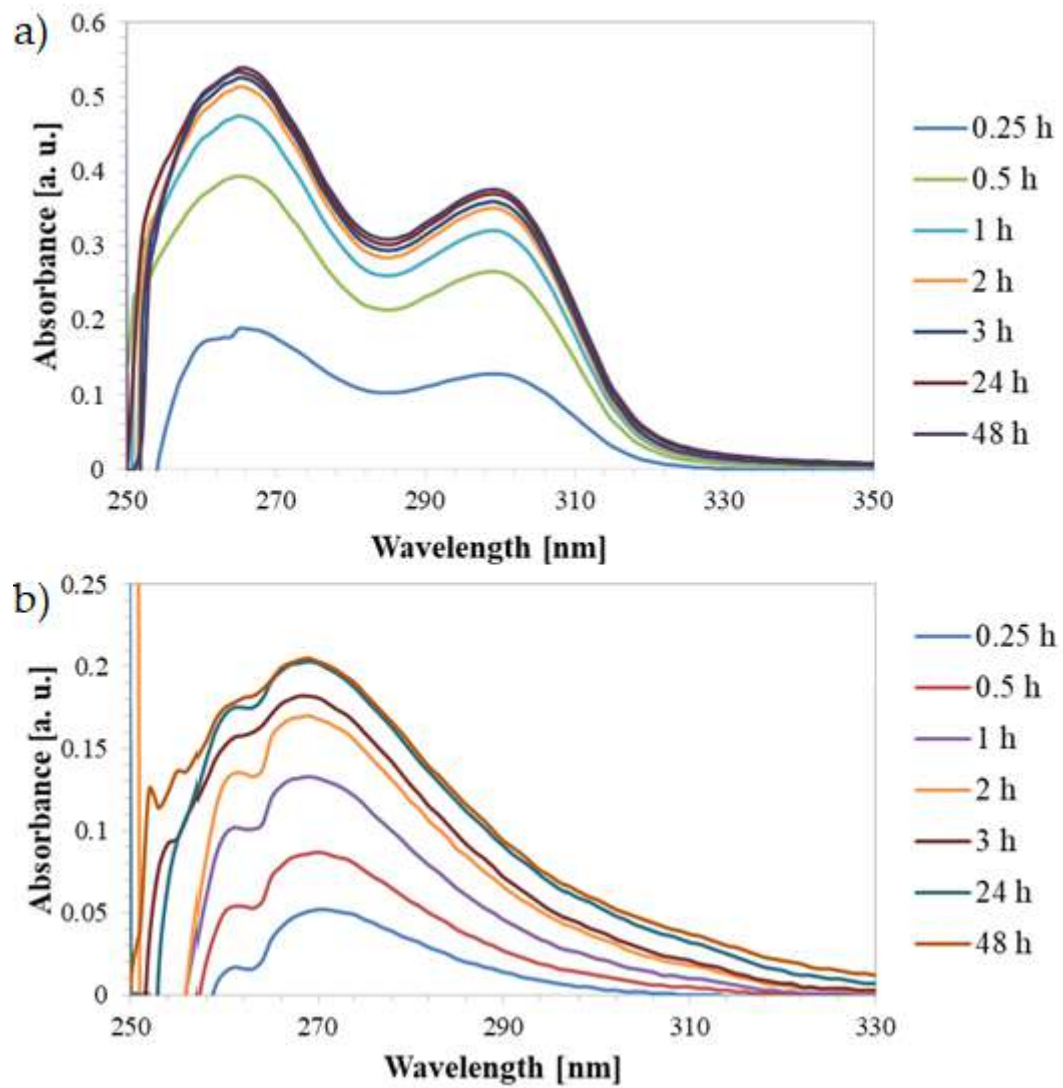


Figure S7. UV-Vis spectra of released drug for a) G2_PAS, and b) G2_CLV systems.

PUBLIKACJA P.2

Linear Copolymers Based on Choline Ionic Liquid Carrying Anti-Tuberculosis Drugs: Influence of Anion Type on Physicochemical Properties and Drug Release.

Niesyto, K., Neugebauer, D.

International Journal of Molecular Sciences 2021, 22, 284



Article

Linear Copolymers Based on Choline Ionic Liquid Carrying Anti-Tuberculosis Drugs: Influence of Anion Type on Physicochemical Properties and Drug Release

Katarzyna Niesyto and Dorota Neugebauer *

Department of Physical Chemistry and Technology of Polymers, Faculty of Chemistry, Silesian University of Technology, 44-100 Gliwice, Poland; Katarzyna.Niesyto@polsl.pl

* Correspondence: Dorota.Neugebauer@polsl.pl

Abstract: In this study, drug nanocarriers were designed using linear copolymers with different contents of cholinium-based ionic liquid units, i.e., [2-(methacryloyloxy)ethyl]trimethylammonium chloride (TMAMA/Cl: 25, 50, and 75 mol%). The amphiphilicity of the copolymers was evaluated on the basis of their critical micelle concentration (CMC = 0.055–0.079 mg/mL), and their hydrophilicities were determined by water contact angles (WCA = 17°–46°). The chloride anions in the polymer chain were involved in ionic exchange reactions to introduce pharmaceutical anions, i.e., *p*-aminosalicylate (PAS[−]), clavulanate (CLV[−]), piperacillin (PIP[−]), and fusidate (FUS[−]), which are established antibacterial agents for treating lung and respiratory diseases. The exchange reaction efficiency decreased in the following order: CLV[−] > PAS[−] > PIP[−] >> FUS[−]. The hydrophilicity of the ionic drug conjugates was slightly reduced, as indicated by the increased WCA values. The major fraction of particles with sizes ~20 nm was detected in systems with at least 50% TMAMA carrying PAS or PIP. The influence of the drug character and carrier structure was also observed in the kinetic profiles of the release processes driven by the exchange with phosphate anions (0.5–6.4 μg/mL). The obtained polymer-drug ionic conjugates (especially that with PAS) are promising carriers with potential medical applications.



Citation: Niesyto, K.; Neugebauer, D. Linear Copolymers Based on Choline Ionic Liquid Carrying Anti-Tuberculosis Drugs: Influence of Anion Type on Physicochemical Properties and Drug Release. *Int. J. Mol. Sci.* **2021**, *22*, 284. <https://doi.org/10.3390/ijms22010284>

Received: 13 December 2020

Accepted: 27 December 2020

Published: 30 December 2020

Publisher's Note: MDPI stays neutral with regard to jurisdictional claims in published maps and institutional affiliations.



Copyright: © 2020 by the authors. Licensee MDPI, Basel, Switzerland. This article is an open access article distributed under the terms and conditions of the Creative Commons Attribution (CC BY) license (<https://creativecommons.org/licenses/by/4.0/>).

Keywords: choline; anion exchange; antibacterial activity; polymer carriers

1. Introduction

Polymer-based drug delivery systems (DDS) are of great interest to the scientific community because of their various advantages. These vehicles improve the pharmacokinetics and pharmacodynamics involved in transporting the drug to the destination of therapeutic action [1–4]. Therefore, the most requested systems are the targeted and controlled DDS [5–8]. The delivery properties can be adjusted by modifying the polymer structure to avoid the uncontrolled rate of drug release [9–11]. Drug release can also be activated by specific conditions that are characteristic of unhealthy cells, i.e., pH, temperature, or ionic strength [12–15]. The responsiveness of polymer vehicles to pH changes are commonly used in the treatment of cancer cells due to their acidic reaction, which is an opposite to alkaline environment in healthy cells [16]. Additionally, the unhealthy cells usually gain higher temperature, which is exploited by temperature-responsive polymer carriers for specific behavior in the conditions of their lower or upper critical solution temperature [17]. Mechanisms based on ionic strength are characteristic for polymers containing ionic groups. Ion exchange controlled release systems are applied in delivery of ionic drugs, which can be attached to polymer matrix by ionic interactions. The ion delivery depends on the type and geometry of ionic carrier, charge intensity, and coordination number of ionic groups, as well as ionic strength of polymer solution [18].

Diverse types of carrier are known, some of them are polymer-drug conjugates, in which the latter component is connected directly to the polymeric matrix by a chemical

bond or through the linker [19,20]. If the conjugate has amphiphilic properties, the drug can be encapsulated inside the self-assembled structure [21], thus constituting dual drug co-delivery systems, which have also been applied in combined therapies [22,23]. Compared with traditional drugs, the presence of a polymer carrier is intended to ensure the solubility of the hydrophobic drug in aqueous solution, which is desirable to optimize the drug's effect on the human body [24,25]. Conjugate design requires individualized strategies that involve introducing the appropriate type of connection between the drug and the polymeric matrix to achieve the desired release profile [26,27].

Ionic liquids (ILs), which are popular in various fields of chemistry, are also convenient for drug delivery because of their ionic nature and ion exchange capabilities, which are useful to tune biochemical properties and to generate pharmaceutical activity. As a result, the drug (in an anionic or cationic form) can be introduced into polymer matrix, wherein it is ionically bonded with a counterion [28]. Choline ((2-hydroxyethyl)trimethylammonium chloride), as an IL with vitamin-like functions, is a known carrier of anti-inflammatory salicylates and can be applied as a biological cation owing to its biocompatibility and antibacterial properties [29–31]. Moreover, this molecule and its phosphoryl derivative are capable of degradation under anaerobic conditions [32,33]. The (phosphoryl)choline in a methacrylate-functionalized form has been polymerized to obtain a biocompatible poly(ionic liquid) (PIL) for pharmacological and medical applications. For example, poly(2-methacryloyloxyethyl) phosphorylcholine has been reported as a suitable component of implants, medical devices, or DDS [34–36]. Similarly, poly[2-(methacryloyloxy)ethyl]trimethylammonium chloride (PTMAMA) has demonstrated bactericidal and fungicidal properties [37]. Moreover, its high hydrophilicity can be modified by incorporating hydrophobic units into the polymer chain or by exchanging with hydrophobic anions to yield the amphiphilic copolymer [38], which can create micellar systems in aqueous solution and consequently enable encapsulation of non-ionic drugs [39]. On the other hand, the combination of quaternary ammonium cations with chloride counter ions has been convenient for anion exchange reactions to introduce the ionic drug [40], thus forming the ionic type of polymer-drug conjugates. These systems comprised the graft topology of PTMAMA carrying the pharmaceutical anions, such as salicylate [41], *p*-aminosalicylate, or clavulanate [42]. In these cases, the drug release occurred in the solution containing the stronger ions (i.e., phosphate ions), which is in contrast to conventional conjugates, where the drug is released by hydrolytic degradation of a linker (usually ester- or amide-type). Other PIL-based DDSs have been reported for poly(imidazolium salt)s carrying naproxen anions [43] or poly(guanidinium salt)s with antibiotic anions [44].

In the present work, we describe linear PILs based on [2-(methacryloyloxy)ethyl]trimethylammonium chloride (TMAMA) as the universal matrix for potential polymer-drug ionic conjugates. These copolymers with varied ionic group contents were synthesized via controlled polymerization reaction (i.e., atom transfer radical polymerization (ATRP)). New drug delivery systems were designed by employing the anion exchange reaction with selected drugs in ionic form, such as *p*-aminosalicylic (PAS^-), clavulanic (CLV^-), fusidic (FUS^-), and piperacillin (PIP^-) anions as the antibacterial agents. *p*-Aminosalicylic acid has antitubercular activity, which extinguishes the growth and multiplication of *Mycobacterium tuberculosis*, leading to cell apoptosis, so it is predominantly used to support the action of other anti-tuberculosis drugs. Clavulanic acid isolated from *Streptomyces* is a weak antimicrobial agent and β -lactamase inhibitor that precludes deactivation of antibiotic in combination therapy for bacterial infections (i.e., acute bronchitis and upper respiratory tract infections). Piperacillin acid as an ampicillin-derived antibiotic with broad-spectrum bactericidal activity, and it is clinically efficient in the treatment of infections caused by *Streptococcus pneumoniae*, including lung diseases. Fusidic acid is a natural steroid antibiotic that shows bacteriostatic activity without the corticosteroid effects, and it is effective against *Bordetella pertussis* and *Staphylococcus aureus*, which damage the respiratory system. The aforementioned drugs are typically administered orally during conventional treatments. The influence of the carrier composition and the anion type on the physicochemical proper-

ties, exchange effect, and progress of pharmaceuticals release are investigated in this work, in order to inform the design single-drug delivery systems with potential for the treatment of lung and respiratory diseases. Previously, PAS^- and CLV^- based systems have been studied in combination with PTMAMA graft copolymers [42]. However, in those cases the TMAMA units were located in the side chains, which were formed by grafting from polymethacrylate macroinitiator. Similarly to linear copolymers they were varied with content of ionic units, but in the grafted ones this range was narrower (13–46%), and the TMAMA copolymer side chains were significantly shorter (16–65 repeating units). Fundamental difference was the grafting degree (25% and 50%) defining the distribution density of side chains attached to the hydrophobic backbone. Thus, the linear TMAMA copolymers were investigated to evaluate their delivery potential in comparison to analogous ionic carriers with graft topology.

2. Results and Discussion

Several carriers were designed with statistically distributed ionic units, which act as polymer-drug conjugates. To obtain such systems, PILs containing an ionic monomer (i.e., TMAMA/Cl as M1) in combination with methyl methacrylate (MMA as M2) as a comonomer were copolymerized in different ratios (C1: 25/75, C2: 50/50, and C3: 75/25) by ATRP at 40 °C. The reaction was initiated by ethyl 2-bromoisobutyrate (EBiB) and catalyzed by a copper bromide/*N,N,N',N'',N'''*-pentamethyldiethylenetriamine (CuBr/PMDETA) complex. As a result, linear copolymers were prepared with varying content of ionic units, which corresponded to the initial proportion of TMAMA/MMA in the reaction mixture (Figure 1, Table 1). In our previous studies on the copolymerization of TMAMA and MMA formation of statistical copolymers was postulated due to comparable relative reactivity ratios of comonomers, that is $r_{\text{TMAMA/Cl}} = 1.13$ and $r_{\text{MMA}} = 0.88$ [38].

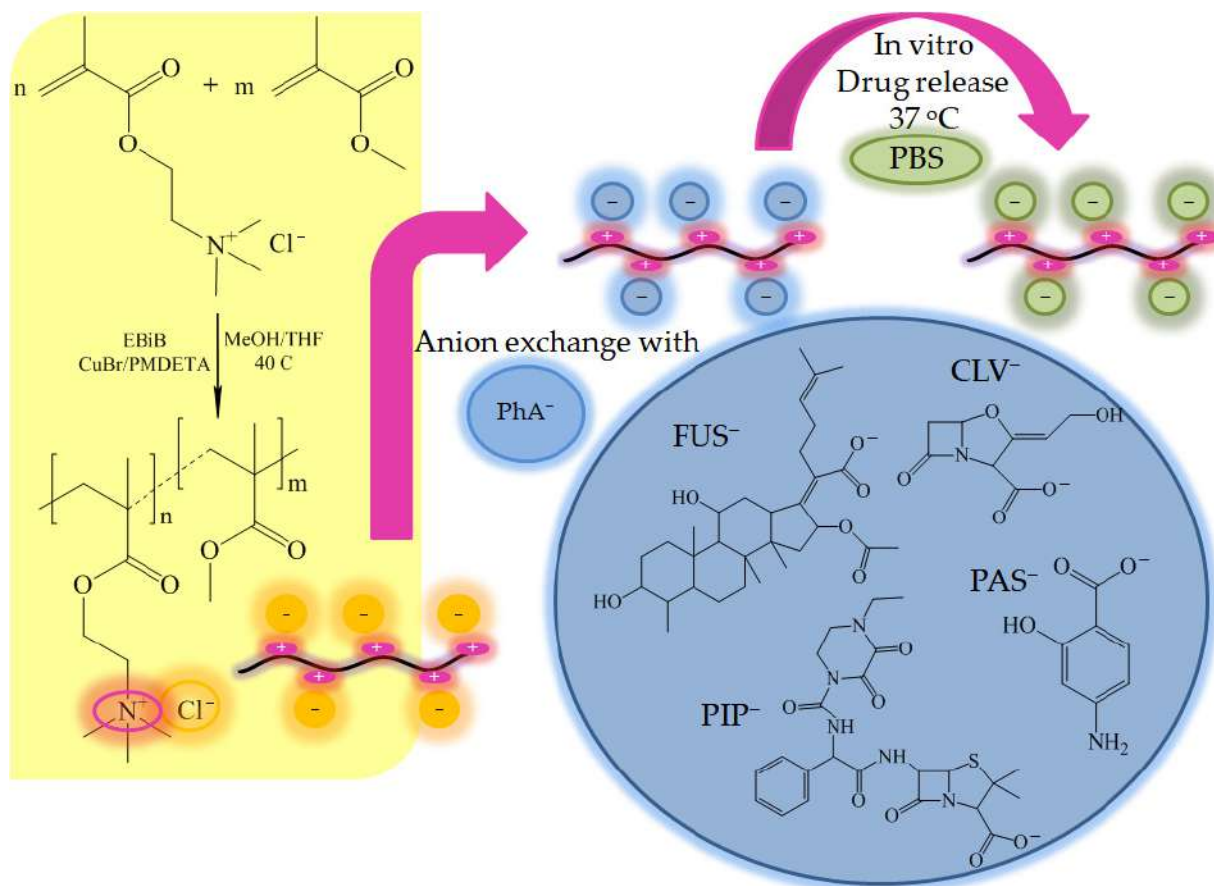


Figure 1. Schematic anion exchange pathway for obtaining linear TMAMA-based copolymers.

Table 1. Characteristics of linear copolymers based on choline ionic liquid (IL) synthesized by atom transfer radical polymerization (ATRP).

No.	M1/M2	¹ H NMR ^a					SEC ^b		
		X _{M1} (%)	X _{M2} (%)	DP _{M1}	DP _n	F _{M1} (%)	M _n × 10 ³ (g/mol)	M _n × 10 ³ (g/mol)	Đ
C1	25/75	59.8	62.3	90	370	24	46.9	5.7	1.74
C2	50/50	78.6	80.5	236	477	49	73.3	11.9	1.36
C3	75/25	88.1	86.6	396	526	75	95.5	16.7	1.27

M1: TMAMA/Cl, M2: MMA; conditions: C1: [M1+M2]₀: [EBiB]₀: [CuBr]₀: [PMDETA]₀ = 600:1:1:1, 24 h, methanol:THF = 3:1 v/v, where methanol:M1 = 1:1 v/wt., 40 °C; X_{M1} and X_{M2} are conversions of TMAMA/Cl and MMA, respectively; DP_{M1} is polymerization degree of TMAMA/Cl units; DP_n is polymerization degree; F_{M1} is content of TMAMA/Cl fraction in the polymer. ^a deuterated dimethyl sulfoxide (DMSO-d₆), tetramethylsilane (TMS) internal standard; ^b tetrahydrofuran (THF) solvent, polystyrene calibration.

The use of methanol as co-solvent in the reaction mixture can be disadvantageous because of possible transesterification of TMAMA/Cl to MMA as side reaction during polymerization [45,46]. Our previous studies showed that it can be minimized effectively at reduced amount of methanol (1 mL per 1 g of TMAMA) and at higher initial content of TMAMA (≥25%) [38]. Thus the use of optimized conditions of copolymerization, i.e., ratios of TMAMA/MMA (25/75, 50/50, 75/25), and low amount of methanol in the reaction mixture (1 mL per 1 g of TMAMA), allowed excluding transesterification, which was confirmed by the calculated content of ionic fraction (F_{M1}) in the copolymer (it was different from that initial by 1%).

The copolymer structure was confirmed by proton nuclear magnetic resonance (¹H NMR) spectroscopy, which revealed proton signals from methyl groups at 1.4–0.6 ppm and methylene groups at 2.0–1.6 ppm in the main chain (Figure 2). Additionally, signals from methoxy protons at 3.7–3.5 ppm in MMA units, and from oxyethylene and methyl groups in the ammonium cation of TMAMA/Cl units (4H at 4.6–4.1 ppm and 9H groups at 3.4 and 3.3 ppm, respectively) confirmed the incorporation of both monomers into the polymer chain. The ¹H NMR analysis of the reaction mixture allowed for the determination of monomer conversions (Table 1) using the integration of vinyl proton signals assigned to unreacted TMAMA and MMA (6.2–6.1 ppm and 6.1–6.0 ppm, respectively) relative to signals corresponding to the protons in substituents (both reacted and unreacted monomers), i.e., 9H in -(CH₃)₃N⁺ and 3H in -OCH₃, respectively. The conversion values could then be used to calculate the other parameters, including the polymerization degree, the ionic unit contents, and the polymer molecular weight (Table 1). The compositions of the final copolymers C1, C2, and C3 containing 24%, 49%, and 75% TMAMA units, respectively, were guaranteed by properly assumed initial ratio of monomers. The controlled polymerization was also verified by the size-exclusion chromatography (SEC) results, supporting low dispersity indices of the polymers with longer chains (Đ < 1.4 at DP_n > 450). The exception for C1 suggests that a lower reaction rate in a system containing predominantly MMA promoted the occurrence of side reactions (Table 1).

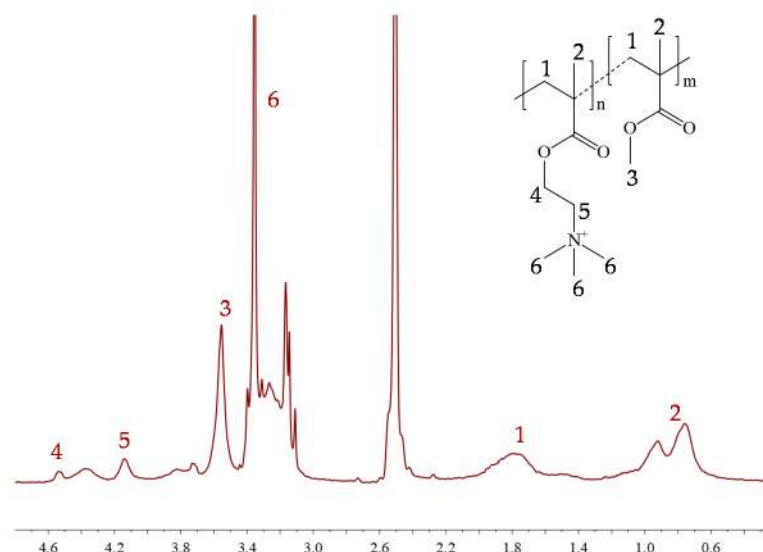


Figure 2. ^1H NMR spectrum of linear copolymer of TMAMA/Cl C1, where n is DP_{M1} and m is DP_{M2} .

The amphiphilic nature of the linear copolymers was investigated via goniometry; specifically, measuring the interfacial tension (IFT) of polymer aqueous solution in a concentration series ($C = 0.008\text{--}0.5\text{ mg/mL}$). The crossing point on a plot of IFT values vs. $\log C$ of measured samples was determined as the critical micelle concentration (CMC; Figure 3a), which defines the polymer's ability to form micellar structures in aqueous solution. The CMC values increased as the content of TMAMA ionic units increased (Figure 3b).

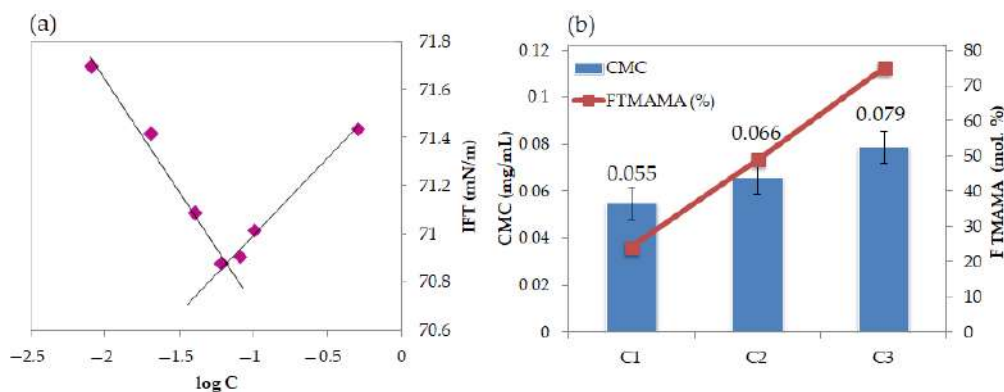


Figure 3. (a) Variation in the interfacial tension with the logarithm of the linear copolymer C2 concentration in aqueous solution at $25\text{ }^\circ\text{C}$; (b) influence of polymer chain length on critical micelle concentration (CMC) value.

The presence of cationic units with chloride counter ions statistically distributed along the polymer chain was advantageous for the anion exchange reaction to generate pharmaceutical activity. The drug in ionic form was introduced to the polymer matrix by dissolving and mixing with the polymer for 48 h. The studied pharmaceutical salts (i.e., sodium or potassium PAS, CLV, PIP, and FUS) were selected based on their antibacterial and bacteriostatic activity. The introduction of pharmaceutical anion (PhA) into chloride based copolymers was analyzed by Fourier-transform infrared spectroscopy (FT-IR), where the characteristic bands were identified. Before anion exchange the chloride copolymers were recognized by the presence of absorption peaks corresponding to C-O and C=O stretching vibration of ester groups (1150 cm^{-1} and 1720 cm^{-1} , respectively), C-H (1450 cm^{-1} , $2800\text{--}3100\text{ cm}^{-1}$), as well as C-N (950 cm^{-1}) in the quaternary nitrogen group of TMAMA units (Figure S1). After anion exchange the new bands appeared at $800\text{--}1000\text{ cm}^{-1}$ and 1600 cm^{-1} (aromatic C=C) due to PAS and PIP, at 1550 cm^{-1} (alkene C=C) due to CLV and

FUS, 1250 cm^{-1} (C-S) due to PIP. Moreover, a broad signal characteristic for O-H and N-H stretching vibrations ($3250\text{--}3600\text{ cm}^{-1}$) was detected as the representative for all types of anions, whereas signal in range of $2845\text{--}3000\text{ cm}^{-1}$ was significantly more intense in the system with CLV due to content of large number of aliphatic and cyclic C-H bonding.

A new characteristic signals assigned to the bonded drugs were also detected in the ^1H NMR spectra (see detailed data of chemical shifts in the Supporting Materials). The protons becoming from the polymer matrix are observed at low ppm region (4.58–0.46 ppm, Figure S2a). After anion exchange to PAS^- the conjugation was confirmed by the presence of signals in the range of 4.9–7.3 ppm, including protons from benzene ring (Figure S2b). In the case of CLV, PIP, and FUS (Figure S2c–e), the protons corresponding to PhA were overlapped with those for the copolymer carrier. Theoretically, the pharmaceutical anions could generate the nucleophilic attack on the carbon of carbonyl group to form carboxylic groups in the copolymer. However, both carboxylic acids and their deprotonated forms are rather weak nucleophiles, thus they should not be effective in the case of the detachment of methyl and 2-trimethylammonium ethyl groups situated at ester bonding. The lack of signal at higher chemical shifts (12–13 ppm) in the ^1H NMR spectra of the ionic conjugates confirms that the acidic hydrolysis was not activated (Figure S2).

The degree of anion exchange was determined based on the drug content (DC), which was evaluated with ultraviolet-visible light spectroscopy (UV-Vis). DC values represent the percentage contribution of pharmaceutical ions in the copolymer (Table 2). In the exchange reactions, the least effective ionic drug was FUS (7–11%), but CLV, PAS, and PIP, demonstrated satisfactory degrees of exchange, reaching levels of 65–95%, 59–82%, and 42–48%, respectively. These results suggest that the nature of the anion has a significant impact on the degree of exchange, and that pharmaceutical compounds with less steric hindrance (i.e., PAS and CLV) were especially beneficial in the anion replacement reaction. Additionally, the drug content was improved when the TMAMA content was increased to 50%, but a larger quantity of ionic units limited the exchange yield (Figure 4). The PIP and FUS anions may have encountered problems finding the chloride exchange sites because they are larger molecules. The structures of PAS, CLV, and PIP contain the nitrogen atoms, which provide their higher coordination number, and they enhance the anion affinity to trimethylammonium substituents. As a result, these pharmaceutical anions were introduced in large amounts. A different effect was noticed in the case of FUS, which is a rigid structure of four conjugated rings, thus exhibiting lower affinity for the hydrophilic moieties. These results are in good correlation with another important factor, which is the water solubility of the salt/anion, which is the most limited for FUS, and then increases in the order $\text{PIP}^- < \text{PAS}^- < \text{CLV}^-$, according to Databank Online.

Table 2. Data for exchanged and released pharmaceutical anion (PhA) in the TMAMA-based polymers.

No.	Drug Exchange				Drug Release			
	DC (%)				Amount of Released PhA (%)			
	(Concentration of Introduced PhA ($\mu\text{g/mL}$))				(Concentration of Released PhA ($\mu\text{g/mL}$))			
	PAS^-	CLV^-	PIP^-	FUS^-	PAS^-	CLV^-	PIP^-	FUS^-
C1	75.8 (16.9)	65.6 (14.6)	42.6 (9.5)	7.8 (1.7)	32.7 (5.3)	5.3 (0.8)	8.1 (0.8)	65.7 (1.1)
C2	82.2 (18.2)	95.3 (21.2)	-	9.7 (2.2)	34.9 (6.4)	9.3 (2.0)	-	21.1 (0.5)
C3	59.3 (6.6)	81.7 (18.1)	47.5 (10.5)	10.7 (2.4)	45.4 (3.0)	7.7 (1.4)	7.3 (0.8)	49.5 (1.2)

DC is drug content; PAS^- is *p*-aminosalicylic, CLV^- is clavulanic, FUS^- is fusidic, and PIP^- is piperacillin anion.

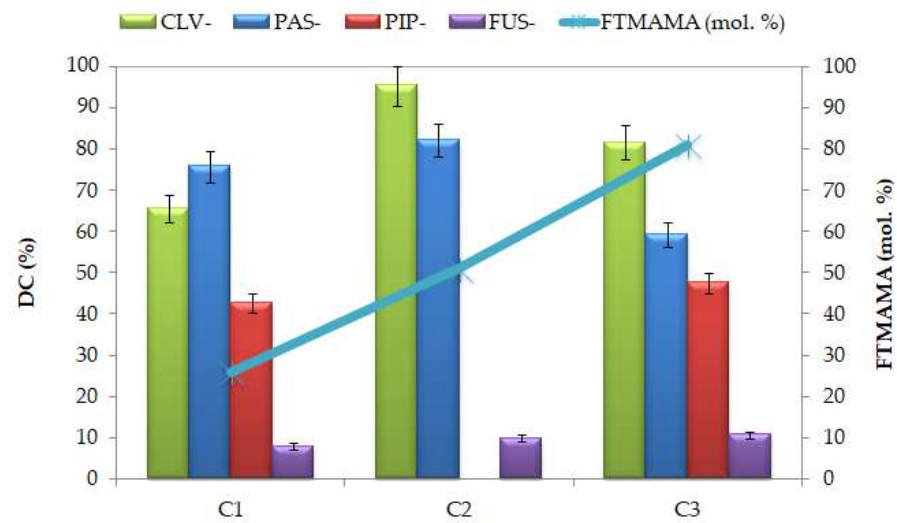


Figure 4. Effect of anion type and content of ionic fractions on the drug content.

The hydrophilicities of the introduced pharmaceutical anions were evaluated by determining the water contact angle via goniometry using the sessile drop method. Aqueous solutions of the polymer systems (0.3 mg/mL in methanol) were applied to thoroughly cleaned glass plates by a spin-coating method, where the centrifugal force allowed for the homogeneous distribution of polymer across the surface to form a film. The water contact angles (WCA) values (presented in Figure 5) showed a decreasing trend with increasing content of ionic units (F_{M1}) for all studied systems, including those with the pharmaceutical anions.

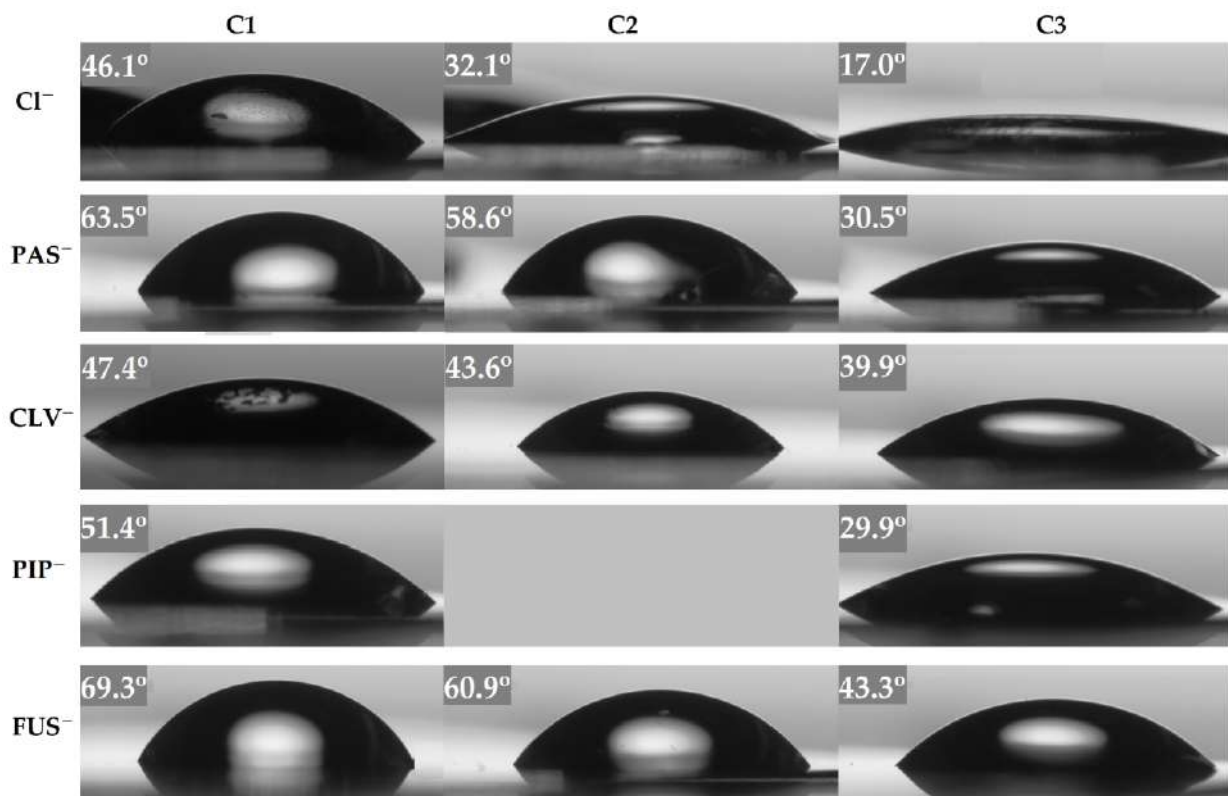


Figure 5. Changes in surface wettability depending on the copolymer and counter-ion, illustrated by goniometry camera.

The WCA values for polymer matrices containing Cl anions changed from 46° to 17°, indicating that they were hydrophilic systems. The same correlation between WCA and TMAMA content has been described previously for graft copolymers with TMAMA units in the side chains [42], but their wettability was lower than that of the linear copolymers studied herein because of the hydrophobic backbone. After anion exchange, the wettability of the polymer films was reduced, yielding higher WCA values relative to their polymer matrices, meaning that the selected drugs did not improve the hydrophilicity of ionic conjugates. Among the tested systems, the FUS-bearing polymers were the most dissimilar (43–69°), although the drug content was the smallest, indicating the specificity of the steroid structure of the introduced anions. Figure 5 shows the visual changes in the contact angles of the individual systems, which illustrate the differences in the wettability of surfaces covered with PIL layers. The composition of the polymer matrix, the type of drug, and the exchange efficiency influence the hydrophilicity of the system. These parameters are also responsible for the ratios of TMAMA/PhA to TMAMA/Cl units present in the polymer chain due to incomplete exchange.

The physicochemical characteristics of the chloride-based copolymers and their ionic drug conjugates were evaluated using dynamic light scattering (DLS) measurements. Before exchange, the hydrodynamic diameters (D_h) of copolymer particles were ranged in 240–300 nm showing no dependency on the ionic content. Copolymer C1 containing PAS and PIP showed similar behavior, forming two equal-volume fractions, with particle sizes of 274 and 12 nm, 291 and 9 nm, respectively. This result indicates that the self-assembled micelles easily aggregated because of the high content of hydrophobic fraction in C1 ($F_{\text{MMA}} = 75\%$). In contrast, C2 and C3 the fraction of smaller particles ($D_h \sim 20$ nm) prevailed (67–80%). Additionally, the particles were characterized by a low size distribution (PDI = 0.38–0.46). In the copolymers with CLV, one dominant fraction was observed (75–80%), wherein the particles reached larger sizes (169–306 nm) and their polydispersity indices were higher (0.8–1). However, C1/CLV particles were smaller than C1 conjugated with PAS or PIP. The formation of large particles as the higher level of self-assemblies was observed due to aggregation effect of micelles in water solution. The self-organized linear TMAMA copolymers probably form the superstructures of entangled chains with statistically distributed ionic and hydrophobic groups, which can be situated in their outer part. Thus, the external hydrophobic moieties participating in the π -stacking interaction and hydrogen bonding between hydrophilic moieties (especially in the conjugates), were responsible for attraction polymer assemblies to result in aggregates (>470 nm, 20%) and super-aggregates (>1000 nm, <10%). The details are presented in Table 3 and illustrated by the DLS histograms in Figure 6.

Table 3. Hydrodynamic diameters of poly(ionic liquid) (PIL) particles determined by dynamic light scattering (DLS) ^a.

No.	Cl ⁻			PAS ⁻			CLV ⁻			PIP ⁻		
	D_h (nm)	f (%)	PDI	D_h (nm)	f (%)	PDI	D_h (nm)	f (%)	PDI	D_h (nm)	f (%)	PDI
C1	239	62.7	0.723	274	49.9	0.605	169	73.4	0.809	291	43.7	0.496
	1–5	35.6		12	47.4		7	20.8		9	48.0	
C2	301	93.9	0.471	24	75.3	0.442	306	80.9	1.000	-	-	-
	5	6.1		926	22.1		15	17.0		-	-	
C3	237	76.3	0.506	20	67.2	0.457	217	75.6	0.791	23	80.5	0.381
	2	23.7		475	20.6		16	23.8		772	19.5	

Where f is an fraction content of particles, ^a measurements based on the intensity at a copolymer concentration in aqueous solution of 1 mg/mL.

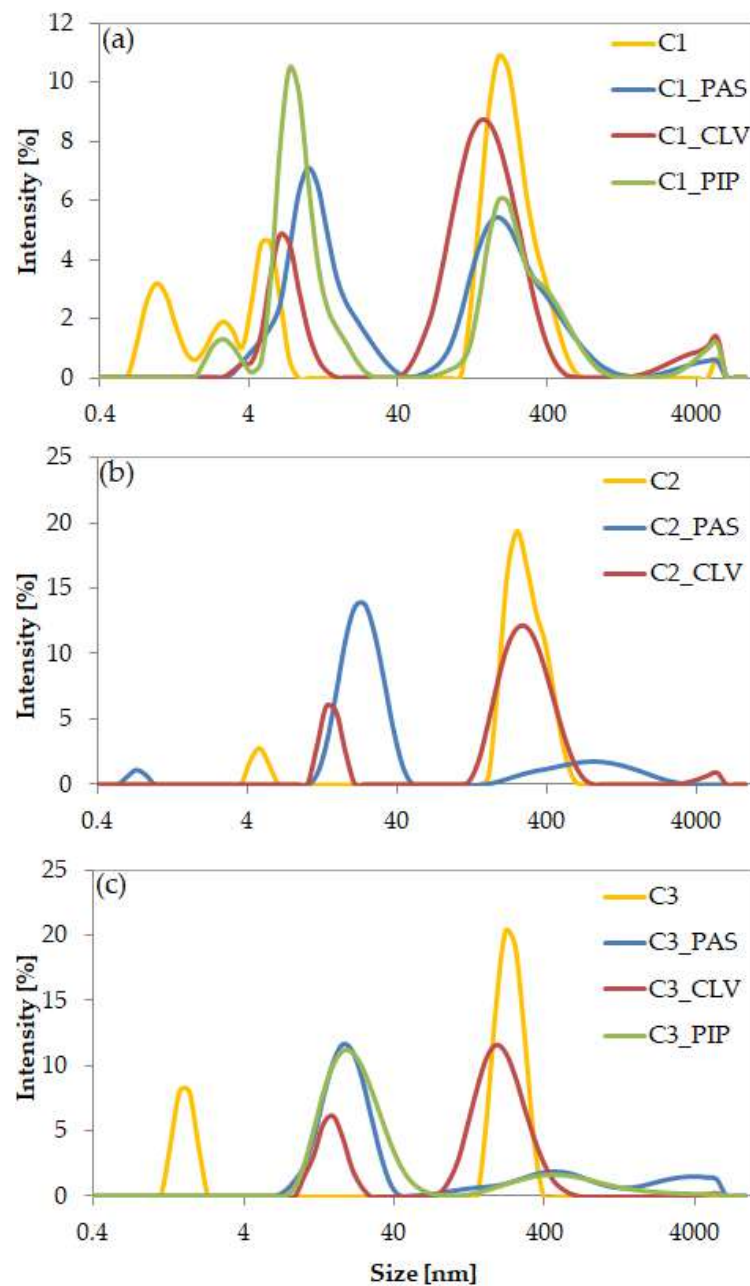


Figure 6. DLS histograms for particles of (a) C1, (b) C2, and (c) C3 systems in deionized water at 25 °C.

The release of the selected drugs in non-ionic forms has been reported for the non-ionic polymers used in the encapsulation of these compounds via physical interactions, for example: poly(ϵ -caprolactone)-*b*-polyethylene glycol-*b*-poly(ϵ -caprolactone) polymersomes with loaded clavulanic acid (16%), which was released in 35% after 24 h and 60% after 170 h [47], poly(ethylene glycol) methyl ether-*b*-poly(lactide-*co*-glycolide) with loaded PIP/tazobactam to design the effective antibiofilm [48], poly(DL-lactic-*co*-glycolic acid) and poly(3-hydroxybutyric acid-*co*-3-hydroxyvaleric acid) microspheres with encapsulated fusidic acid (76–89%), which was released up to 80% [49].

Previous *in vitro* studies into the mechanism of anionic drug release from ionic carriers have indicated that the phosphate anions from phosphate buffered saline (PBS) can exchange with the biologically active anions conjugated to the polymer matrix [36]. Systems based on TMAMA copolymers have been investigated for delivery of salicylate or sulfacetamide counterions [39]. As it was noticed, the anion exchange properties strongly

depended on the nature of both ionic polymer and ionic drug. Thus, the chloride anions were exchanged by the salicylate ones in 50%, and then they were exchanged by phosphates anions in 35–60% demonstrating the “burst” effect within 4 h, whereas in the case of sulfacetamide systems PhA introduction was efficient in 98%, but its release occurred in only 11%.

During drug release via dialysis in PBS (pH = 7.4 in 37 °C), the samples were collected at designated time intervals, and the maximum absorptions of the free pharmaceuticals were measured using UV-Vis. The burst release of PAS[−] and CLV[−] was observed around 1–1.5 h, and the release continued up to 4 h, when small changes in the kinetics profiles resulted in the plateau state. For the systems containing PIP[−] and FUS[−], which have large steric hindrance, the release process occurred over a longer time, as indicated by the visible changes in free drug concentration detected for up to 48 h, especially for PIP systems (Figure 7). Generally, four different release profiles depending on the burst drug release point and more or less suddenly attained plateau are demonstrated. According to that the PAS, FUS, and CLV based systems in comparison to polymers bearing PIP seem to be more effective in the release rate of those anions. The rapid release of the drug in the first 4 h suggests their localization in the external groups, whereas the remaining anions could be trapped inside. This hypothesis can be concluded especially for PIP systems, where the effective drug release followed after 1 h. The remaining drug anions trapped inside the core need higher ionic strength to suppress interactions and then to diffuse through the entangled matrix, which can be additionally limited by the rigidity and steric hindrance of pharmaceutical molecule. The best delivery properties considering both drug content and amount of the released drug were exhibited by PAS systems, because 60–80% of the drug was attached and 33–46% was released. This was associated with a high concentration of released drug (3.0–6.4 µg/mL; Table 2). Although the systems with FUS[−] could exchange large amounts of pharmaceuticals with phosphate anions (21–66%) probably due to repulsive effect magnified by steric structure of FUS, the low drug content (~2 µg/mL) led to a significantly lower concentration of the released drug (0.5–1.2 µg/mL). Low release percentage levels were achieved by the systems containing CLV[−] and PIP[−] (~10%) corresponding to 0.8–2.0 mg/mL, in spite of a relatively large drug contents in CLV[−] and PIP[−] systems (mean ~80% vs. 40%). This opposite behavior in relation to FUS can be also explained by the way of anions conjugation and high stability of conjugates due to strong attraction in entangled core and lower coordination number of phosphate anions.

The previous tested micelles based on TMAMA grafted copolymers formed micelles, where the core was composed mainly of hydrophobic backbone; in turn, the shell included grafted chains with cationic groups. Thus, the pharmaceutical anions were arranged only outside the core. In comparison with linear copolymers, the easier access to the pharmaceutical ions in grafted ones should facilitate drug release, but this aspect is much more composite due to higher stability of the graft polymer with the micelle-like structure. The exchange of Cl[−] onto PAS[−] and CLV[−] in the graft polymer matrix was yielded at 31–64% and 79–100%, respectively, and then the exchange onto phosphate anions was carried out during drug release in 20–42% (3–9 µg/mL from 1 mg of drug conjugates) for PAS and 25–73% (11–31 µg/mL) for CLV within 3 h [42]. These results indicated similar levels of PAS release independently on polymer topology, whereas the percentage amounts of released CLV was ~10 times lower for the linear polymers. The burst effect was much less significant for graft copolymers, especially those with higher grafting degree. It shows that the change in structural parameters of copolymer carrier caused by macromolecule topology can be strategic for individual exchange and release properties for the same pharmaceutical anion.

Different mathematical models were applied to describe the *in vitro* drug release. The fitting levels for kinetics profiles were interpreted by correlation coefficients (R^2), which determined adequate model describing the release mechanisms. The release of PAS, CLV, PIP, and FUS anions represented by first-order kinetics ($R^2 = 0.75–0.95, 0.98, 0.95–0.97, 0.84–0.99$, respectively) indicated the dependence of drug release rate on the

concentration (Figure 8a–d). The Higuchi model, presented as a function of the percentage of remaining anions in relation to the square root of time (Figure 8e–h), was the most fitted for PIP conjugates showing the highest values of the R^2 above 0.97. However, the CLV and FUS systems also achieved good correlation with this model ($R^2 = 0.81$ – 0.99). Hence, it can be postulated that the anion drug release followed diffusion controlled mechanism. Moreover, it was found that the Korsmeyer–Peppas model, which distinguishes Fickian and non-Fickian diffusion estimated by the diffusion exponent (n , calculated from equation $M_t/M = kt^n$, Table S1) similarly to Higuchi model, was also represented by a high fitting degree (0.8–0.99; Figure S3). System C3/PIP indicated the diffusion exponent value in the range of equal $0.45 < n < 0.89$, so the drug release occurred by non-Fickian diffusion, whereas in the case of C1/PIP it was higher than 0.89, which implies non-Fickian super case-II transport. The release of PhA by other systems can be described by quasi-Fickian process ($n \leq 0.45$). These results mean that the diffusion process of released anions is slower than the anion exchange as consequence of the break of ionic bonding between PhA and trimethylammonium moieties in the polymer.

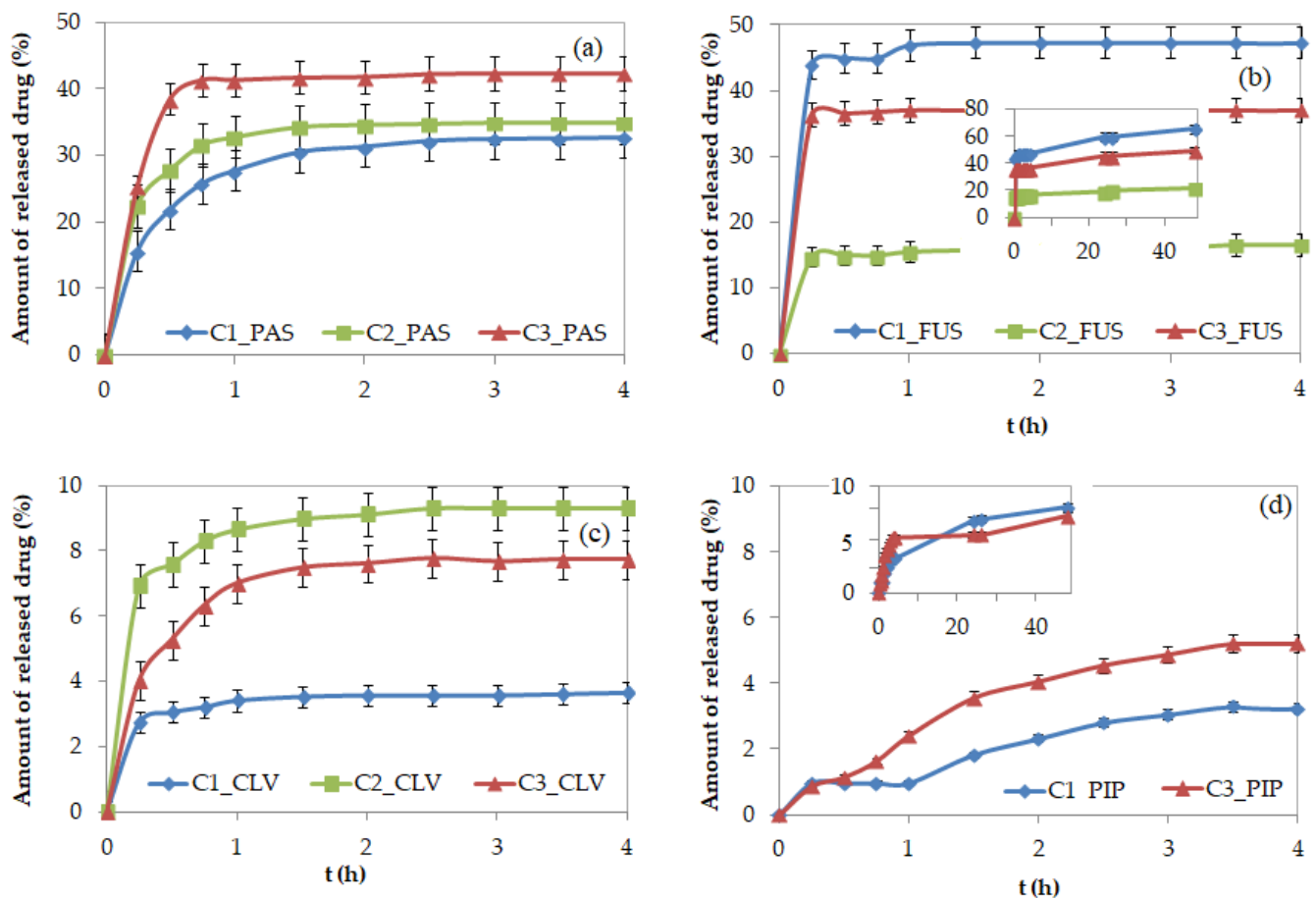


Figure 7. Kinetic release profiles of (a) PAS, (b) FUS, (c) CLV, and (d) PIP anions from conjugates based on PILs.

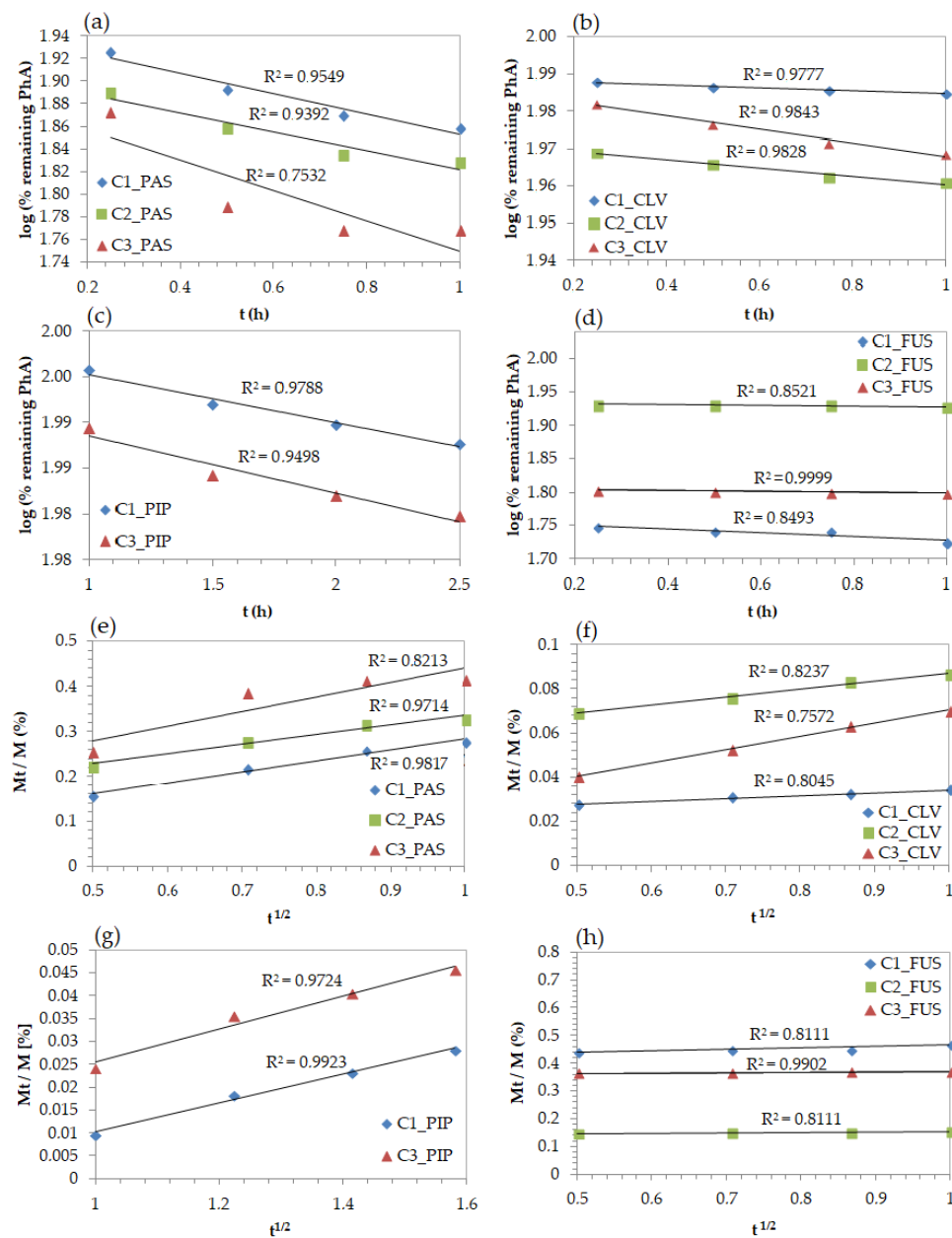


Figure 8. Kinetics profiles by models of first order (a–d), and Higuchi's (e–h) for release of PAS, CLV, PIP, and FUS anions from conjugates based on PILs.

3. Materials and Methods

The methyl methacrylate (MMA; Alfa Aesar, Warsaw, Poland) was dried using molecular sieves (type 4Å, Chempur, Piekary Śląskie, Poland). The [2-(methacryloyloxy)ethyl]-trimethylammonium chloride (TMAMA/Cl; 80% aq. solution, Sigma-Aldrich, Poznań, Poland) was dried to a constant weight under reduced pressure. Methanol and tetrahydrofuran (THF) were purchased from Chempur (Piekary Śląskie, Poland) and dried over the same molecular sieves as MMA. Copper(I) bromide (CuBr; Fluka, 98%, Steinheim, Germany) was purified using a procedure described previously in the literature [42]. *N,N,N',N'',N''*-pentamethyldiethylenetriamine (PMDETA, 98%), ethyl 2-bromoisobutyrate (EBiB, 98%), potassium clavulanate (KCLV), and bis(trifluoromethane)sulfonimide lithium salt (LiTf₂N) were obtained from Sigma Aldrich (Poznań, Polska). Sodium *p*-aminosalicylate (NaPAS, 98%), sodium piperacillin (NaPIP, 99%), and sodium fusidate (NaFUS, 98.8%) were purchased from Alfa Aesar (Warsaw, Poland) and used without further purification.

3.1. Characterization

¹H-NMR spectra were recorded using a UNITY/NOVA spectrometer (300 MHz, Varian, Mulgrave, Victoria, Australia). The measurements were executed in deuterated dimethyl sulfoxide (DMSO-d₆) with tetramethylsilane (TMS) as the internal standard. The molecular weight (M_n) and dispersity index (\mathcal{D}) were estimated using size exclusion chromatography (SEC) in THF (1100 Agilent 1260 Infinity with differential refractometer MDS RI detector, Agilent Technologies, Santa Clara, CA, USA) at 40 °C with a flow rate of 0.8 mL/min using a pre-column guard (5 × 7.5 mm) and a PLGel 5 μm MIXED-C 300 column (7.5 × 300 mm). The calculations were based on polystyrene standards (580–300,000 g/mol). Fourier-transform infrared spectroscopy (FT-IR) was conducted with Spectrum Two 1000 FT-IR Infrared Spectrometer with attenuated total reflection (ATR) (Perkin Elmer, Waltham, MA, USA). The critical micelle concentration (CMC) was determined via interfacial tension measurements of aqueous polymer solutions with concentrations in the range of 8×10^{-3} to 0.5 mg/mL, which were performed with the pendant drop method using a goniometer (OCA 15EC, DataPhysics, Filderstadt, Germany). SCA20_U software was used for data collection and processing. The same software module was also employed for the water contact angle (WCA) measurements carried by the sessile drop method, in which a drop of water (4 μL) was placed on the polymer film. The polymer film was prepared by spin coating the polymer solution in methanol (0.3 mg/mL), which was applied on degreased glass plates. The hydrodynamic diameter (D_h) of particles and polydispersity index (PDI) were measured by dynamic light scattering (DLS) using a Zetasizer Nano-S90 instrument (Malvern Technologies, Malvern, UK). He-Ne laser operated at 4 mW was the source of light scattered at 633 nm. Samples diluted in water (1.0 mg/mL) after filtration (MCE Syringe Filters, hydrophilic M.E. Cellulose membrane with pore diameter: 0.45 μm) were introduced into poly(methyl methacrylate) cells, which were placed in the compartment thermostated at 25 °C. Each measurement was repeated three times to obtain an average value. Data were analyzed using the cumulant method. The drug release process was monitored by ultraviolet-visible spectroscopy (UV-Vis; Evolution 300 spectrometer, Thermo Fisher Scientific, Waltham, MA, USA) on the samples acquired at suitable time intervals. This method allowed the determination of the drug content (DC) and the amount of released pharmaceutical anions (PAS⁻, CLV⁻, PIP⁻, or FUS⁻).

3.2. Synthesis of Linear Copolymers Bearing Cl⁻ (Example for C1)

Comonomers TMAMA (2 g, 9.63 mmol) and MMA (3.08 mL, 28.88 mmol), methanol (3 mL), and THF (1 mL) were added into a Schlenk flask. The mixture was degassed by two freeze-pump-thaw cycles. Then, EBiB (9.52 μL, 0.06 mmol) was added as the ATRP initiator, and the degassing cycle was repeated once again before the initial sample (0.1 mL) was taken. The reaction was catalyzed by a CuBr/PMDETA complex (9.21 mg, 0.06 mmol/13.40 μL, 0.06 mmol). The reaction ran for 24 h at 40 °C and was stopped by exposing the mixture to the air. The polymer was dissolved in methanol and precipitated twice in a chloroform-diethyl ether mixture, then dried under vacuum. ¹H-NMR (300 MHz, DMSO-d₆, ppm): 4.58–4.50 (2H, -O-CH₂-), 4.21–4.08 (2H, -CH₂-N⁺), 3.66–3.46 (3H, -OCH₃), 3.42–3.31 (9H, -N⁺(CH₃)₃), 2.09–1.60 (2H, -CH₂-), 1.40–0.46 (3H, -CH₃).

3.3. Anion Exchange Reaction in Polymer Matrix (Example for C1)

The copolymer C1 (28.11 mg, including 0.05 mmol of ionic units) was dissolved in methanol (1 mL) and mixed with the proper pharmaceutical salt (i.e., NaPAS (11.70 mg, 0.06 mmol), KCLV (11.36 mg, 0.06 mmol), NaFUS (29.86 mg, 0.06 mmol), or NaPIP (29.91 mg, 0.06 mmol)). The reaction was carried out for 48 h. The ionic conjugates with pharmaceutical anions (PhA) were obtained after drying under reduced pressure.

To analyze the molecular weight and dispersity index of the synthesized chloride-containing copolymers (insoluble in standard SEC solvents, including THF), the ion exchange of chloride anions with bistriflimide ions was performed. Copolymer C1 (3.82 mg, including 0.01 mmol of ionic units) was dissolved in methanol, and then, LiTf₂N salt

(2.16 mg, 0.01 mmol) was added. The polymer with exchanged anions (Tf_2N^-) was dried under reduced pressure to give the final product.

3.4. Drug Release of Pharmaceutical Anions

The conjugate with pharmaceutical anions (1.0 mg) was dissolved in 1 mL of phosphate buffered saline (PBS) aqueous solution ($\text{pH} = 7.4$). Then, 1 mL of polymer solution was placed into a dialysis membrane bag ($\text{MWCO} = 3.5 \text{ kDa}$) and put into a glass vial filled with 45 mL PBS. Then, the solution was stirred at 37°C for 48 h. During the drug release, buffer samples (2.5 mL) were collected at consistent time intervals and analyzed on a UV-Vis spectrophotometer. The absorbance of PAS, CLV, FUS, or PIP was measured at 261, 258, 256, or 260 nm, respectively. The quantitative content of the drug in PBS was calculated based on the prepared calibration curve and appointed absorbance maximum wavelengths for the anions with antibacterial activity.

4. Conclusions

Several choline-based copolymers were synthesized by ATRP with different content of ionic units (i.e., 25%, 50%, and 75%), with the ability for self-assembly at CMC below 0.08 mg/mL . The presence of trimethylammonium groups and chloride anions in the main polymer chain was convenient for introducing various pharmaceutical anions with antibacterial properties via an exchange reaction. The resulting conjugates, which act as nanocarriers of ionic drugs, could be applied as oral medicines, owing to their suitable particle sizes (19–306 nm). The conjugated drugs did not exhibit significantly different levels of hydrophilicity in comparison with their chloride matrices, which was confirmed by the wettability of the polymer films evaluated by WCA (the maximum increment was 25°). The developed systems were capable of effectively carrying PAS, CLV, and PIP anions, with contents of 59–82%, 66–95%, and 43–47%, respectively. During the release process, PAS anions were removed by phosphate ions from the polymer systems in the largest amounts (33–46%; 3–6 $\mu\text{g/mL}$). The specific attractive force of CLV and PIP anions to the polymer matrix likely inhibited the release of the drug, and they were replaced at $\sim 10\%$. The low content of FUS anions induced significant release (21–66%). The designed ionic conjugates carrying pharmaceutical anions with antibacterial activity may represent interesting systems with potential applications for lung and respiratory treatment, especially because of their physicochemical characteristics and preliminary drug delivery results.

Supplementary Materials: The following are available online at <https://www.mdpi.com/1422-0067/22/1/284/s1>.

Author Contributions: K.N.: data curation, formal analysis, funding acquisition, investigation, project administration, and writing—original draft; D.N.: conceptualization, methodology, project administration, writing—review and editing, and supervision. All authors have read and agreed to the published version of the manuscript.

Funding: This research was funded by the Polish Budget Funds for Scientific Research in 2020 as core funding for R&D activities in the Silesian University of Technology—funding for young scientists, grant number 04/040/BKM20/0131, and by the National Science Center under the OPUS grant number 2017/27/B/ST5/00960.

Institutional Review Board Statement: Not applicable.

Informed Consent Statement: Not applicable.

Data Availability Statement: Not applicable.

Conflicts of Interest: The authors declare no conflict of interest.

Abbreviations

ATRP	Atom transfer radical polymerization
CLV	Clavulanate
CMC	Critical micelle concentration
DC	Drug content
DDS	Drug delivery system
DLS	Dynamic light scattering
DMSO-d ₆	Deuterated dimethyl sulfoxide
EBiB	Ethyl 2-bromoisobutyrate
FUS	Fusidate
IFT	Interfacial tension
LiTf ₂ N	Bis(trifluoromethane)sulfonimide lithium salt
MMA	Methyl methacrylate
NMR	Nuclear magnetic resonance
PAS	<i>p</i> -Aminosalicylate
PBS	Phosphate buffered saline
PDI	Polydispersity index
PhA	Pharmaceutical anion
PIL	Poly(ionic liquid)
PIP [−]	Piperacillin
PMDETA	<i>N,N,N',N'',N'''</i> -pentamethyldiethylenetriamine
SEC	Size exclusion chromatography
THF	Tetrahydrofuran
TMAMA/Cl	[2-(methacryloyloxy)ethyl]trimethylammonium chloride
TMS	Tetramethylsilane
UV-Vis	Ultraviolet-visible light spectroscopy
WCA	Water contact angle

References

- Deshpande, A.; Rhodes, C.; Shah, N.; Malick, A. Controlled-Release Drug Delivery Systems for Prolonged Gastric Residence: An Overview. *Drug Dev. Ind. Pharm.* **1996**, *22*, 531–539. [[CrossRef](#)]
- Gupta, P.; Vermani, K.; Garg, S. Hydrogels: From controlled release to pH-responsive drug delivery. *Drug Discov. Today* **2002**, *7*, 569–579. [[CrossRef](#)]
- Liechty, W.; Kryscio, D.; Slaughter, B.; Peppas, N. Polymers for Drug Delivery Systems. *Annu. Rev. Chem. Biomol. Eng.* **2010**, *1*, 149–173. [[CrossRef](#)]
- Deb, P.; Kokaz, S.; Abed, S.; Paradkar, A.; Tekade, R. Pharmaceutical and Biomedical Applications of Polymers. In *Advances in Pharmaceutical Product Development and Research, Basic Fundamentals of Drug Delivery*; Tekade, R.K., Ed.; Academic Press: Cambridge, MA, USA, 2019; pp. 203–267.
- Li, H.; Wu, C.; Xia, M.; Zhao, H.; Zhao, M.; Hou, J.; Li, R.; Wei, L.; Zhang, L. Targeted and controlled drug delivery using a temperature and ultra-violet responsive liposome with excellent breast cancer suppressing ability. *RSC Adv.* **2015**, *5*, 27630–27639. [[CrossRef](#)]
- Langer, R.; Peppas, N. Chemical and Physical Structure of Polymers as Carriers for Controlled Release of Bioactive Agents, a Review. *JMS Rev. Macromol. Chem. Phys.* **1983**, *23*, 61–126. [[CrossRef](#)]
- Lee, J.; Yeo, Y. Controlled Drug Release from Pharmaceutical Nanocarriers. *Chem. Eng. Sci.* **2015**, *125*, 75–84. [[CrossRef](#)]
- Zhu, C.; Song, X.; Zhou, W.; Wen, Y.; Wang, X. An efficient cell-targeting and intracellular controlled-release drug delivery system based on MSN-PEM-aptamer conjugates. *J. Mater. Chem.* **2009**, *19*, 7765–7770. [[CrossRef](#)]
- Neugebauer, D.; Mielańczyk, A.; Bielas, R.; Odrobińska, J.; Kupczak, M.; Niesyto, K. Ionic Polymethacrylate Based Delivery Systems: Effect of Carrier Topology and Drug Loading. *Pharmaceutics* **2019**, *11*, 337. [[CrossRef](#)]
- Odrobińska, J.; Niesyto, K.; Erfurt, K.; Siewniak, A.; Mielańczyk, A.; Neugebauer, D. Retinol-Containing Graft Copolymers for Delivery of Skin-Curing Agents. *Pharmaceutics* **2019**, *11*, 378.
- Kohay, H.; Can Sarisozen, C.; Sawant, R.; Jhaveri, A.; Torchilin, V.; Mishael, Y. PEG-PE/Clay Composite Carriers for Doxorubicin: Effect of Composite Structure on Release, Cell Interaction and Cytotoxicity. *Acta Biomater.* **2017**, *55*, 443–454. [[CrossRef](#)]
- Qing, G.; Li, M.; Deng, L.; Lv, Z.; Ding, P.; Sun, T. Smart Drug Release Systems Based on Stimuli-Responsive Polymers. *Mini Rev. Med. Chem.* **2012**, *12*, 1–12. [[CrossRef](#)]
- Choi, S.; Zhang, Y.; Xia, Y. A Temperature-Sensitive Drug Release System Based on Phase-Change materials. *Angew. Chem. Int. Ed.* **2010**, *49*, 7904–7908. [[CrossRef](#)] [[PubMed](#)]
- Zhang, X.; Zhuo, R.; Cui, J.; Zhang, J. A novel thermo-responsive drug delivery system with positive controlled release. *Int. J. Pharm.* **2002**, *235*, 43–50. [[CrossRef](#)]

15. Garcia, M.C. Ionic-strength-responsive polymers for drug delivery applications. In *Stimuli Responsive Polymeric Nanocarriers for Drug Delivery Applications*; Makhlof, A.S., Ed.; Elsevier: Amsterdam, The Netherlands, 2018; pp. 393–409.
16. Tang, H.; Zhao, W.; Yu, J.; Li, Y.; Zhao, C. Recent Development of pH-Responsive Polymers for Cancer Nanomedicine. *Molecules* **2019**, *24*, 4. [[CrossRef](#)]
17. Abdollahi, A.; Roghani-Mamaqani, H.; Razavi, B.; Salami-Kalajahi, M. The light-controlling of temperature-responsivity in stimuli-responsive polymers. *Polym. Chem.* **2019**, *10*, 5686–5720. [[CrossRef](#)]
18. Anand, V.; Kandarapu, R.; Garg, S. Ion-exchange resins: Carrying drug delivery forward. *Drug Discov. Today* **2001**, *6*, 905–914. [[CrossRef](#)]
19. Ekladios, I.; Colson, Y.; Grinstaff, M. Polymer-drug conjugate therapeutics: Advances, insights and prospects. *Nat. Rev. Drug Discov.* **2019**, *18*, 273–294. [[CrossRef](#)]
20. Kumar, L.; Verma, S.; Vaidya, B.; Mehra, N. Nanocarrier-Assisted Antimicrobial Therapy Against Intracellular Pathogens. In *Nanostructures for Antimicrobial Therapy*; Ficai, A., Grumezescu, A.M., Eds.; Elsevier: Amsterdam, The Netherlands, 2017; pp. 293–324.
21. Yokoyama, M.; Kwon, G.; Okano, T.; Sakurai, Y.; Seto, T.; Kataoka, K. Preparation of Micelle-Forming Polymer-Drug Conjugates. *Bioconjugate Chem.* **1992**, *3*, 295–301. [[CrossRef](#)]
22. He, C.; Tang, Z.; Tian, H.; Chen, X. Co-delivery of chemotherapeutics and proteins for synergistic therapy. *Adv. Drug Deliv. Rev.* **2016**, *98*, 64–76. [[CrossRef](#)]
23. Sun, J.; Chen, Y.; Huang, Y.; Zhao, W.; Liu, Y.; Venkataramanan, R.; Lu, B.; Li, S. Programmable co-delivery of the immune checkpoint inhibitor NIG919 and chemotherapeutic doxorubicin via a redox-responsive immunostimulatory polymeric prodrug carrier. *Acta. Pharmacol. Sin.* **2017**, *38*, 823–834. [[CrossRef](#)]
24. Larson, N.; Ghandehari, H. Polymeric Conjugates for Drug Delivery. *Chem. Mater.* **2012**, *24*, 840–853. [[CrossRef](#)] [[PubMed](#)]
25. Pasut, G.; Veronese, F. Polymer–drug conjugation, recent achievements and general strategies. *Prog. Polym. Sci.* **2007**, *32*, 933–961. [[CrossRef](#)]
26. Yu, Y.; Chen, C.-K.; Law, W.-C.; Mok, J.; Zou, J.; Prasad, P.N.; Cheng, C. Well-Defined Degradable Brush Polymer–Drug Conjugates for Sustained Delivery of Paclitaxel. *Mol. Pharm.* **2013**, *10*, 867–874. [[CrossRef](#)] [[PubMed](#)]
27. Mielańczyk, A.; Neugebauer, D. Designing Drug Conjugates Based on Sugar Decorated V-Shape and Star Polymethacrylates: Influence of Composition and Architecture of Polymeric Carrier. *Bioconjugate Chem.* **2015**, *26*, 2303–2310. [[CrossRef](#)]
28. Araújo, J.; Florindo, C.; Pereiro, A.; Vieira, N.; Matias, A.; Duarte, C.; Marrucho, I. Cholinium-based ionic liquids with pharmaceutically active anions. *RSC Adv.* **2014**, *4*, 28126–28132. [[CrossRef](#)]
29. Islam, R.; Chowdhury, R.; Wakabayashi, R.; Tahara, Y.; Kamiya, N.; Moniruzzaman, M.; Goto, M. Choline and amino acid based biocompatible ionic liquid mediated transdermal delivery of the sparingly soluble drug acyclovir. *Int. J. Pharm.* **2020**, *582*, 119335. [[CrossRef](#)]
30. Islam, R.; Chowdhury, R.; Wakabayashi, R.; Kamiya, N.; Moniruzzaman, M.; Goto, M. Ionic Liquid-In-Oil Microemulsions Prepared with Biocompatible Choline Carboxylic Acids for Improving the Transdermal Delivery of a Sparingly Soluble Drug. *Pharmaceutics* **2020**, *12*, 392. [[CrossRef](#)]
31. Tanner, E.; Curreri, A.; Balkaran, J.; Selig-Wober, N.; Yang, A.; Kendig, C.; Fluhr, M.; Kim, N.; Mitragotri, S. Design Principles of Ionic Liquids for Transdermal Drug Delivery. *Adv. Mater.* **2019**, *31*, 1901103. [[CrossRef](#)]
32. Boethling, R.; Sommer, E.; DiFiore, D. Designing Small Molecules for Biodegradability. *Chem. Rev.* **2007**, *107*, 2207–2227. [[CrossRef](#)]
33. Jameson, E.; Quareshy, M.; Chem, Y. Methodological considerations for the identification of choline and carnitine-degrading bacteria in the gut. *Methods* **2018**, *149*, 42–48. [[CrossRef](#)]
34. Iwasaki, Y.; Ishihara, K. Cell membrane-inspired phospholipid polymers for developing medical devices with excellent biointerfaces. *Sci. Technol. Adv. Mater.* **2012**, *13*, 064101. [[CrossRef](#)] [[PubMed](#)]
35. Lewis, A.; Tang, Y.; Brocchini, S.; Choi, J.; Godwin, A. Poly(2-methacryloyloxyethyl phosphorylcholine) for Protein Conjugation. *Bioconjugate Chem.* **2008**, *19*, 2144–2155. [[CrossRef](#)] [[PubMed](#)]
36. Hu, G.; Emrick, T. Functional Choline Phosphate Polymers. *J. Am. Chem. Soc.* **2016**, *138*, 1828–1831. [[CrossRef](#)] [[PubMed](#)]
37. Shiga, T.; Mori, H.; Uemura, K.; Moriuchi, R.; Dohra, H.; Yamawaki-Ogata, A.; Narita, Y.; Saito, A.; Kotsuchibashi, Y. Evaluation of the Bactericidal and Fungicidal Activities of Poly([2-(methacryloyloxy)ethyl]trimethyl Ammonium Chloride)(Poly (METAC))-Based Materials. *Polymers* **2018**, *10*, 947. [[CrossRef](#)] [[PubMed](#)]
38. Bielas, R.; Mielańczyk, A.; Siewniak, A.; Neugebauer, D. Trimethylammonium-based polymethacrylate ionic liquids with tunable hydrophilicity and charge distribution as carriers of salicylate anions. *ACS Sustain. Chem. Eng.* **2016**, *4*, 4181–4191. [[CrossRef](#)]
39. Bielas, R.; Siewniak, A.; Skonieczna, M.; Adamiec, M.; Mielańczyk, Ł.; Neugebauer, D. Choline based polymethacrylate matrix with pharmaceutical cations as co-delivery system for antibacterial and anti-inflammatory combined therapy. *J. Mol. Liq.* **2019**, *285*, 114–122. [[CrossRef](#)]
40. Bielas, R.; Łukowiec, D.; Neugebauer, D. Drug delivery via anion exchange of salicylate decorating poly(meth)acrylates based on pharmaceutical ionic liquid. *New J. Chem.* **2017**, *21*, 12801–12807. [[CrossRef](#)]
41. Bielas, R.; Mielańczyk, A.; Skonieczna, M.; Mielańczyk, Ł.; Neugebauer, D. Choline supported poly(ionic liquid) graft copolymers as novel delivery systems of anionic pharmaceuticals for anti-inflammatory and anti-coagulant therapy. *Sci. Rep.* **2019**, *9*, 14410. [[CrossRef](#)]

42. Niesyto, K.; Neugebauer, D. Synthesis and Characterization of Ionic Graft Copolymers: Introduction and In Vitro Release of Antibacterial Drug by Anion Exchange. *Polymers* **2020**, *12*, 2159. [[CrossRef](#)]
43. Hosseinzadeh, F.; Mahkam, M.; Galehassadi, M. Synthesis and characterization of ionic liquid functionalized polymers for drug delivery of an anti-inflammatory drug. *Des. Monomers Polym.* **2012**, *15*, 279–388. [[CrossRef](#)]
44. Gorbunova, M.; Lemkina, L.; Borisova, I. New guanidine-containing polyelectrolytes as advanced antibacterial materials. *Eur. Polym. J.* **2018**, *105*, 426–433. [[CrossRef](#)]
45. Li, Y.; Armes, S.; Jin, X.; Zhu, S. Direct Synthesis of Well-Defined Quaternized Homopolymers and Diblock Copolymers via ATRP in Protic Media. *Macromolecules* **2003**, *36*, 8268–8275. [[CrossRef](#)]
46. Visnevskij, C.; Makuska, R. SARA ATRP in Aqueous Solutions Containing Supplemental Redox Intermediate: Controlled Polymerization of [2- (Methacryloyloxy)ethyl] trimethylammonium Chloride. *Macromolecules* **2013**, *46*, 4764–4771. [[CrossRef](#)]
47. Danafar, H. Preparation and characterization of PCL-PEG-PCL polymersomes for delivery of clavulanic acid. *Cogent. Med.* **2016**, *3*, 1235245. [[CrossRef](#)]
48. Morteza, M.; Roya, S.; Hamed, H.; Amir, Z.; Abolfazl, A. Synthesis and evaluation of polymeric micelle containing piperacillin/tazobactam for enhanced antibacterial activity. *Drug Deliv.* **2019**, *26*, 1292–1299. [[CrossRef](#)] [[PubMed](#)]
49. Yang, C.; Plackett, D.; Needham, D.; Burt, H. PLGA and PHBV Microsphere Formulations and Solid-State Characterization: Possible Implications for Local Delivery of Fusidic Acid for the Treatment and Prevention of Orthopaedic Infections. *Pharm. Res.* **2009**, *26*, 1644–1656. [[CrossRef](#)]

Linear copolymers based on choline ionic liquid carrying anti-tuberculosis drugs: influence of anion type on physicochemical properties and drug release

Katarzyna Niesyto ¹, Dorota Neugebauer ^{1*}

¹ Department of Physical Chemistry and Technology of Polymers, Faculty of Chemistry, Silesian University of Technology, 44-100 Gliwice, Poland

* Correspondence: Dorota.Neugebauer@polsl.pl

Content:

Figure S1. FT-IR spectra for C1 copolymer and its conjugates with PAS, CLV, PIP and FUS.

Figure S2. ¹H NMR spectra of (a) linear copolymer C1 vs (b) PAS, (c) CLV, (d) PIP and (e) FUS contained conjugates.

Figure S3. Kinetics profiles by Korsmeyer-Peppas model for release of (a) PAS, (b) CLV, (c) PIP, and (d) FUS anions from conjugates based on PILs.

Table S1. Fitting and diffusion coefficients of drug release kinetics by Korsmeyer-Peppas model.

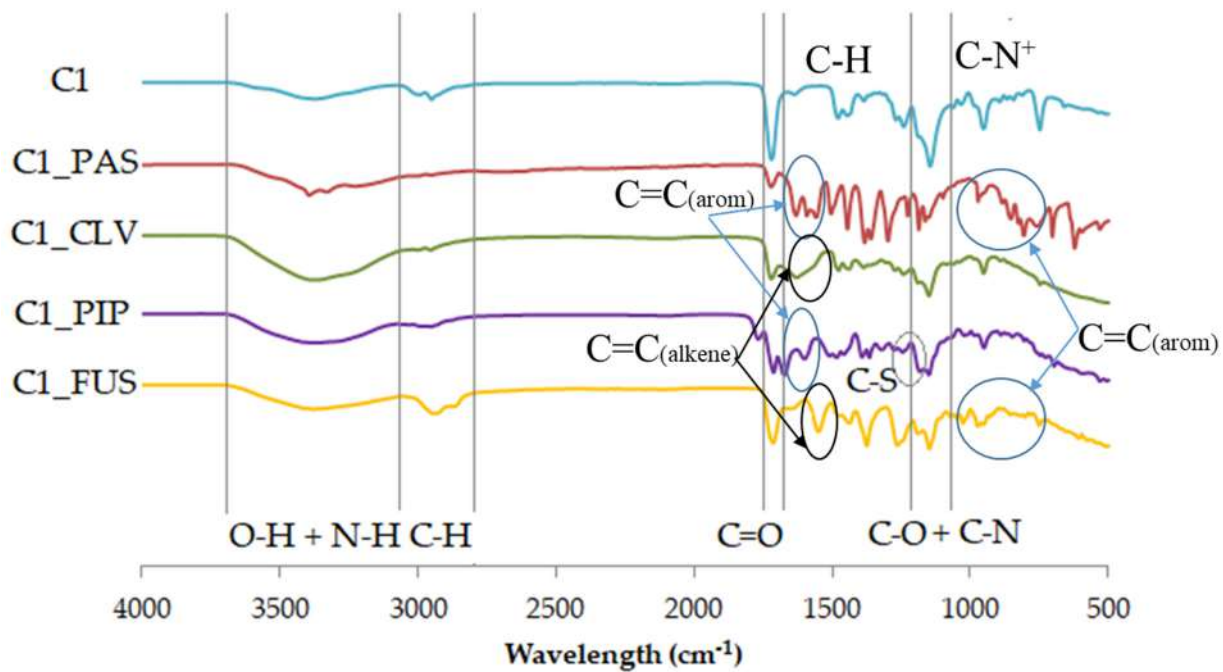


Figure S1. FT-IR spectra for C1 copolymer and its conjugates with PAS, CLV, PIP and FUS.

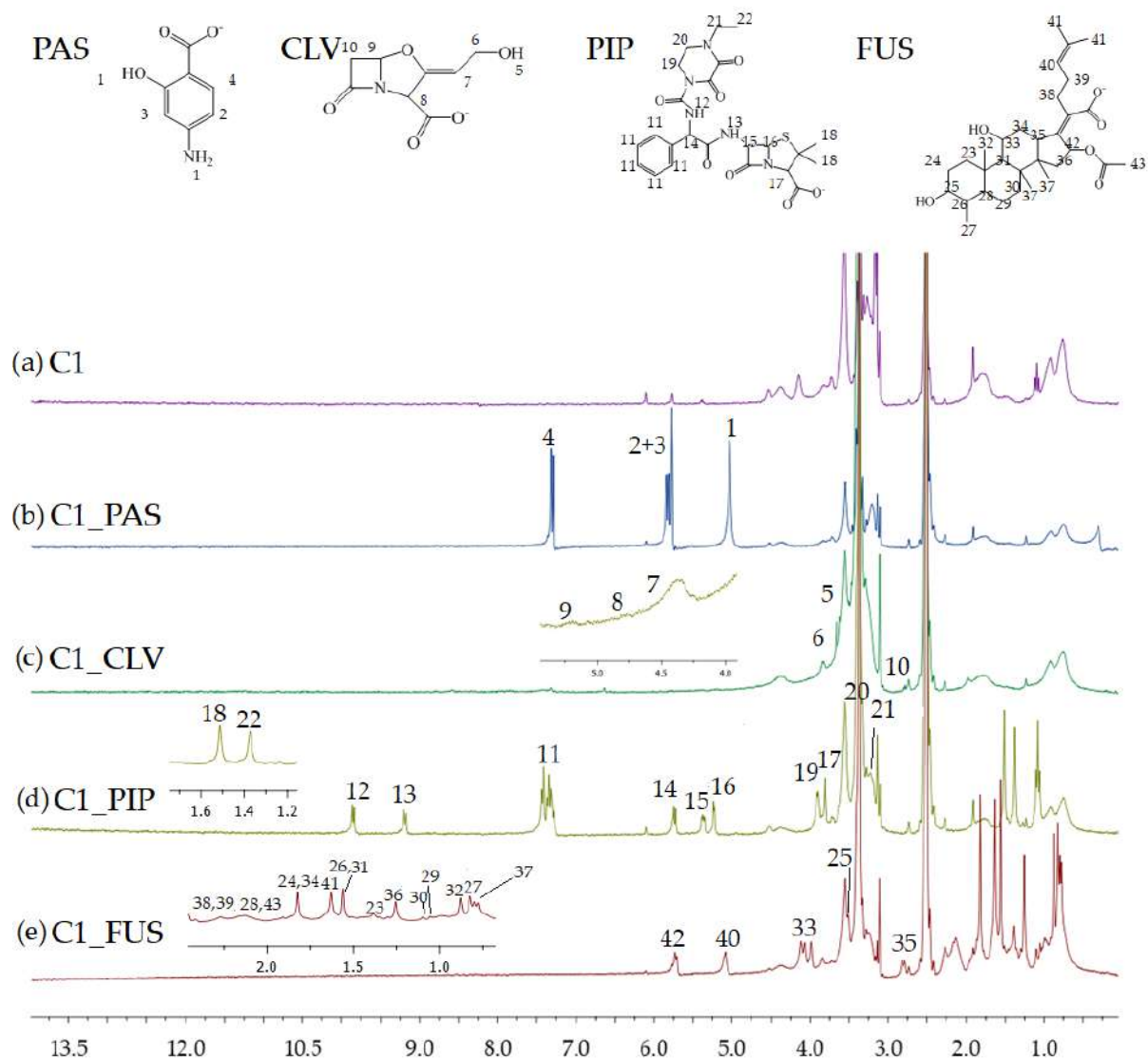


Figure S2. ^1H NMR spectra of (a) linear copolymer C1 vs (b) PAS, (c) CLV, (d) PIP and (e) FUS contained conjugates.

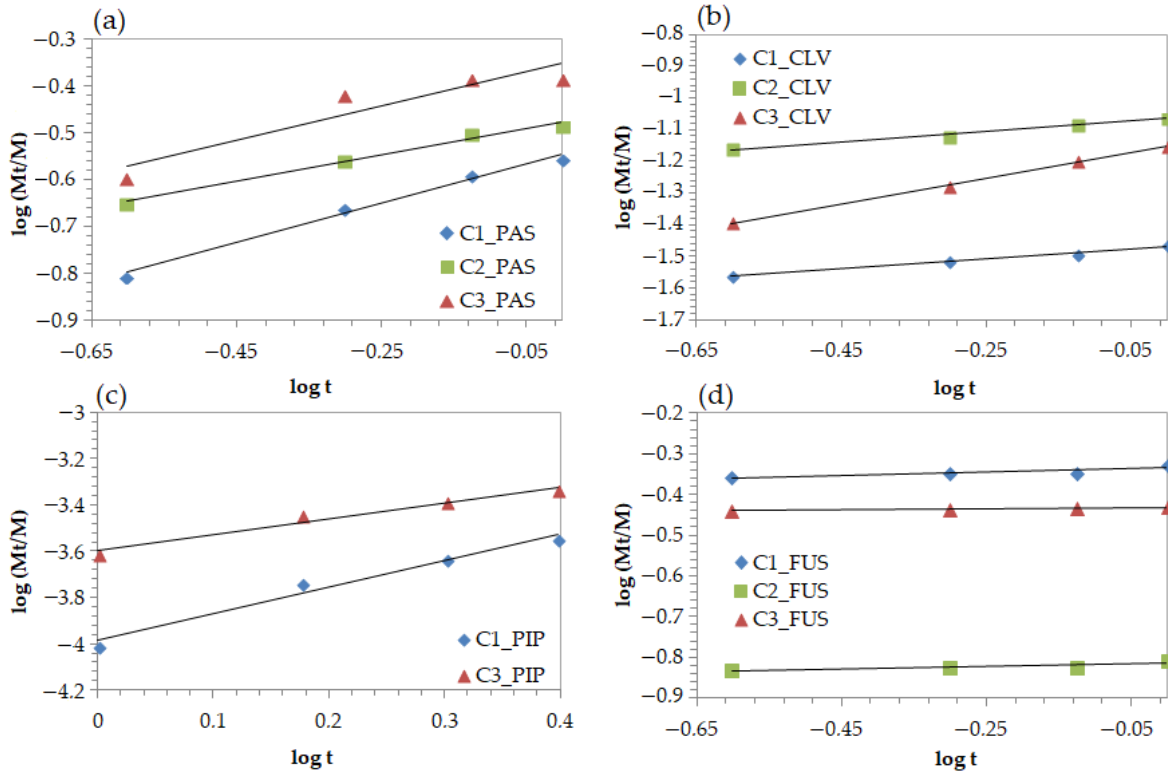


Figure S3. Kinetics profiles by Korsmeyer-Peppas model for release of (a) PAS, (b) CLV, (c) PIP, and (d) FUS anions from conjugates based on PILs.

Table S1. Fitting and diffusion coefficients of drug release kinetics by Korsmeyer-Peppas model.

No.	PAS ⁻		CLV ⁻		PIP ⁻		FUS ⁻	
	R ²	n	R ²	n	R ²	n	R ²	n
C1	0.9887	0.4233	0.9950	0.1551	0.9723	1.1499	0.7667	0.0402
C2	0.9866	0.2838	0.9877	0.1635	-	-	0.7654	0.0324
C3	0.8735	0.3644	0.9988	0.4035	0.9652	0.6870	0.9619	0.0140

PUBLIKACJA P.3

Dual-Drug Delivery via the Self-Assembled Conjugates of Choline-Functionalized Graft Copolymers.

Niesyto, K., Mazur, A., Neugebauer, D.

Materials 2022, 15, 4457

Article

Dual-Drug Delivery via the Self-Assembled Conjugates of Choline-Functionalized Graft Copolymers

Katarzyna Niesyto , Aleksy Mazur and Dorota Neugebauer * 

Department of Physical Chemistry and Technology of Polymers, Faculty of Chemistry, Silesian University of Technology, 44-100 Gliwice, Poland; katarzyna.niesyto@polsl.pl (K.N.); aleksy.mazur@gmail.com (A.M.)

* Correspondence: dneugebauer@polsl.pl

Abstract: Graft copolymers based on a choline ionic liquid (IL), [2-(methacryloyloxy)ethyl]-trimethylammonium chloride (TMAMA), were obtained by atom transfer radical polymerization. The presence of chloride counterions in the trimethylammonium groups promoted anion exchange to introduce fusidate anions (FUS, 32–55 mol.%) as the pharmaceutical anions. Both the choline-based IL copolymers and their ionic drug-carrier conjugates (FUS systems as the first type, 26–208 nm) formed micellar structures (CMC = 0.011–0.025 mg/mL). The amphiphilic systems were advantageous for the encapsulation of rifampicin (RIF, 40–67 mol.%), a well-known antibiotic, resulting in single-drug (RIF systems as the second type, 40–95 nm) and dual-drug systems (FUS/RIF as the third type, 31–65 nm). The obtained systems released significant amounts of drugs (FUS > RIF), which could be adjusted by the content of ionic units and the length of the copolymer side chains. The dual-drug systems released 31–55% FUS (4.3–5.6 µg/mL) and 19–31% RIF (3.3–4.0 µg/mL), and these results were slightly lower than those for the single-drug systems, reaching 45–81% for FUS (3.8–8.2 µg/mL) and 20–37% for RIF (3.4–4.0 µg/mL). The designed polymer systems show potential as co-delivery systems for combined therapy against drug-resistant strains using two drugs in one formula instead of the separate delivery of two drugs.

Keywords: graft copolymers; dual-drug delivery systems; polymer carriers



Citation: Niesyto, K.; Mazur, A.; Neugebauer, D. Dual-Drug Delivery via the Self-Assembled Conjugates of Choline-Functionalized Graft Copolymers. *Materials* **2022**, *15*, 4457. <https://doi.org/10.3390/ma15134457>

Academic Editors: Diganta B. Das and Fernando Gomes de Souza Junior

Received: 27 May 2022

Accepted: 21 June 2022

Published: 24 June 2022

Publisher's Note: MDPI stays neutral with regard to jurisdictional claims in published maps and institutional affiliations.



Copyright: © 2022 by the authors. Licensee MDPI, Basel, Switzerland. This article is an open access article distributed under the terms and conditions of the Creative Commons Attribution (CC BY) license (<https://creativecommons.org/licenses/by/4.0/>).

1. Introduction

Polymer nanocarriers have recently gained enormous attention due to their potential applications as fluorescent biosensors and markers [1,2], as well as in drug delivery systems (DDSs) [3–6]. A wide range of biocompatible polymer matrices can be pre-designed, and their properties can be adjusted to meet the specific needs of a given carrier [7]. Controlled drug release, with a limited increase in drug concentration in the body, is one of the main advantages of nanocarriers [8–10]. Generally, DDSs are used to improve the effectiveness of standard drugs and conventional treatments.

Depending on a polymer's structure, drugs can be bound to a nanocarrier in various ways. Amphiphilic polymers are composed of hydrophobic and hydrophilic units, which allow them to form micellar structures, in which a drug can be physically encapsulated into the core [11,12]. Such structures can be obtained by coupling polymer segments or via the copolymerization of monomers with different solubilities. Of particular note are amphiphilic copolymers based on ionic liquids (ILs), which are considered to be green solvents. Due to their unique properties, such as chemical and thermal stability and high ionic conductivity, they have been applied in various industries [13,14]. The most important properties of DDSs are the high biocompatibility and low toxicity of many ILs, which can improve the pharmacokinetic and pharmacodynamic properties of the drugs being transported [15–17]. Some of them, i.e., cholinium-based ILs, show biological functions [18–21]. Micelles based on IL (co)polymers have been studied for the encapsulation

and delivery of various active pharmaceutical ingredients (APIs), e.g., erythromycin, indomethacin, quercetin [22], curcumin [23,24], acyclovir [25], paclitaxel [26], dopamine [27], and doxorubicin [28,29].

The ionic structure of IL-based polymers can be applied for ionic exchange. This approach enables the introduction of APIs in ionic form into a polymer to produce ionic conjugates. Various cations, such as imidazolium, lidocainum, cholinium, and guanidinium, have been employed in polymers to carry ionic ibuprofenate [30,31], ampicillin [32,33], (acetyl)salicylate, or aspirin [34]. In the case of a matrix decorated with cholinium ILs, there are reports of anion exchange and the delivery of various anions based on mefenamic acid [35,36], nalidixic, niflumic, pyrazinoic, and picolinic acids [37], salicylate [22,38], *p*-aminosalicylate, clavulanate [39], fusidate, and piperacillin [40]. The aforementioned systems have focused on delivering a single drug introduced via encapsulation or ion exchange. The specificity of IL-based polymers that also exhibit amphiphilicity favors the combination of both of these abilities to obtain systems with a dual pharmacological action. In this case, the biological activity of the polyIL (PIL) conjugate conferred by the ionic drug can be doubled by encapsulating a second drug (non-ionic) into the micelle core.

Herein, we report PIL grafted copolymers as the matrices for innovative dual-drug delivery systems based on micelles of ionic conjugates (Figure 1). These systems are advantageous, especially for combined therapies. For this purpose, our previously designed graft copolymers based on a polymerizable IL, [2-(methacryloyloxy)ethyl]trimethylammonium chloride (TMAMA) [39], were applied. This IL-monomer was chosen due to the presence of a biologically active choline group, its advantageous non-toxicity, and its high biocompatibility. Cytotoxicity tests indicated the non-toxic action of IL-graft copolymers against normal BEAS-2B cell lines. Moreover, their selective biological action was observed versus normal and lung cancer cell lines [21]. Furthermore, the ionic structure of IL units was convenient for the ionic exchange reaction, which in this study, was used to introduce fusidate anions (FUS^-) into the side chains of the copolymer. The selected API anion corresponds to fusidic acid, which is a natural bacteriostatic antibiotic with a steroidal structure that can inhibit the synthesis of bacterial proteins. This drug is also used in the treatment of lung diseases due to its effective action against strains of, e.g., *Staphylococcus aureus*, *Bordetella pertussis*, *Mycobacterium leprae*, and *Mycobacterium tuberculosis*. The amphiphilicity of polymer-FUS conjugates encouraged us to encapsulate the antibacterial drug, rifampicin (RIF), which is conventionally applied for the treatment of tuberculosis. Bacterial resistance has been frequently noticed during treatment with fusidic acid alone; hence, a combination therapy based on drugs containing fusidic acid (and its sodium salt) and rifampicin was used to obtain a better treatment effect. However, a formulation containing both rifampicin and fusidate is not commercially available, and they are currently used as separate medicines, i.e., Rifampicin TZF and Fucidin[®]. In our studies, the efficiencies of dual DDSs (RIF/ FUS^-) were compared with the single DDSs (micellar with RIF vs. ionic conjugate with FUS^-) by monitoring the content of the drugs and their *in vitro* release under conditions approximate to human fluids (phosphate-buffered saline, PBS at pH = 7.4) to show the improved applicability in relation to their single-drug carrier analogs.

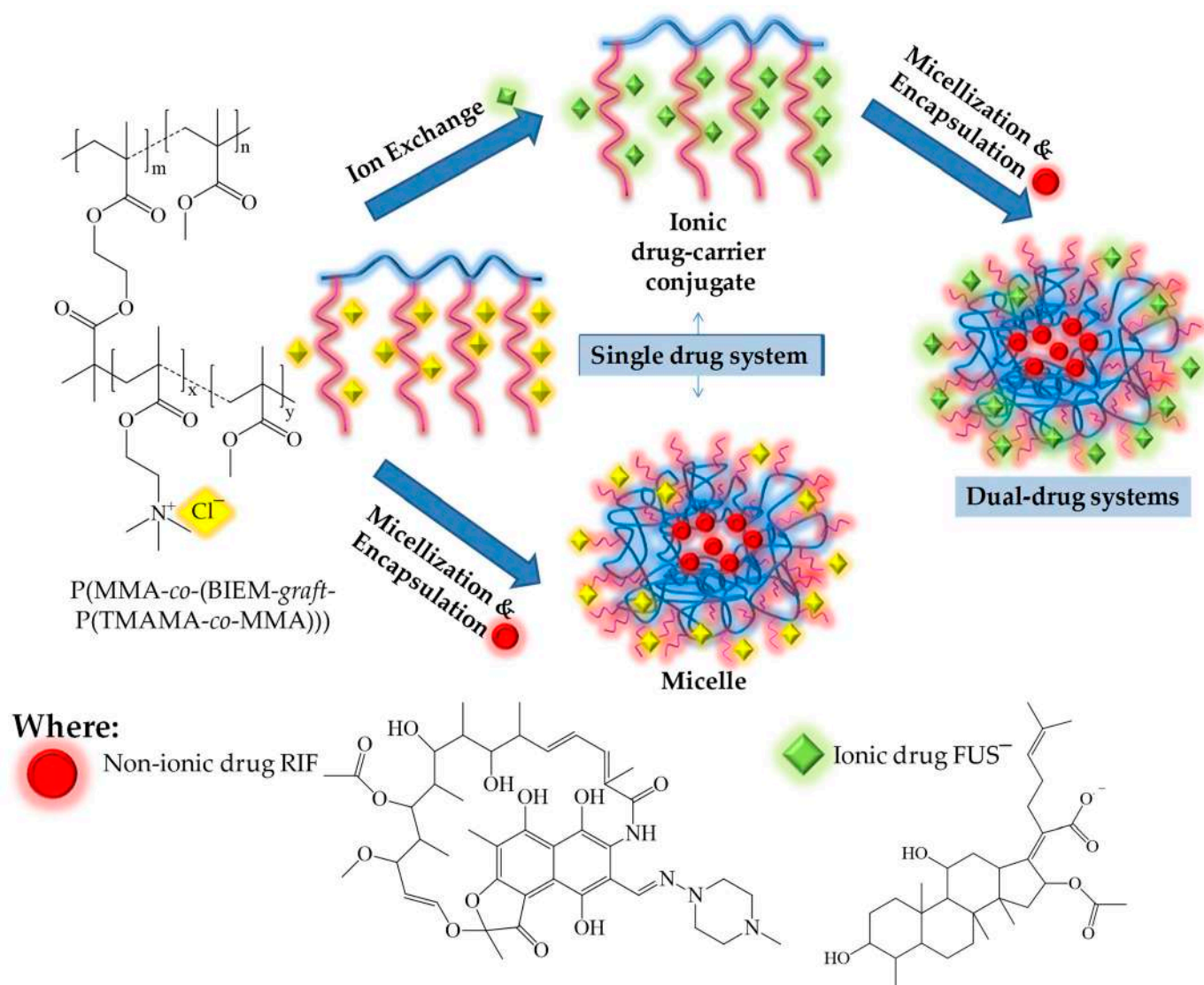


Figure 1. Schematic route of the amphiphilic graft copolymer based on TMAMA and various types of drug carriers.

2. Materials and Methods

Methyl methacrylate (MMA, Alfa Aesar, Warsaw, Poland) and [2-(methacryloyloxy)ethyl]trimethylammonium chloride (TMAMA, 80% aq. solution, Sigma-Aldrich, Poznan, Poland) were dried using molecular sieves or under vacuum, respectively. Copper(I) chloride (CuCl, Fluka, 98%, Steinheim, Germany) was purged according to procedures described previously [39]. Methanol was obtained from Chempur (Piekary Śląskie, Poland). Rifampicin (RIF, 97%) and sodium fusidate (FUS, 98.8%) were purchased from Alfa Aesar (Warsaw, Poland) and used without prior purification. Phosphate-buffered saline (PBS), 2,2'-bipyridine (bpy), and tetrahydrofuran (THF) were obtained from Sigma-Aldrich (Poznań, Poland).

2.1. Synthesis of Ionic Graft Copolymers Bearing Cl⁻ or FUS⁻

The preparation of copolymers of methyl methacrylate and 2-(2-bromoisobutyryloxy)ethyl methacrylate (P(MMA-co-BIEM)) with different contents of bromoester active groups (25% or 50%), which were used as the multifunctional macroinitiators (MI) in a “grafting-from” strategy, have been described previously [39].

Comonomers TMAMA (1.80 g, 8.66 mmol), MMA (0.913 mL, 8.57 mmol), methanol (2 mL), THF (1 mL), MI with 25% of initiating bromoester groups (97.17 mg), and bpy (27.07 mg, 0.18 mmol) were placed into a Schlenk flask. Two freeze-pump-thaw cycles were carried out, and then the catalyst CuCl (12.91 mg, 0.08 mmol) was added to the mixture. The reaction was carried out at 40 °C for 2 h. The reaction was stopped by exposing the mixture to air. The polymer was precipitated in a chloroform–diethyl ether mixture and then dried under vacuum.

The obtained graft copolymer I (21.0 mg, including 0.06 mmol of TMAMA units) was dissolved in 1 mL of methanol. Next, the sodium salt of fusidic acid (FUS, 29.8 mg; 0.06 mmol) was inserted into the polymer solution. The ion-exchange reaction was performed for 48 h at room temperature. The conjugate I_FUS was obtained after drying under reduced pressure.

2.2. Encapsulation and Micellization

The amphiphilic graft copolymer (20 mg) and RIF in a weight ratio of 1:1 were dissolved in methanol (2 mL). Then, deionized water was dropped into the mixture (4 mL, two-fold excess of water relative to the solvent) and stirred for 24 h. Next, the methanol was evaporated, and the aqueous fraction was collected and lyophilized to obtain a solid product.

The same procedure was applied to form single-drug systems based on copolymers with chloride anions and dual-drug systems, in which the conjugates with FUS anions were mixed with the non-ionic RIF.

2.3. Drug Release Studies of Ionic and Non-Ionic Drugs

The obtained conjugate/micelle/dual-system (1.0 mg) was dissolved in 1 mL of PBS solution (pH = 7.4). Next, the mixture (1 mL) was transferred to a dialysis membrane bag (MWCO = 3.5 kDa), which was placed in a glass vial filled with 45 mL of PBS. Drug release experiments were performed, under stirring, at 37 °C. The samples (0.5 mL) were taken at appropriate time intervals and mixed with 0.5 mL of methanol. The samples prepared in this way were analyzed on a UV-Vis spectrophotometer, observing the absorption maximum at $\lambda = 207$ nm for FUS[−] and 330 nm for RIF.

2.4. Characterization

¹H NMR spectra were recorded using a UNITY/NOVA (Varian, Mulgrave, Victoria, Australia) spectrometer operating at 300 MHz. The measurements were performed by dissolving samples in deuterated dimethyl sulfoxide (DMSO) with tetramethylsilane (TMS) as an internal standard. Molecular weight and dispersity index (M_n and \mathcal{D}) were estimated by size-exclusion chromatography (SEC). Measurements were performed on a chromatograph (Ultimate 3000 with differential refractometer RefractoMax 521 detector, Thermo Fisher Scientific, Waltham, MA, USA) in DMF containing 10 mM LiBr at 50 °C with a flow rate of 0.25 mL/min using a TSKgel Guard SuperMPHZ-H 6 μ m pre-column (4.6 mm \times 2 cm) and two TSKgel SuperMultiporeHZ-H 6 μ m columns (4.6 mm \times 15 cm), or in water with a flow rate of 0.35 mL/min using a TSKgel SuperAW3000 4 μ m column (6.0 mm \times 15 cm) and a TSKgel SuperAW-H Guard pre-column (4.6 mm \times 35 mm). The calculations were based on poly(ethylene oxide) (PEO) standards (982–969,000 g/mol). The critical micelle concentration (CMC) was evaluated by measuring the interfacial tension (IFT) using the pendant drop method on a goniometer (OCA 15EC, DataPhysics, Filderstadt, Germany). For this purpose, a series of aqueous polymer solutions (0.0006–0.06 mg/mL) was prepared. The same apparatus was also used for contact angle (CA) measurements using the sessile drop method. The polymer solution in methanol (0.3 mg/mL) was spin-coated on a thin glass plate. Next, deionized water (4 μ L) was dropped onto the thin polymer layer, and the CA was measured. The data were collected and processed by SCA20_U software. The hydrodynamic diameters (D_h) of particles and polydispersity indexes (PDI) were measured by dynamic light scattering (DLS) using a Zetasizer Nano-S90 (Malvern Technologies, Malvern, UK). Samples were placed in poly(methyl methacrylate) (PMMA) cells after dilution with

a solvent (0.5 mg/mL). Then, they were put into the thermostatted cell compartment of the instrument at 25 °C. Each measurement was repeated three times to obtain an average value. Ultraviolet-visible light spectroscopy (UV-Vis, spectrometer Evolution 300, Thermo Fisher Scientific, Waltham, MA, USA) was used to determine the anionic drug content (DC) in conjugates or the non-ionic drug loading content (DLC) in micelles, as well as the amount of the drug released during in vitro studies. The measurements were carried out in quartz cuvettes.

3. Results

The graft copolymers were obtained by atom-transfer radical polymerization (ATRP) catalyzed with CuCl/bpy complex in THF/methanol at 40 °C. The backbone was constructed from copolymers of methyl methacrylate and 2-(2-bromoisobutyryloxy)ethyl methacrylate (P(MMA-co-BIEM)) with various contents of bromoester initiating groups (25% or 50%). Side chains, which were grafted from these active groups in the multifunctional macroinitiator (MI), represented the structure of copolymers of [2-(methacryloyloxy)ethyl]-trimethylammonium chloride, in different ratios, with methyl methacrylate (P(TMAMA-co-MMA)) (25:75; 50:50). The polymers contained various grafting degrees (DG = 26 or 46 mol.%), depending on the number of initiating groups (Table 1). The structure of graft copolymers was confirmed using the ¹H NMR spectroscopy (Figure S1).

Table 1. Data for P(MMA-co-(BIEM-graft-P(TMAMA-co-MMA))) graft copolymers synthesized by ATRP. Data from [39].

No.	n _{sc}	DG (mol.%)	F _{TMAMA} ^a (mol.%)	DP _{sc} ^a	M _n ^a × 10 ^{−3} (g/mol)	Đ ^b
I	48	26	39	35	273.1	1.15
II	133	46	36	28	583.5	1.03 ^c
III			18	65	1090.5	1.11

Conditions: I, II: [TMAMA]₀: [MMA]₀: [MI]₀: [CuCl]₀: [bpy]₀ = 50:50:1:1:2, III: [TMAMA]₀: [MMA]₀: [MI]₀: [CuCl]₀: [bpy]₀ = 25:75:1:1:2, methanol/THF = 2:1 v/v; 1:1 v/wt, 40 °C. The main chain MI_I: MMA/BIEM = 75/25; DP_n = 186; MI_{II-III}: MMA/BIEM = 50/50; DP_n = 292, where DP_n is the polymerization degree of the main chain. n_{sc} is the number of side chains; DG is the degree of grafting, equal to n_{sc} per total DP_n of the polymer backbone; DP_{sc} is the polymerization degree of the side chains; F_{TMAMA} is the content of TMAMA in the side chains; ^a determined with ¹H NMR using monomer conversion calculated for the reaction mixture by estimating the integration of signals for unreacted TMAMA (6.07 ppm) and MMA (6.02 ppm) in relation to the constant intensity of the pyrene signal (8.26–8.18 ppm) as the internal standard; ^b determined by SEC (PEO calibration in DMF or ^c in H₂O).

Graft copolymers I–III were used as the matrices to obtain different types of carriers (Figure 1). Chloride anions included in TMAMA units, which were distributed along the side chains in the polymer, served as ion-exchange species. Fusidate (FUS) sodium salt was selected as the API to obtain drug-carrier ionic conjugates. The efficiency of the exchange reaction using FUS anions was evaluated by the drug content (DC), which refers to the percentage of ionic drugs in the copolymer, determined by UV-Vis (Figure 2). The most effective exchange yielding DC > 50% took place in polymer I, which was characterized by a shorter main chain and loosely-distributed grafts (DG = 26 mol.%). A higher steric hindrance in the densely-grafted side chains (DG = 46 mol.%) likely caused tighter packing of the IL units, which corresponded to the lower efficacy of the Cl[−] exchange to FUS[−] in copolymers II–III (~35%).

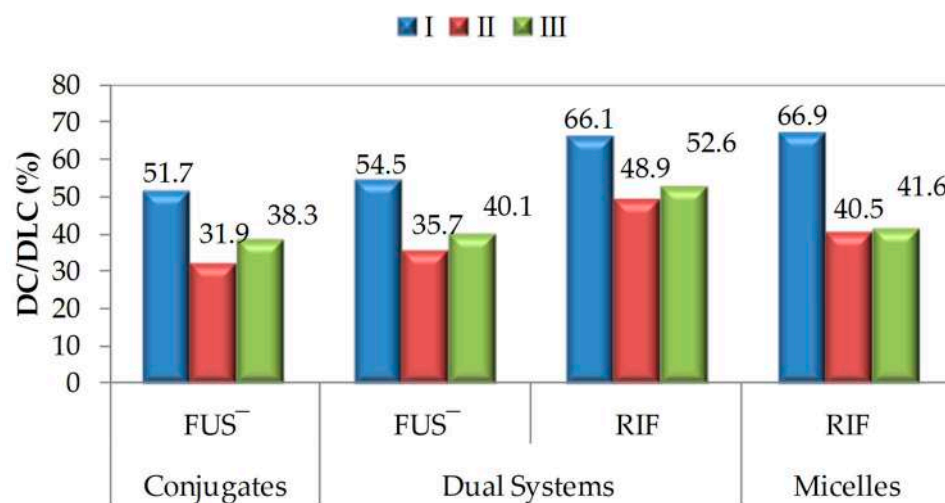


Figure 2. DC/DLC values of FUS or RIF for various carriers based on graft copolymers I–III, where: DC refers to the amount of conjugated ionic drug, and DLC relates to the amount of non-ionic drug encapsulated in the micelle core.

The amphiphilic properties of graft copolymers I–III and their conjugates with FUS were determined by the critical micelle concentration (CMC). For this purpose, the interfacial tension (IFT) was measured using goniometry for the polymer/conjugate series in an aqueous solution, with a selected concentration range of $C = 6 \times 10^{-4}$ –0.06 mg/mL. The crossover point on an IFT vs. $\log C$ plot was used to set the value of the CMC (Figure S2). The results in Table 2 show that the exchange of Cl^- to FUS^- changed the CMC for copolymer I (0.013 vs. 0.025 mg/mL), whereas these values were similar for copolymers with a higher graft density. The CMC values for FUS conjugates increased with the TMAMA fraction. The self-assembly behavior of the graft copolymers, including those bearing fusidate counterions, makes them suitable candidates for the encapsulation of non-ionic drugs to obtain dual-drug systems based on micellar conjugates.

Table 2. Characterization of aqueous solution and surface wettability for graft copolymers and their conjugates with FUS^- .

	CMC ^a (mg/mL)		CA ^b (°)	
	Cl^- (Data from [39])	FUS^-	Cl^- (Data from [39])	FUS^-
I	0.013	0.025	56.3	51.0
II	0.020	0.020	48.3	35.3
III	0.011	0.012	44.3	43.2

^a Evaluated using the crossover point of IFT and $\log C$ of polymer/conjugate; ^b estimated using the water sessile drop method on a polymer film by goniometry.

Goniometry is a convenient method for measuring the water contact angle (CA, Table 2) using the sessile drop technique. The evaluation of a polymer film's wettability indirectly describes the hydrophilic-hydrophobic balance in the macromolecule. It also helps show the specific influence of the polymer structure, including the type of counterion (Cl^- vs. FUS^-). Polymer I, with the highest amount of hydrophilic TMAMA units in the grafts and the lowest molecular weight ($I:F_{\text{TMAMA}} = 43\%$; $M_n = 273.1 \times 10^3$ g/mol), was characterized by the highest CA (56.3° and 51.0°, for carriers bearing Cl^- and FUS^- anions, respectively). The CA values slightly decreased after counterion exchange to FUS^- due to the higher hydrophilicity of the FUS^- systems. The differences in the water contact angles for the FUS conjugates are shown in Figure 3.

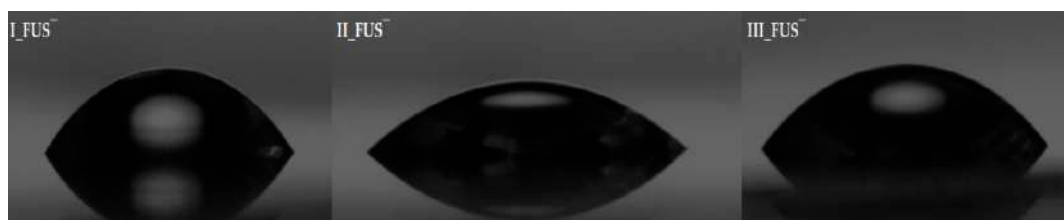


Figure 3. Screen shots during sessile water drop measurements for FUS conjugates.

The amphiphilicity of the given structures allowed them to form micelles via self-organization. Therefore, both the copolymer with chloride counterions and conjugates with ionic drugs were used as the matrices for encapsulating the non-ionic drug rifampicin (RIF) in the micelle core. Rifampicin is a bactericidal antibiotic used to treat respiratory diseases caused by, e.g., *Mycobacterium tuberculosis*, *Streptococcus pyogenes*, and *Streptococcus pneumoniae*. The action mechanism of RIF is based on bacterial DNA polymerase blocking, which inhibits bacterial RNA and protein synthesis. Because of this, RIF is also combined with FUS to ensure an effective defense against many microorganisms that cause respiratory diseases. Marsot et al. also discovered drug–drug interaction between RIF and FUS [41]. Bel et al. noted that FUS increased the bioavailability and concentration of RIF in plasma, while decreasing its clearance [42]. Moreover, RIF can potentially induce the metabolism of FUS and reduce its concentration. Therefore, a dual-drug system formulation for the co-delivery of these agents (FUS and RIF) is clinically relevant.

The degree of non-ionic drug encapsulation, namely the drug loading content (DLC), was calculated as a percentage of the drug loading concentration to the total concentration of the copolymer/conjugate and the loaded drug, using UV-Vis spectroscopy. Similar to FUS exchange, the encapsulation of RIF was the most efficient in copolymer I (Figure 2). It was also observed that the presence of an anionic drug in the polymer did not greatly impact its encapsulation (in micelles of a single-drug system, $DLC_{RIF} = 66.9\%$ vs. the dual-drug system, $DLC_{RIF} = 66.1\%$). A similar trend was observed when II or III was used as the matrix, but they could encapsulate RIF in lower amounts, i.e., 50% and 40%, respectively.

The hydrodynamic diameters (D_h) of the obtained carriers were determined by DLS in an aqueous solution. Figure 4 shows the histograms of polymer particles, and the detailed data are presented in Table S1. Compared with previously studied chloride-based copolymers [39], the introduction of FUS anions increased the particle sizes, except for system III (Cl^- : 105 nm vs. FUS^- : 95 nm). FUS^- conjugates I and II formed two fractions of particles at 30 nm and 200 nm. However, in the latter system, the larger particles were the dominant fraction. Similar differences were observed for both types of systems after the micellization of RIF, but the particle sizes of the dominant fraction were evaluated to be 30–40 nm (52–55%) and 51–97 nm (90–94%). The highest molecular weight of copolymer III helped generate monomodal particles, which depended on the system and reached sizes of 95 nm (FUS^- conjugate), 94 nm (RIF micelles), and 65 nm (micellar conjugate FUS^- /RIF).

In vitro drug release studies were performed in PBS (pH = 7.4) for samples (0.5 mL) taken at appropriate time intervals and measured using UV-Vis at $\lambda_{FUS} = 207$ nm and $\lambda_{RIF} = 330$ nm. The release of ionic and/or non-ionic drugs (Figure 5) showed a biphasic kinetic dependence. An initial burst release was observed at up to 5 h, then a slower release lasted for up to 50 h. In the case of single-drug micelles I_RIF and III_RIF, as well as for all dual-drug systems, the drug release reached a plateau after 24 h. Generally, FUS was released in larger amounts from the conjugates than RIF was from the micelles, representing single-drug systems (Table 3). The highest difference in the release rate of RIF vs. FUS (micelles vs. conjugates), 37% vs. 80%, was observed for system III. This effect was reduced by using half-length grafts in system I (20% vs. 50%, respectively). Finally, the release rates were comparable with the shortest side chains, when DP did not exceed 30 units. The combination of FUS and RIF in the dual-drug system also caused a more rapid release of FUS anions than did the encapsulated RIF. Additionally, studies on the double

systems indicated that the encapsulated RIF was released slightly more slowly than from the single-drug micelles. Similarly, the release of FUS anions was reduced compared with the single-drug conjugates. In all cases, the highest amount of the drug was released from the densely-grafted polymer III, which was characterized by the lowest fraction of TMAMA units (18%) in the longest side chains ($DP_{SC} = 65$), independent of the drug delivery form of the carrier. The final concentrations of co-released drugs indicated excess FUS, where the RIF:FUS ratio was equal to 0.7–0.8:1. Currently, pharmaceutical formulations containing both RIF and FUS are not commercially available, but Drancourt et al. proved the positive effect of this drug combination on drug-resistant strains in a ratio of 0.6:1 [43]. Therefore, our results for dual FUS/RIF systems are promising for the simultaneous delivery of two drugs, which could be applied in lung disease therapies against drug-resistant strains.

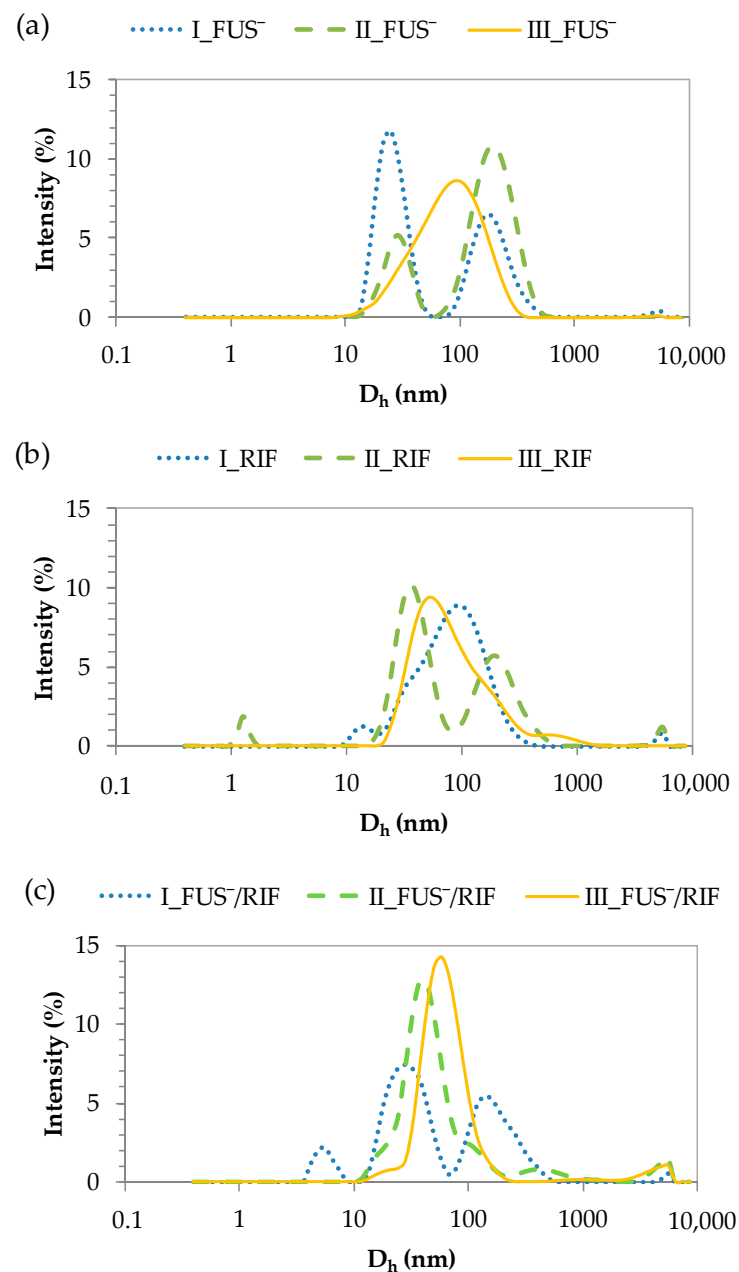


Figure 4. DLS histograms for particles in single systems with (a) FUS⁻, (b) RIF, and (c) dual systems.

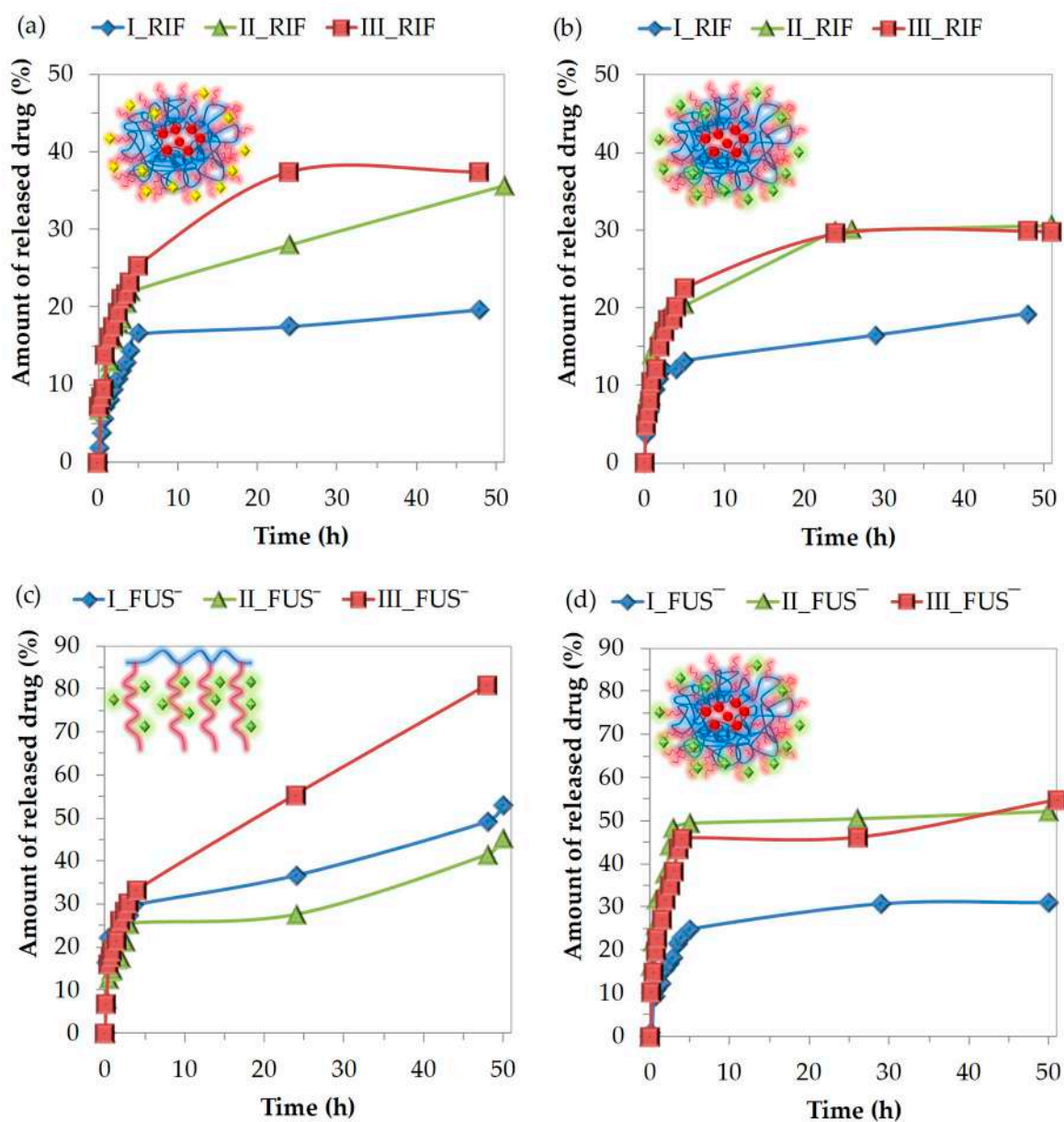


Figure 5. Kinetic release profiles of RIF from various types of carriers: (a) micelles and (b) dual-drug systems or FUS from (c) conjugates and (d) dual-drug systems, based on PIL graft copolymers I–III.

Table 3. Data for drugs released from carriers I–II based on TMAMA.

	Conjugates		Dual-Drug Systems				Micelles	
	FUS ⁻		FUS ⁻		RIF		RIF	
	ARD (%)	CD (µg/mL)	ARD (%)	CD (µg/mL)	ARD (%)	CD (µg/mL)	ARD (%)	CD (µg/mL)
I	52.82	7.18	30.84	4.31	19.19	3.29	19.65	3.37
II	45.23	3.80	52.11	4.65	30.57	3.88	35.64	3.70
III	81.32	8.21	54.84	5.57	29.91	4.03	37.37	3.98

ARD is the amount of released drug; CD is the concentration of the drug released after 48–50 h.

4. Conclusions

Graft copolymers with various contents of IL units were tested for obtaining three types of carriers, i.e., single-drug systems with conjugated FUS or encapsulated RIF, as well as dual-drug systems with conjugated FUS and encapsulated RIF. The drug delivery properties of these systems were verified. The ionic structure of the tested copolymers allowed for an ion exchange reaction of chloride anions to FUS^- , which resulted in ionic drug-carrier conjugates. Both chloride-based copolymers and FUS conjugates showed the ability to self-organize; thus, they could be applied for the encapsulation of the non-ionic drug RIF in polymer micelle superstructures. The entrapment of RIF in the self-assembled conjugates with FUS^- was advantageous for achieving dual-drug systems for co-delivery applications. Drugs were successfully introduced into both conjugates and/or micellar carriers ($\text{FUS} \leq 54\%$ and $\text{RIF} \leq 67\%$). There was no significant effect of the anion type (chloride vs. pharmaceutical fusidate) on the RIF encapsulation efficiency. The sizes of the self-assembled particles for the main fraction decreased in the following order: FUS conjugates (26–208 nm, 58–100%), RIF micelles (40–97 nm, 55–96%), and micellar conjugates FUS/RIF (31–65 nm, 52–95%). During in vitro studies in PBS, an initial burst release was observed. The amounts of the drugs released varied in a wide range, between 19–81%, depended on the side chain length and ionic content of the polymer, as well as the drug and carrier type. In conclusion, the selected trimethylammonium-containing graft copolymers are sufficient for obtaining single-drug systems in the form of micelles or ionic conjugates. They are also suitable as innovative dual-drug systems carrying two drugs, connected by a polymer matrix, in different ways (physically vs. ionically). The selected drugs (RIF and FUS) can be used for antibacterial treatment, including drug-resistant bacterial strains and combined therapy, with simultaneous drug co-delivery.

Supplementary Materials: The following supporting information can be downloaded at: <https://www.mdpi.com/article/10.3390/ma15134457/s1>, Figure S1: Representative ^1H NMR spectrum of graft copolymer I; Figure S2: Representative plot of interfacial tension vs. logarithm of the conjugate concentration Π_{FUS} in aqueous solution at 25 °C; Table S1: Hydrodynamic diameters (D_h) of nanoparticles determined using DLS.

Author Contributions: K.N.: data curation, formal analysis, investigation, and writing—original draft; A.M.: data curation and investigation; D.N.: conceptualization, methodology, funding acquisition, project administration, writing—review and editing, and supervision. All authors have read and agreed to the published version of the manuscript.

Funding: This research was funded by the National Science Center, grant no. 2017/27/B/ST5/00960 and the publication fee is financed by the Rector's pro-quality grant no. 04/040/RGJ21/0153.

Institutional Review Board Statement: Not applicable.

Informed Consent Statement: Not applicable.

Data Availability Statement: Not applicable.

Acknowledgments: The authors thank Anna Mielańczyk for carrying out the DLS analyses and Sylwia Waśkiewicz for carrying out the GPC analyses.

Conflicts of Interest: The authors declare no conflict of interest.

References

1. Lai, W.-F. Non-conjugated polymers with intrinsic luminescence for drug delivery. *J. Drug Deliv. Sci. Technol.* **2020**, *59*, 101916. [[CrossRef](#)]
2. Bielas, R.; Wróbel-Marek, J.; Kurczyńska, E.U.; Neugebauer, D. Pyranine labeled polymer nanoparticles as fluorescent markers for cell wall staining and imaging of movement within apoplast. *Sens. Actuators B Chem.* **2019**, *297*, 126789. [[CrossRef](#)]
3. Shah, A.; Aftab, S.; Nisar, J.; Ashiq, M.; Iftikhar, F. Nanocarriers for targeted drug delivery. *J. Drug. Deliv. Sci. Technol.* **2021**, *62*, 102426. [[CrossRef](#)]
4. Edis, Z.; Wang, J.; Waqas, M.; Ijaz, M.; Ijaz, M. Nanocarriers-Mediated Drug Delivery Systems for Anticancer Agents: An Overview and Perspectives. *Int. J. Nanomed.* **2021**, *16*, 1313–1330. [[CrossRef](#)] [[PubMed](#)]

5. Kingsley, J.; Dou, H.; Morehead, J.; Rabinow, B.; Gendelman, H.; Destache, C. Nanotechnology: A Focus on Nanoparticles as a Drug Delivery System. *J. Neuroimmune Pharmacol.* **2006**, *1*, 340–350. [[CrossRef](#)]
6. Wilczewska, A.; Niemirowicz, K.; Markiewicz, K.; Car, H. Nanoparticles as drug delivery systems. *Pharmacol. Rep.* **2012**, *64*, 1020–1037. [[CrossRef](#)]
7. Rani, A.; Asgher, M.; Qamae, S.; Khalid, N. Nanostructure-mediated delivery of therapeutic drugs—A comprehensive review. *Int. J. Chem. Biochem. Sci.* **2019**, *15*, 5–14.
8. Natarajan, J.; Nugraha, C.; Ng, X.; Venkatraman, S. Sustained-release from nanocarriers: A review. *J. Control. Release* **2014**, *193*, 122–138. [[CrossRef](#)]
9. Salim, M.; Minamikawa, H.; Sugimura, A.; Hashim, R. Amphiphilic designer nano-carriers for controlled release: From drug delivery to diagnostics. *Med. Chem. Commun.* **2014**, *5*, 1602–1618. [[CrossRef](#)]
10. Singh, S.; Pandey, V.; Tewari, R.; Agarwal, V. Nanoparticle based drug delivery system: Advantages and applications. *Indian. J. Sci. Technol.* **2011**, *4*, 177–184. [[CrossRef](#)]
11. Adams, M.; Lavasanifar, A.; Kwon, G. Amphiphilic block copolymers for drug delivery. *J. Pharm. Sci.* **2003**, *92*, 1343–1355. [[CrossRef](#)] [[PubMed](#)]
12. Jones, M.; Leroux, J. Polymeric micelles—A new generation of colloidal drug carriers. *Eur. J. Pharm. Biopharm.* **1999**, *48*, 101–111. [[CrossRef](#)]
13. Huddleston, J.; Visser, A.; Reichert, W.; Willauer, H.; Broker, G.; Rogers, R. Characterization and comparison of hydrophilic and hydrophobic room temperature ionic liquids incorporating the imidazolium cation. *Green Chem.* **2001**, *3*, 156–164. [[CrossRef](#)]
14. Freire, M.; Teles, A.; Rocha, M.; Schröder, B.; Neves, C.; Carvalho, P.; Evtuguin, D.; Santos, L.; Coutinho, J. Thermophysical Characterization of Ionic Liquids Able To Dissolve Biomass. *J. Chem. Eng. Data.* **2011**, *56*, 4813–4822. [[CrossRef](#)]
15. Moshikur, R.; Chowdhury, M.; Moniruzzaman, M.; Goto, M. Biocompatible ionic liquids and their application in pharmaceuticals. *Green Chem.* **2020**, *22*, 8116–8139. [[CrossRef](#)]
16. Gomes, J.; Silva, S.; Reis, R. Biocompatible ionic liquids: Fundamental behaviours and applications. *Chem. Soc. Rev.* **2019**, *48*, 4317–4335. [[CrossRef](#)] [[PubMed](#)]
17. Wood, N.; Stephens, G. Accelerating the discovery of biocompatible ionic liquids. *Phys. Chem. Chem. Phys.* **2010**, *12*, 1670–1674. [[CrossRef](#)] [[PubMed](#)]
18. Fukaya, Y.; Iizuka, Y.; Sekikawa, K.; Ohno, H. Bio ionic liquids: Room temperature ionic liquids composed wholly of biomaterials. *Green Chem.* **2007**, *9*, 1155. [[CrossRef](#)]
19. Pernak, J.; Syguda, A.; Mirska, I.; Pernak, A.; Nawrot, J.; Prądzyńska, A.; Griffin, S.; Rogers, R. Choline-derivative-based ionic liquids. *Chem. Eur. J.* **2007**, *13*, 6817–6827. [[CrossRef](#)]
20. Taha, M.; Almeida, M.; Silva, F.; Domingues, P.; Ventura, S.; Coutinho, J.; Freire, M. Novel Biocompatible and Self-buffering Ionic Liquids for Biopharmaceutical Applications. *Chem. Eur. J.* **2015**, *21*, 4781–4788. [[CrossRef](#)]
21. Niesyto, K.; Łyżniak, W.; Skonieczna, M.; Neugebauer, D. Biological in vitro evaluation of PIL graft conjugates: Cytotoxicity characteristics. *Int. J. Mol. Sci.* **2021**, *22*, 7741. [[CrossRef](#)] [[PubMed](#)]
22. Bielas, R.; Siewniak, A.; Skonieczna, M.; Adamiec, M.; Mielńczyk, Ł.; Neugebauer, D. Choline based polymethacrylate matrix with pharmaceutical cations as co-delivery system for antibacterial and anti-inflammatory combined therapy. *J. Mol. Liq.* **2019**, *285*, 114–122. [[CrossRef](#)]
23. Ghatak, C.; Rao, V.; Mandal, S.; Ghosh, S.; Sarkar, N. An Understanding of the Modulation of Photophysical Properties of Curcumin inside a Micelle Formed by an Ionic Liquid: A New Possibility of Tunable Drug Delivery System. *J. Phys. Chem. B* **2012**, *116*, 3369–3379. [[CrossRef](#)] [[PubMed](#)]
24. Kurnik, I.S.; D’Angelo, N.; Mazzola, P.; Chorilli, M.; Kamei, D.; Pereira, J.; Vicente, A.; Lopes, A. Polymeric micelles using cholinium-based ionic liquids for the encapsulation and release of hydrophobic drug molecules. *Biomater. Sci.* **2021**, *9*, 2183–2196. [[CrossRef](#)]
25. Moniruzzaman, M.; Tahara, Y.; Tamura, M.; Kamiya, N.; Goto, M. Ionic liquid-assisted transdermal delivery of sparingly soluble drugs. *Chem. Commun.* **2010**, *46*, 1452. [[CrossRef](#)]
26. Ali, M.; Moshikur, R.; Wakabayashi, R.; Moniruzzaman, M.; Goto, M. Biocompatible Ionic Liquid-Mediated Micelles for Enhanced Transdermal Delivery of Paclitaxel. *ACS Appl. Mater. Interfaces* **2021**, *13*, 19745–19755. [[CrossRef](#)] [[PubMed](#)]
27. Mahajan, S.; Sharma, R.; Mahajan, R. An Investigation of Drug Binding Ability of a Surface Active Ionic Liquid: Micellization, Electrochemical, and Spectroscopic Studies. *Langmuir* **2012**, *28*, 17238–17246. [[CrossRef](#)] [[PubMed](#)]
28. Lu, B.; Li, Y.; Wang, Z.; Wang, B.; Pan, X.; Zhao, W.; Ma, W.; Zhang, J. Dual Responsive Hyaluronic Acid Graft Poly(ionic liquid) Block Copolymer Micelle for Efficient CD44 Targeted Antitumor Drug Delivery. *New J. Chem.* **2019**, *43*, 12275–12282. [[CrossRef](#)]
29. Lu, B.; Zhou, G.; Xiao, F.; He, Q.; Zhang, J. Stimuli-Responsive Poly(ionic liquid) Nanoparticle for Controlled Drug Delivery. *J. Mater. Chem. B* **2020**, *8*, 7994–8001. [[CrossRef](#)]
30. Viau, L.; Tourné-Péteilh, C.; Devoisselle, J.; Vioux, A. Ionogels as drug delivery system: One-step sol–gel synthesis using imidazolium ibuprofenate ionic liquid. *Chem. Commun.* **2010**, *46*, 228–230. [[CrossRef](#)]
31. Bica, K.; Rodríguez, H.; Gurau, G.; Andreea Cojocar, O.; Riisager, A.; Fehrmann, R.; Rogers, R. Pharmaceutically active ionic liquids with solids handling, enhanced thermal stability, and fast release. *Chem. Commun.* **2012**, *48*, 5422. [[CrossRef](#)] [[PubMed](#)]
32. Ferraz, R.; Branco, L.; Marrucho, I.; Araújo, J.; Rebelo, L.; da Ponte, M.; Prudencio, C.; Noronha, J.; Petrovski, Ž. Development of novel ionic liquids based on ampicillin. *Med. Chem. Commun.* **2012**, *3*, 494. [[CrossRef](#)]

33. Gorbunova, M.; Lemkina, L.; Borisova, I. New guanidine-containing polyelectrolytes as advanced antibacterial materials. *Eur. Polym. J.* **2018**, *105*, 426–433. [[CrossRef](#)]
34. Bica, K.; Rijkssen, C.; Nieuwenhuyzen, M.; Rogers, R. In search of pure liquid salt forms of aspirin: Ionic liquid approaches with acetylsalicylic acid and salicylic acid. *Phys. Chem. Chem. Phys.* **2010**, *12*, 2011. [[CrossRef](#)]
35. Halayqa, M.; Zawadzki, M.; Domańska, U.; Plichta, A. API-ammonium ionic liquid–Polymer compounds as a potential tool for delivery systems. *J. Mol. Liq.* **2017**, *248*, 972–980. [[CrossRef](#)]
36. Halayqa, M.; Zawadzki, M.; Domańska, U.; Plichta, A. Polymer–Ionic liquid–Pharmaceutical conjugates as drug delivery systems. *J. Mol. Struct.* **2019**, *1180*, 573–584. [[CrossRef](#)]
37. Araújo, J.; Florindo, C.; Pereiro, A.; Vieira, N.; Matias, A.; Duarte, C.; Rebelo, L.; Marrucho, I. Cholinium-based ionic liquids with pharmaceutically active anions. *RSC Adv.* **2014**, *4*, 28126–28132. [[CrossRef](#)]
38. Bielas, R.; Łukowiec, D.; Neugebauer, D. Drug delivery via anion exchange of salicylate decorating poly(meth)acrylates based on a pharmaceutical ionic liquid. *New J. Chem.* **2017**, *41*, 12801–12807. [[CrossRef](#)]
39. Niesyto, K.; Neugebauer, D. Synthesis and Characterization of Ionic Graft Copolymers: Introduction and In Vitro Release of Antibacterial Drug by Anion Exchange. *Polymers.* **2020**, *12*, 2159. [[CrossRef](#)]
40. Niesyto, K.; Neugebauer, D. Linear Copolymers Based on Choline Ionic Liquid Carrying Anti-Tuberculosis Drugs: Influence of Anion Type on Physicochemical Properties and Drug Release. *Int. J. Mol. Sci.* **2021**, *22*, 284. [[CrossRef](#)]
41. Marsot, A.; Ménard, A.; Dupouey, J.; Muziotti, C.; Guilhaumou, R.; Blin, O. Population pharmacokinetics of rifampicin in adult patients with osteoarticular infections: Interaction with fusidic acid. *Br. J. Clin. Pharmacol.* **2017**, *83*, 1039–1047. [[CrossRef](#)] [[PubMed](#)]
42. Bel, F.; Bourguignon, L.; Tod, M.; Ferry, T.; Goutelle, S. Mechanisms of drug–drug interaction between rifampicin and fusidic acid. *Br. J. Clin. Pharm.* **2017**, *83*, 1862–1864. [[CrossRef](#)] [[PubMed](#)]
43. Drancourt, M.; Stein, A.; Argenson, J.N.; Roiron, R.; Groulier, P.; Raoult, D. Oral treatment of *Staphylococcus* spp. infected orthopaedic implants with fusidic acid or ofloxacin in combination with rifampicin. *J. Antimicrob. Chemother.* **1997**, *39*, 235–240. [[PubMed](#)]

Supporting Information

Dual drug delivery via self-assembled conjugates of choline functionalized graft copolymers

Katarzyna Niesyto, Aleksy Mazur and Dorota Neugebauer *

* Department of Physical Chemistry and Technology of Polymers, Faculty of Chemistry, Silesian University of Technology, 44-100 Gliwice, Poland

* Correspondence: Dorota.Neugebauer@polsl.pl

Contents:

Figure S1. Representative ^1H NMR spectrum of graft copolymer I.

Figure S2. Representative plot of interfacial tension vs logarithm of the conjugate concentration Π_{FUS} in aqueous solution at 25 °C.

Table S1. Hydrodynamic diameters (D_h) of nanoparticles determined using DLS.

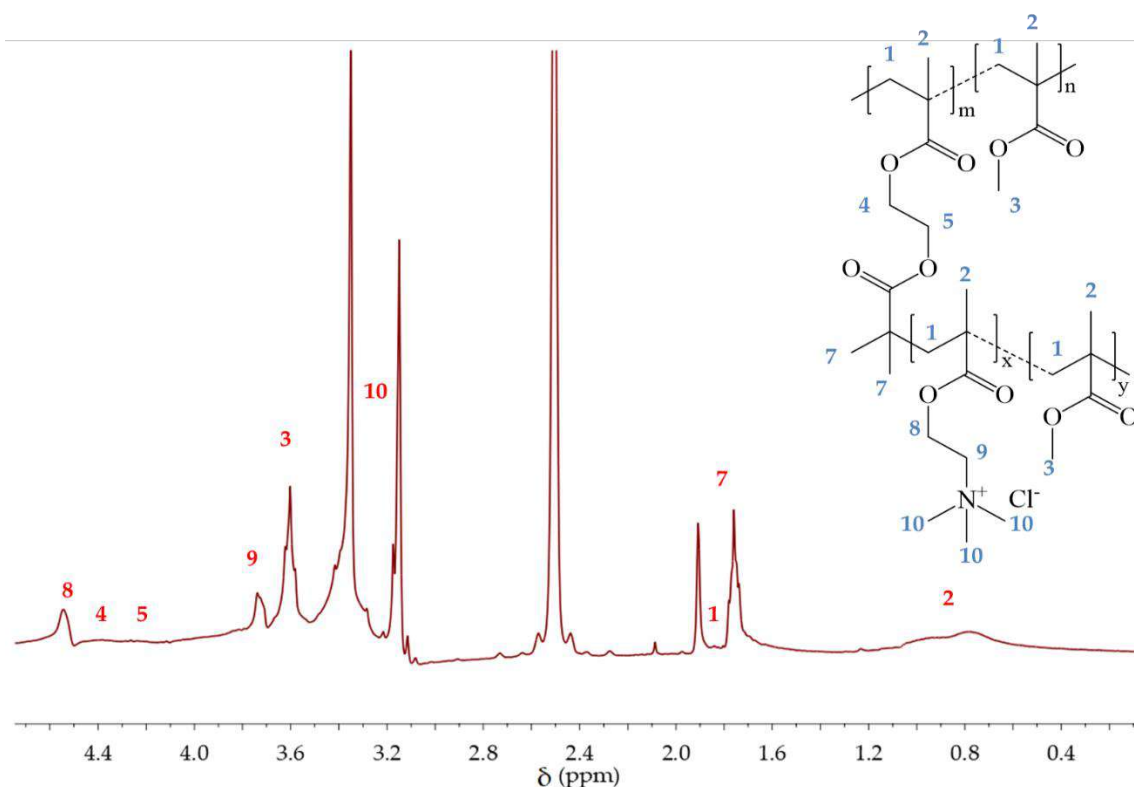
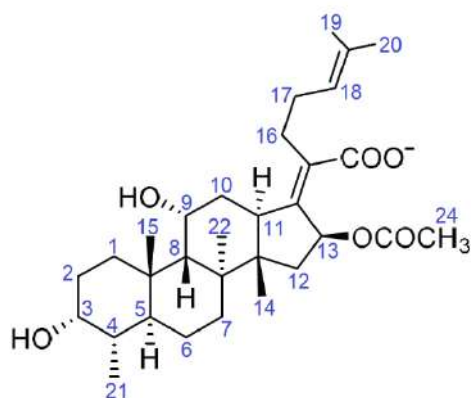


Figure S1. Representative ^1H NMR spectrum of graft copolymer I.

^1H NMR (DMSO- d_6 , δ , ppm): 4.63-4.43 (2H, $-\text{CH}_2\text{-O-}$), 4.47-4.28 (2H, $-\text{CH}_2\text{-OOC-C-}(\text{CH}_3)_2\text{Br}$), 4.28-4.08 (2H, $-\text{COO-CH}_2$), 3.86-3.65 (2H, $-\text{CH}_2\text{-N}^+$), 3.65-3.47 (3H, $-\text{O-CH}_3$), 3.42-3.01 (9H, $-\text{N}^+(\text{CH}_3)_3$, 1.98-1.82 (6H, $-(\text{CH}_3)_2\text{Br}$ initiating moiety), 1.4-0.51 (3H, $-\text{CH}_3$ backbone).

After exchange of Cl^- by FUS^- , the new signals appeared in ^1H NMR (DMSO- d_6 , δ , ppm): 0.7-0.9 (3x3H, $-\text{CH}_3$ at ring, #14,15,21), 0.9-1.2 (3x2H and 3x1H, $-\text{CH}_2$ in ring, #1(1H),2(2H), 6(2H),7(2H),10(1H),12(1H)), 1.25 (3H, $-\text{CH}_3$ at ring, #22), 1.3-1.4 (2x1H, CH in ring, CH-CH_3 , #8,4), 1.6-1.7 (2x3H, $-\text{CH}_3$, #19,20), 1.8 (3H, $-\text{OCOCH}_3$ #24), 2.02-2.17 (2x2H, $-\text{CH}_2$, #16,17), 2.17-2.33 (3x1H, $-\text{CH}_2$ in ring, #1(1H),10(1H),12(1H)), 4.0-4.2 (2x1H, CH-OH , #3,9), 5.10 (1H, $-\text{CH=}$ #18), 5.88 (1H, $-\text{CH-COOCH}_3$ #13).



FUS^-

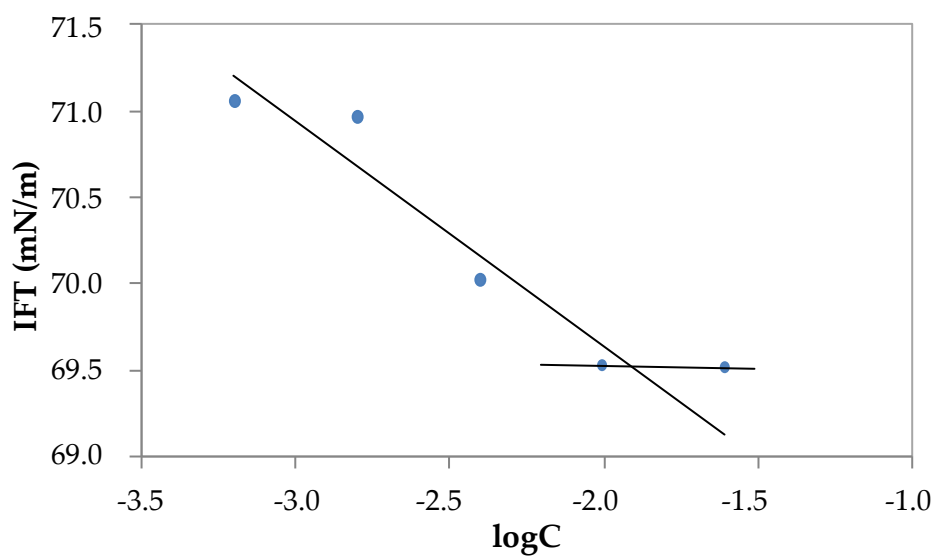


Figure S2. Representative plot of interfacial tension vs logarithm of the conjugate concentration II_FUS in aqueous solution at 25 °C.

Table S1. Hydrodynamic diameters (D_h) of nanoparticles determined using DLS^a.

	CF (37)			FUS ⁻			RIF			FUS ⁻ /RIF		
	PDI	Size (nm)	Intensity (%)	PDI	Size (nm)	Intensity (%)	PDI	Size (nm)	Intensity (%)	PDI	Size (nm)	Intensity (%)
I	0.454	18 125	64 32	0.424	26 199	58 41	0.436	97 14	94 5	0.23	31 184	52 40
II	0.241	72	100	0.564	208 29	83 7	0.377	40 216	55 40	0.371	51 531	90 6
III	0.293	105	99	0.281	95	100	0.269	94	96	0.27	65	95

^aconcentration of copolymer in water: 1 or 0.5 mg/mL.

PUBLIKACJA P.4

Ionic Liquid-based Polymer Matrices for Single and Dual Drug Delivery: Impact of Structural Topology on Characteristics and In Vitro Delivery Efficiency

Niesyto, K., Keihankhadiv, S., Mazur, A., Mielańczyk, A., Neugebauer, D.

International Journal of Molecular Sciences 2024, 25, 1292



Article

Ionic Liquid-Based Polymer Matrices for Single and Dual Drug Delivery: Impact of Structural Topology on Characteristics and In Vitro Delivery Efficiency

Katarzyna Niesyto , Shadi Keihankhadiv , Aleksy Mazur , Anna Mielańczyk and Dorota Neugebauer *

Department of Physical Chemistry and Technology of Polymers, Faculty of Chemistry, Silesian University of Technology, 44-100 Gliwice, Poland; katarzyna.niesyto@polsl.pl (K.N.); shadi.keihankhadiv@polsl.pl (S.K.); aleksy.mazur@polsl.pl (A.M.); anna.mielanczyk@polsl.pl (A.M.)

* Correspondence: dorota.neugebauer@polsl.pl

Abstract: Previously reported amphiphilic linear and graft copolymers, derived from the ionic liquid [2-(methacryloyloxy)ethyl]trimethylammonium chloride (TMAMA_{Cl}⁺), along with their conjugates obtained through modification either before or after polymerization with *p*-aminosalicylate anions (TMAMA_{PAS}⁺), were employed as matrices in drug delivery systems (DDSs). Based on the counterion type in TMAMA units, they were categorized into single drug systems, manifesting as ionic polymers with chloride counterions and loaded isoniazid (ISO), and dual drug systems, featuring ISO loaded in self-assembled PAS conjugates. The amphiphilic nature of these copolymers was substantiated through the determination of the critical micelle concentration (CMC), revealing an increase in values post-ion exchange (from 0.011–0.063 mg/mL to 0.027–0.181 mg/mL). The self-assembling properties were favorable for ISO encapsulation, with drug loading content (DLC) ranging between 15 and 85% in both single and dual systems. In vitro studies indicated ISO release percentages between 16 and 61% and PAS release percentages between 20 and 98%. Basic cytotoxicity assessments using the 2,5-diphenyl-2H-tetrazolium bromide (MTT) test affirmed the non-toxicity of the studied systems toward human non-tumorigenic lung epithelial cell line (BEAS-2B) cell lines, particularly in the case of dual systems bearing both ISO and PAS simultaneously. These results confirmed the effectiveness of polymeric carriers in drug delivery, demonstrating their potential for co-delivery in combination therapy.

Keywords: co-delivery systems; single drug systems; dual drug systems; poly(ionic liquid)s; graft copolymers; linear copolymers; *p*-aminosalicylate; isoniazid



Citation: Niesyto, K.; Keihankhadiv, S.; Mazur, A.; Mielańczyk, A.; Neugebauer, D. Ionic Liquid-Based Polymer Matrices for Single and Dual Drug Delivery: Impact of Structural Topology on Characteristics and In Vitro Delivery Efficiency. *Int. J. Mol. Sci.* **2024**, *25*, 1292. <https://doi.org/10.3390/ijms25021292>

Academic Editor: Piotr Dobrzynski

Received: 13 December 2023

Revised: 15 January 2024

Accepted: 18 January 2024

Published: 20 January 2024



Copyright: © 2024 by the authors. Licensee MDPI, Basel, Switzerland. This article is an open access article distributed under the terms and conditions of the Creative Commons Attribution (CC BY) license (<https://creativecommons.org/licenses/by/4.0/>).

1. Introduction

The use of nanocarriers has emerged as a highly promising strategy in the field of drug delivery systems (DDSs) [1–5]. These systems aim to prevent harmful side effects, reduce drug degradation, enhance drug accumulation within specific target zones, and improve overall drug bioavailability [6–11]. A diverse range of drug carriers is extensively employed, such as lipoproteins, liposomes, hydrogels, conjugates, capsules, particles, as well as micellar systems [12–14]. Among the latter, polymeric micelles representing nano-scale dimension superstructures are formed in an aqueous environment by self-assembling amphiphilic polymers with different types, including linear and graft, block, and stimuli-sensitive [15–18]. They are notable for their considerable potential, attributed to their dual-phase arrangement, featuring an inner core and an outer shell [19,20]. The hydrophobic core of micelles offers a conducive environment for solubilizing water-insoluble drugs, enabling their effective loading and delivery to the designated targets [21,22]. Moreover, they demonstrate kinetic stability in the bloodstream due to low critical micelle concentrations (CMCs) [23], leading to prolonged circulation duration and controlled release [24–27].

Among amphiphilic copolymers, a group of polymerized ionic liquids (PILs) stands out, which have the form of salts due to the presence of ion pairs [28–31]. Their characteristics encompass chemical and thermal stability, high ionic conductivity, adaptable polarity providing a variety of solubility, and fitting the other properties by counterion exchange dependently on the future application [28,31–36]. In recent years, they have been investigated [37–39], in the formation of ionic drug conjugates [40], and polymeric micelles [41,42]. Notably, choline, as a water-soluble trimethylammonium salt with a chloride anion, is commonly employed as a naturally derived cationic constituent in biocompatible monomers generating antibacterial properties [43–46] and improved pharmacodynamic and pharmacokinetic effects of the carried drug [47]. A commercially available choline ester of methacrylic acid, [2-(methacryloyloxy)ethyl]trimethylammonium chloride (TMAMA_{Cl}⁺), has been applied to design the choline-based PILs. Furthermore, they have been modified to the pharmaceutically active polymer conjugates by replacing chloride anion with the pharmaceutical anion, such as sulfacetamide [48], fusidate [49,50], piperacillin [51], clavulanate, and p-aminosalicylate (PAS) [37,38]. However, anion exchange has also been performed for this choline-based monomer to incorporate the pharmaceutical anion, such as cloxacillin [52], fusidate [52], salicylate [53], and PAS [54], where the resulting pharmaceutically functionalized choline monomers have been employed in the synthesis of drug-PIL ionic conjugates.

The self-assembled PILs have also been investigated as polymer matrices with the ability to encapsulate and deliver active pharmaceuticals, such as paclitaxel [55], dopamine [56], curcumin [57,58], doxorubicin [59,60], acyclovir [61,62], PAS [63], etc. In addition, PIL systems containing salicylate anions and encapsulated erythromycin have been reported to exhibit effective drug content and release [48]. In the case of dual drug systems, they are promising in combination therapy, increasing the effectiveness of treatment, for example in the presence of drug-resistant strains, as well as being more convenient because both drugs are delivered in one formulation.

In our studies, linear and graft choline-based PILs were investigated as matrices for single and dual drug delivery systems (Figure 1). The specific structure of copolymers led to obtaining the ionic drug conjugates, whose amphiphilic properties allowed for the encapsulation of a non-ionic drug. The polymerizable TMAMA_{Cl}⁺ and modified [2-(methacryloyloxy)ethyl]trimethylammonium p-aminosalicylate (TMAMA_{PAS}⁺) have been employed earlier for the synthesis of linear polymers [54,63] and graft copolymers [51,64]. Moreover, the graft copolymers based on the TMAMA_{Cl}⁺ modified by anion exchange to obtain the PAS[−] conjugates have also been reported [51]. The amphiphilic characteristics of the selected polymers established a favorable environment for encapsulating isoniazid (ISO), which is a first-line anti-tuberculosis drug [65]. ISO exhibits strong early bactericidal activity by inhibiting the action in the synthesis of mycolic acids in *Mycobacterium tuberculosis* [66,67] and interindividual variability in the pharmacokinetic effects [68,69]. Furthermore, it can be used in a multidrug treatment when combined with another antituberculosis drug like the second-line PAS [70], which has the potential to extend the effective duration of ISO by retarding its acetylation path [71]. Our current research incorporated the preparation and characterization of ISO-loaded self-assembling nanocarriers based on linear and graft PILs as the single drug systems, and ionic drug conjugates as the dual drug systems carrying PAS anions and encapsulated ISO. Drug release *in vitro* studies were conducted in phosphate-buffered saline (PBS) simulating human body fluids at a pH of 7.4 at 37 °C to assess the potential of choline-based polymers differing in topology and composition for effective delivery of ISO and ISO/PAS.

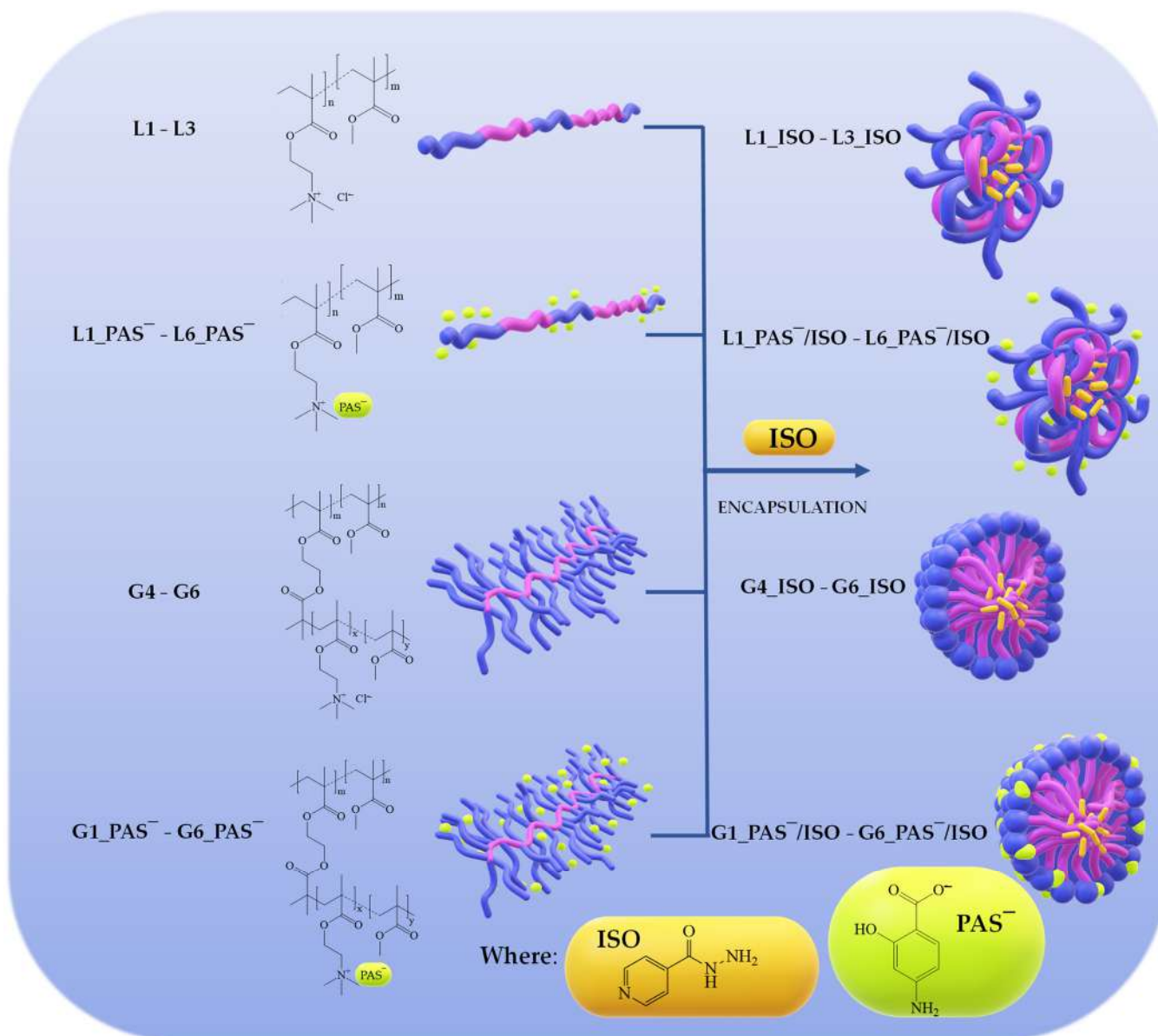


Figure 1. Schematic route of the linear and graft PIIls to single and dual drug delivery systems combining PAS anions and encapsulated ISO.

2. Results and Discussion

2.1. TMAMA-Based Linear and Graft Copolymers as Drug Carriers

The utilization of polymerizable ionic liquids (ILs), specifically TMAMA-Cl⁻ or TMAMA-PAS⁻, in copolymerization with MMA via atom transfer radical polymerization (ATRP), yielded linear copolymers denoted as P(TMAMA-co-MMA) (Table 1) [54,63]. In this process, a low molecular weight initiator, ethyl 2-bromoisobutyrate, was applied. Moreover, graft copolymers were synthesized (Table 2) [51,64], wherein the chains of P(TMAMA-co-MMA) were grown by *grafting from* multifunctional macroinitiators containing 18–48% of 2-(2-bromoisobutyryloxy)ethyl methacrylate initiating units. Within each topological group of polymers, distinctions were made between polymers with Cl⁻ (L1–L3 vs. G4–G6), polymers with PAS⁻ directly introduced by the polymerization of pharmaceutically functionalized monomeric IL (L4_PAS⁻–L6_PAS⁻ vs. G1_PAS⁻–G3_PAS⁻), and polymers modified with PAS anions indirectly introduced by the post-polymerization exchange reaction of Cl anions in the polymer matrix using the sodium salt of PAS (L1_PAS⁻–L3_PAS⁻, G4_PAS⁻–G6_PAS⁻).

Table 1. Basic characteristics of linear copolymers [54,63].

No.	DP _{TMAMA}	DP _n	F _{TMAMA} (mol.%)	M _n (g/mol)	Đ	DC (%)
L1						
L1_PAS ⁻	71	390	18	46,700	1.12	- 37
L2						
L2_PAS ⁻	52	203	26	26,900	1.26	- 34
L3						
L3_PAS ⁻	224	497	45	73,800	1.96	- 51
L4_PAS ⁻	68	272	25	42,500	1.29	24
L5_PAS ⁻	139	190	74	50,300	1.33	42
L6_PAS ⁻	261	279	93	86,500	1.5500	47

Where: DP_{TMAMA}—polymerization degree of TMAMA units; DP_n—total polymerization degree; F_{TMAMA}—the content of TMAMA units in the copolymer; M_n—average molecular weight; Đ—dispersity index; DC—drug content of PAS⁻.

Table 2. Basic characteristics of graft copolymers [51,64].

No.	n _{sc}	DG (%)	DP _{sc}	DP _{TMAMA}	F _{TMAMA} (mol.%)	M _n (g/mol)	Đ	DC (%)
G1_PAS ⁻	99	48	89	35	40	841,900	1.40	43
G2_PAS ⁻			35	20	57	431,300	1.36	35
G3_PAS ⁻	65	18	75	55	73	405,000	1.46	39
G4								
G4_PAS ⁻	48	26	35	15	39	273,100	1.15	- 32
G5								
G5_PAS ⁻			28	11	36	583,500	1.03	- 36
G6	133	46						
G6_PAS ⁻			65	12	18	1,090,500	1.11	- 37

Where: n_{sc}—the number of the side chains; DG—the degree of grafting, equal to n_{sc} per polymerization degree of the main chain; DP_{sc}—the polymerization degree of the side chains, F_{TMAMA}—content of TMAMA in the side chains; M_n—average molecular weight; Đ—dispersity index; DC—drug content of PAS⁻.

The initial ratios of comonomers TMAMA:MMA in the controlled polymerization facilitated the adjustment of the ionic content (F_{TMAMA}) in the main chain of linear copolymers (18–45% of TMAMA_{Cl}⁻ vs. 25–93% of TMAMA_{PAS}⁻ units) or in the side chains of graft copolymers (18–39% of TMAMA_{Cl}⁻ vs. 40–73% of TMAMA_{PAS}⁻ units). Nevertheless, a higher content of TMAMA_{PAS}⁻ led to the conclusion that it polymerized at a higher rate than its analog TMAMA_{Cl}⁻, under analogical conditions. Furthermore, an increase in the number of initiating sites in MI corresponding to a higher grafting degree (DG) and the highest polymerization degree relating to the longest side chains (DP_{sc}) contributed to the reduction of the ionic fraction.

The relationship between copolymer composition and the initial composition of the comonomer mixture was examined to validate the statistical structure for the majority of copolymers, as indicated by F_{M1}~f_{M1}, signifying comparable reactivities of comonomers (Figure S1). For copolymers L5_PAS⁻, L6_PAS⁻, and G2_PAS⁻, G3_PAS⁻, the ionic content was higher than the initial ionic monomer content in the reaction mixture (F_{M1} > f_{M1}), suggesting that these conjugates can be categorized as gradient copolymers with a dominant TMAMA fraction. They facilitate the segregation of hydrophilic and hydrophobic parts, leading to a more pronounced formation of core-shell micelles compared to statistical copolymers. The nanoparticles formed by statistical copolymers result from interactions causing the shrinkage of entangled polymeric chains. In the case of graft copolymers, functioning as non-linear block copolymers, phase separation is facilitated by the main chain, generating a water-insoluble core, while side chains with either statistical or gradient structures form a layer around the core.

The introduction of PAS counterions into the polymer through the polymerization of TMAMA_{PAS}⁻ resulted in single drug delivery systems. UV-vis analysis indicated that

the drug content of PAS (DC, Tables 1 and 2) reached 24–47% in the linear copolymers L4_PAS⁻–L6_PAS⁻, increasing with the ionic content, and 35–43% in the graft copolymers G1_PAS⁻–G3_PAS⁻, increasing with both DG and F_{TMAMA}, as well as the length of side chains. In copolymers with chloride counterions, ionic exchange was beneficial for introducing the PAS counterions as pharmaceutical ones, transforming L1–L3 to L1_PAS⁻–L3_PAS⁻ and G4–G6 to G4_PAS⁻–G6_PAS⁻ with satisfactory DC levels ranging 34–51% and 32–37% [51], respectively. The highest DC was observed in sample L3_PAS⁻, comparable to L6_PAS⁻, corresponding to the highest F_{TMAMA} in the linear copolymer in both series. Graft copolymers G4_PAS⁻–G6_PAS⁻, which contained lower DP_{TMAMA} than directly obtained G1_PAS⁻–G3_PAS⁻ conjugates, achieved similar DCs (32–37% vs. 35–43%, respectively). These results demonstrated more controlled DC adjustment by structural parameters for copolymers derived from TMAMA_PAS⁻ than in the case of post-polymerization modification of polymers yielding exchange to PAS⁻. The excess chloride anions could be locally reduced by the steric hindrance of entangled polymer chains, influencing the exchange efficiency as an additional parameter.

2.2. Wettability and Amphiphilic Properties

Wettability measurements were conducted through goniometry using the sessile water drop method on a polymer film applied to a glass plate via spin coating. The aim was to determine the water contact angle (WCA) as a parameter for assessing the degree of hydrophilicity in the polymer systems.

The results for linear copolymers showed that an increase in ionic fraction content led to a reduction in WCA (Figure 2a). For Cl⁻-based polymers (L1–L3), this reduction ranged from 53° to 39°, while for PAS-based polymers (L4_PAS⁻–L6_PAS⁻), it ranged from 48° to 30° [63]. Comparing polymers containing PAS anions (L4_PAS⁻) to their Cl⁻ counterparts (L2) with a similar amount of ionic fraction (~26%), the films of the latter exhibited lower surface wetting, correlated with slightly higher WCAs. This indicated reduced water interaction with the polymer surface, suggesting lower hydrophilicity.

Similarly, in the case of graft copolymers G1_PAS⁻–G3_PAS⁻, there was a trend of decreasing WCA with increasing F_{TMAMA}, in contrast to the series of polymers G4–G6 with chloride anions (Figure 2b). Among them, G3_PAS⁻ exhibited the highest wettability, characterized by loosely grafted long side chains and the highest ionic content. In Cl⁻-containing graft copolymers, the highest grafting degree and the longest side chains in relation to the lowest content of the TMAMA fraction contributed to the high degree of hydrophilicity in copolymer G6 [51]. The exchange of Cl⁻ anions with PAS ones induced a reduction in WCA values (from 56.3–44.3° to 45.7–30.3°), resulting in films with higher wettability after introducing the drug into the polymer matrix. Moreover, these films were more hydrophilic than those in the series G1_PAS⁻–G3_PAS⁻ obtained by the direct incorporation of the anionic drug via PAS IL monomer, especially when compared with the densely grafted G5_PAS⁻ and G6_PAS⁻.

Due to amphiphilic properties, these polymers were able to form self-assembled systems in aqueous solutions, creating a conducive environment for drug encapsulation through physical interactions with the polymer matrix. To assess self-organization and drug entrapment abilities, the critical micelle concentration (CMC) was determined for both linear and graft polymers based on PILs. The CMC values were obtained through goniometry, defining the interfacial tension (IFT) of aqueous solutions of the tested polymer systems in various concentrations ($c = 5 \times 10^{-4}$ –0.3 mg/mL) to identify the cross-over point in the IFT vs. logC plot (Figure S2).

For linear copolymers with chloride anions (L1–L3, F_{TMAMA} = 18–45%), CMC values ranged from 0.037 to 0.063 mg/mL. In contrast, PAS-based copolymers (L4_PAS⁻–L6_PAS⁻) showed a broader range of CMCs from 0.027 to 0.181 mg/mL due to higher ionic content (25–93%) (Figure 2c). An increase in CMC correlated with an elevation in the ionic fraction content was observed in both copolymer series. Comparing analogous copolymers based on Cl⁻ vs. PAS⁻ (L2 vs. L4_PAS⁻) with similar F_{TMAMA} parameters but differences in

DP_n and DP_{TMAMA} , the latter polymer self-assembled at a lower concentration (0.046 vs. 0.027 mg/mL) due to its longer polymethacrylate chains providing lower solubility. This result emphasized the significant impact of anions within the copolymer matrix on interactions between polymer chains, thereby altering the overall self-assembly behavior.

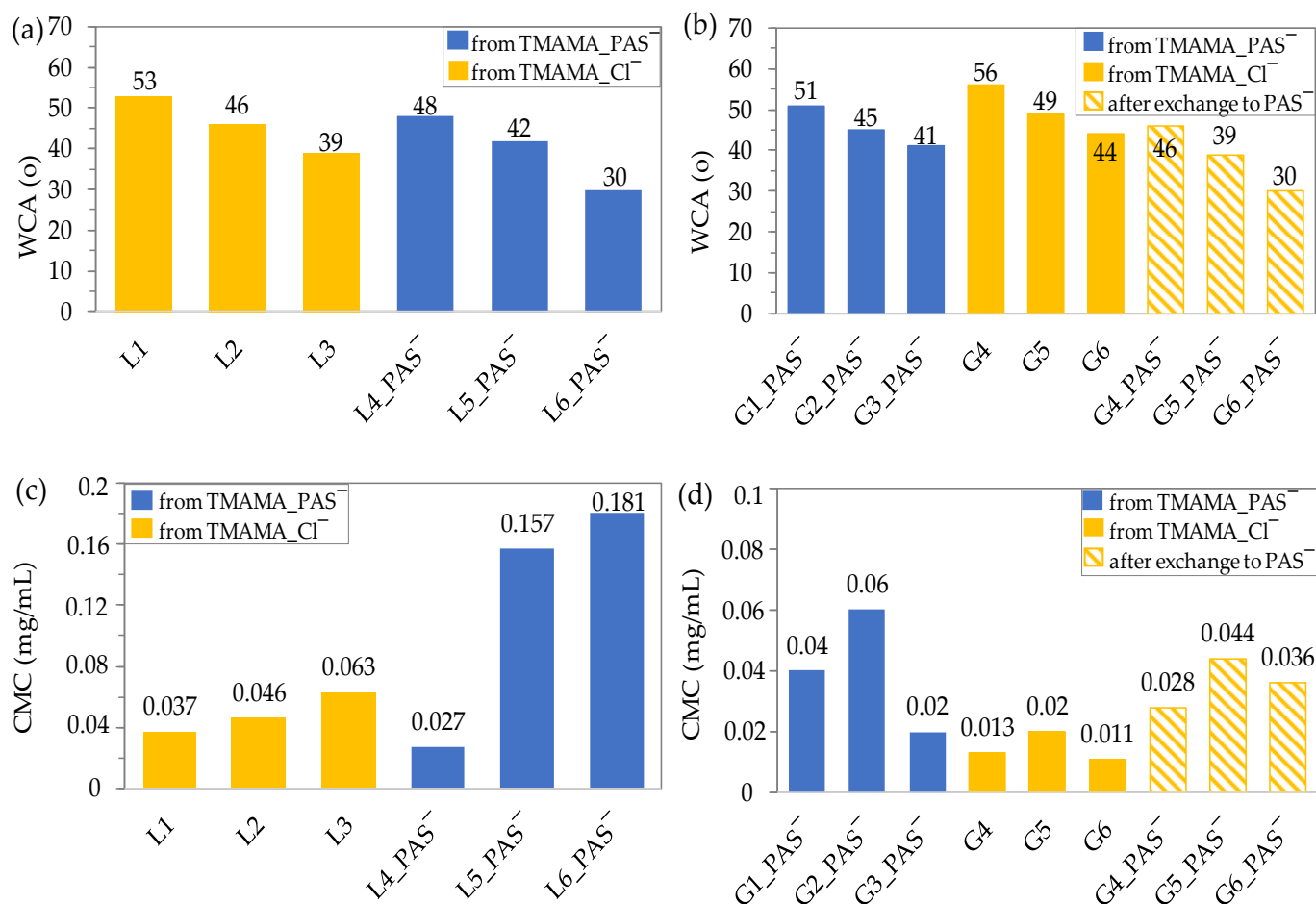


Figure 2. Evaluation through WCA of copolymer film spin-coated on glass plate (linear (a) and graft (b)) and CMCs of copolymers in aqueous solutions (linear (c) and graft (d)) determined by goniometry.

Among graft copolymers based on TMAMA_PAS⁻ IL, G3_PAS⁻ exhibited the lowest CMC (0.020 mg/mL, Figure 2d), despite its high ionic content (73 mol%), with elevated DP_{sc} contributing to better stabilization of nanoparticles. Additionally, G1_PAS⁻, containing a lower TMAMA fraction and a higher DP_{sc} , formed nanostructures at a higher polymer concentration (0.04 mg/mL) than G3_PAS⁻. The highest CMC (three times higher than G3_PAS⁻), was detected for G2_PAS⁻ (0.06 mg/mL), characterized by significantly short side chains. In the series of graft copolymers containing Cl⁻, the highest CMC value was obtained for G5 (0.02 mg/mL), characterized by the shortest side chains and the highest ionic fraction. Two other polymers, G4 with loosely distributed chains (DG = 26%) and the highest F_{TMAMA} (39%), and G6 with densely distributed grafts (DG = 46%) and the lowest F_{TMAMA} (18%), achieved comparable CMC values (0.013 and 0.011 mg/mL, respectively). The findings allow us to conclude that the length of side chains and the arrangement of ionic groups along them exert a significant influence on the self-assembling behavior of graft copolymers and CMC values.

Comparing the series of G4–G6 with the modified G4_PAS⁻–G6_PAS⁻, the PAS conjugation improved polymer solubility in aqueous solution, increasing CMC values (0.013 vs. 0.028 mg/mL; 0.020 vs. 0.044 mg/mL; 0.011 vs. 0.036 mg/mL). However, these values were

lower than those for G1_PAS⁻-G3_PAS⁻, influenced by factors such as a larger content of PAS anions (DC = 43% vs. 32%) in the case of G1_PAS⁻ vs. G4_PAS⁻ with similar ionic fraction content ($F_{\text{TMAMA}} \sim 40\%$) or larger content of TMAMA fraction for G2_PAS⁻ vs. G5_PAS⁻ ($F_{\text{TMAMA}} = 57\%$ vs. 36%) with similar drug content (DC = 35%). The opposite correlation was observed when comparing the pair of polymers G3_PAS⁻ vs. G6_PAS⁻ (both with long side chains $\text{DP}_{\text{sc}} = 75$ vs. 65), which varied significantly by ionic fraction content ($F_{\text{TMAMA}} = 73\%$ vs. 18%) and grafting degree (DG = 18% vs. 46%). In this case, a lower density of side chains, despite the high content of ionic fraction, appeared to be beneficial for the self-assembling nanocarrier formation at lower concentrations (0.02 vs. 0.036 mg/mL, respectively).

In general, both the linear and the graft copolymers demonstrated low CMCs, classifying them as promising candidates for self-assembly behavior, favorable for the physical entrapment of drugs.

2.3. Encapsulation of Isoniazid

Considering the self-assembling properties, all types of polymers were utilized as matrices for the encapsulation of ISO to design nanoparticles with loaded drugs, as illustrated in Figure 1. The carriers, based on the PIL copolymers with chloride anions, were pharmaceutically activated by drug encapsulation as a single drug delivery system. In turn, the PAS conjugates with loaded ISO resulted in a dual drug system. The ISO loading by copolymers was preliminarily confirmed using ¹H NMR (Figure 3), showing in spectrum, characteristic signals related to the dispersed ISO in the matrix. These signals include protons in the aromatic ring at 7.73 and 8.7 ppm (c, b: 1H+1H, -CH), in the amide group at 10.1 ppm (a: 1H, -NH), and in the amine group at 4.5–5.3 ppm (d: 2H, -NH₂). In the case of PAS conjugates, the signals of the PAS drug corresponding to the aromatic protons (B, C: 2H, 5.8–5.7 ppm) and amine (D: 2H, 5.2–4.3 ppm) were also observed.

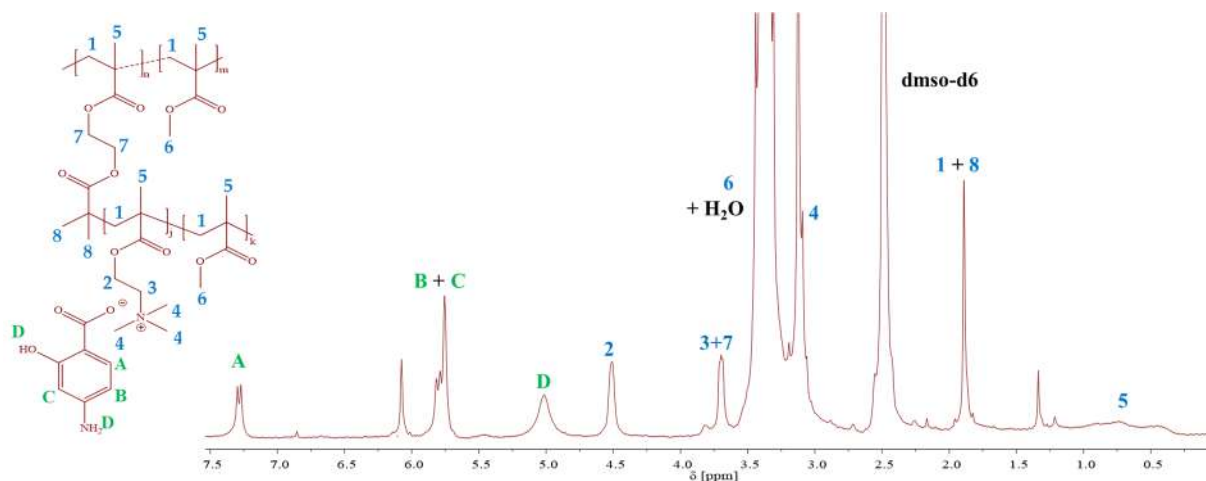


Figure 3. Representative ¹H NMR spectra of the PAS conjugate based on graft copolymer with encapsulated ISO (G3_PAS⁻/ISO).

The DC of PAS in the copolymers remained consistent throughout the self-assembling process (Tables 1 and 2, Figure 4). The drug loading content (DLC) of ISO in the copolymer nanocarriers was determined through UV-vis measurements. The DLC varied depending on the copolymer topology and composition, including the type of anions. For linear copolymers, DLC values reached 28–43% in L1–L3 and 22–23% in L1_PAS⁻-L3_PAS⁻, compared to 30–47% in L4_PAS⁻-L6_PAS⁻ (Figure 4a). These results suggest that a larger amount of TMAMA fraction with PAS counterions limited the efficiency of ISO encapsulation.

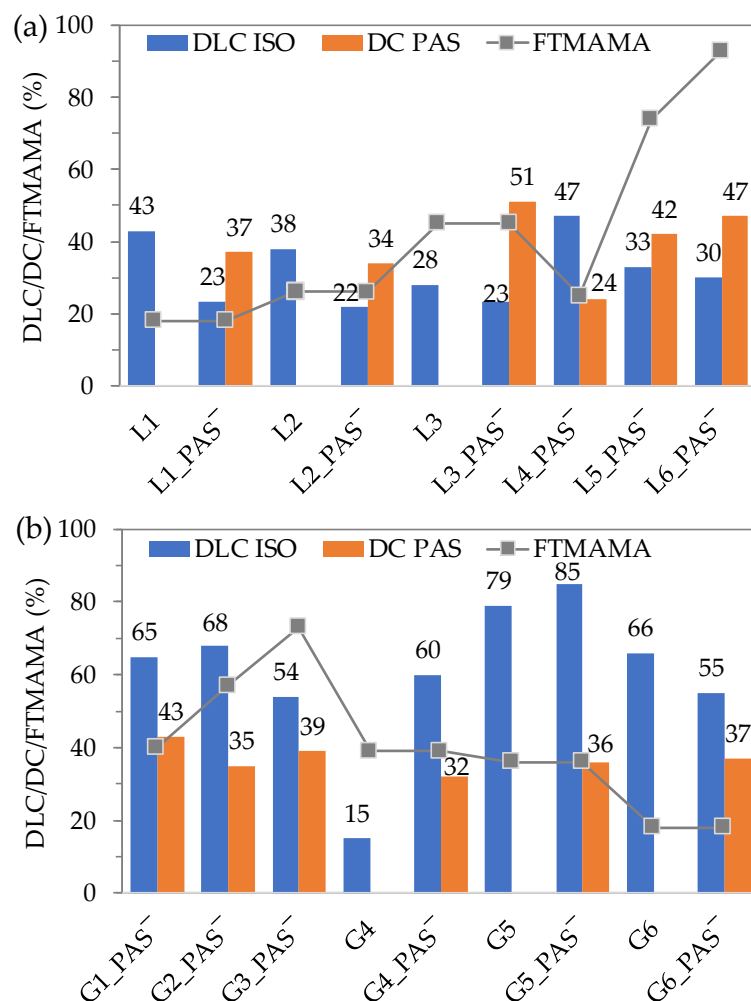


Figure 4. Drug content of PAS anions and drug loading content of ISO in relation to the content of ionic fraction in linear (a) and graft (b) copolymers of single and dual drug systems.

In the graft copolymer systems, the efficiency of ISO encapsulation depends on the carrier type. Generally, the process was executed with a high DLC: 54–68% for G1_PAS⁻–G3_PAS⁻, 15–79% for G4–G6, and 55–85% for G4_PAS⁻–G6_PAS⁻ (Figure 4b). Although the drug entrapment in the first series did not significantly vary, it was most successful for G2_PAS⁻, characterized by a lower DP_{sc} and a higher DG, which did not hinder encapsulation. It is plausible that a high DP_{TMAMA}, and consequently a high PAS content, occupied most of the space available for ISO, leading to a noticeable reduction in DLC for G3_PAS⁻. For the G4 and G5 systems, the presence of PAS enhanced the ISO loading effect, especially in the case of G4 (15 vs. 60% for single vs. dual system), while in G5, DLC did not rise substantially (79 vs. 85% for single vs. dual system). The opposite relationship was observed for G6 systems, but similarly to G5, the change was not significant (66 vs. 55% for single vs. dual system). In this series of graft copolymers, both G5 systems, characterized by the lowest DP_{sc}, appeared to be the most beneficial, carrying 79% of ISO (single drug system) and 85% of ISO accompanied by 36% of PAS (dual drug system).

The self-assembled conjugate systems, which are peculiar entangled polymeric chains as dual systems, present a distinctive combination of PAS and ISO drugs. They bind with the polymer matrix via ionic bonds and physical interaction, respectively. This generates different mechanisms for their release. In the case of pharmaceutical anions, the release occurs through exchange by phosphate anions present in physiological fluids, whereas the nonionic drug is removed from polymeric chains via diffusion. This specific strategy can be

advantageous in the controlled delivery of both drugs, achieving an enhanced therapeutic effect.

2.4. Hydrodynamic Diameters of Self-Assembled Conjugates

The self-assembled conjugates of each group, representing dual systems bearing PAS^- and ISO, were analyzed through DLS to evaluate the hydrodynamic diameters (Dh) of particles in water solutions. The systems mostly created two prevailing fractions, as demonstrated in Figure S3 by DLS histograms for obtained nanoparticles, whereas a schematic illustration of the predominant fractions exceeding 30% is shown in Figure 5. The linear copolymers formed nanoparticles with a size reaching 236–338 nm as the main fraction. The second fraction corresponded to smaller particles (below 50 nm), comprising a lower amount (~20%), apart from L4_ PAS^- /ISO, which exhibited an equivalent fraction of dramatically larger particles with a size of 1527 nm. This phenomenon was observed due to the aggregation effect of the nanoparticles. The hydrophobic moieties in this linear system, where the fraction of hydrophilic TMAMA moieties is low (FTMAMA = 25%), formed nanoparticles through π -stacking interactions. Thus, the higher TMAMA fraction in copolymers with a linear topology has a significant impact on the lower size of formed nanocarriers.

In turn, systems based on graft copolymers formed particles with hydrodynamic diameters in the range of 149–243 nm (G1_ PAS^- /ISO–G2_ PAS^- /ISO) and ~175 nm (G4_ PAS^- /ISO and G6_ PAS^- /ISO) as the prevailing fraction, regardless of variations in DLC or polymer characteristics. The second fraction, with a smaller share, showed structures with sizes between 19 and 44 nm. However, the higher chain packing in the brushes and the high content of the TMAMA fraction in G3_ PAS^- /ISO and G5_ PAS^- /ISO resulted in stronger chain attraction and the formation of small nanocarriers (68 nm and 48 nm, respectively). At the same time, the aggregation effect yielded larger ones with low intensity (250 nm and 1128 nm, respectively). This occurred due to the repulsive interactions between the ionic moieties present in the side chains, especially in the systems characterized by the shortest side chains and the lowest content of TMAMA units. The polydispersity indices were below 0.5, indicating a relatively narrow size distribution of the polymer particles. The previous examination via TEM analysis of the analogical TMAMA-based graft copolymers without encapsulated drug indicated spherical geometry of the self-assembled superstructures [53], which are also assumed for the tested systems.

2.5. In Vitro Drug Release Studies

The in vitro drug release studies were conducted through dialysis under physiological conditions (pH 7.4 at 37 °C) for a duration of 72 h. For the single drug systems based on the linear copolymers, an initial burst was observed, and the encapsulated ISO was released with a relatively low efficiency of 15–29% during the first hour (Figure 6a). However, the opposite trend was noted for the linear PAS conjugates with encapsulated ISO in the dual drug systems L1_ PAS^- /ISO–L3_ PAS^- /ISO, resulting in fast ISO release and slow PAS release, i.e., 71–97% and 13–17%, respectively (Figure 6c). In the case of dual systems L4_ PAS^- /ISO–L6_ PAS^- /ISO based on conjugates obtained directly from TMAMA_ PAS^- , differences in co-release of these drugs were less pronounced, but twice the amount of PAS was released compared to ISO, 31–54% vs. 18–30% (Figure 6d).

In comparison to the single L1–L3 systems, the presence of the second drug significantly influenced the co-release, enhancing ISO release while limiting PAS release. In the case of linear copolymers, the ionic chains could encapsulate the anionic drug inside the tangles, creating a hybrid interior. This means that some fraction of conjugated PAS anions could be entrapped between the polymer chains, limiting PAS release. On the other hand, ISO, physically bound to the matrix, could interact with present PAS ions, causing a repulsive effect and enhancing ISO release. The further release occurred at a slower rate with slight changes in the amounts of released drug (ARD), except for L3_ISO with the highest content of the ionic fraction, achieving complete drug release within 72 h. The final

ARD values are presented in Figure 7a, showing that ISO was released in larger amounts from the single linear systems (43–98%) than in the analogous dual systems (31–100%). Additionally, the ARD of ISO was similar to the ARD of PAS (48–50%) with the exception of L4_PAS⁻/ISO, where it was significantly different, yielding a release of 31% of ISO and 79% of PAS⁻.

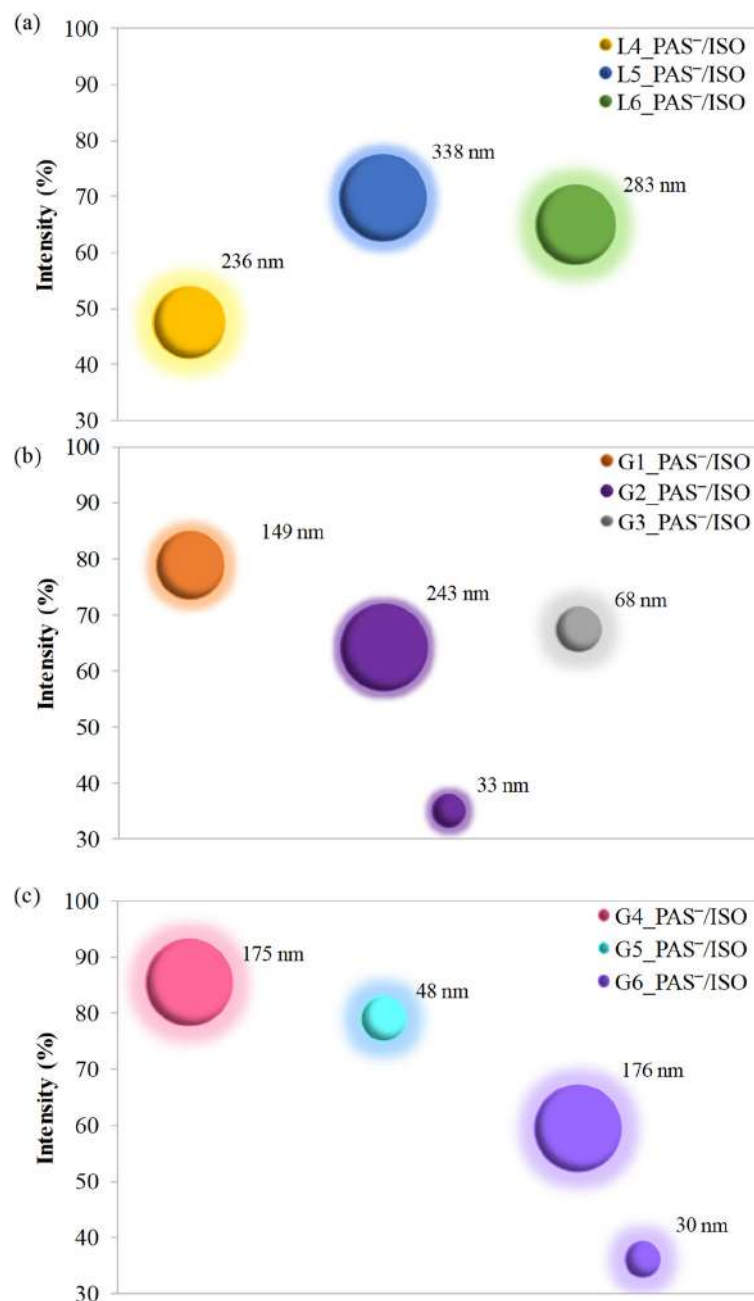


Figure 5. Hydrodynamic diameters (Dh) of L4–L6_PAS⁻/ISO⁻ (a), G1–G3_PAS⁻/ISO⁻ (b) and G4–G6_PAS⁻/ISO⁻ (c), ISO-loaded polymer nanoparticles determined via DLS.

Similar to the linear copolymer systems, the release profiles for the graft copolymers generally exhibited an initial rapid logarithmic increase in ARD within the first hour, followed by a nearly linear expansion of ARD up to 72 h. The highest amounts of ISO were released within the first hour, reaching 36–46% for G1_PAS⁻–G3_PAS⁻ (Figure 6e), 15–60% for G4–G6 (Figure 6b), and 11–26% for G4_PAS⁻–G6_PAS⁻ (Figure 6f). However, subsequent drug release was limited due to the enhanced stability of the nanocarriers, as evidenced by their low CMC values. Specifically, G2_PAS⁻ exhibited a faster rate of ISO

release, resulting in a higher ARD compared to G3_PAS⁻ with the same grafting degree but longer side chains and higher TMAMA content (54% vs. 41%, respectively). Compared to ARD from the conjugates containing only PAS prepared directly from TMAMA_PAS⁻ [64], the presence of ISO marginally reduced PAS release, with G1 dropping from 100% to 94% and G2 from 91% to 87%. An exception was G3, where ARD ranged from 75% to 93% due to intensified repulsive interactions between PAS anions. Less effective release of ISO was observed for the graft copolymers G4–G6 and their PAS conjugates, with the exception of the G4 system characterized by the short backbone and lower grafting density, and simultaneously the highest TMAMA content in this series of polymers. In this single drug system, the ARD of ISO was twice as high as in its dual analog (61% vs. 29%, respectively), whereas the release profiles for G5 and G6 were comparable in the single and dual systems, yielding ~20% of ISO ARD with no impact of the ionic PAS presence. Thus, G5 was found to be the most advantageous for ISO release, indicating that the less packaging of the side chains bearing Cl⁻ was favorable for drug transport, attributable to the smaller steric effect allowing superior access to the drug for release.

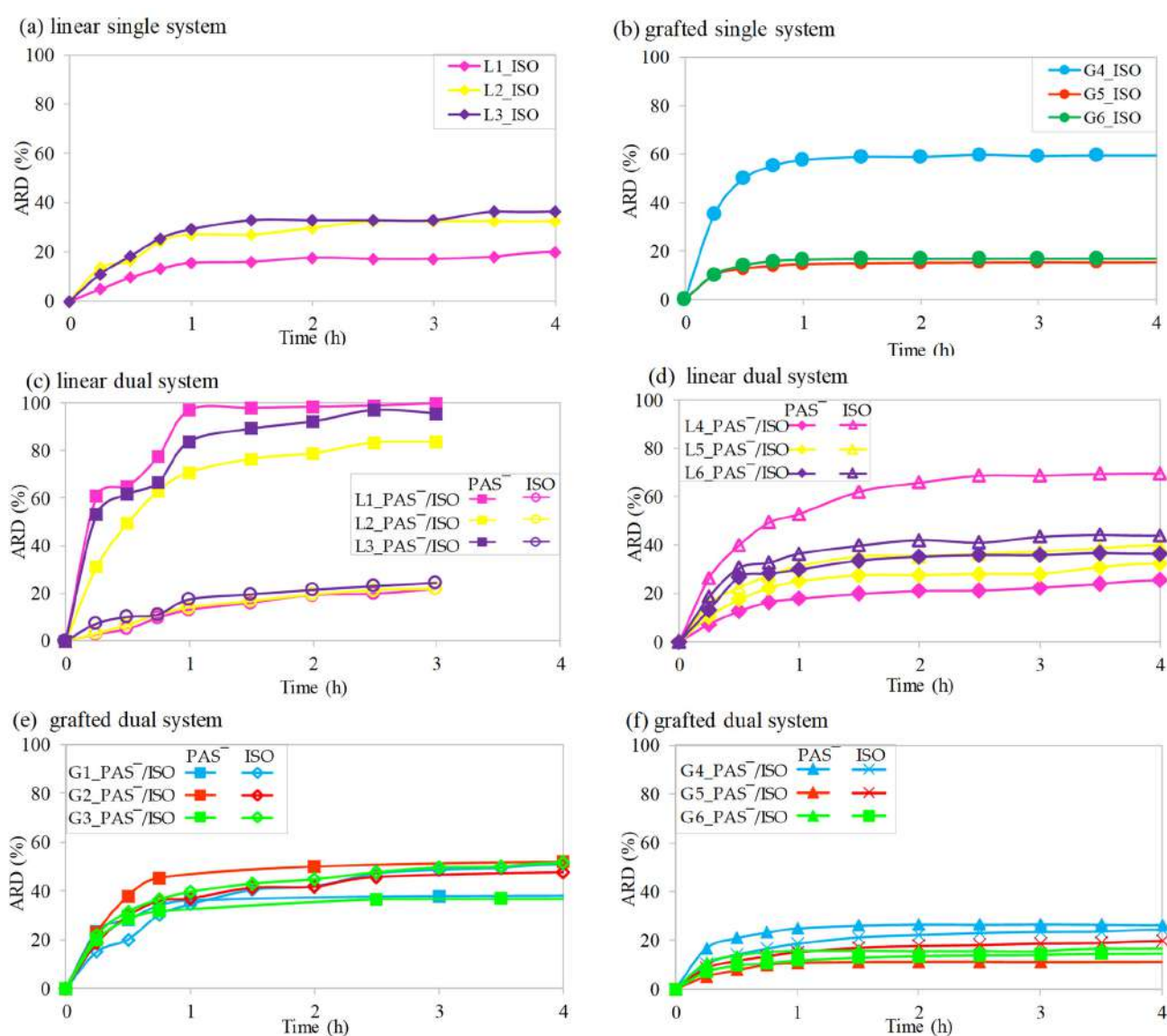


Figure 6. Drug release profiles for single drug systems based on copolymers with encapsulated ISO: L1–L3 (a), G4–G6 (b), and dual drug systems: L1_PAS⁻/ISO–L3_PAS⁻/ISO (c), L4_PAS⁻/ISO–L6_PAS⁻/ISO (d), G1_PAS⁻/ISO–G3_PAS⁻/ISO (e), G4_PAS⁻/ISO–G6_PAS⁻/ISO (f).

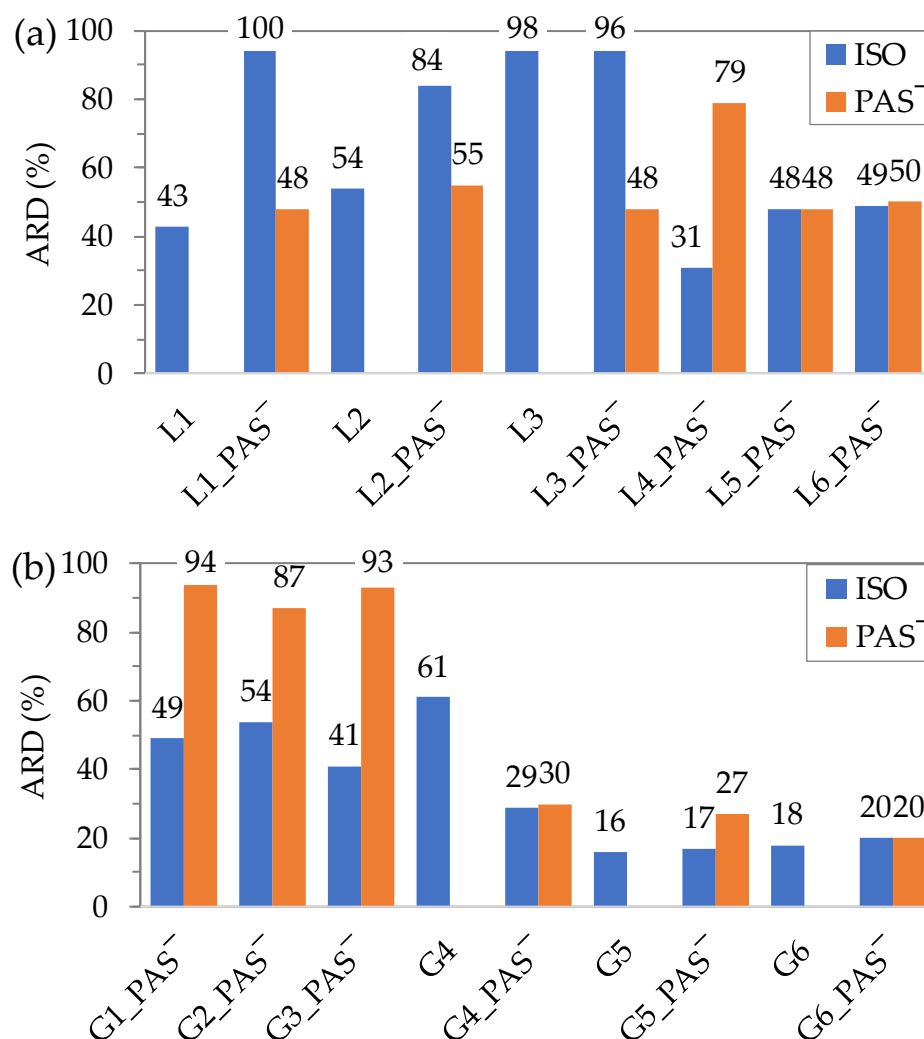


Figure 7. Amount of released drug by linear (a) and graft (b) copolymers of single and dual drug systems in PBS (pH 7.4 at 37 °C).

In the case of ionic drug release, the graft copolymers G1_PAS⁻–G3_PAS⁻ in dual drug systems demonstrated highly effective replacement of PAS anions by phosphate ones ranging between 87 and 94%, with a burst effect in the first hour (~50%), regardless of the polymer's characteristics and ionic content (Figure 6e). The higher release rate of the anionic PAS in comparison to the encapsulated ISO was different from that for the polymer modified with PAS⁻ to conjugates G4_PAS⁻–G6_PAS⁻ (Figure 6f), where ARD values of PAS and ISO were comparable. A marked discrepancy in ARD percentages emerges when contrasting the PAS conjugates obtained directly via PAS IL monomer and the PAS conjugates prepared through polymer modification via exchange of Cl to PAS (G1_PAS⁻–G3_PAS⁻ vs. G4_PAS⁻–G6_PAS⁻) (Figure 7b). The PAS release from the first series was induced by the combined influence of high F_{TMAMA} and DP_{sc} or F_{TMAMA} and DG , which amplified the repulsive forces among PAS anions. The possible partial encapsulation of PAS species during the anion exchange process in G4-, G5-, and G6-based matrices might further stabilize the nanoparticles, leading to a diminished ARD. Additionally, in these carriers, probably the PAS ions were more hidden in the polymer matrix, slowing down the drug release. It also elucidates the reduced amount of released ISO from G4_PAS⁻/ISO–G6_PAS⁻/ISO systems. Comparing dual systems of both types of graft copolymers, the burst release phase was prolonged from 2.5h to 4h for G4_PAS⁻/ISO–G6_PAS⁻/ISO.

2.6. In Vitro Cytotoxicity Assay

Previous reports on the cytotoxic evaluation of linear and graft copolymers based on TMAMA as matrices for drug delivery systems indicated non-cytotoxic effects towards normal human bronchial epithelial cells (BEAS-2B) and cytotoxic effects on adenocarcinomic human alveolar basal epithelial cells (A549) [72,73]. Basic cytotoxicity studies were conducted using the colorimetric MTT assay at various concentrations of polymer systems (3–100 $\mu\text{g}/\text{mL}$) on BEAS-2B cell lines to assess their impact on cell viability. For these tests, model samples were selected from the individual groups: L5_PAS⁻ vs. L5_PAS⁻/ISO, and G2_PAS⁻/ISO vs. G6_ISO vs. G6_PAS⁻/ISO. Following the administration of samples, treated cell lines were incubated for 72 h under standard conditions.

Cytotoxicity increased with concentration, as depicted in Figure 8. The single system with PAS⁻ (L5_PAS⁻) exhibited the most pronounced cytotoxic effect at the highest concentration (100 $\mu\text{g}/\text{mL}$), where cell viability decreased to 24%. In comparison to PAS conjugates based on grafted systems described previously [72], the survival rate for G6_PAS⁻ equal to 54%. Interestingly, the addition of a second drug in dual systems caused a significant decrease in cytotoxicity, evident for L5_PAS⁻/ISO and for G6_PAS⁻/ISO at the highest concentration. Moreover, at concentrations below 100 $\mu\text{g}/\text{mL}$, L5_PAS⁻/ISO did not exhibit any cytotoxicity, and its action on BEAS-2B cell lines resulted in increased cell viabilities. In contrast, the addition of the highest concentration of the single drug system G6_ISO caused the least decrease in viability, indicating that this sample is less cytotoxic at the highest tested concentration. Cell treatment with G2_PAS⁻/ISO at the highest concentration reduced cell viability by up to 60%, similar to L5_PAS⁻/ISO.

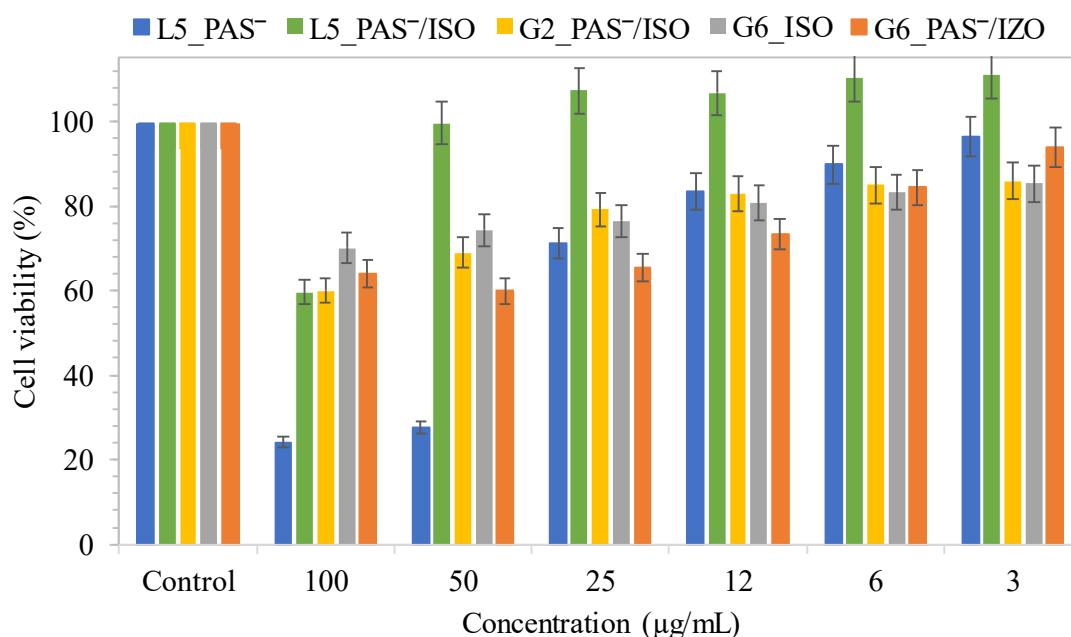


Figure 8. Cell viability of single and dual drug systems bearing PAS⁻ or/and ISO as a selected model drug delivery systems consisted of linear or graft PIL-based copolymers at different concentrations for BEAS-2B cell line treatment, after 72 h of incubation in comparison to the controls (100%).

The percentage of cell coverage, i.e., confluence, was determined after 72 h of incubation at two different concentrations of dual systems, namely 3 and 100 $\mu\text{g}/\text{mL}$. Confluence, reflecting the impact of sample treatment on BEAS-2B cell lines and influenced by cell death, was measured as a percentage relative to untreated control cells. In each sample, a comparison between the highest and lowest concentrations revealed an increase in confluence at the lowest concentration (25% vs. 98% in L5_PAS⁻/ISO; 89% vs. 103% in G2_PAS⁻/ISO; 73% vs. 101% in G6_PAS⁻/ISO) (Figure 9a). The treatment with the L5_PAS⁻/ISO system at the highest concentration led to significant cell proliferation (confluence ~25%), resulting

in the smallest coverage compared to other tested systems. However, this system did not induce any harmful effects on BEAS-2B cell lines at low concentrations. Treatment with graft polymer systems at 100 $\mu\text{g}/\text{mL}$ induced cell death only up to 11% and 27% in G2_PAS⁻/ISO and G6_PAS⁻/ISO, respectively. Microscopic pictures are presented in Figure 9b. The results indicated that these systems exhibit weak or non-cytotoxic effects against BEAS-2B cell lines, especially at low concentrations.

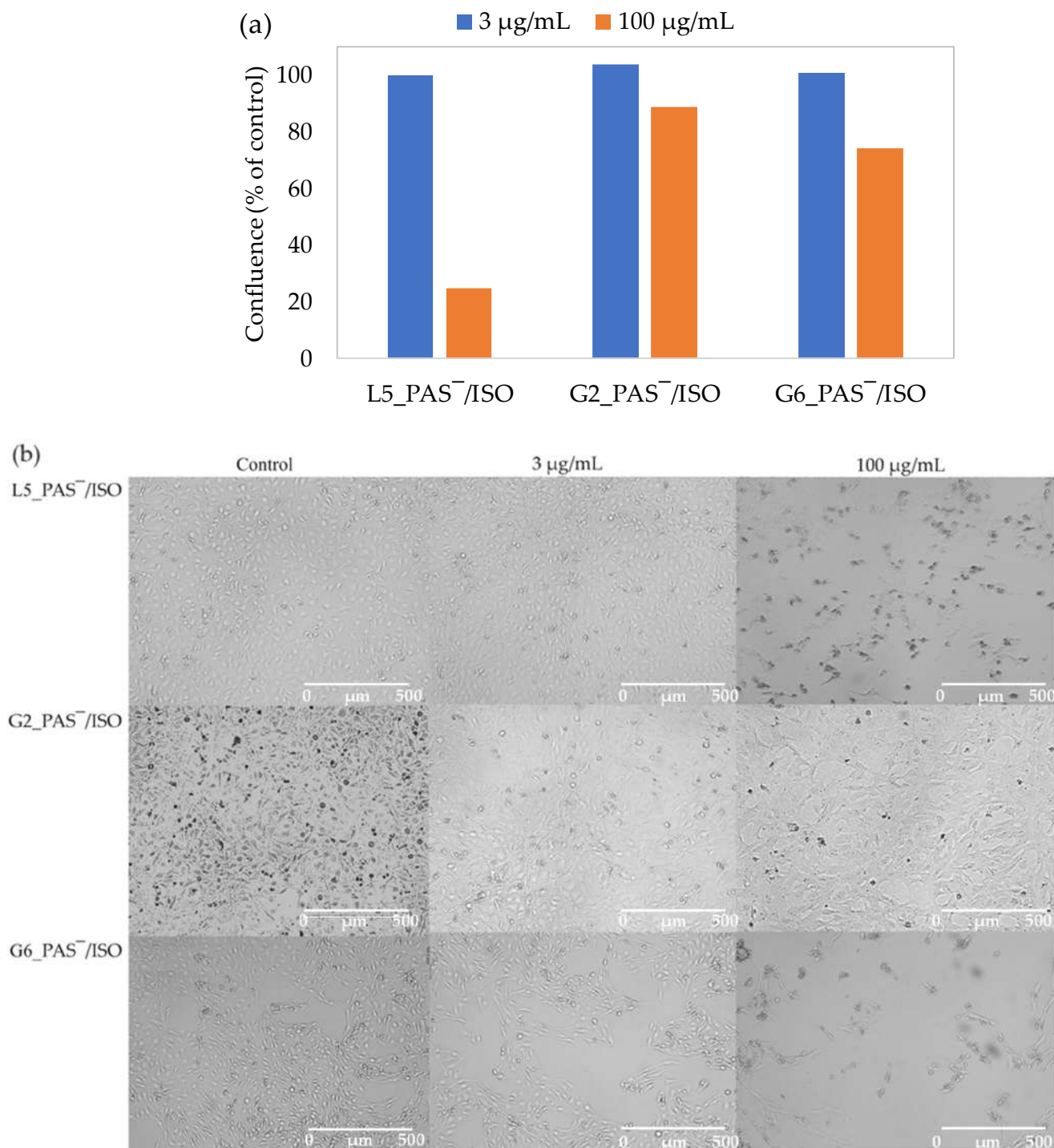


Figure 9. The confluence of dual systems L5_PAS⁻/ISO, G2_PAS⁻/ISO, and G6_PAS⁻/ISO against BEAS-2B cell line (a), and microscopic pictures taken with a Live Cell Analyzer for untreated control cells vs. treated BEAS-2B cell lines with the dual systems L5_PAS⁻/ISO, G2_PAS⁻/ISO and G6_PAS⁻/ISO in concentrations 3 $\mu\text{g}/\text{mL}$ and 100 $\mu\text{g}/\text{mL}$ (b).

3. Materials and Methods

Linear copolymers based on TMAMA/Cl⁻ (L1–L3) or TMAMA/PAS⁻ (L4_PAS⁻–L6_PAS⁻) were synthesized as it was reported [56]. Graft copolymers based on TMAMA/PAS⁻ (G1_PAS⁻–G3_PAS⁻) [64] or TMAMA/Cl⁻ (G4–G6) [51] were synthesized by grafting from multifunctional macroinitiator. The conjugates L1_PAS⁻–L3_PAS⁻ [50] and G4_PAS⁻–G6_PAS⁻ [51] were prepared through ionic exchange of Cl⁻ in the reaction of PAS salt with polymer L1–L3 and G4–G6, respectively. Tetrahydrofuran (THF), methanol (MeOH), isoniazid (ISO), phosphate-buffered saline (PBS), DMEM-F12 medium, and 3-(4,5-dimethyl-thiazol-2-yl)-2,5-diphenyltetrazolium bromide (MTT) were received from Sigma-Aldrich (Poznań, Poland). Human bronchial epithelial cells (BEAS-2B) were purchased from ATCC (Cat# ATCC[®] CRL-9609; Manassas, VA, USA).

3.1. Encapsulation of ISO

Linear or graft copolymer bearing Cl counterions, or the conjugates with PAS⁻ (20 mg) and ISO (20 mg) was dissolved in methanol (2 mL). After dissolving, the deionized water (4 mL) was added dropwise into the mixture and stirred for 24 h. Then the organic solvent evaporated, whereas the aqueous fraction was lyophilized to obtain the solid product. As a result, the single drug systems bearing ISO or dual drug ones bearing PAS⁻ and ISO were obtained.

3.2. In Vitro Drug Release Studies

Single or dual drug system (1.0 mg) was dissolved in PBS (pH = 7.4), where the concentration of the mixture was equal to 1 mg/mL. The 1 mL of the obtained solution was introduced to the dialysis membrane bag (MWCO = 3.5 kDa), which then was put into a vial filled with 44 mL of PBS. The drug release studies were carried out at a temperature of 37 °C with constant stirring. The buffer solution samples (2.5 mL) were taken to estimate the concentration of the released drug using UV–vis spectroscopy, measuring absorbance at $\lambda = 265$ nm for ISO and $\lambda = 305$ nm for PAS⁻.

3.3. Cell Growth and Cytotoxicity Assay

Cells were grown in a DMEM-F12 medium in sterile culture bottles characterized by 75 cm² of culture area, with 10% (*v/v*) FBS at 37 °C in the incubator (humidified atmosphere with 5% CO₂). The cell cultures (10,000 cells per well) were placed in a 96-well plate for MTT tests in 0.2 mL of medium 24 h before adding polymer systems.

The MTT assay was estimated in the 96-well plates. Untreated samples were left in the first row and outer columns of wells as the controls. A series of concentrations (100–3.125 µg/mL) of the examined compounds was prepared in the remaining wells. The treated and control cells were incubated for 72 h in standard conditions. The solutions were then taken out and 50 µL of MTT solution (concentration 0.5 mg/mL in RPMI 1640 without phenol red) was added to the wells. After 2 h of incubation, the solution was removed from the wells. Formed formazan crystals were flooded and dissolved in 75 µL of isopropanol:HCl mixture (*v/v* = 1:0.04). The cytotoxicity was estimated via measurement of the formazan absorbance at 570 nm in a microplate reader. Measurements were repeated three times. The results were presented as the percentage fraction of the control. The cell viability and confluence analyses were performed with the use of a Live Cell Analyzer. After 72 h of incubation, the microscopic images were taken from treated and untreated cells.

3.4. Characterization

¹H-NMR spectra were recorded with a UNITY/NOVA (Varian, Mulgrave, Victoria, Australia) spectrometer operating at 300 MHz. The measurements were carried out in deuterated dimethyl sulfoxide (DMSO) with tetramethylsilane (TMS) as an internal standard. The spectrum peaks were integrated and fitted using the MestReNova software, version: 6.0.2-5475. The critical micelle concentration (CMC) was evaluated by measuring

the interfacial tension (IFT) using the pendant drop method on a goniometer (OCA 15EC, DataPhysics, Filderstadt, Germany). A series of polymers in aqueous solutions in different concentrations (0.0006–0.15 mg/mL) was prepared. A goniometer was also used for water contact angle determination (WCA), employing the sessile drop method. The polymer solution in methanol (0.3 mg/mL) was transferred by spin-coating on a thin glass plate. Next, 4 μ L of deionized water was dispensed onto the polymer layer, then the WCA value was measured. The result data was processed using SCA20_U software, version: 5.0.38. The hydrodynamic diameters (Dh) of polymer particles and polydispersity index (PDI) were estimated through dynamic light scattering (DLS) using a Zetasizer Nano-S90 (Malvern Technologies, Malvern, UK). Samples in poly(methyl methacrylate) (PMMA) cells (concentration of samples = 1.0 mg/mL) were placed into the thermostatted cell compartment of the device at 25 °C. The measurements were repeated three times, to create an average value. Ultraviolet–visible light spectroscopy (UV–Vis, spectrometer Evolution 300, Thermo Fisher Scientific, Waltham, MA, USA) was used for determination of the ionic drug content (DC), the non-ionic drug loading content (DLC), as well as the amount of the released drug (ARD) during in vitro studies in PBS to estimate the absorbance of PAS[−] and ISO. Viability monitoring and confluence analysis were performed using a Live Cell Analyzer (JuLI™ Br; NanoEnTek Inc., Seoul, Republic of Korea). The cytotoxicity through the MTT test was estimated by measuring the absorbance of the formazan product at 570 nm with the use of a microplate reader (Epoch, BioTek, Winooski, VT, USA).

4. Conclusions

Various types of self-assembled ionic conjugates were obtained as single and dual drug systems constructed from linear and graft PIL-based copolymers. Due to the ionic structure of choline units, the copolymers could carry the drug in anionic form, i.e., PAS[−] (DC = 24–47%). Wettability assessment of chloride-based polymers indicated a hydrophilic nature (WCA = 39–56°), while the PAS conjugates exhibited higher hydrophilicity (WCA = 30–51°). The amphiphilic properties of Cl[−]-based (CMC = 0.037–0.063 μ g/mL vs. 0.011–0.020 μ g/mL for linear vs. graft) and PAS-based polymers (CMC = 0.027–0.181 μ g/mL vs. 0.020–0.060 μ g/mL vs. 0.028–0.044 μ g/mL for linear vs. graft vs. graft modified) enabled the encapsulation of ISO.

The ISO loading was sufficient in both single and dual drug systems, reaching 28–47% for linear, 54–68% for graft, and 15–85 % for graft-modified polymers. ISO was released in similar or lower amounts than PAS (16–61% vs. 20–98%, respectively). The MTT test against normal cells demonstrated low cytotoxicity of single drug systems with ISO, while the dual drug systems bearing ISO and PAS did not show any harmful action. The studies confirmed that the structure of polymers, type, and content of attached/encapsulated drugs can be used to adjust characteristics of wettability, pharmacokinetics, and cytotoxicity of systems. According to the obtained results, the designed PIL carriers, including PAS conjugates, are promising for encapsulation of ISO to attain delivery systems, including those for simultaneous co-delivery of drugs.

Supplementary Materials: The supporting information can be downloaded at <https://www.mdpi.com/article/10.3390/ijms25021292/s1>.

Author Contributions: K.N.: data curation, formal analysis, investigation, an outline and organizing the writing—original draft; S.K.: data curation, formal analysis, investigation, writing—original draft; A.M. (Aleksy Mazur): data curation, formal analysis, investigation, writing—original draft; A.M. (Anna Mielańczyk): GPC and DLS analyses; D.N.: conceptualization, methodology, funding acquisition, project administration, writing—review and editing, supervision. All authors have read and agreed to the published version of the manuscript.

Funding: This research was funded by the National Science Center, grant no. 2017/27/B/ST5/00960. The Grant for Young Scientists was supporting S.K. (BKM-546/RCH4/2023 (04/040/BKM23/0260)) and A.M. (Aleksy Mazur) (BKM-549/RCH4/2023 (04/040/BKM23/0263)).

Institutional Review Board Statement: Not applicable.

Informed Consent Statement: Not applicable.

Data Availability Statement: Data are contained within the article and Supplementary Materials.

Acknowledgments: The biological part was performed in the Biotechnology Center of the Silesian University of Technology in Gliwice. The authors would like to thank Magdalena Skonieczna for her help in cytotoxicity tests.

Conflicts of Interest: The authors declare no conflicts of interest.

References

1. Girija, A.R. 12—Medical Applications of Polymer/Functionalized Nanoparticle Systems. In *Polymer Composites with Functionalized Nanoparticles*; Pielichowski, K., Majka, T.M., Eds.; Elsevier: Amsterdam, The Netherlands, 2019; pp. 381–404.
2. Demetzos, C.; Pippa, N. Advanced drug delivery nanosystems (aDDnSs): A mini-review. *Drug Deliv.* **2014**, *21*, 250–257. [[CrossRef](#)] [[PubMed](#)]
3. Din, F.; Aman, W.; Ullah, I.; Qureshi, O.; Mustamoha, O.; Shafique, S.; Zeb, A. Effective use of nanocarriers as drug delivery systems for the treatment of selected tumors. *Int. J. Nanomed.* **2017**, *12*, 7291–7309. [[CrossRef](#)] [[PubMed](#)]
4. Cukierman, E.; Khan, D. The benefits and challenges associated with the use of drug delivery systems in cancer therapy. *Biochem. Pharmacol.* **2010**, *80*, 762–770. [[CrossRef](#)] [[PubMed](#)]
5. Allen, T. Drug Delivery Systems: Entering the Mainstream. *Science* **2004**, *303*, 1818–1822. [[CrossRef](#)]
6. Ojewole, E.; Macraj, I.; Naidoo, P.; Govender, T. Exploring the use of novel drug delivery systems for antiretroviral drugs. *Eur. J. Pharm. Biopharm.* **2008**, *70*, 697–710. [[CrossRef](#)] [[PubMed](#)]
7. Buddolla, A.L.; Kim, S. Recent insights into the development of nucleic acid-based nanoparticles for tumor-targeted drug delivery. *Colloids Surf. B* **2018**, *172*, 315–322. [[CrossRef](#)] [[PubMed](#)]
8. Duan, Q.; Ma, L.; Zhang, B.; Zhang, Y.; Li, X.; Wang, T.; Zhang, W.; Li, Y.; Sang, S. Construction and application of targeted drug delivery system based on hyaluronic acid and heparin functionalised carbon dots. *Colloids Surf. B* **2020**, *188*, 110768. [[CrossRef](#)]
9. Chacko, I.A.; Ghate, V.M.; Dsouza, L.; Lewis, S.A. Lipid vesicles: A versatile drug delivery platform for dermal and transdermal applications. *Colloids Surf. B* **2020**, *195*, 111262. [[CrossRef](#)]
10. Singh, S.; Pandey, V.; Tewari, R.; Agarwal, V. Nanoparticle based drug delivery system: Advantages and applications. *Indian J. Sci. Technol.* **2011**, *4*, 177–180. [[CrossRef](#)]
11. Gelperina, S.; Kisich, K.; Iseman, M.; Heifets, L. The potential Advantages of Nanoparticle Drug Delivery Systems in Chemotherapy of Tuberculosis. *Am. J. Respir. Crit. Care Med.* **2005**, *172*, 1487–1490. [[CrossRef](#)]
12. Yokoyama, M. Drug targeting with nano-sized carrier systems. *J. Artif. Organs* **2005**, *8*, 77–84. [[CrossRef](#)] [[PubMed](#)]
13. Couvreur, P.; Puisieux, F. Nano- and microparticles for the delivery of polypeptides and proteins. *Adv. Drug Deliv. Rev.* **1993**, *10*, 141–162. [[CrossRef](#)]
14. Ahmad, Z.; Shah, A.; Siddiq, M.; Kraatz, H.B. Polymeric micelles as drug delivery vehicles. *RSC Adv.* **2014**, *4*, 17028–17038. [[CrossRef](#)]
15. García, M.C. 13-Stimuli-responsive polymersomes for drug delivery applications. In *Stimuli Responsive Polymeric Nanocarriers for Drug Delivery Applications*; Makhoulouf, A.S., Abu-Thabit, N.Y., Eds.; Woodhead Publishing: Sawston, UK, 2019; Volume 2, pp. 345–392.
16. Torchilin, V. Structure and design of polymeric surfactant-based drug delivery systems. *J. Control. Release* **2001**, *73*, 137–172. [[CrossRef](#)] [[PubMed](#)]
17. Atanase, L.I. Micellar Drug Delivery Systems Based on Natural Biopolymers. *Polymers* **2021**, *13*, 477. [[CrossRef](#)] [[PubMed](#)]
18. Kulthe, S.; Choudhari, M.; Inamdar, N.; Mourya, V. Polymeric micelles: Authoritative aspects for drug delivery. *Des. Monomers Polym.* **2012**, *15*, 465–521. [[CrossRef](#)]
19. Yokoyama, M. Polymeric micelles as drug carriers: Their lights and shadows. *J. Drug Target.* **2014**, *22*, 576–583. [[CrossRef](#)]
20. Haag, R. Supramolecular Drug-Delivery Systems Based on Polymeric Core–Shell Architectures. *Angew. Chem. Int. Ed.* **2004**, *43*, 278–282. [[CrossRef](#)]
21. Figueiras, A.; Domingues, C.; Jarak, I.; Santos, A.; Parra, A.; Pais, A.; Alvarez-Lorenzo, C.; Concheiro, A.; Kabanov, A.; Cabral, H.; et al. New Advances in Biomedical Application of Polymeric Micelles. *Pharmaceutics* **2022**, *14*, 1700. [[CrossRef](#)]
22. Aliabadi, H.M.; Lavasanifar, A. Polymeric micelles for drug delivery. *Expert Opin. Drug Deliv.* **2005**, *3*, 139–162. [[CrossRef](#)]
23. Ke, X.; Ng, V.; Ono, R.; Chan, J.; Krishnamurthy, S.; Wang, Y.; Hedrick, J.; Yang, Y. Role of non-covalent and covalent interactions in cargo loading capacity and stability of polymeric micelles. *J. Control. Release* **2014**, *193*, 9–26. [[CrossRef](#)] [[PubMed](#)]
24. De, R.; Mahata, M.K.; Kim, K.T. Structure-Based Varieties of Polymeric Nanocarriers and Influences of Their Physicochemical Properties on Drug Delivery Profiles. *Adv. Sci.* **2022**, *9*, 2105373. [[CrossRef](#)] [[PubMed](#)]
25. Tang, Z.; He, C.; Tian, H.; Ding, J.; Hsiao, B.S.; Chu, B.; Chem, X. Polymeric nanostructured materials for biomedical applications. *Prog. Polym. Sci.* **2016**, *60*, 86–128. [[CrossRef](#)]
26. Ghosh, B.; Biswas, S. Polymeric micelles in cancer therapy: State of the art. *J. Control. Release* **2021**, *332*, 127–147. [[CrossRef](#)] [[PubMed](#)]

27. Jhaveri, A.M.; Torchilin, V.P. Multifunctional polymeric micelles for delivery of drugs and siRNA. *Front. Pharmacol.* **2014**, *5*, 77. [[CrossRef](#)] [[PubMed](#)]
28. Wang, B.; Qin, L.; Mu, T.; Xue, Z.; Gao, G. Are Ionic Liquids Chemically Stable? *Chem. Rev.* **2017**, *117*, 7113–7131. [[CrossRef](#)] [[PubMed](#)]
29. Mallakpour, S.; Dinari, M. Ionic Liquids as Green Solvents: Progress and Prospects. In *Green Solvents II: Properties and Applications of Ionic Liquids*; Mohammad, A., Inamuddin, Eds.; Springer: Dordrecht, The Netherlands, 2012; pp. 1–32.
30. Zhao, H. Methods for stabilizing and activating enzymes in ionic liquids—A review. *J. Chem. Technol. Biotechnol.* **2010**, *7*, 891–907. [[CrossRef](#)]
31. Sidat, Z.; Marimuthu, T.; Kumar, P.; du Toit, L.C.; Kondiah, P.P.D.; Choonara, Y.E.; Pillay, V. Ionic Liquids as Potential and Synergistic Permeation Enhancers for Transdermal Drug Delivery. *Pharmaceutics* **2019**, *11*, 96. [[CrossRef](#)]
32. Vijayakrishna, K.; Mecerreyes, D.; Gnanou, Y.; Taton, D. Polymeric Vesicles and Micelles Obtained by Self-Assembly of Ionic Liquid-Based Block Copolymers Triggered by Anion or Solvent Exchange. *Macromolecules* **2009**, *42*, 5167–5174. [[CrossRef](#)]
33. Adawiyah, N.; Moniruzzaman, M.; Hawatulaila, S.; Goto, M. Ionic liquids as a potential tool for drug delivery systems. *Med. Chem. Commun.* **2016**, *7*, 1881–1897. [[CrossRef](#)]
34. Marsh, K.N.; Boxall, J.A.; Lichtenthaler, R. Room temperature ionic liquids and their mixtures—A review. *Fluid Phase Equilibria* **2004**, *219*, 93–98. [[CrossRef](#)]
35. Earle, M.J.; Seddon, K.R. Ionic liquids. Green solvents for the future. *Pure Appl. Chem.* **2000**, *72*, 1391–1398. [[CrossRef](#)]
36. Antonietti, M.; Kuang, D.; Smarsly, B.; Zhou, Y. Ionic Liquids for the Convenient Synthesis of Functional Nanoparticles and Other Inorganic Nanostructures. *Angew. Chem. Int. Ed.* **2004**, *43*, 4988–4992. [[CrossRef](#)] [[PubMed](#)]
37. Kubisa, P. Application of Ionic Liquids as Solvents for Polymerization Processes. *Prog. Polym. Sci.* **2004**, *29*, 3–12. [[CrossRef](#)]
38. Ueki, T.; Watanabe, M. Macromolecules in Ionic Liquids: Progress, Challenges, and Opportunities. *Macromolecules* **2008**, *41*, 3739–3749. [[CrossRef](#)]
39. Lu, J.; Yan, F.; Texter, J. Advanced applications of ionic liquids in polymer science. *Prog. Polym. Sci.* **2009**, *34*, 431–448. [[CrossRef](#)]
40. Halayqa, M.; Zawadzki, M.; Domańska, U.; Plichta, A. Polymer–Ionic liquid–Pharmaceutical conjugates as drug delivery systems. *J. Mol. Struct.* **2019**, *1180*, 573–584. [[CrossRef](#)]
41. Banerjee, P.; Anas, M.; Jana, S.; Mandal, T. Recent developments in stimuli-responsive poly(ionic liquid)s. *J. Polym. Res.* **2020**, *27*, 177. [[CrossRef](#)]
42. He, Y.; Li, Z.; Simone, P.; Lodge, T.P. Self-Assembly of Block Copolymer Micelles in an Ionic Liquid. *J. Am. Chem. Soc.* **2006**, *128*, 2745–2750. [[CrossRef](#)]
43. Tao, D.J.; Cheng, Z.; Chen, F.F.; Li, Z.M.; Hu, N.; Chen, X.S. Synthesis and Thermophysical Properties of Biocompatible Cholinium-Based Amino Acid Ionic Liquids. *J. Chem. Eng. Data* **2013**, *58*, 1542–1548. [[CrossRef](#)]
44. Muhammad, N.; Hossain, M.I.; Man, Z.; El-Harabawi, M.; Bustam, M.A.; Noaman, Y.A.; Alitheen, N.; Ng, M.; Hefter, G.; Yin, C.-Y. Synthesis and Physical Properties of Choline Carboxylate Ionic Liquids. *J. Chem. Eng. Data* **2012**, *57*, 2191–2196. [[CrossRef](#)]
45. Gouveia, W.; Jorge, T.F.; Martins, S.; Meireles, M.; Carolino, M.; Cruz, C.; Almeida, T.; Araujo, M. Toxicity of ionic liquids prepared from biomaterials. *Chemosphere* **2014**, *104*, 51–56. [[CrossRef](#)] [[PubMed](#)]
46. Gomes, J.M.; Silva, S.S.; Reis, R.L. Biocompatible ionic liquids: Fundamental behaviours and applications. *Chem. Soc. Rev.* **2019**, *48*, 4317–4335. [[CrossRef](#)]
47. Li, X.; Ma, N.; Zhang, L.; Ling, G.; Zhang, P. Applications of choline-based ionic liquids in drug delivery. *Int. J. Pharm.* **2022**, *612*, 121366. [[CrossRef](#)] [[PubMed](#)]
48. Bielas, R.; Siewniak, A.; Skonieczna, M.; Adamiec, M.; Mielańczyk, Ł.; Neugebauer, D. Choline based polymethacrylate matrix with pharmaceutical cations as co-delivery system for antibacterial and anti-inflammatory combined therapy. *J. Mol. Liq.* **2019**, *285*, 114–122. [[CrossRef](#)]
49. Niesyto, K.; Mazur, A.; Neugebauer, D. Dual-Drug Delivery via the Self-Assembled Conjugates of Choline-Functionalized Graft Copolymers. *Materials* **2022**, *15*, 4457. [[CrossRef](#)] [[PubMed](#)]
50. Niesyto, K.; Neugebauer, D. Linear Copolymers Based on Choline Ionic Liquid Carrying Anti-Tuberculosis Drugs: Influence of Anion Type on Physicochemical Properties and Drug Release. *Int. J. Mol. Sci.* **2021**, *22*, 284. [[CrossRef](#)] [[PubMed](#)]
51. Niesyto, K.; Neugebauer, D. Synthesis and Characterization of Ionic Graft Copolymers: Introduction and In Vitro Release of Antibacterial Drug by Anion Exchange. *Polymers* **2020**, *12*, 2159. [[CrossRef](#)]
52. Mazur, A.; Niesyto, K.; Neugebauer, D. Pharmaceutical Functionalization of Monomeric Ionic Liquid for the Preparation of Ionic Graft Polymer Conjugates. *Int. J. Mol. Sci.* **2022**, *23*, 14731. [[CrossRef](#)]
53. Bielas, R.; Mielańczyk, A.; Skonieczna, M.; Mielańczyk, Ł.; Neugebauer, D. Choline supported poly(ionic liquid) graft copolymers as novel delivery systems of anionic pharmaceuticals for anti-inflammatory and anti-coagulant therapy. *Sci. Rep.* **2019**, *9*, 14410. [[CrossRef](#)]
54. Keihankhadiv, S.; Neugebauer, D. Synthesis and Characterization of Linear Copolymers Based on Pharmaceutically Functionalized Monomeric Choline Ionic Liquid for Delivery of p-Aminosalicylate. *Pharmaceutics* **2023**, *15*, 860. [[CrossRef](#)] [[PubMed](#)]
55. Ali, M.K.; Moshikur, R.M.; Wakabayashi, R.; Moniruzzaman, M.; Goto, M. Biocompatible Ionic Liquid-Mediated Micelles for Enhanced Transdermal Delivery of Paclitaxel. *ACS Appl. Mater. Interfaces* **2021**, *13*, 19745–19755. [[CrossRef](#)] [[PubMed](#)]
56. Mahajan, S.; Sharma, R.; Mahajan, R.K. An Investigation of Drug Binding Ability of a Surface Active Ionic Liquid: Micellization, Electrochemical, and Spectroscopic Studies. *Langmuir* **2012**, *28*, 17238–17246. [[CrossRef](#)] [[PubMed](#)]

57. Ghatak, C.; Rao, V.G.; Mandal, S.; Ghosh, S.; Sarkar, N. An Understanding of the Modulation of Photophysical Properties of Curcumin inside a Micelle Formed by an Ionic Liquid: A New Possibility of Tunable Drug Delivery System. *J. Phys. Chem. B* **2012**, *116*, 3369–3379. [[CrossRef](#)] [[PubMed](#)]
58. Kurnik, I.S.; D'Angelo, N.A.; Mazzola, P.G.; Chorilli, M.; Kamei, D.T.; Pereira, J.F.; Vicente, A.A.; Lopes, A.M. Polymeric micelles using cholinium-based ionic liquids for the encapsulation and release of hydrophobic drug molecules. *Biomater. Sci.* **2021**, *9*, 2183–2196. [[CrossRef](#)] [[PubMed](#)]
59. Lu, B.; Li, Y.; Wang, Z.; Wang, B.; Pan, X.; Zhao, W.; Ma, X.; Zhang, J. A dual responsive hyaluronic acid graft poly(ionic liquid) block copolymer micelle for an efficient CD44-targeted antitumor drug delivery. *New J. Chem.* **2019**, *43*, 12275–12282. [[CrossRef](#)]
60. Lu, B.; Zhou, G.; Xiao, F.; He, Q.; Zhang, J. Stimuli-responsive poly(ionic liquid) nanoparticles for controlled drug delivery. *J. Mater. Chem. B* **2020**, *8*, 7994–8001. [[CrossRef](#)]
61. Moniruzzaman, M.; Tahara, Y.; Tamura, M.; Kamiya, N.; Goto, M. Ionic liquid-assisted transdermal delivery of sparingly soluble drugs. *Chem. Comm.* **2010**, *46*, 1452–1454. [[CrossRef](#)]
62. Sawdon, A.J.; Peng, C.A. Polymeric micelles for acyclovir drug delivery. *Colloids Surf. B* **2014**, *122*, 738–745. [[CrossRef](#)]
63. Keihankhadiv, S.; Neugebauer, D. Self-Assembling Polymers with p-Aminosalicylate Anions Supported by Encapsulation of p-Aminosalicylate for the Improvement of Drug Content and Release Efficiency. *Pharmaceuticals* **2023**, *16*, 1502. [[CrossRef](#)]
64. Mazur, A.; Neugebauer, D. Characterization of Graft Copolymers Synthesized from p-Aminosalicylate Functionalized Monomeric Choline Ionic Liquid. *Pharmaceutics* **2023**, *15*, 2556. [[CrossRef](#)] [[PubMed](#)]
65. Soedarsono, S.; Jayanti, R.P.; Mertaniasih, N.M.; Kusmiati, T.; Permatasari, A.; Indrawanto, D.W.; Charisma, A.N.; Yuliwulandari, R.; Long, N.P.; Choi, Y.K.; et al. Development of population pharmacokinetics model of isoniazid in Indonesian patients with tuberculosis. *Int. J. Infect. Dis.* **2022**, *117*, 8–14. [[CrossRef](#)] [[PubMed](#)]
66. Takayama, K.; Schnoes, H.K.; Armstrong, E.L.; Boyle, R.W. Site of inhibitory action of isoniazid in the synthesis of mycolic acids in *Mycobacterium tuberculosis*. *J. Lipid Res.* **1975**, *16*, 308–317. [[CrossRef](#)] [[PubMed](#)]
67. Jindani, A.; Aber, V.R.; Edwards, E.A.; Mitchison, D.A. The Early Bactericidal Activity of Drugs in Patients with Pulmonary Tuberculosis. *Am. Rev. Respir. Dis.* **1980**, *121*, 939–949. [[PubMed](#)]
68. McIlleron, H.; Wash, P.; Burger, A.; Norman, J.; Folb, P.I.; Smith, P. Determinants of Rifampin, Isoniazid, Pyrazinamide, and Ethambutol Pharmacokinetics in a Cohort of Tuberculosis Patients. *Antimicrob. Agents Chemother.* **2006**, *50*, 1170–1177. [[CrossRef](#)] [[PubMed](#)]
69. Kinzig-Schippers, M.; Tomalik-Scharte, D.; Jetter, A.; Scheidel, B.; Jakob, V.; Rodamer, M.; Cascorbi, I.; Doroshenko, O.; Sorgel, F.; Fuhr, U. Should We Use N-Acetyltransferase Type 2 Genotyping To Personalize Isoniazid Doses? *Antimicrob. Agents Chemother.* **2005**, *49*, 1733–1738. [[CrossRef](#)] [[PubMed](#)]
70. Zhang, T.; Jiang, G.; Wen, S.; Huo, F.; Wang, F.; Huang, H.; Pang, Y. Para-aminosalicylic acid increases the susceptibility to isoniazid in clinical isolates of *Mycobacterium tuberculosis*. *Infect. Drug Resist.* **2019**, *12*, 825–829. [[CrossRef](#)]
71. Jennne, J.W. Partial purification and properties of the isoniazid transacetylase in human liver. Its relationship to the acetylation of p-aminosalicylic acid. *J. Clin. Investig.* **1965**, *44*, 1992–2002. [[CrossRef](#)]
72. Niesyto, K.; Łyżniak, W.; Skonieczna, M.; Neugebauer, D. Biological In Vitro Evaluation of PIL Graft Conjugates: Cytotoxicity Characteristics. *Int. J. Mol. Sci.* **2021**, *22*, 7741. [[CrossRef](#)]
73. Niesyto, K.; Skonieczna, M.; Adamiec-Organisćok, M.; Neugebauer, D. Toxicity evaluation of choline ionic liquid-based nanocarriers of pharmaceutical agents for lung treatment. *J. Biomed. Mater. Res. Part B Appl. Biomater.* **2023**, *7*, 1374–1385. [[CrossRef](#)]

Disclaimer/Publisher's Note: The statements, opinions and data contained in all publications are solely those of the individual author(s) and contributor(s) and not of MDPI and/or the editor(s). MDPI and/or the editor(s) disclaim responsibility for any injury to people or property resulting from any ideas, methods, instructions or products referred to in the content.

Ionic Liquid based Polymer Matrices for Single and Dual Drug Delivery: Impact of Structural Topology on Characteristics and In Vitro Delivery Efficiency

Katarzyna Niesyto ¹, Shadi Keihankhadiv ¹, Aleksy Mazur ¹, Anna Mielńczyk ¹, Dorota Neugebauer ¹

¹ Department of Physical Chemistry and Technology of Polymers, Faculty of Chemistry, Silesian University of Technology, 44-100 Gliwice, Poland; Katarzyna.Niesyto@polsl.pl (K.N.); Shadi.Keihankhadiv@polsl.pl (S.K.); Aleksy.Mazur@polsl.pl (A.Ma.), Anna.Mielancyk@polsl.pl (A.Mi.)

* Correspondence: Dorota.Neugebauer@polsl.pl (D.N.)

Content:

Figure S1. Copolymer composition vs. initial composition of the comonomer mixture.

Figure S2. Exemplary variation of the surface tension with the logarithm of the concentration of linear copolymer (a) L3, and grafted copolymers (b) G5 and (c) G5_PAS⁻ conjugate in aqueous solution at 25°C.

Figure S3. DLS histograms for nanoparticles based on ISO loaded (a) linear copolymers, (b) graft copolymers prepared from TMAMA_PAS, and (c) modified graft copolymers prepared from TMAMA_Cl as dual drug systems in deionized water at 25 °C.

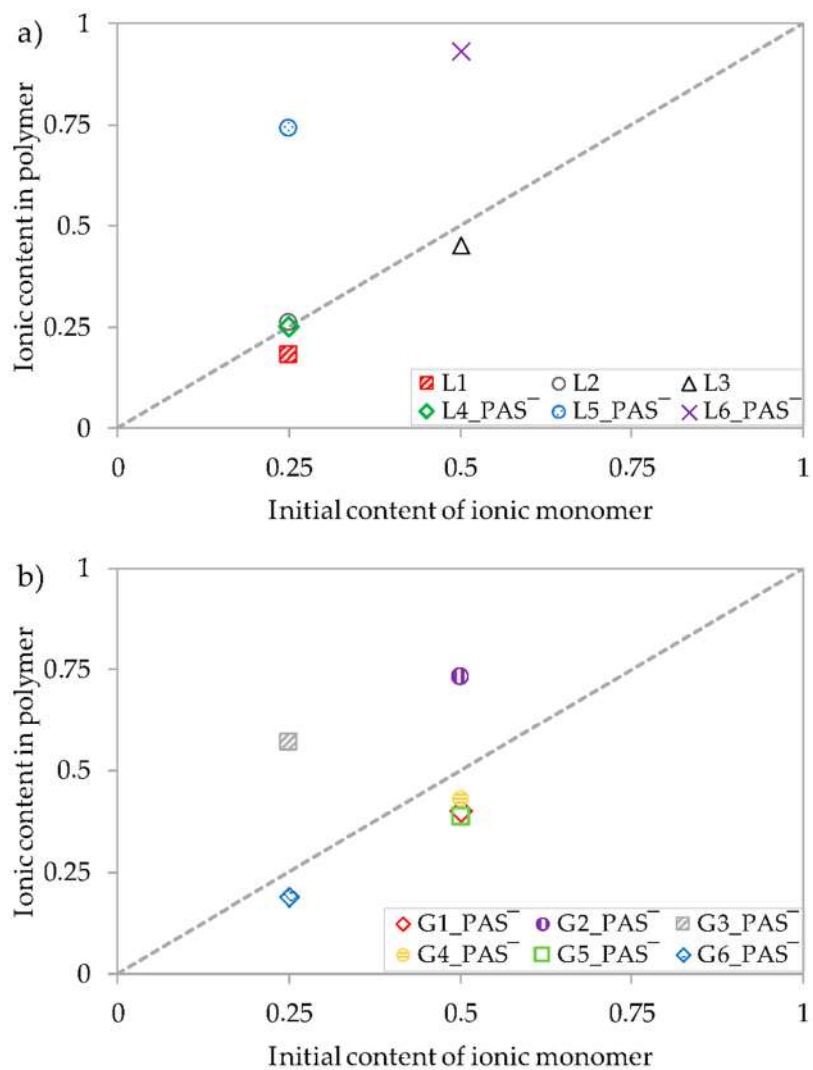


Figure S1. Copolymer composition vs. initial composition of the comonomer mixture.

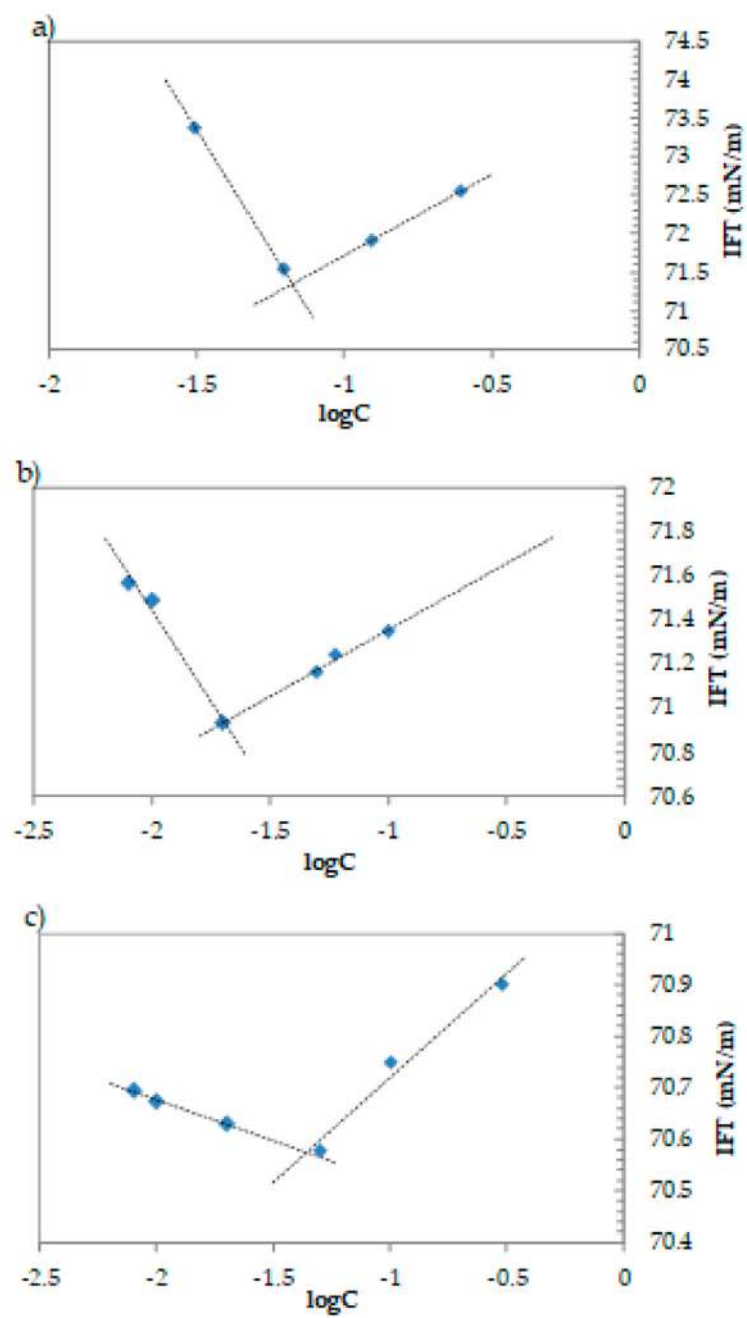


Figure S2. Exemplary variation of the surface tension with the logarithm of the concentration of linear copolymer (a) L3, and grafted copolymers (b) G5 and (c) G5_PAS⁻ conjugate in aqueous solution at 25°C.

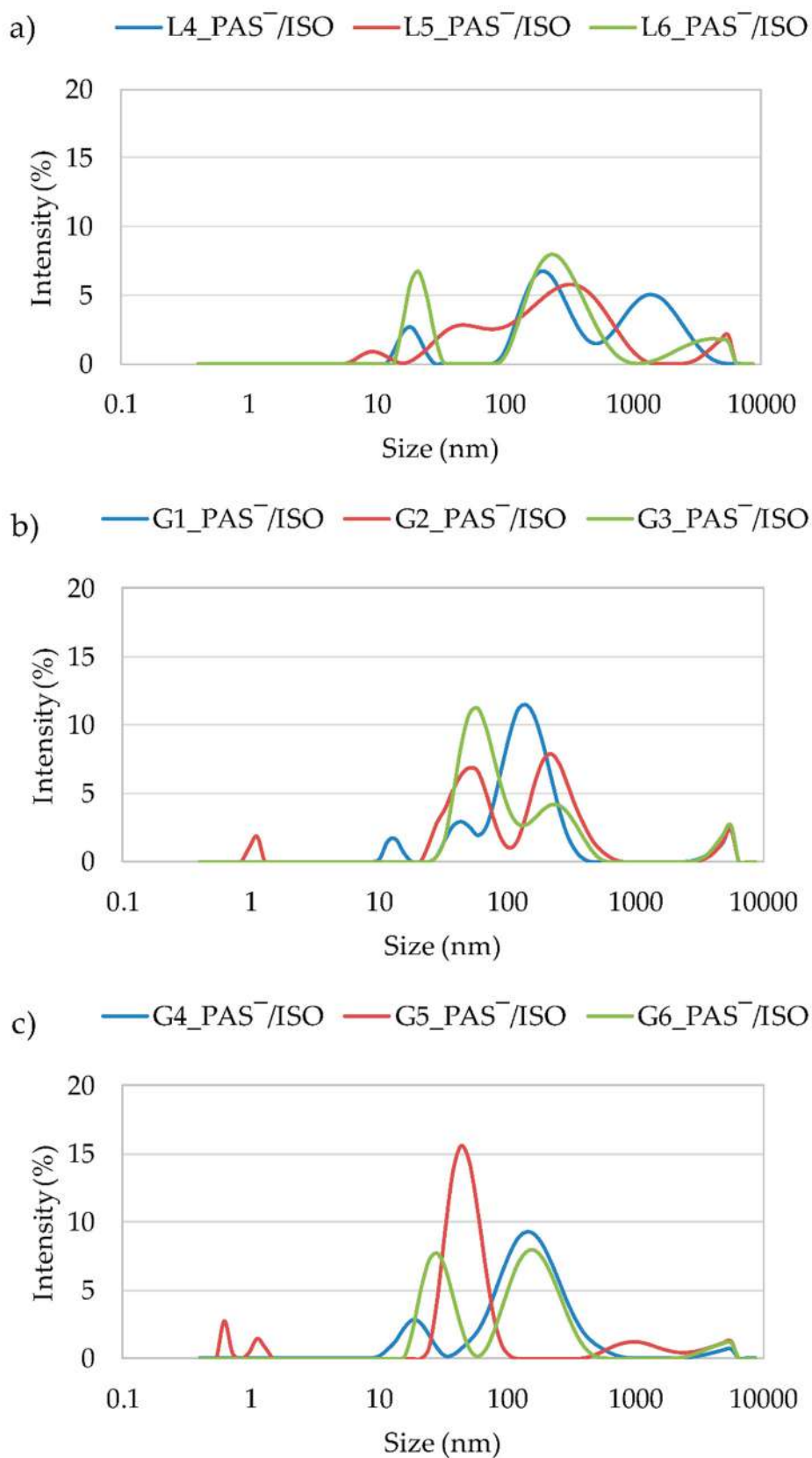


Figure S3. DLS histograms for nanoparticles based on ISO loaded (a) linear copolymers, (b) graft copolymers prepared from TMAMA_PAS, and (c) modified graft copolymers prepared from TMAMA_Cl as dual drug systems in deionized water at 25 °C.

PUBLIKACJA P.5

Piperacillin/Tazobactam co-delivery by micellar ionic conjugate systems carrying pharmaceutical anions and encapsulated drug

Niesyto, K., Mazur, A., Neugebauer, D.

Pharmaceutics 2024, 16, 198

Article

Piperacillin/Tazobactam Co-Delivery by Micellar Ionic Conjugate Systems Carrying Pharmaceutical Anions and Encapsulated Drug

Katarzyna Niesyto , Aleksy Mazur  and Dorota Neugebauer* 

Department of Physical Chemistry and Technology of Polymers, Faculty of Chemistry, Silesian University of Technology, 44-100 Gliwice, Poland; katarzyna.niesyto@polsl.pl (K.N.); aleksy.mazur@polsl.pl (A.M.)

* Correspondence: dorota.neugebauer@polsl.pl

Abstract: Previously obtained amphiphilic graft copolymers based on [2-(methacryloyloxy)ethyl]trimethylammonium chloride (TMAMA) ionic liquid were used as the matrices of three types of nanocarriers, i.e., conjugates with ionic piperacillin (PIP) and micelles with tazobactam (TAZ), which represented single systems, and dual systems bearing PIP anions and encapsulated TAZ for co-delivery. The exchange of Cl anions in TMAMA units with PIP ones resulted in a yield of 45.6–72.7 mol.%. The self-assembling properties were confirmed by the critical micelle concentration (CMC), which, after ion exchange, increased significantly (from 0.011–0.020 mg/mL to 0.041–0.073 mg/mL). The amphiphilic properties were beneficial for TAZ encapsulation to reach drug loading contents (DLCs) in the ranges of 37.2–69.5 mol.% and 50.4–80.4 mol.% and to form particles with sizes of 97–319 nm and 24–192 nm in the single and dual systems, respectively. In vitro studies indicated that the ionically conjugated drug (PIP) was released in quantities of 66–81% (7.8–15.0 µg/mL) from single-drug systems and 21–25% (2.6–3.9 µg/mL) from dual-drug systems. The release of encapsulated TAZ was more efficient, achieving 47–98% (7.5–9.0 µg/mL) release from the single systems and 47–69% (9.6–10.4 µg/mL) release from the dual ones. Basic cytotoxicity studies showed non-toxicity of the polymer matrices, while the introduction of the selected drugs induced cytotoxicity against normal human bronchial epithelial cells (BEAS-2B) with the increase in concentration.

Keywords: co-delivery systems; PIL; piperacillin; tazobactam; encapsulation

Citation: Niesyto, K.; Mazur, A.; Neugebauer, D. Piperacillin/Tazobactam Co-Delivery by Micellar Ionic Conjugate Systems Carrying Pharmaceutical Anions and Encapsulated Drug. *Pharmaceutics* **2024**, *16*, 198. <https://doi.org/10.3390/pharmaceutics16020198>

Academic Editor: Rokšana Markiewicz

Received: 22 December 2023

Revised: 19 January 2024

Accepted: 22 January 2024

Published: 30 January 2024



Copyright: © 2024 by the authors. Licensee MDPI, Basel, Switzerland. This article is an open access article distributed under the terms and conditions of the Creative Commons Attribution (CC BY) license (<https://creativecommons.org/licenses/by/4.0/>).

1. Introduction

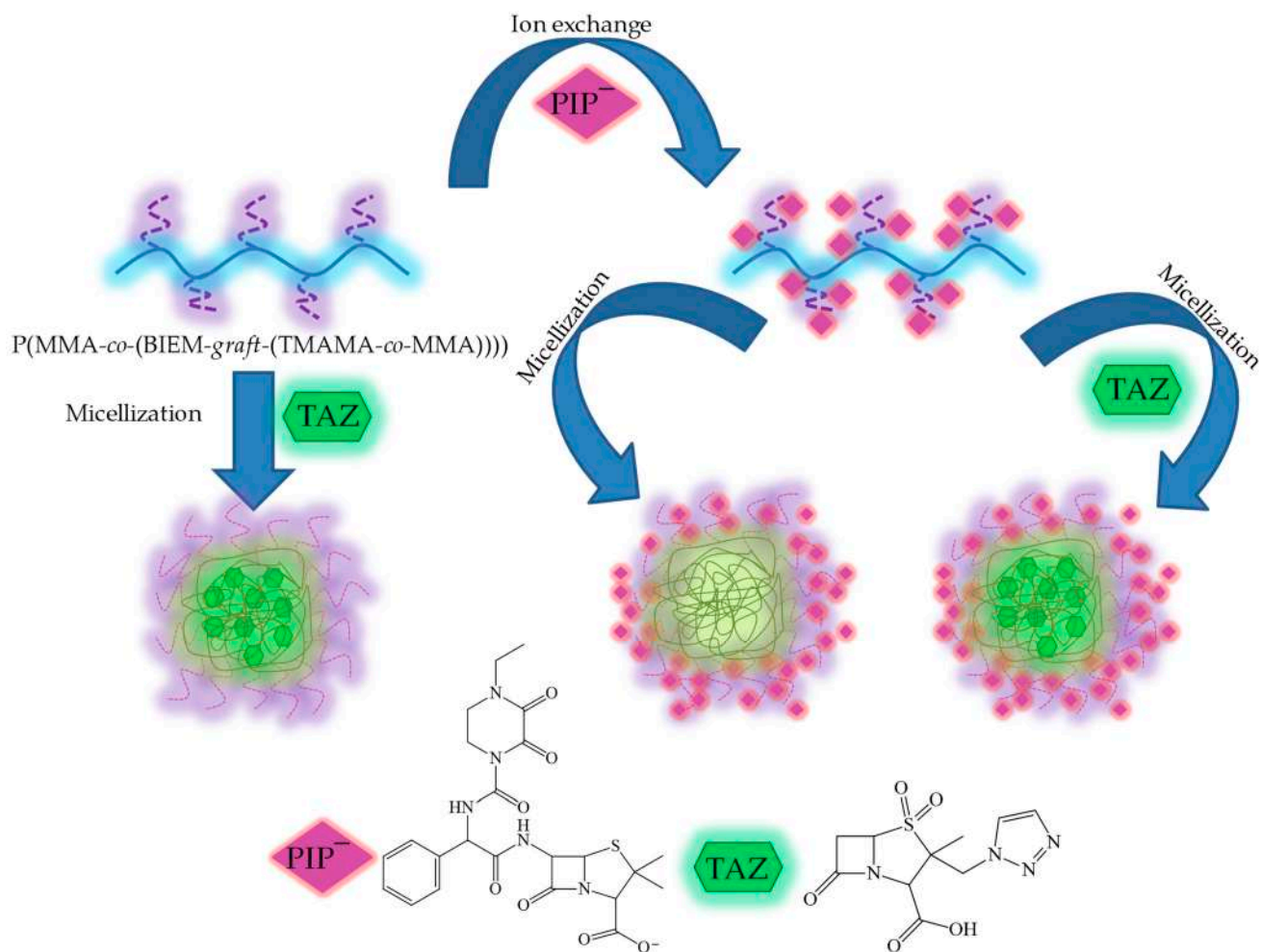
Versatility of application, as well as the possibility of designing drug carriers, has resulted in drug delivery systems (DDSs) gaining high interest among polymer scientists. In past years, DDSs have been studied to improve the healing effect and potential of drugs [1–5]. There are a few factors, i.e., toxicity, non-stability, and poor solubility of the drugs, that limit the capacity of pharmaceuticals. Functional polymers, in addition to being able to transport the drug to the desired place, perform various tasks, for example, enhancing bioavailability or bioactivity, drug protection from undesired external factors, and drug decomposition, or even enhancing the solubility of the drug [6–8]. The composition of the polymer that constitutes the matrix is fundamental to obtaining the desired carrier with appropriate properties. There are many types of carriers, and those based on poly(ionic liquids) (PILs) deserve special attention due to the unique properties of ionic liquids.

PILs comprise ions in their structure and have the specific properties of ionic liquids (ILs), such as high thermal stability, high solvating power, and low vapor pressure [9–11]. Moreover, PILs demonstrate unrepeatable properties due to the combined architecture of the polymer and ILs [12,13]. From the DDS design and pharmacological points of view, ILs are useful in the development of new pharmaceutical agents and in the organic synthesis of pharmaceuticals as green solvents, which facilitates the purification and isolation of pharmaceutical compounds [14–17]. Moreover, ILs and PILs can affect the solubility

of ionically bounded drugs [18–21]; they can serve as prodrugs [22–25]; and by properly selecting the polymer chain and the pharmaceutical counterion, the fine tuning of their properties is possible [26,27]. Many PILs have non-toxic, biocompatible, and self-assembly properties, which give them the possibility of being matrices of nanocarriers in DDSs, as has been reported, for example, for imidazolium PIL-based polymers [28]. Spherical nanoparticles prepared from an amphiphilic block copolymer with PIL units have been studied in doxorubicin delivery [29]. The same drug has been successfully encapsulated and delivered by phosphonium PIL-based nanoparticles [30]. On the other hand, the more sophisticated structure of cholinium PIL-based graft copolymers is designed to carry *p*-aminosalicylate, clavulanate [31], cloxacillin [32], and fusidate [33].

One of the main problems in chemotherapy is overcoming drug resistance and improving therapy. Therefore, using dual-drug systems for combination therapy that includes various pharmaceuticals with synergistic action has become a desired method [34–36]. There are few diverse approaches to obtaining dual-drug systems, but those based on PILs are still not well known and need extensive investigations. In the literature, there are only a few examples of the use of polymers based on ionic liquids for the simultaneous release of different drugs. For example, polymeric multi-branched IL-based chitosan nanocarriers for simultaneous delivery of doxorubicin and methotrexate have been reported [37]. Dual systems have also been studied by our group; the polymer carriers based on choline ionic liquid demonstrated successful delivery of salicylate and erythromycin [38], fusidate and rifampicin [33], and fusidate and cloxacillin [32] as pairs of drugs with a synergistic effect.

In this paper, we present a study on well-defined graft copolymers which incorporate water-soluble [2-(methacryloyloxy)ethyl]trimethylammonium chloride (TMAMA) IL units in their side chains, as outlined in reference [31]. These copolymers serve as matrices for the development of single- and dual-drug delivery systems. The biological nature of the polymers was generated by introducing TMAMA as the derivative of choline, which has a complex role in living organisms, including the synthesis of neurotransmitters, the transformation of betaine for methyl-group metabolism, and the synthesis of cell membrane components and lipoproteins. Due to the presence of ionic moieties in the side chains, the ion exchange of chloride with ionic drugs was possible, thereby modifying the polymer. On the other hand, the amphiphilic polymers were also verified in terms of the capability of non-ionic drug encapsulation. For this purpose, piperacillin (PIP) in ionic form was selected as a model drug to obtain ionic polymer–drug conjugates, whereas tazobactam (TAZ) was the second type of model drug with a non-ionic nature beneficial for loading in the formed micelles. Recently, our group reported polymer–PIP-based ionic conjugates with a linear topology [39], but the graft copolymers with a specific structure formed more stable self-assembled nanostructures than their linear analogs, providing different drug release profiles. TAZ and PIP are commonly applied as a standard formulation of drugs with a broad spectrum of antibacterial action, also known as the commercial product Zosyn[®]. So far, PIP/TAZ have been co-encapsulated in micelles [40], incorporated into hydrogels [41], and mixed with nanocomposites [42]. In our studies, these two drugs were introduced via different bonding types to diverge their co-release rate, whereby the encapsulated drug loaded through physical interactions was more readily available for drug release than the ionically conjugated drug. Therefore, to show the influence of drug nature and polymer matrix composition, as well as drug connection type, three types of carriers were examined, i.e., ionic conjugates (PIP) and micelles (TAZ) as single DDSs and micelle-forming polymer–drug conjugates carrying TAZ and PIP with synergistic action as a dual system (Scheme 1). Their potential was verified through the determination of drug contents and/or loading efficiency, kinetic profiles of *in vitro* drug release in phosphate-buffered saline (PBS) imitating human fluids (pH 7.4, 37 °C), and cytotoxicity against the BEAS-2B cell line using an MTT assay.



Scheme 1. Schematic routes of single- and double-drug systems with piperacillin anions and tazobactam as model drugs.

2. Materials and Methods

Graft copolymers (GP1–GP3) based on PILs with choline cations and chloride counterions (Table 1) were synthesized through controlled radical polymerization and characterized according to previously described procedures [31,43]. Sodium piperacillin (NaPIP; 99%) and tazobactam (TAZ; 94%) were purchased from Alfa Aesar (Warsaw, Poland) and used without prior purification. Methanol was obtained from Chempur (Piekary Śląskie, Poland). Phosphate-buffered saline (PBS) was obtained from Sigma-Aldrich (Poznań, Polska). DMEM-F12 medium and 3-(4,5-dimethyl-thiazol-2-yl)-2,5-diphenyltetrazolium bromide (MTT) were received from Aldrich (Poznań, Poland). Human bronchial epithelial cells (BEAS-2B) were purchased from ATCC (Cat# ATCC[®] CRL-9609; Manassas, VA, USA).

Table 1. Data for TMAMA-based graft copolymers [31].

No.	n_{sc}	DG (mol. %)	DP_{sc}	F_{TMAMA} (mol. %)	$M_n \times 10^{-3}$ (g/mol)	M_w/M_n
GP1	48	26	35	39	273.1	1.15
GP2	133	46	28	36	583.5	1.03
GP3	133	46	65	18	1090.5	1.11

n_{sc} —the number of side chains; DG—the degree of grafting, equal to n_{sc} per total DP_n , where $DP_{n,GP1} = 186$ and $DP_{n,GP2,GP3} = 292$; F_{TMAMA} —the content of TMAMA in the side chains; M_n —average number of molecular weight; M_w/M_n —molecular weight distribution.

2.1. Synthesis of Ionic Conjugates Bearing PIP Anions (Example of GP1_PIP⁻)

Copolymer GP1 (21 mg, including 0.05 mmol TMAMA units) was dissolved in methanol (1 mL). Subsequently, pharmaceutical PIP sodium salt (29.9 mg, 0.05 mmol) was added to the mixture in equimolar ratio to the TMAMA units in the polymer chain. The reaction was carried out for 48 h at room temperature. Then, the polymer system was dried under reduced pressure, resulting in the formation of conjugate GP1_PIP⁻.

2.2. Encapsulation of TAZ

A graft copolymer bearing chloride counterions (20 mg) and TAZ (20 mg) was dissolved in methanol (2 mL). After complete dissolution, a two-fold excess of deionized water was added to the mixture and stirred for 24 h. Subsequently, the organic solvent was evaporated. The resulting aqueous fraction was then lyophilized, yielding the solid product.

The same procedure was used to obtain dual systems containing two types of drugs, PIP and TAZ. In this case, the ionic PIP-based polymer conjugate (20 mg) was dissolved with TAZ (20 mg) in methanol.

2.3. In Vitro Drug Release Studies

Single-/dual-drug systems (1.0 mg) were dissolved to achieve a concentration of 1 mg/mL in PBS (pH = 7.4). A volume of 1 mL of the obtained mixture was introduced to a dialysis membrane bag (MWCO = 3.5 kDa) and placed into a glass vial containing 45 mL of PBS. The drug release experiment was conducted at a temperature of 37 °C under constant stirring. Samples of the buffer solution (0.5 mL) were taken and mixed with an equal volume of methanol to determine the concentration of released drug using UV-Vis spectroscopy, measuring absorbance at $\lambda = 277$ nm for PIP anions and $\lambda = 210$ nm for TAZ. The data obtained from the measurements are presented in release profiles as means \pm SDs.

2.4. Cell Growth and MTT Cytotoxicity Assay

Cells were cultured in a DMEM-F12 medium in sterile culture bottles, characterized by 75 cm² of culture area, supplemented with 10% (*v/v*) FBS at 37 °C in the incubator (humidified atmosphere with 5% CO₂). The cell cultures were placed in a 96-well plate for MTT tests with 10,000 cells per well. A total of 10,000 cells were placed into 96-well plates in 0.2 mL of medium 24 h before polymer systems were added.

Control samples were prepared in the first row and outer columns of wells. Dilutions of the tested compounds (3.125–100 μ g/mL) were prepared in the left wells (0.1 mL). The treated and control cells were then incubated for 72 h under standard conditions. Subsequently, the solutions were removed, and 50 μ L of MTT solution (0.5 mg/mL in RPMI 1640 without phenol red) was added into each well. After 1–2 h of incubation, the MTT solution was aspirated. The created formazan crystals were dissolved in 75 μ L of isopropanol:HCl mixture (*v/v* = 1:0.04). Cytotoxicity was evaluated by measuring the absorbance of the formazan product at 570 nm using a microplate reader. Measurements were repeated three times (six technical repetitions for each concentration). The results were presented as the percentage fraction of the control. Cell viability monitoring and confluence analysis were performed using a live cell analyzer. After 72 h of incubation, microscopic images of both treated and untreated cells were captured. Data obtained from measurements are presented as means \pm SDs.

2.5. Characterization

Critical micelle concentration (CMC) was determined by measuring interfacial tension (IFT) using the pendant drop method on a goniometer (OCA 15EC; DataPhysics, Filderstadt, Germany). For this purpose, a series of aqueous polymer solutions (0.0006–0.15 mg/mL) were prepared. The goniometer was also used for evaluating the contact angle (CA) using the sessile drop method. The polymer solution in methanol (0.3 mg/mL) was spin-coated on a thin glass plate. Next, 4 μ L of deionized water was dispensed onto the polymer layer; then, the CA value was measured. The data were collected and processed with SCA20_U

software 5.0.38. The hydrodynamic diameter (D_h) of particles and the polydispersity index (PDI) were measured with dynamic light scattering (DLS) using a nanoparticle analyzer, NANOTRAC Flex (Microtrac Retsch GmbH, Haan, Germany; Dimensions LS software 1.1.0.), equipped with an external “dip-in” probe with 180° backscattering. Samples were placed and measured in 1.5 mL glass vials after dilution with deionized water (1.0 mg/mL) at 25 °C. Each measurement was repeated three times to create an average value. Ultraviolet–visible light spectroscopy (UV-Vis; spectrometer Evolution 300; Thermo Fisher Scientific, Waltham, MA, USA) was used to determine the ionic drug content (DC) or the non-ionic drug loading content (DLC), as well as the amount of drug released during in vitro studies in PBS with the addition of methanol. The calculations were based on the estimated absorbance of detected pharmaceuticals at proper wavelengths (277 nm for PIP and 210 nm for TAZ) to determine their concentrations using the calibration curve equations using standard formulas [31]. The measurements were carried out in quartz cuvettes. Viability monitoring and confluence analysis were performed using a live cell analyzer (JuLI™ Br; NanoEnTek Inc., Seoul, Korea). The cytotoxicity according to the MTT test was evaluated by measuring the absorbance of formazan product at 570 nm with the use of a microplate reader (Epoch; BioTek, Winooski, VT, USA).

3. Results and Discussion

The graft polymers (GP1–GP3) were composed of methyl methacrylate and 2-(2-bromoisobutyryloxy)ethyl methacrylate copolymers as the main chain, decorated by [2-(methacryloyloxy)ethyl]trimethylammonium chloride and methyl methacrylate copolymers as the grafts (P(MMA-co-(BIEM-graft-(TMAMA-co-MMA)))) [31]. The copolymers varied in terms of the number of side chains ($n_{sc} = 48–133$), grafting degree (DG = 26–46%), polymerization degree of side chains ($DP_{sc} = 28–65$), and content of TMAMA units ($F_{TMAMA} = 18–36$ mol.%) (Table 1). These designed graft copolymers with advanced structures are dedicated to antibacterial treatment, including combination therapy.

The self-assembling characteristics of the graft copolymers with Cl anions have already been evaluated with critical micelle concentration values (CMC; Table 2) ranging from 0.011 to 0.020 mg/mL [31]. The amphiphilicity of these copolymers allowed for non-ionic drug encapsulation, resulting in micelles as a single-drug delivery system (Scheme 1). To assess the loading capability, tazobactam (TAZ) was used as a model drug. TAZ is a penicillanic acid derivative with a β -lactam antibiotic structure which works as a β -lactamase inhibitor commonly used with β -lactam antibiotics, such as piperacillin, to protect them from bacterial destruction [44]. The copolymer structure directly influenced the efficiency of encapsulation (Figure 1). In the case of copolymer GP1, with a lower number of side chains represented by a lower degree of grafting, encapsulation proceeded to the highest degree, leading to a nearly 70% drug loading in the micelles. For copolymers GP2 and GP3, with a higher number of side chains and a higher degree of grafting, encapsulation was less effective (DLC = 43.5% and 37.2%, respectively). Additionally, it was observed that the degree of encapsulation increased with the fraction of TMAMA units. Thus, both a high fraction of TMAMA units (as the hydrophilic fraction) and a lower density of side chains may have a beneficial effect on TAZ encapsulation inside the micelles formed by choline-based copolymers with Cl counterions.

Subsequently, due to the presence of TMAMA units in the side chains of graft copolymers, the exchange reaction from chloride to pharmaceutical anions was possible. Consequently, piperacillin (PIP) anions were introduced into the polymer structure, and polymer–drug ionic conjugates were obtained as a second series of single DDSs (Scheme 1). Piperacillin, a β -lactam antibiotic with a broad spectrum of action, was used as the model drug in this case. Its mechanism focuses on blocking bacterial cell wall biosynthesis (transpeptidation) due to the structural similarity to the natural substances used by bacteria to build the cell wall. The drug content (DC; Figure 1), determined with the UV-Vis method, suggested that the exchange between chloride and PIP ions was the most effective in the case of copolymer GP3 (~73%), characterized by the highest grafting density

and the longest side chains. Lower DC values were detected for GP1 (53%) and GP2 (45%), characterized by doubly shorter grafts and doubly higher content of ionic fraction (above 35 mol.%). It is possible that the high amount of MMA in the side chains led to a lower packing of the copolymer matrix, resulting in a looser distribution of ionic TMAMA units, facilitating access to them.

Table 2. Characteristics of choline-based copolymers with Cl and after exchange with PIP anions using the goniometric method.

No.	CMC ^a (mg/mL)		Contact Angle ^b (°)	
	Cl (23)	PIP	Cl (23)	PIP
GP1	0.013	0.073	56.3	36.1
GP2	0.020	0.041	48.9	35.5
GP3	0.011	0.044	44.3	44.3

CMC: critical micelle concentration; ^a measured through IFT at a series of concentrations; ^b measured using sessile drop method on the polymer film (0.3 mg/mL polymer solution spin-coated on glass plate).

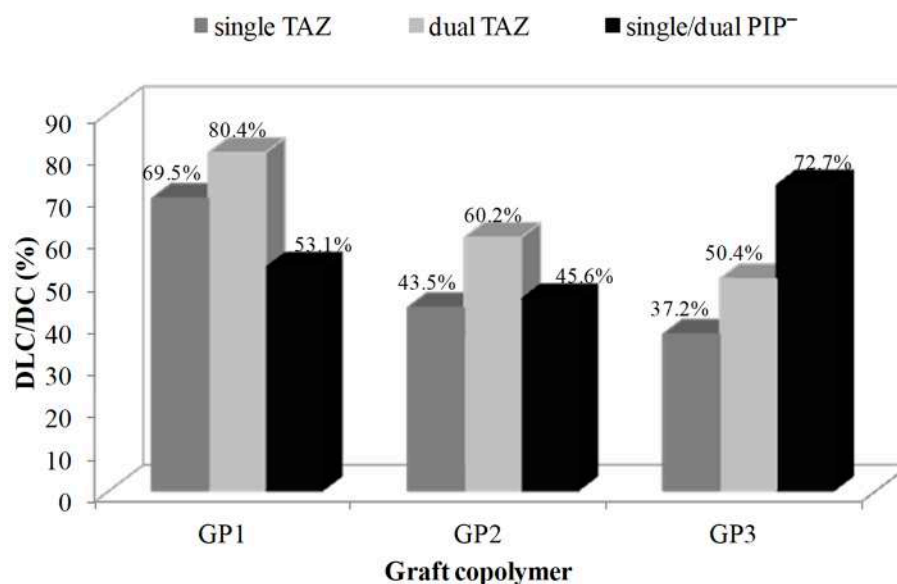


Figure 1. Drug loading contents of TAZ vs. drug contents of PIP anions in single and dual polymeric systems.

Following ion exchange, the amphiphilic properties of graft copolymers needed verification for their use in further encapsulation of a second drug. The CMC values of the ionic PIP polymer conjugates were determined using the goniometric method, where the intersection of two straight lines on the interfacial tension (IFT) versus the negative logarithm of concentration ($-\log C$) plot was employed as the standard procedure. In comparison to the initial graft copolymers with Cl anions, the CMCs after conjugation with PIP significantly increased, yielding values in the range of 0.041–0.073 mg/mL (Table 1). However, the conjugates were still able to form micelles. Therefore, drug encapsulation was possible, and they could be employed as matrices for dual-drug systems, representing a third type of the studied carriers.

The polymer characteristics were also examined to determine the surface wettability of PIP conjugate films. For this purpose, solutions of conjugates at a concentration 0.3 mg/mL in methanol were prepared. The glass plates were deeply cleaned for thin polymeric layer application. The spin-coating method was used to obtain a homogeneous polymer layer. Then, the goniometer was applied to measure the contact angle (CA) using the sessile drop method. After anion exchange between chloride anions and PIP ones, the CA values decreased as follows: GP1: 56.3° vs. 36.1°; GP2: 48.9° vs. 35.5°. On the contrary, we did

not notice any changes in the case of GP3 (Table 2). The highest reduction was observed in GP1_PIP, which was also characterized by the highest increase in CMC. Considering CMC and CA values, it can be concluded that conjugation with a chosen ionic drug induced an enhancement in the hydrophilicity of the polymer systems. Additionally, they became more hydrophilic with the increase in the content of ionic fraction, which is an opposite correlation with respect to the chloride-based systems. The photos from goniometric measurements are present in Figure 2.

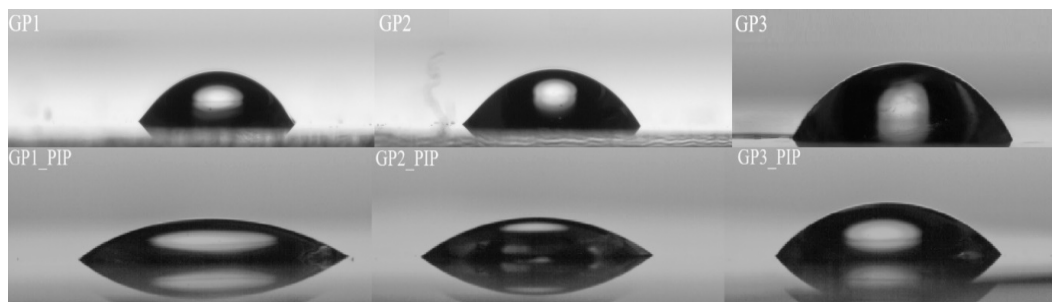


Figure 2. Screen shots of contact angles on polymer films of GP1–GP3 vs. GP1_PIP–GP3_PIP measured using the goniometric method.

The particle sizes of the single- and dual-drug systems were assessed with dynamic light scattering (DLS) measurements (Table 3, Figure S1). The encapsulation of TAZ in chloride-based copolymers created monodisperse particles for GP1 and GP3 ranging between 319 nm and 247 nm, while in GP2, the prevailing fraction (>40%) demonstrated particles of 97 nm. A higher grafting degree of copolymers resulted in the aggregation of nanoparticles, especially for G2 (~10%) and insignificantly for G3. In the case of PIP polymer conjugates, the predominant fraction (>68%) consisted of nanoparticles in the size range of 20–31 nm. The π -stacking interaction, attributed to PIP conjugation with the polymer containing the highest TMAMA fraction, was responsible for the attraction of GP1 polymer assemblies (>1700 nm, 10%). Dual-drug systems showed a tendency for the formation of two prevailing fractions in the size range of 24–192 nm, indicating smaller particles than TAZ-encapsulating single-drug systems and relatively similar to analogous PIP conjugates. Generally, the longest side chains and the highest DC of PIP in the GP3 sample favored a repulsion effect, leading to larger nanoparticles as small aggregates in a significant fraction (451 nm in 32% for single systems and 770 nm in 46% for the dual systems).

Table 3. Hydrodynamic diameters of PIL-based particles determined using DLS.

	D_h (nm)	TAZ Fraction (%)	PDI	D_h (nm)	PIP ⁻ Fraction (%)	PDI	D_h (nm)	PIP ⁻ /TAZ Fraction (%)	PDI
GP1	319	100	0.004	20	77.8	0.26	24	42.4	0.36
				244	11.7		192	55.2	
				1714	10.5		1875	2.4	
GP2	16	24.4	0.17				26	67.1	0.42
	97	41.3							
	504	24.9					83	32.9	
	5430	9.4							
GP3	247	97.4	0.09	31	68.3	1.15	48	54.3	1.06
	6000	2.6		451	31.7		770	45.7	

In vitro drug release from single- and dual-drug systems was conducted at 37 °C in phosphate-buffered saline (PBS; pH = 7.4). The concentration of free drug was monitored

within 48 h using UV-Vis spectrometry (Table 4). A similar trend was observed in the case of copolymers GP1 and GP2. In both instances, equivalent amounts of non-ionic TAZ were released from single and dual systems, constituting 47% and ~70%, respectively. This indicates no discernible effect of the conjugated PIP in the polymer matrix (Figure 3a,b). However, considering the different DLC values, which were higher for dual systems, the concentrations of free TAZ exhibited slight variations (GP1: 8.30 $\mu\text{g/mL}$ vs. 9.60 $\mu\text{g/mL}$; GP2: 7.52 $\mu\text{g/mL}$ vs. 10.41 $\mu\text{g/mL}$ for single and dual systems, respectively). On the other hand, release from the GP3 matrix in a single system progressed to a very high amount of free TAZ (98%), while the presence of PIP anions as the accompanying drug limited the release of encapsulated TAZ to 64%. Despite this, the lower DLC in the micelles than in the double system resulted in a significant concentration of free TAZ (~9 $\mu\text{g/mL}$). The release of ionic PIP, occurring through exchange with phosphate anions present in the solution, was pronounced for the single system (Figure 3c,d), leading to substantial drug concentrations (7–15 $\mu\text{g/mL}$). In turn, the presence of encapsulated TAZ in the micellar PIP conjugates significantly restricted the release of ionic PIP to 21–25% (2.6–3.9 $\mu\text{g/mL}$). In a previous study [25], analogous systems with a different pair of drugs, i.e., ionic fusidate and non-ionic rifampicin, were described. The release was not only influenced by the structure of the polymer matrix, but it could also be limited/improved by the presence of the combined drug and the method of drug introduction (chemical bonding or physical interactions).

Table 4. Drug release data for single and dual systems GP1–GP3.

	Single System		Dual System		Single System		Dual System	
	TAZ		TAZ		PIP		PIP	
	%	C ($\mu\text{g/mL}$)	%	C ($\mu\text{g/mL}$)	%	C ($\mu\text{g/mL}$)	%	C ($\mu\text{g/mL}$)
GP1	47	8.30	47	9.60	79	10.81	25	3.41
GP2	68	7.52	69	10.41	66	7.76	23	2.64
GP3	98	9.04	64	8.27	81	15.04	21	3.94

The *in vitro* release of the tested drugs was also analyzed using kinetic models, i.e., the first-order, Higuchi, and Korsmeyer-Peppas model equations (Table 5, Figure S2). The samples did not conform to the zero-order model equation, primarily due to the independence of concentration from drug release. The high correlation coefficients (R^2), particularly for PIP conjugate systems ($R^2 \geq 0.90$) in the first-order equation, illustrate the time dependence on the percentage of remaining drug. Both single and double systems containing TAZ were characterized by R^2 values ranging from 0.77 to 0.96, with the lowest value being observed for the GP3 single system. The elevated R^2 values suggest a good fit, allowing the results to be described by this equation. The Higuchi model equation plots depict the function of the square root of time against cumulative percentage drug release, providing insights into the mechanism of controlled drug diffusion. The drug release profiles of ionic PIP and non-ionic TAZ for all studied systems were linear on the Higuchi plots ($R^2 = 0.89$ – 0.99), indicating diffusion-dependent release. The diffusion of the ionic drug was also assessed using the Korsmeyer–Peppas model equation ($M_t/M = kt^n$). The release exponent (n), determined using this equation, characterizes different release mechanisms. Several single systems (GP1_TAZ, GP1_PIP, GP2_PIP, and GP3_PIP) and TAZ in dual system GP2_PIP⁻/TAZ can be described by a quasi-Fickian process ($n \geq 0.45$), while other systems exhibited non-Fickian-type release, indicative of anomalous drug transport ($0.45 < n < 0.89$).

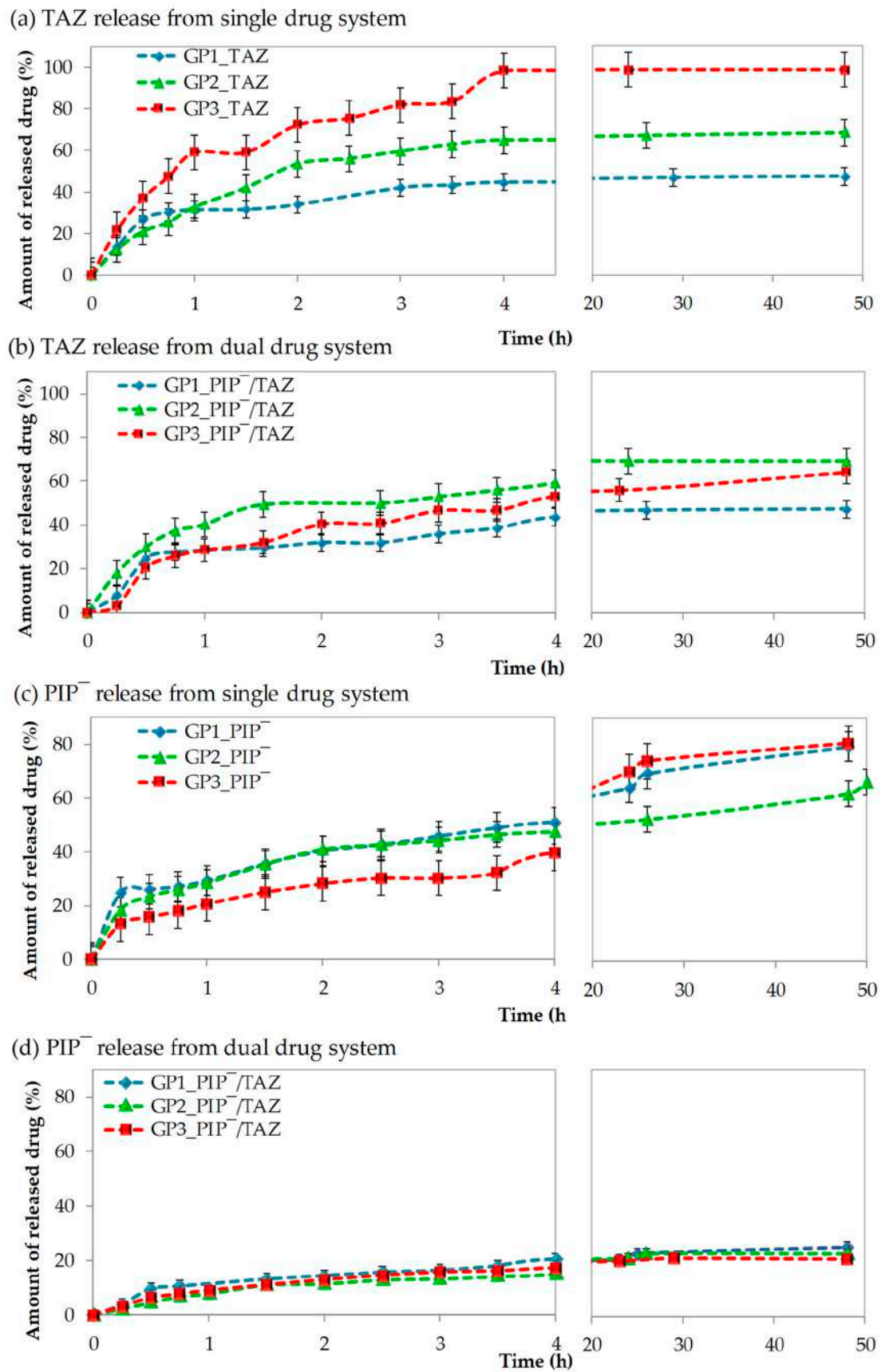
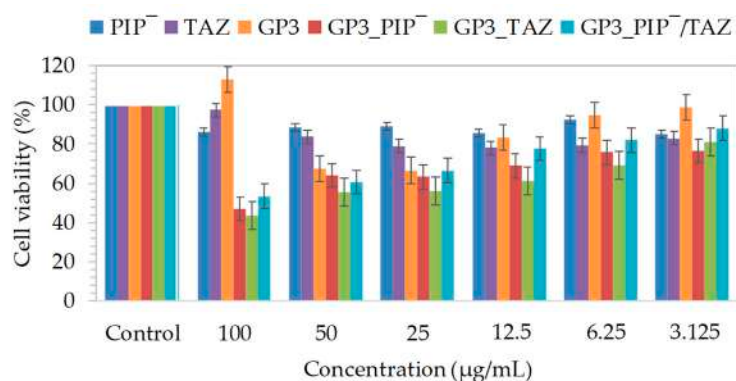


Figure 3. Release profiles of TAZ (a,b) and PIP⁻ (c,d) from systems based on graft copolymers.

Table 5. Correlation coefficients (R^2) and drug release exponents (n) of kinetic model equations.

Drug	Type	Matrix	First-Order Model R^2	Higuchi Model R^2	Korsmeyer–Peppas Model R^2	n
TAZ	Single	GP1	0.88	0.89	0.87	0.35
		GP2	0.96	0.98	0.99	0.60
		GP3	0.77	0.96	0.96	0.48
	Dual	GP1	0.83	0.84	0.77	0.46
		GP2	0.88	0.91	0.92	0.38
		GP3	0.93	0.94	0.79	0.80
PIP ⁻	Single	GP1	0.99	0.98	0.94	0.29
		GP2	0.94	0.98	0.98	0.36
		GP3	0.95	0.97	0.99	0.38
	Dual	GP1	0.91	0.94	0.90	0.48
		GP2	0.90	0.97	0.97	0.64
		GP3	0.91	0.99	0.95	0.56

The previously reported biological studies of graft polymer systems demonstrated selective activity, inducing a negative effect on the tumor adeno-carcinomic human alveolar basal epithelial (A549) cell line, while they did not cause negative changes in normal human bronchial epithelial (BEAS-2B) cells [43]. In this study, co-delivery systems carrying PIP and TAZ were evaluated in BEAS-2B cells to exclude potential cytotoxic effects. Analyses, including colorimetric MTT assays and microscopic measurements of confluence, were conducted before and after treatment with dual system GP3 as a model (Figure 4). Cell viability assays were performed at various concentrations (3.125–100 $\mu\text{g}/\text{mL}$). Following treatment with single systems, such as samples GP3_PIP⁻ and GP3_TAZ, as well as dual system GP3_PIP⁻/TAZ, the affected cell lines were incubated for 72 h under standard conditions. Studies indicated that cytotoxicity increased with concentration, with cell viability dropping below 50% only at the highest concentration (100 $\mu\text{g}/\text{mL}$). Lower concentrations caused a slight decrease in viability, and the lowest tested concentration (3.125 $\mu\text{g}/\text{mL}$) did not significantly induce cell death. Notably, dual systems exhibited lower cytotoxicity compared with their single counterparts. Higher concentrations of polymer systems containing the drugs demonstrated increased cytotoxicity, while lower concentrations showed no significant differences compared with the action of free drugs against the BEAS-2B cell line. The confluence of cells treated with the tested compounds after 72 h of incubation was evaluated by comparing them to untreated control cells. The addition of systems with PIP⁻ did not cause any significant changes, or it even led to an increase in confluence, while TAZ incorporation induced a decrease in cell coverage (Figure 5). Microscopic images are presented in Figure 6.

**Figure 4.** Cell viability of PIP, TAZ, and GP3 bearing PIP⁻ or/and TAZ at different concentrations for treatment of BEAS-2B cell line after 72 h of incubation in comparison to the controls (100%).

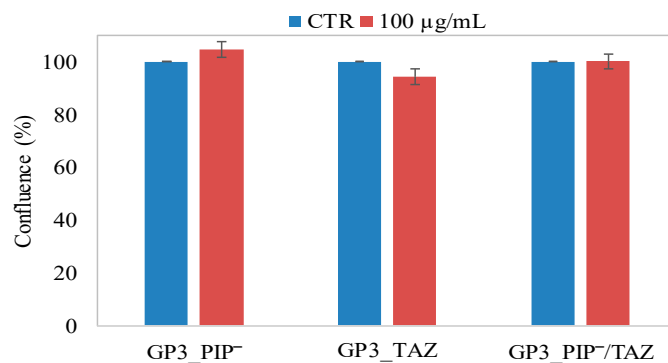


Figure 5. Confluence of BEAS-2B cell lines treated with single and dual systems of GP3 graft polymer for 72 h at the concentration of 100 µg/mL. Results are presented as percent of controls.

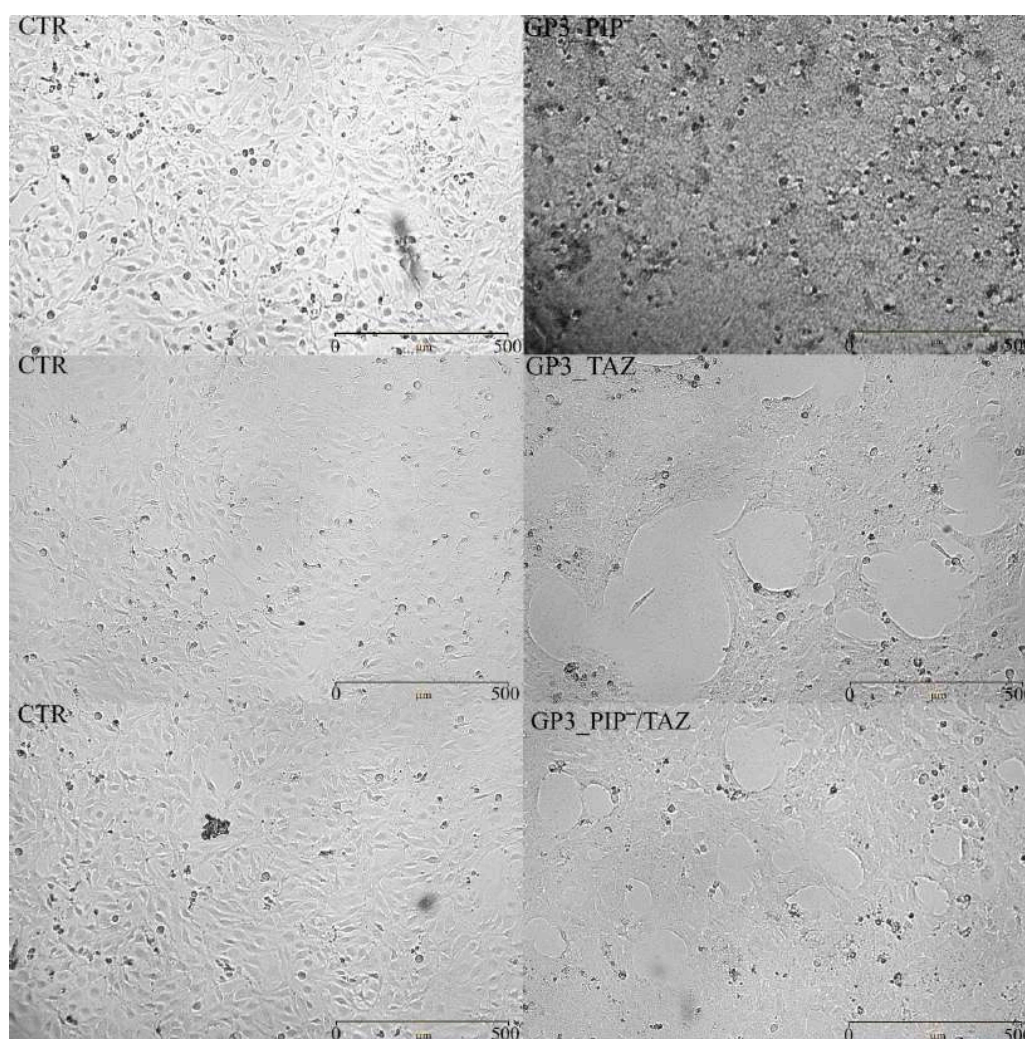


Figure 6. Microscopic images obtained with live cell analyzer of untreated control cells vs. BEAS-2B cells treated with single- or dual-drug delivery graft copolymer systems. The scale bar represents 500 µm.

4. Conclusions

Graft copolymers based on [2-(methacryloyloxy)ethyl]trimethylammonium chloride (TMAMA) units were employed as single-drug carriers, namely, conjugates with ionic piperacillin (PIP) and micelles loaded with tazobactam (TAZ), and dual-drug carriers with ionically conjugated piperacillin and encapsulated tazobactam for co-delivery applications.

The polymers exhibited the capability to exchange chloride ions with PIP, resulting in a DC in the range of 45–73%. The amphiphilic properties of TMAMA-based graft copolymers, as estimated according to CMCs (values ranging from 0.011 to 0.073 mg/mL), proved advantageous for TAZ encapsulation in both single and dual systems (DLCs of 37–70% and 50–80%, respectively). The self-assembling copolymers with encapsulated TAZ formed particles of smaller sizes in dual-drug systems (24–192 nm) compared with single ones (97–319 nm). In vitro release studies on the single-drug systems revealed 66–81% of free PIP (7.8–15.0 µg/mL) and 47–98% of free TAZ (7.5–9.0 µg/mL) after 48 h. In dual-drug co-delivery systems bearing both PIP⁻ and TAZ, there was an inhibitory effect on the release of ionically bound PIP (21–25%, 2.6–3.9 µg/mL), while it did not influence the release of non-ionic TAZ (achieving 47–69%). However, due to high DLC values, the concentrations of free TAZ were improved (9.6–10.4 µg/mL). In vitro cytotoxicity studies indicated a negligible effect on cell viability at low concentrations. Therefore, these designed polymers show promise as carriers for the conjugation and/or encapsulation of PIP and TAZ, serving as co-delivery systems for the simultaneous release of two drugs.

Supplementary Materials: The following supporting information can be downloaded at: <https://www.mdpi.com/article/10.3390/pharmaceutics16020198/s1>, Figure S1: DLS histograms for nanoparticles based on (a) GP1, (b) GP2, and (c) GP3 copolymers, Figure S2: Kinetic profiles according to models of first order, Higuchi, and Korsmeyer–Peppas for release of TAZ from (a) single systems and (b) dual systems, as well as PIP release from (c) single systems and (d) dual systems based on the grafted copolymers.

Author Contributions: K.N.: data curation; formal analysis; investigation; outline and organization of the writing—original draft. A.M.: formal analysis and investigation. D.N.: conceptualization; methodology; funding acquisition; project administration; writing—review and editing; supervision. All authors have read and agreed to the published version of the manuscript.

Funding: This research was funded by the National Science Center, grant No. 2017/27/B/ST5/00960.

Institutional Review Board Statement: Not applicable.

Informed Consent Statement: Not applicable.

Data Availability Statement: The original contributions presented in the study are included in the article/supplementary material; further inquiries can be directed to the corresponding author/s.

Acknowledgments: The biological part was performed at Biotechnology Center of Silesian University of Technology in Gliwice. The authors would like to thank Magdalena Skonieczna for help in cytotoxicity tests.

Conflicts of Interest: The authors declare no conflicts of interest.

References

1. Coelho, J.F.; Ferreira, P.C.; Alves, P.; Cordeiro, R.; Fonseca, A.C.; Góis, J.R.; Gil, M.H. Drug delivery systems: Advanced technologies potentially applicable in personalized treatments. *EPMA J.* **2010**, *1*, 164–209. [[CrossRef](#)]
2. Zhang, Y.; Chan, H.F.; Leong, K.W. Advanced materials and processing for drug delivery: The past and the future. *Adv. Drug Deliv. Rev.* **2013**, *65*, 104–120. [[CrossRef](#)]
3. Tiwari, G.; Tiwari, R.; Bannerjee, S.; Bhati, L.; Pandey, S.; Pandey, P.; Sriwastawa, B. Drug delivery systems: An updated review. *Int. J. Pharm. Investig.* **2012**, *2*, 2. [[CrossRef](#)]
4. Adepu, S.; Ramakrishna, S. Controlled Drug Delivery Systems: Current Status and Future Directions. *Molecules* **2021**, *26*, 5905. [[CrossRef](#)]
5. Ezike, T.C.; Okpala, U.S.; Onoja, U.L.; Nwike, C.P.; Ezeako, E.C.; Okpara, O.J.; Okoroafor, C.C.; Eze, S.C.; Kalu, O.L.; Odoh, E.C.; et al. Advances in drug delivery systems, challenges and future directions. *Heliyon* **2023**, *9*, 17488. [[CrossRef](#)]
6. Pushpamalar, J.; Meganathan, P.; Tan, H.L.; Dahlan, N.A.; Ooi, L.T.; Neerooa, B.N.H.M.; Essa, R.Z.; Shameli, K.; Teow, S.Y. Development of a Polysaccharide-Based Hydrogel Drug Delivery System (DDS): An Update. *Gels* **2021**, *7*, 153. [[CrossRef](#)] [[PubMed](#)]
7. Li, C.; Wang, J.; Wang, Y.; Gao, H.; Wei, G.; Huang, Y.; Haijun Yu, H.; Gan, Y.; Wang, Y.; Mei, L.; et al. Recent progress in drug delivery. *Acta Pharm. Sin. B* **2019**, *9*, 1145–1162. [[CrossRef](#)]

8. Patra, J.K.; Das, G.; Fraceto, L.F.; Ramos Campos, E.V.; del Pilar Rodriguez-Torres, M.; Acosta-Torres, L.S.; Diaz-Torres, L.A.; Grillo, R.; Swamy, M.K.; Sharma, S.; et al. Nano based drug delivery systems: Recent developments and future prospects. *J. Nanobiotechnol.* **2018**, *16*, 71. [[CrossRef](#)] [[PubMed](#)]
9. Lei, Z.; Chen, B.; Koo, M.-K.; MacFarlane, D.R. Introduction: Ionic Liquids. *Chem. Rev.* **2017**, *10*, 6633–6635. [[CrossRef](#)]
10. Clare, B.; Sirwardana, A.; MacFarlane, D.R. Synthesis, Purification and Characterization of Ionic Liquids. In *Ionic Liquids; Topics in Current Chemistry*; Springer: Berlin/Heidelberg, Germany, 2010; Volume 290, pp. 1–40.
11. Forsyth, S.A.; Pringle, J.M.; MacFarlane, D.R. Ionic Liquids—An Overview. *Aust. J. Chem.* **2004**, *57*, 113. [[CrossRef](#)]
12. Kausar, A. Research Progress in Frontiers of Poly(Ionic Liquid)s: A Review. *Polym. Plast. Technol. Eng.* **2017**, *56*, 1823–1838. [[CrossRef](#)]
13. Yuan, J.; Markus Antonietti, M. Poly(ionic liquid)s: Polymers expanding classical property profiles. *Polymer* **2011**, *52*, 1469–1482. [[CrossRef](#)]
14. Qader, I.B.; Prasad, K. Recent developments on Ionic Liquids and Deep Eutectic Solvents for Drug Delivery Applications. *Pharm. Res.* **2022**, *39*, 2367–2377. [[CrossRef](#)] [[PubMed](#)]
15. Chen, J.; Xie, F.; Chen, L.; Li, X. Ionic liquids for preparation of biopolymer materials for drug/gene delivery: A review. *Green Chem.* **2018**, *20*, 4169–4200. [[CrossRef](#)]
16. Pedro, S.N.; Freire, C.S.R.; Silvestre, A.J.D.; Freire, M.G. Ionic Liquids in Drug Delivery. *Encyclopedia* **2021**, *1*, 324–339. [[CrossRef](#)]
17. Md Moshikur, R.; Chowdhury, M.R.; Moniruzzaman, M.; Goto, M. Biocompatible ionic liquids and their application in pharmaceuticals. *Green Chem.* **2020**, *22*, 8116–8139. [[CrossRef](#)]
18. Lu, B.; Bo, Y.; Yi, M.; Wang, Z.; Zhang, J.; Zhu, Z.; Zhao, Y.; Zhang, J. Enhancing the Solubility and Transdermal Delivery of Drugs Using Ionic Liquid-In-Oil Microemulsions. *Adv. Funct. Mater.* **2021**, *31*, 2102794. [[CrossRef](#)]
19. Ait-Touchente, Z.; Zine, N.; Jaffrezic-Renault, N.; Errachid, A.; Lebaz, N.; Fessi, H.; Elaissari, A. Exploring the Versatility of Microemulsions in Cutaneous Drug Delivery: Opportunities and Challenges. *Nanomaterials* **2023**, *13*, 1688. [[CrossRef](#)]
20. Liu, C.; Chen, B.; Shi, W.; Huang, W.; Qian, H. Ionic Liquids for Enhanced Drug Delivery: Recent Progress and Prevailing Challenges. *Mol. Pharm.* **2022**, *19*, 1033–1046. [[CrossRef](#)]
21. Shukla, M.K.; Tiwari, H.; Verma, R.; Dong, W.-L.; Azizov, S.; Kumar, B.; Pandey, S.; Kumar, D. Role and Recent Advancements of Ionic Liquids in Drug Delivery Systems. *Pharmaceutics* **2023**, *15*, 702. [[CrossRef](#)]
22. Cojocaru, O.A.; Bica, K.; Gurau, G.; Narita, A.; McCrary, P.D.; Shamshina, J.L.; Barber, P.S.; Rogers, R.D. Prodrug ionic liquids: Functionalizing neutral active pharmaceutical ingredients to take advantage of the ionic liquid form. *Med. Chem. Comm.* **2013**, *4*, 559. [[CrossRef](#)]
23. Zhang, W.; Guo, Y.; Yang, J.; Tang, G.; Zhang, J.; Cao, Y. Prodrug Based on Ionic Liquids for Dual-Triggered Release of Thiabendazole. *ACS Omega* **2023**, *8*, 3484–3492. [[CrossRef](#)] [[PubMed](#)]
24. Moshikur, R.M.; Chowdhury, M.R.; Wakabayashi, R.; Tahara, Y.; Moniruzzaman, M.; Goto, M. Ionic liquids with methotrexate moieties as a potential anticancer prodrug: Synthesis, characterization and solubility evaluation. *J. Mol. Liq.* **2019**, *278*, 226–233. [[CrossRef](#)]
25. Cojocaru, O.; Shamshina, J.; Rogers, R. Review/Preview: Prodrug Ionic Liquids Combining the Prodrug and Ionic Liquid Strategies to Active Pharmaceutical Ingredients. *Chim. Oggi-Chem. Today* **2013**, *31*, 24–29.
26. Pedro, S.; Freire, C.; Silvestre, A.; Freire, M. The Role of Ionic Liquids in the Pharmaceutical Field: An Overview of Relevant Applications. *Int. J. Mol. Sci.* **2020**, *21*, 8298. [[CrossRef](#)]
27. Liu, C.; Raza, F.; Qian, H.; Tian, X. Recent advances in poly(ionic liquid)s for biomedical application. *Biomater. Sci.* **2022**, *10*, 2524–2539. [[CrossRef](#)] [[PubMed](#)]
28. Guo, J.; Zhou, Y.; Qiu, L.; Yuan, C.; Yan, F. Self-assembly of amphiphilic random co-poly(ionic liquid)s: The effect of anions, molecular weight, and molecular weight distribution. *Polym. Chem.* **2013**, *4*, 4004–4009. [[CrossRef](#)]
29. Lu, B.; Zhou, G.; Xiao, F.; He, Q.; Zhang, J. Stimuli-Responsive Poly(ionic liquid) Nanoparticle for Controlled Drug Delivery. *J. Mater. Chem. B.* **2020**, *8*, 7994–8001. [[CrossRef](#)]
30. Fan, S.-Y.; Hao, Y.-N.; Zhang, W.-X.; Kapasi, A.; Shu, Y.; Wang, J.-H.; Chen, W. Poly(ionic liquid)-Gated CuCo₂S₄ for pH-/Thermo-Triggered Drug Release and Photoacoustic Imaging. *ACS Appl. Mater. Interfaces* **2020**, *12*, 9000–9007. [[CrossRef](#)]
31. Niesyto, K.; Neugebauer, D. Synthesis and Characterization of Ionic Graft Copolymers: Introduction and In Vitro Release of Antibacterial Drug by Anion Exchange. *Polymers* **2020**, *12*, 2159. [[CrossRef](#)]
32. Mazur, A.; Niesyto, K.; Neugebauer, D. Pharmaceutical Functionalization of Monomeric Ionic Liquid for the Preparation of Ionic Graft Polymer Conjugates. *Int. J. Mol. Sci.* **2022**, *23*, 14731. [[CrossRef](#)]
33. Niesyto, K.; Mazur, A.; Neugebauer, D. Dual-Drug Delivery via the Self-Assembled Conjugates of Choline-Functionalized Graft Copolymers. *Materials* **2022**, *15*, 4457. [[CrossRef](#)] [[PubMed](#)]
34. Tu, Y.; Zheng, R.; Yu, F.; Xiao, X.; Jiang, M.; Yuan, Y. Dual drug delivery system with flexible and controllable drug ratios for synergistic chemotherapy. *Sci. China Chem.* **2021**, *64*, 1020–1030. [[CrossRef](#)]
35. Xiao, Y.; Gao, Y.; Li, F.; Deng, Z. Combinational dual drug delivery system to enhance the care and treatment of gastric cancer patients. *Drug Deliv.* **2020**, *27*, 1491–1500. [[CrossRef](#)] [[PubMed](#)]
36. Wei, L.; Cai, C.; Lin, J.; Chen, T. Dual-drug delivery system based on hydrogel/micelle composites. *Biomaterials* **2009**, *30*, 2606–2613. [[CrossRef](#)] [[PubMed](#)]

37. Rahimi, M.; Shafiei-Irannejad, V.; Safa, K.D.; Salehi, R. Multi-branched ionic liquid-chitosan as a smart and biocompatible nano-vehicle for combination chemotherapy with stealth and targeted properties. *Carbohydr. Polym.* **2018**, *196*, 299–312. [[CrossRef](#)]
38. Bielas, R.; Siewniak, A.; Skonieczna, M.; Adamiec, M.; Mielańczyk, Ł.; Neugebauer, D. Choline based polymethacrylate matrix with pharmaceutical cations as co-delivery system for antibacterial and anti-inflammatory combined therapy. *J. Mol. Liq.* **2019**, *285*, 114–122. [[CrossRef](#)]
39. Niesyto, K.; Neugebauer, D. Linear Copolymers Based on Choline Ionic Liquid Carrying Anti-Tuberculosis Drugs: Influence of Anion Type on Physicochemical Properties and Drug Release. *Int. J. Mol. Sci.* **2021**, *22*, 284. [[CrossRef](#)]
40. Milani, M.; Salehi, R.; Hamishehkar, H.; Zarebkohan, A.; Akbarzadeh, A. Synthesis and evaluation of polymeric micelle containing piperacillin/tazobactam for enhanced antibacterial activity. *Drug Delivery* **2019**, *26*, 1292–1299.
41. Pulat, M.; Tan, N.; Onurdağ, F.K. Swelling dynamics of IPN hydrogels including acrylamide-acrylic acid-chitosan and evaluation of their potential for controlled release of piperacillin-tazobactam. *J. Appl. Polym. Sci.* **2011**, *120*, 441–450. [[CrossRef](#)]
42. Mahata, D.; Jana, M.; Jana, A.; Mukherjee, A.; Mondal, N.; Saha, T.; Sen, S.; Nando, G.B.; Mukhopadhyay, C.K.; Chakraborty, R.; et al. Lignin-graft-Polyoxazoline Conjugated Triazole a Novel Anti-Infective Ointment to Control Persistent Inflammation. *Sci. Rep.* **2017**, *7*, 46412. [[CrossRef](#)] [[PubMed](#)]
43. Niesyto, K.; Łyżniak, W.; Skonieczna, M.; Neugebauer, D. Biological in vitro evaluation of PIL graft conjugates: Cytotoxicity characteristics. *Int. J. Mol. Sci.* **2021**, *22*, 7741. [[CrossRef](#)] [[PubMed](#)]
44. Rodríguez-Villodres, Á.; Gutiérrez Linares, A.; Gálvez-Benitez, L.; Pachón, J.; Lepe, J.A.; Smani, Y. Semirapid Detection of Piperacillin/Tazobactam Resistance and Extended-Spectrum Resistance to β -Lactams/ β -Lactamase Inhibitors in Clinical Isolates of *Escherichia coli*. *Microbiol. Spectr.* **2021**, *9*, e0080121. [[CrossRef](#)] [[PubMed](#)]

Disclaimer/Publisher's Note: The statements, opinions and data contained in all publications are solely those of the individual author(s) and contributor(s) and not of MDPI and/or the editor(s). MDPI and/or the editor(s) disclaim responsibility for any injury to people or property resulting from any ideas, methods, instructions or products referred to in the content.

Piperacillin/Tazobactam Co-Delivery by Micellar Ionic Conjugate Systems Carrying Pharmaceutical Anions and Encapsulated Drug

Katarzyna Niesyto, Aleksy Mazur and Dorota Neugebauer *

Department of Physical Chemistry and Technology of Polymers, Faculty of Chemistry,
Silesian University of Technology, 44-100 Gliwice, Poland;
katarzyna.niesyto@polsl.pl (K.N.); aleksy.mazur@polsl.pl (A.M.)

* Correspondence: dorota.neugebauer@polsl.pl

Content:

Figure S1. DLS histograms for nanoparticles based on a) GP1, b) GP2, and c) GP3 copolymer.

Figure S2. Kinetics profiles by models of first order, Higuchi and Korsmeyer-Peppas for release of TAZ from a) single and b) dual systems; as well as PIP release from c) single and d) dual systems based on the grafted copolymers.

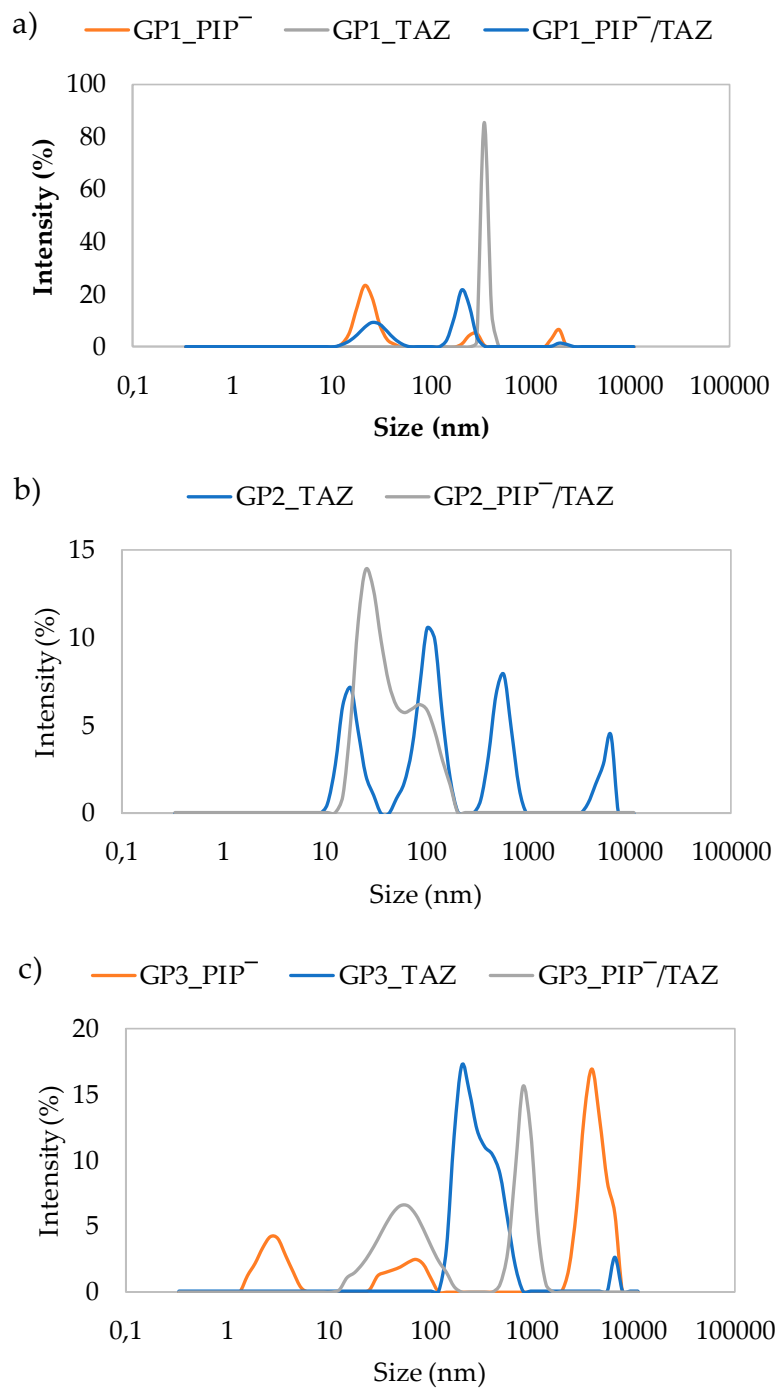


Figure S1. DLS histograms for nanoparticles based on a) GP1, b) GP2, and c) GP3 copolymer.

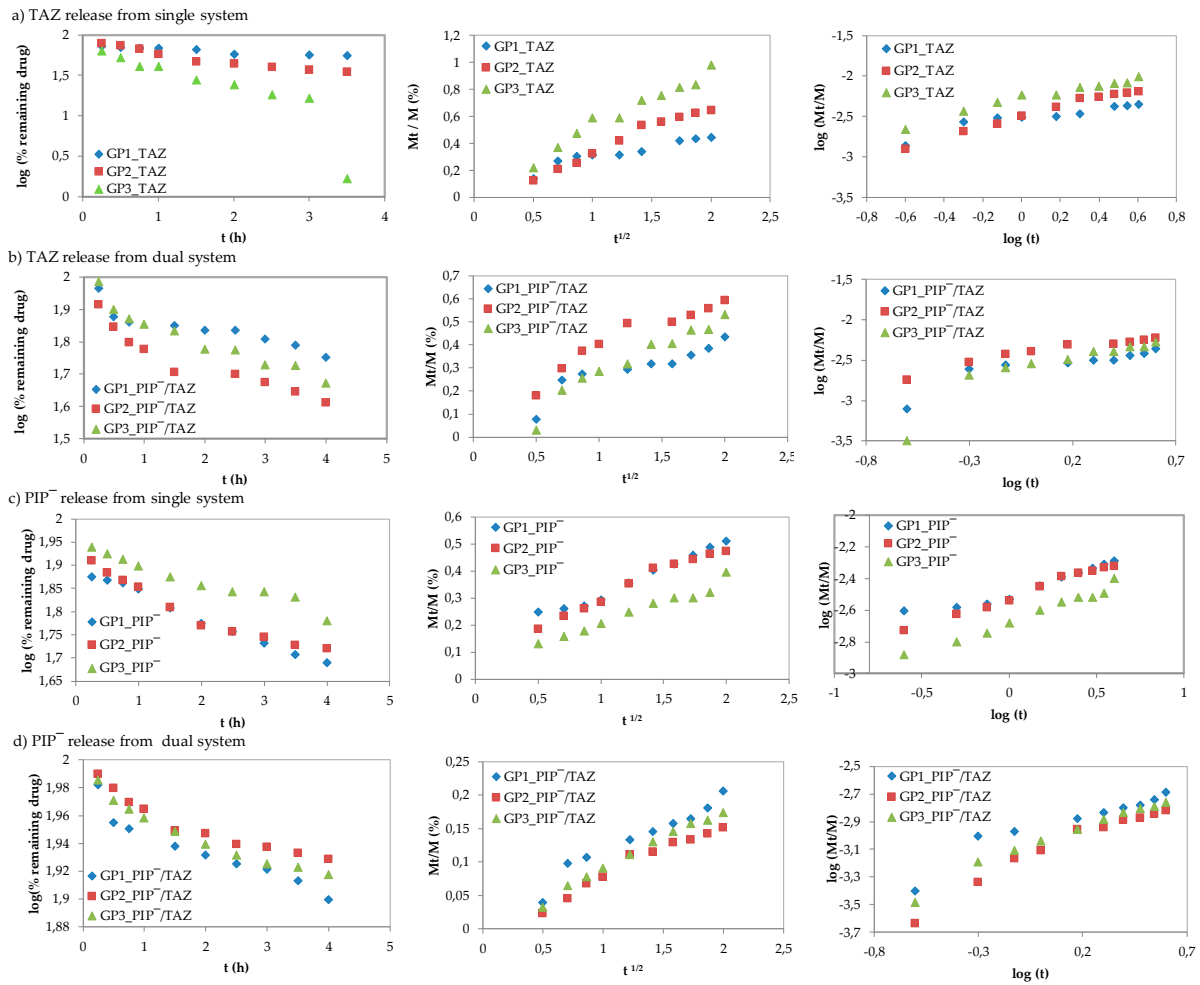


Figure S2. Kinetics profiles by models of first order (left column), Higuchi (central column) and Korsmeyer-Peppas (right column) for release of TAZ from a) single and b) dual systems; as well as PIP release from c) single and d) dual systems based on the grafted copolymers.

PUBLIKACJA P.6

Biological in vitro evaluation of PIL graft conjugates: cytotoxicity characteristics

Niesyto, K., Łyżniak, W., Skonieczna, M., Neugebauer, D.

International Journal of Molecular Sciences 2021, 22, 7741



Article

Biological In Vitro Evaluation of PIL Graft Conjugates: Cytotoxicity Characteristics

Katarzyna Niesyto ¹, Wiktoria Łyżniak ¹, Magdalena Skonieczna ^{2,3,*} and Dorota Neugebauer ^{1,*}

¹ Department of Physical Chemistry and Technology of Polymers, Faculty of Chemistry, Silesian University of Technology, 44-100 Gliwice, Poland; katarzyna.niesyto@polsl.pl (K.N.); wiktlyz002@student.polsl.pl (W.Ł.)

² Department of Systems Biology and Engineering, Silesian University of Technology, Akademicka 16, 44-100 Gliwice, Poland

³ Biotechnology Centre, Silesian University of Technology, Krzywoustego 8, 44-100 Gliwice, Poland

* Correspondence: Magdalena.Skonieczna@polsl.pl (M.S.); Dorota.Neugebauer@polsl.pl (D.N.)

Abstract: In vitro cytotoxicity of polymer-carriers, which in the side chains contain the cholinium ionic liquid units with chloride (Cl) or pharmaceutical anions dedicated for antituberculosis therapy, i.e., *p*-aminosalicylate (PAS) and clavulanate (CLV), was investigated. The carriers and drug conjugates were examined, in the concentration range of 3.125–100 µg/mL, against human bronchial epithelial cells (BEAS-2B) and adenocarcinomic human alveolar basal epithelial cells (A549) as an experimental model cancer cell line possibly coexisting in tuberculosis. The cytotoxicity was evaluated by MTT test and confluency index, as well as by the cytometric analyses, including Annexin-V FITC apoptosis assay. The polymer systems showed supporting activity towards the normal cells and no tumor progress, especially at the highest concentration (100 µg/mL). The analysis of cell death did not show meaningful changes in the case of the BEAS-2B, whereas in the A549 cell line, the cytostatic activity was observed, especially for the drug-free carriers, causing death in up to 80% of cells. This can be regulated by the polymer structure, including the content of cationic units, side-chain length and density, as well as the type and content of pharmaceutical anions. The results of MTT tests, confluency, as well as cytometric analyses, distinguished the polymer systems with Cl/PAS/CLV containing 26% of grafting degree and 43% of ionic units or 46% of grafting degree and 18% of ionic units as the optimal systems.

Keywords: graft copolymers; PIL; ionic conjugates; cytotoxicity; antituberculosis drugs



Citation: Niesyto, K.; Łyżniak, W.; Skonieczna, M.; Neugebauer, D. Biological In Vitro Evaluation of PIL Graft Conjugates: Cytotoxicity Characteristics. *Int. J. Mol. Sci.* **2021**, *22*, 7741. <https://doi.org/10.3390/ijms22147741>

Academic Editor: Jesus Vicente De Julián Ortiz

Received: 9 July 2021
Accepted: 17 July 2021
Published: 20 July 2021

Publisher's Note: MDPI stays neutral with regard to jurisdictional claims in published maps and institutional affiliations.



Copyright: © 2021 by the authors. Licensee MDPI, Basel, Switzerland. This article is an open access article distributed under the terms and conditions of the Creative Commons Attribution (CC BY) license (<https://creativecommons.org/licenses/by/4.0/>).

1. Introduction

In medicine, nano-sized materials can be applied as drug vehicles [1,2], where polymer-carriers improve a drug's effect on the body through controlled release [3,4]. They are beneficial for limiting the side effects of low molecular weight medicine, i.e., exceeding the permissible dose of the drug [3]. In drug delivery systems (DDS), the bioactive substances can be loaded/encapsulated via physical interactions or chemically attached by a polymer matrix. The latter, known as the polymer-drug conjugates [5–7], are characterized by their stability, depending on the type of bonding, which requires the presence of specific sites in the polymer chain to ensure drug conjugation.

Ionic strength seems to be advantageous for ionic drug attachment [8,9]. In these cases, the carriers contain ionic groups, which are usually provided by ionic liquids (IL) as suitable (co)monomers introduced into the polymer chain [10–12]. Many of them are known as biocompatible, especially those based on choline chloride with cationic trimethylammonium groups [13–17]. Moreover, many poly(ionic liquid)s (PILs) are non-toxic in nature and show biological activity, which is desirable in medicine [18,19]. The carriers varied with structure and topology based on ILs have been designed via amphiphilic linear polymers, i.e., from vinylimidazolium [20], imidazolium [21], pyridinium [22] or

guanidinium-type IL [23]. Numerous reports have been devoted to the use of phosphorylcholine IL as a co-monomer to obtain linear block copolymers [24,25], whereas those with graft topology and containing ionic units, i.e., imidazolium [26] or choline-type IL [12,27] in the side chains, have been investigated with significantly lower attention. In the case of the ionic polymer structure, drugs can be carried in ionic form as counterions, i.e., nicotinic, salicylic, ampicillin, naproxen, ibuprofenate anions [28–30], as well as in nonionic form as loaded guests [31], or both forms as the systems for combined therapy [32].

Drugs released from carriers travel along the body, where both the polymer and the active substance may have a direct effect on normal and diseased cells. Therefore, the optimal pharmacokinetics in correlation with the selective cytotoxicity of DDS is crucial in pharmaceutical therapy, where drug activity is expected toward diseased cells and can be utilized against tumor cells. Basic research to understand how a drug or carrier will respond in the body is supported by cell line assays [33]. Using in vitro models, with normal epithelial BEAS-2B and cancer A549 cells existing in a human respiratory system, the biological activity of tested compounds could be described. For further applications, most of the inhaled agents against different human diseases, such as tuberculosis, in the preliminary studies were tested using a standard cytotoxicity assay. Not only active substances but also components of drug delivery systems should be carefully studied in the first step of potential application. Contamination of the physiological microbiome of the human respiratory system with malignant pathogens could result in diseases. The main goal of a novel drug should be focused on the intelligent selectivity, with neutral action against healthy cells, cytostatic action against cancer cells and antimicrobial activity against resistant pathogens.

Ionic drug-carrier conjugates based on graft copolymers containing ionic liquid units in the side chains, i.e., (2-trimethylammonium)ethyl methacrylate and methyl methacrylate copolymer (P(TMAMA-*co*-MMA)), have been designed to attach to ionic drugs, such as *p*-aminosalicylate (PAS) and clavulanate (CLV), which are common drugs used in lung diseases treatment, especially tuberculosis [27]. The infected cells are easily exposed to other pathogens, i.e., responsible for progress of cancer cells. Therefore, the drug systems were tested on human bronchial epithelial (BEAS-2B) as normal cells to check their non-toxic activity and adenocarcinomic human alveolar basal epithelial cells (A549) cells to exclude their supportive effect on tumor cells. PIL carriers varying with the type of counterions, that is, Cl, PAS or CLV, were selected for the evaluation of cytotoxicity, which may be adjusted by possible correlations with the polymer structure parameters (content of TMAMA units, grafting degree and length of side chains). This verification was supported by in vitro cytotoxicity tests, that is, the colorimetric tests applying 3-(4,5-dimethylthiazol-2-yl)-2,5-diphenyltetrazolium bromide (MTT), as well as cell cycle and apoptosis assays with the use of flow cytometry.

2. Results

Well-defined ionic graft copolymers, i.e., polymethacrylate backbones decorated by polymethacrylate grafts functionalized with ionic TMAMA moieties, were selected for biological studies, including both free carriers with chloride anions, as well as those carrying the pharmaceutical anions PAS and CLV as the cytostatic on cell lines and potentially antituberculosis drugs (Figure 1). Previous physicochemical reports have indicated that these systems are promising for drug delivery, in which the content of the anionic drug can be regulated by the content of TMAMA and then by the efficiency of anionic exchange of chloride to the drug [27]. Their self-assembling behavior in aqueous solutions has already been proven by the determination of critical micelle concentration (CMC), which reached values of 0.01–0.02 mg/mL for Cl based systems and slightly higher in the case of PAS/CLV containing systems (0.03–0.04 mg/mL). The evaluated carriers varied by backbone and side-chain length (n_{mc} and n_{sc} , respectively), as well as number and content of ionic units (n_{TMAMA} and F_{TMAMA} , respectively). Additionally, the conjugates differed with the type and content of ionic drugs (DC_{PAS} , DC_{CLV}). The structural characteristics of carriers I–IV,

including polymer-drug conjugates, are presented in Table 1. Chosen systems were evaluated for their cytotoxicity towards human bronchial epithelial cells (BEAS-2B) to exclude toxic action on normal cells and adenocarcinomic human alveolar basal epithelial cells (A549), known as non-small lung carcinoma cell line, to exclude the expression of cancer activity. Some of the novel drugs could over-stimulate the cancerogenesis or cancer cells proliferation. The tests to exclude that activity were made.

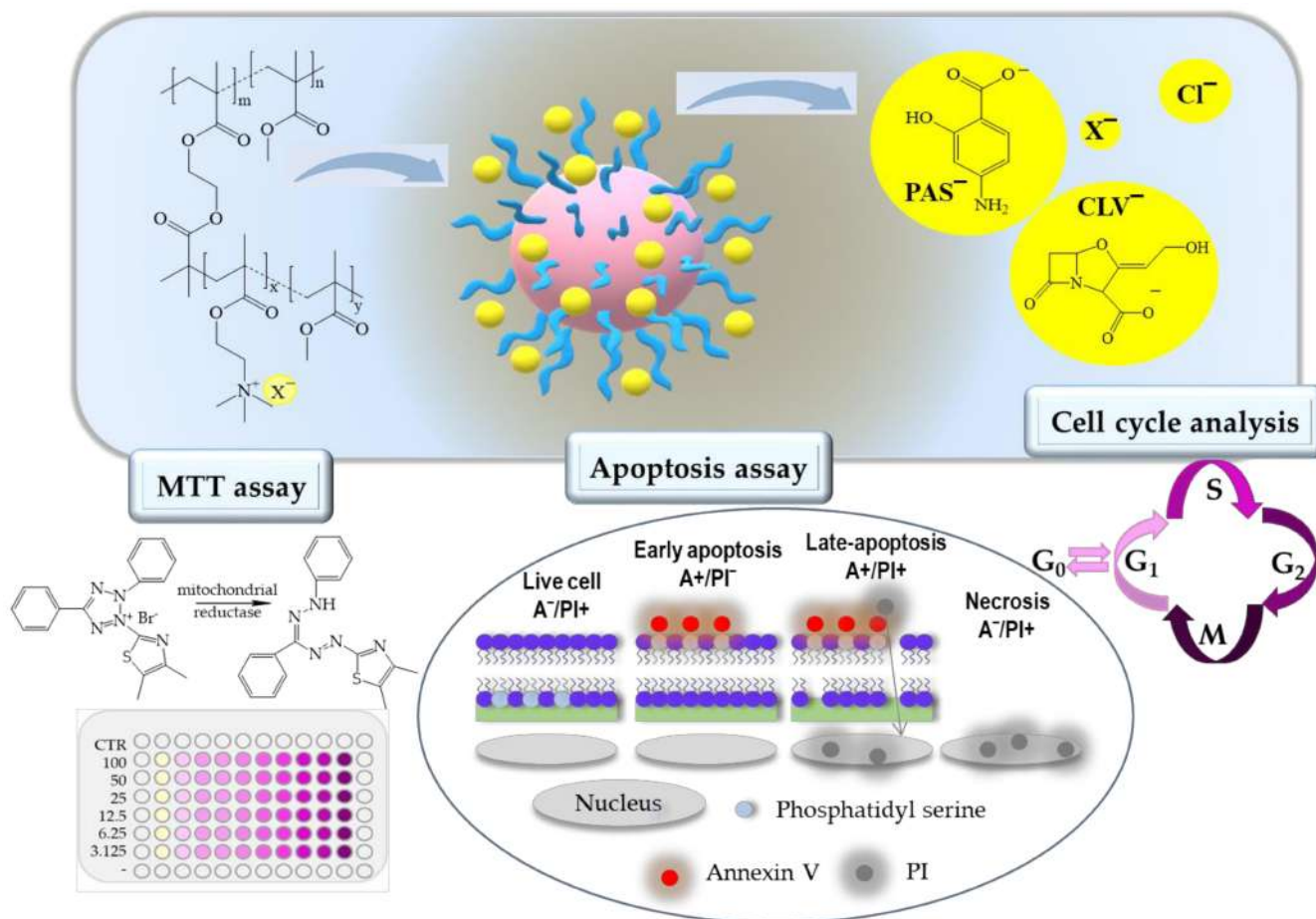


Figure 1. PIL and their conjugates with pharmaceutical anions for cytotoxicity evaluation.

Table 1. Characteristics of amphiphilic graft copolymers and conjugates with PAS^- and CLV^- ^a.

No.	n_{mc}	DG (mol.%)	n_{SC}/n_{TMAMA}	F_{TMAMA} (mol.%)	$M_n \times 10^{-3}$ (g/mol)	\bar{D}	DC (mol.%)	
							PAS	CLV
I	183	26	24/5	21	168.6	1.90	63.9	78.6
II			35/15	43	273.1	1.31	36.2	100.0
III	259	46	65/12	18	1090.5	1.11	37.0	66.3
IV			28/11	39	583.5	-	36.5	88.7

where: n_{mc} is the number of units in the main chain, DG is grafting degree, n_{sc} and n_{TMAMA} are numbers of repeating units in side chains and TMAMA units, respectively, F_{TMAMA} is the content of ionic hydrophilic units in side chains, M_n is average molecular weight, \bar{D} is dispersity index, DC is drug content; ^a procedures, calculations and more detailed physicochemical data are reported in ref. [27].

2.1. MTT Cytotoxicity Assay

One of the most popular cytotoxicity assays is the colorimetric MTT test, which allows the determination of the viability of cells after treatment and assesses a drug's effect on proliferation. During the assay, due to the mitochondrial reductase, the reaction substrate—yellow water-soluble 3-(4,5-dimethylthiazol-2-yl)-2,5-diphenyltetrazolium bromide (MTT)—is modified by mammalian cells. The insoluble purple product (E,Z)-

5-(4,5-dimethylthiazol-2-yl)-1,3-diphenylformazan (formazan) directly appertains to the number of living cells [34–37]. Cell viability assays were performed at a series of concentrations (100–3.125 $\mu\text{g}/\text{mL}$) of nanocarriers I–IV, without pharmaceutical anions and their conjugates with PAS^- and CLV^- . After treatment with all kinds of samples, poisoned cell lines were incubated for 72 h in standard conditions. Tested compounds showed cytotoxic activity against the tumor A549 cell line (Figure 2a–c). The cytotoxicity of carriers bearing Cl^- is higher in comparison to their conjugates with PAS^- or CLV^- . Moreover, an increase in cytotoxicity measured by the percentage value of cell viability was observed with an increase in polymer concentration (100 vs. 3.125 $\mu\text{g}/\text{mL}$; I: 33% vs. 73%; II: 23% vs. 85%; III: 28 vs. 106%; IV: 42% vs. 82%). Similarly, for drug conjugates, cytotoxicity also increased with concentration. However, this effect was slightly lower than the case of the copolymers without the drug at a concentration of 100 $\mu\text{g}/\text{mL}$ (PAS 64% (I), 36% (II), 46% (III), 70% (IV); CLV : 58%, 23%, 55%, 109%, respectively). In the case of the BEAS-2B cell line, treatment with nanocarriers bearing PAS^- caused the same dependence. At low concentrations, the negative effect was not observed, while higher drug concentrations interfere with proliferation (Figure 2e). After treatment with the copolymers and their CLV conjugates, a completely different relationship was observed (Figure 2d,f). The action of I_CLV , which induced an increase in toxicity with increasing concentration, was opposite to the IV_CLV system, which had a decreased toxic effect. In the range of low concentrations (3.125–12.5 $\mu\text{g}/\text{mL}$) of polymers I–III, and II_CLV and III_CLV conjugates, an increase in cytotoxicity was perceived with increasing concentration, whereas at higher concentrations (25–100 $\mu\text{g}/\text{mL}$), the toxic effect decreased. The highest tested concentrations of polymer systems did not cause cytotoxicity. These results indicated that as the concentration increases, the cells adapt, and their proliferation is improved. This phenomenon is called hormesis, which was described previously for doxorubicin-conjugates based on sugar core toward MCF-7 cell lines [38]. The inverse relationship of the action on BEAS-2B and A549 cell lines suggests that the compounds are selective for normal and cancer lung cells, which is a huge advantage.

The percentage of the culture's surface that is covered by cells, called confluence, was measured after 72 h of incubation at a concentration 100 $\mu\text{g}/\text{mL}$ of the polymer sample. Generally, the confluence is regulated by programmed cell death (apoptosis). For the BEAS-2B cell line, in the case of copolymers bearing Cl^- , an increase of the confluence of I, II, III and IV was observed in comparison to the control cells (Figure 3a). A similar relationship was observed for conjugates with PAS and CLV , where in most cases, the confluence reached almost 100%. In two cases, for I_CLV and IV_PAS , the confluence was lower than for the control cells, reaching ~40%. The increasing regularity means that adding these systems to the cells does not adversely affect the reproduction and activity of the BEAS-2B cells, and in most cases, this effect is even intensified. For the A549 cell line, the opposite relation was perceived (Figure 3b). The confluence for free carriers I, II, IV and conjugates I_CLV , III_CLV , I_PAS , II_PAS , III_PAS and IV_PAS decreased in comparison to their control cells. Adding of II, II_CLV and IV_CLV systems did not have any effect on proliferation.

In relation to the MTT cytotoxicity assay, as well as the confluence of treated and untreated cells, including both normal (BEAS-2B) and tumor (A549) ones, the most optimal systems corresponded to II and III, with no exception to their PAS/CLV conjugates. They represented different structural parameters (Table 1), which means that there are more options to improve the cytotoxic activity in the designed polymer-carriers. In the case of sample II, lower grafting degree (26 mol.%) and densely distributed TMAMA units in the side chains reaching 43 mol.% are favorable for obtaining the suitable biological characteristics in relation to the tested cell lines. In turn, the lower TMAMA contribution (18 mol.%) in the copolymer III in combination with a larger number of side chains corresponding to a higher grafting degree (36%) also appeared advantageous in these studies. Both of them were capable of working selectively, showing cytotoxic activity for A549 and neutral for BEAS-2B. Microscopic images and a comparison of untreated and treated cells by polymer

(I/II and III) and conjugates with PAS⁻ and CLV⁻ (I_PAS, I_CLV) are presented in Figure 4 and Figure S1.

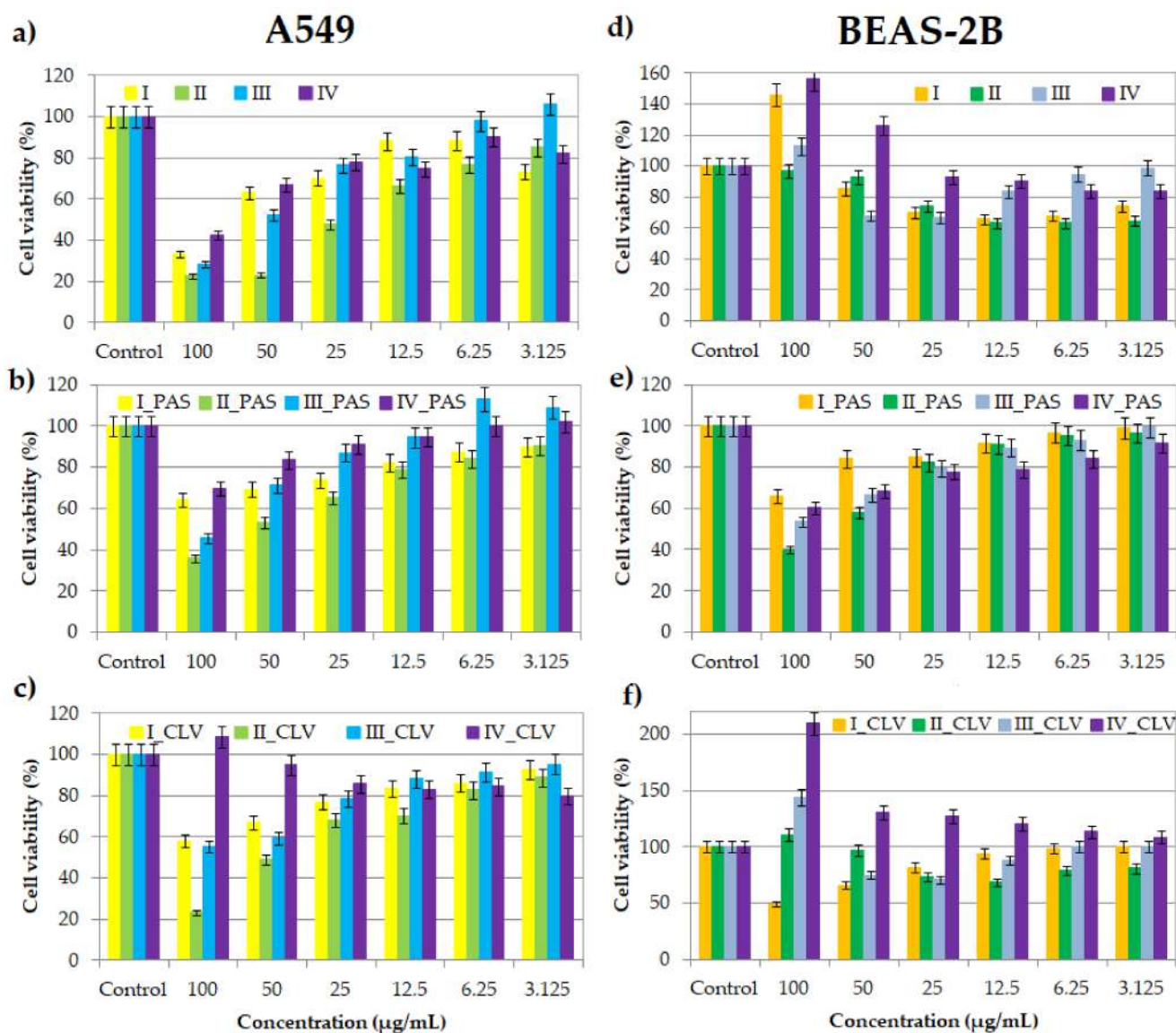


Figure 2. Cell viability of graft copolymers I, II, III and IV (a,d), and their conjugates with PAS (b,e) and CLV (c,f) at different concentrations for treatment of A549 and BEAS-2B cell lines, after 72 h of incubation in comparison to the untreated controls (100%).

2.2. Cytometric Analyses by Flow Cytometry

2.2.1. Apoptosis Assay

Flow cytometry is currently used for observing changes in the cell cycle generated by drugs, apoptosis and cell cycle assay [39–42]. Cell death occurs as a result of the cytotoxic effect. Both the programmed death and the sudden, uncontrolled death may occur to cause cell damage (i.e., in response to the compound action). Flow cytometry allows understanding the processes in cells, permits the determination and analysis of the parameters of normal cells, as well as the cytotoxicity of compounds, especially due to tumor cells. The uncontrolled ability to reproduce, characteristic drug and apoptosis resistance are specific to cancerous cells. In this study, the Annexin-V apoptosis assay was performed to describe the type of cell death induced by a system solution with the drug using the respiratory BEAS-2B and A549 cell lines and 100 μg/mL of free carrier/conjugate dose.

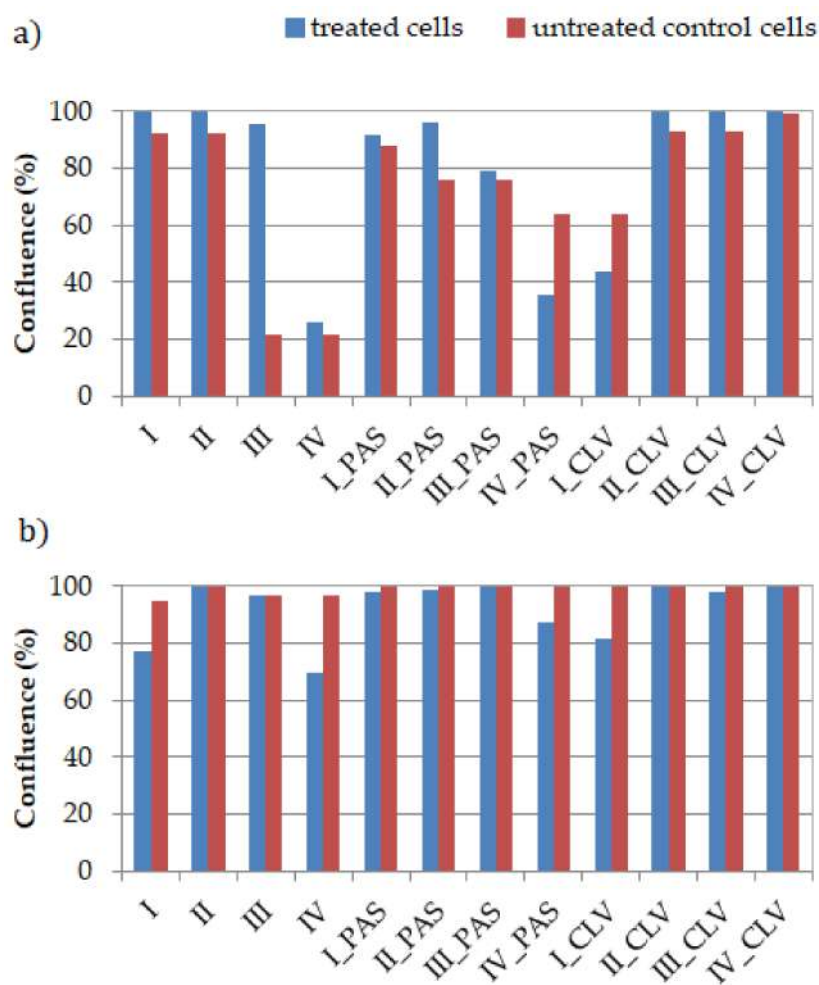


Figure 3. The confluence of polymer/conjugate (treated cells) in comparison to untreated control cells for (a) BEAS-2B and (b) A549 cell lines.

The A549 treatment effects indicated an increase in the necrotic state of cell death (Figure 5a, Table S1). The topology, number of side chains, and content of trimethylammonium groups, such as the type of conjugated anion, had a significant effect on cell death. The most visible changes were caused after treatment with free carriers I ($A^-/PI^+ = 48.8\%$), II ($A^-/PI^+ = 48.1\%$) and III ($A^-/PI^+ = 53.0\%$) in comparison to control cells ($A^-/PI^+ = 21.3\%$). Furthermore, an increase in the apoptotic state (A^+/PI^- and A^+/PI^+) was noticed for the treatment with free carriers (I: 9.2% ; II: 19.0% ; III: 14.6% ; IV: 5.0%), where for the control cells, it was equal to 0.04% . Most cells survived after treatment with IV, similar to CTR cells ($A^-/PI^- = 75.2\%$, 78.66% , respectively). The addition of PAS^- did not have a large impact on the change in the number of living cells. In the case of I_PAS and IV_PAS, the apoptosis phase (A^+/PI^- and A^+/PI^+) increased to 12.8% and 2.9% , respectively. Similarly, the treatment with CLV systems resulted in adaptation and increased cell survival. Generally, the free carriers containing trimethylammonium groups with chloride counterions showed anti-tumor action against the A549 cell line, with an exception for IV, which can be explained by the low content of TMAMA units in relatively short side chains densely grafted on the backbone. This effect was also reduced by the presence of pharmaceutical anions, such as PAS, and especially CLV.

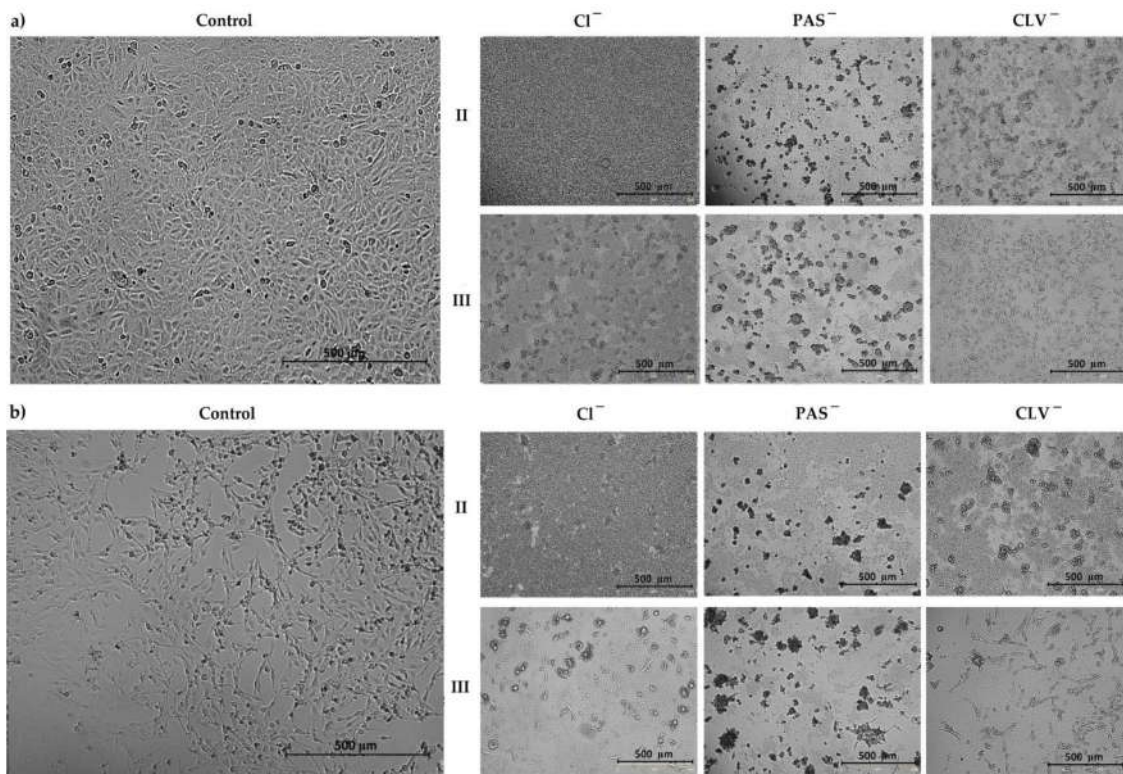


Figure 4. Microscopic images by Live Cell Analyzer for untreated control cells vs. treated (a) A549 and (b) BEAS-2B cells by polymer II and III with Cl^- , PAS^- and CLV^- counterions. The scale bar represents 500 μm .

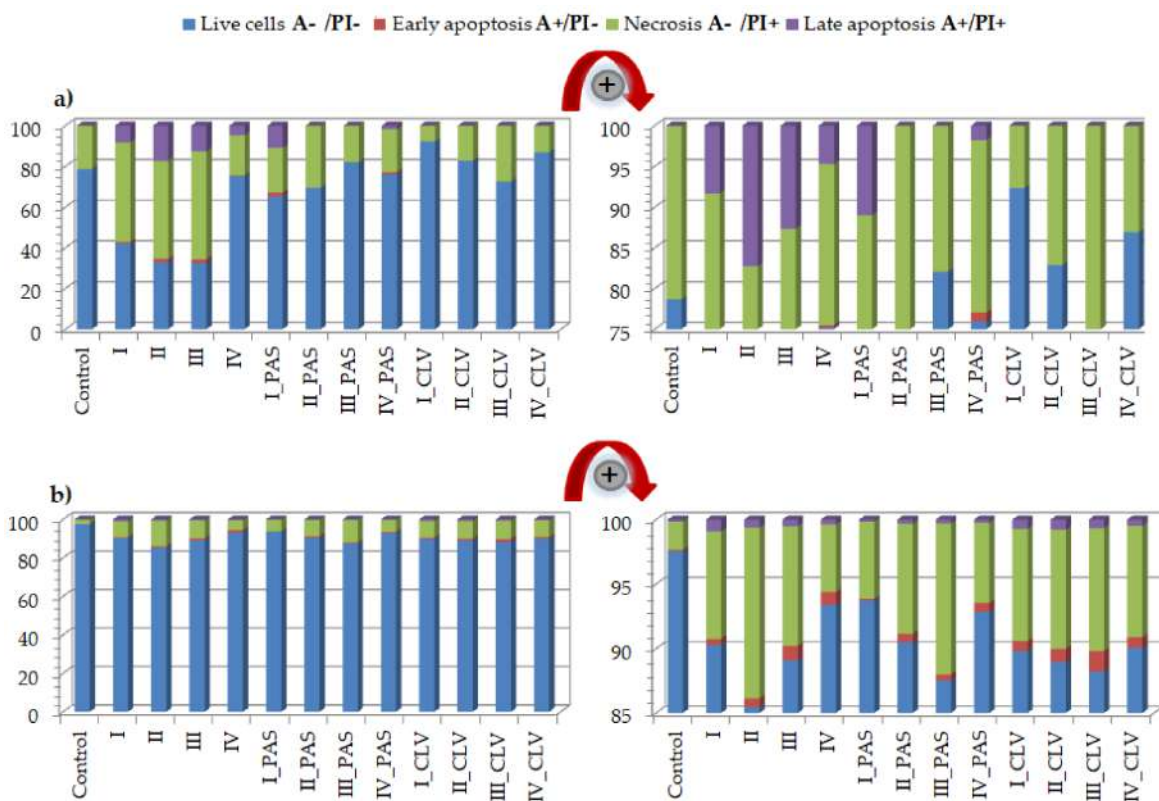


Figure 5. Annexin-V apoptosis assay results for (a) A549 and (b) BEAS-2B cell lines after the treatment of free carriers/conjugates and 72 h of incubation.

The results for the BEAS-2B cell line also demonstrated the increase of necrotic state in comparison to the control (CTR A−/PI+ = 2.2%) (Figure 5b, Table S2). The changes were especially noticeable for cells treated by free carriers II, III and their conjugates II_PAS, III_PAS, II_CLV and III_CLV. A slightly lower effect was noticed for graft copolymers I and IV bearing Cl[−], PAS[−] and CLV[−], where the necrosis was two to four times higher than in the control cells. However, the CLV anions had a greater effect on necrotic death. In each system, an increase in the apoptotic state was observed; nevertheless, the PAS conjugates had a minor effect (Figure 4b zoom in). Most importantly, these systems had no significant effect on the alteration of cell survival (A−/PI− = 85.5%–93.7%; whereas CTR A−/PI− = 97.5%), which suggests that tested carriers are non-toxic against BEAS-2B cell lines. The effects of polymeric carriers and their conjugates on cells are presented on representative plots of cell populations in Figure 6 and Figure S2.

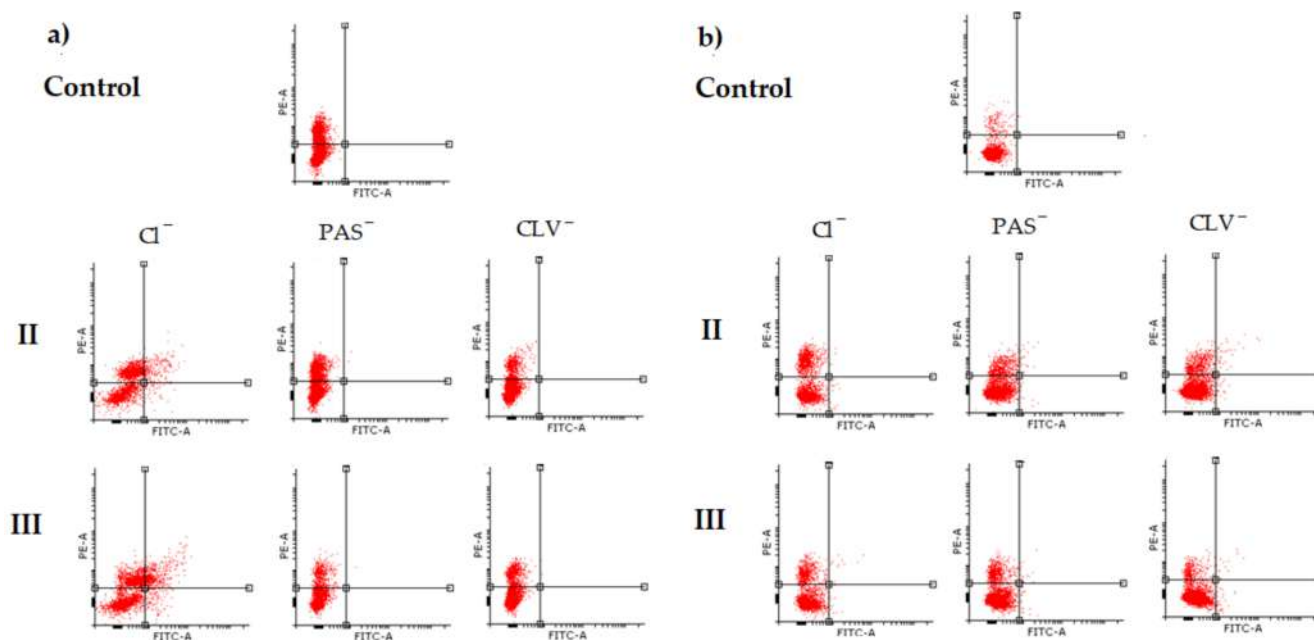


Figure 6. Representative plots of II and III cell populations determined by flow cytometric analysis in (a) A549 and (b) BEAS-2B cell lines.

2.2.2. Cell Cycle Analysis

Cytometric methods allow for the determination of the polymer sample effect on the cell cycle, which goes through several phases (Figure 7). The phases start at zero, which is the resting phase (G0), then proceed to the cell growth phases defined as cellular division and beginning of DNA synthesis (G1), then to replication (S) and mitosis start (I), ending in mitosis of cells (M). Cell cycle analysis was performed in A549 and BEAS-2B lines treated by free carriers and their conjugates with PAS or CLV in one dosage (100 µg/mL) and incubated for 72 h. The cell lines were characterized by a natural rapid proliferation rate, and the extinction of cell cultures occurred in untreated control cell wells due to the crowding and contact inhibition of cells after 72 h. Therefore, for both A549 and BEAS-2B, many cells died and appeared in the sub-G1 phase.

In the case of the treated cells, the blockade of the cycle followed, and the G0/G1 and S phases increased relative to the untreated control. Those changes mainly proved that the compounds were not cytotoxic to the tested cells. Significant growth of the G0/G1 phase was also noted for the A549 cell line. The arrest in this phase means that these compounds act as cytostatics and cause cell cycle disorders. The smallest effect was supported by CLV conjugates, while the cells have been trapped in the S phase. Similarly, the BEAS-2B cells were arrested in the S phase after treatment by all systems. Because of the polymer system action, which could act as an intercalator, the replication was blocked. Nevertheless, in

the S phase, there is a chance that the repair systems of cells and cell division will take place. The I/M phase did not change significantly after drug treatment for both A549 and BEAS-2B lines. The detailed data of cell cycles are presented in Tables S3 and S4.

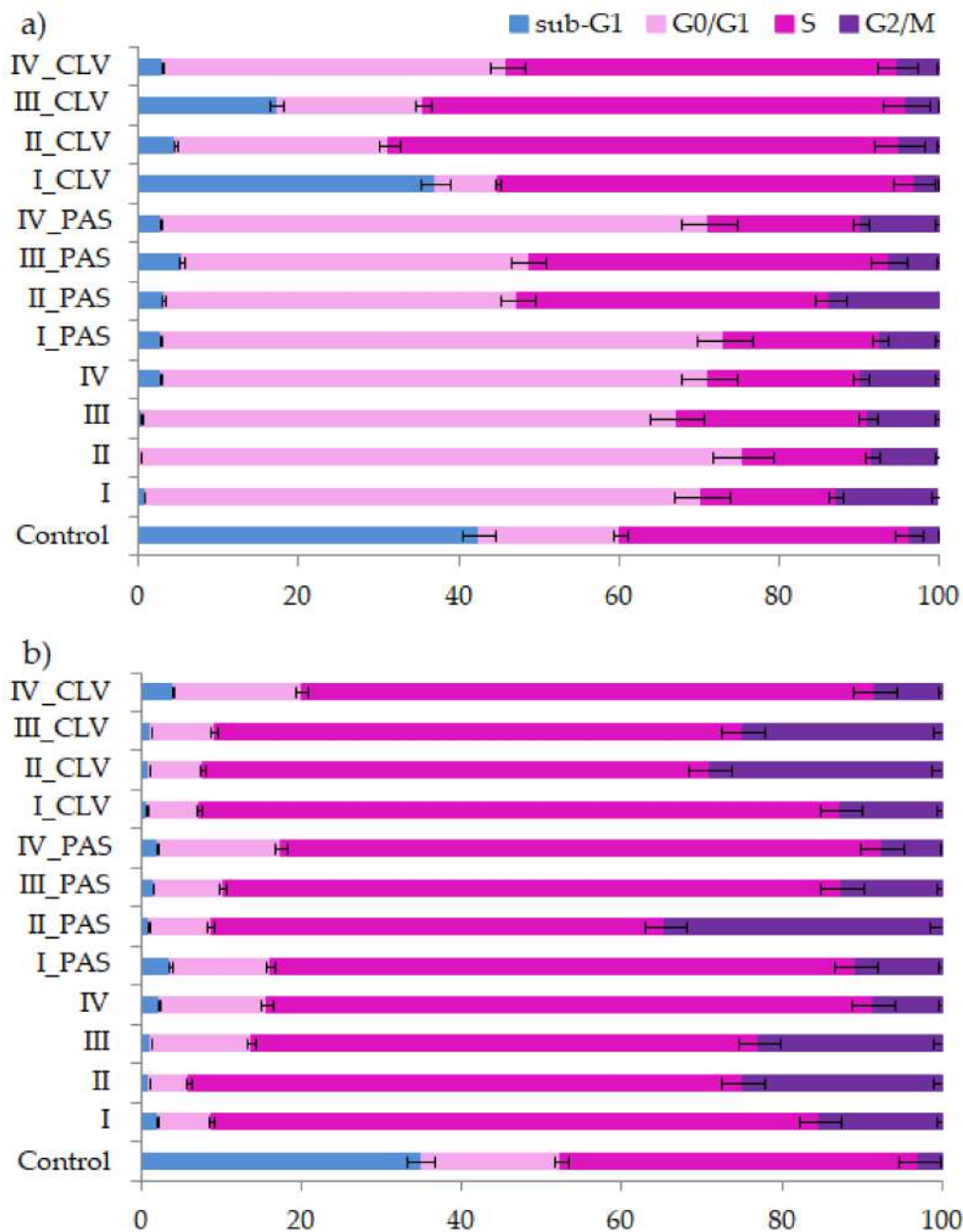


Figure 7. Cell cycle analysis of (a) A549 and (b) BEAS-2B cell lines treated by carriers I–IV or conjugates with PAS and CLV.

3. Materials and Methods

3.1. Materials

Sodium phosphate buffer saline (PBS, pH = 7.4), DMEM-F12 medium, 3-(4,5-dimethylthiazol-2-yl)-2,5-diphenyltetrazolium bromide (MTT) and trypsin were received from Aldrich (Poznań, Poland). Propidium iodide solution (PI, BD Biosciences, San Jose, CA, USA), Annexin-V apoptosis assay (BioLegend, San Diego, CA, USA), physiological saline (PBS without Ca and Mg, PAN-Biotech GmbH, Aidenbach, Germany), fetal bovine serum (FBS, EURx, Gdańsk, Poland) and Annexin-V binding buffer (BD Biosciences, San Jose, CA, USA) were used without prior preparation. Human bronchial epithelial cells (BEAS-

2B) and adenocarcinomic human alveolar basal epithelial cells (A549) were purchased from ATCC (Cat# ATCC[®]CRL-9609; Manassas, VA, USA). Graft copolymers containing TMAMA units with chloride counterions were synthesized by controlled atom transfer radical polymerization, whereas their conjugates with *p*-aminosalicylic (PAS) or clavulanic (CLV) anions were obtained by chloride anion exchange, according to previously described procedures [27].

3.2. Characterization

Viability monitoring, cell density and confluence analysis were performed using Live Cell Analyzer (JuLI[™] Br; NanoEnTek Inc., Seoul, Korea). The cytotoxicity was evaluated by measuring the absorbance of the formazan product at 570 nm with the use of a microplate reader (Epoch, BioTek, Winooski, VT, USA). Apoptosis and cell cycle analysis were carried out with the use of an Aria III flow cytometer (Becton Dickinson; Franklin Lakes, NJ, USA). Cytometric analyses were performed using PE configuration (547 nm excitation; emission: 585 nm) or FITC configuration (488 nm excitation; emission: LP mirror 503, BP filter 530/30).

3.3. Cell Culture

Cells were grown in a DMEM-F12 medium in sterile culture bottles (75 cm² of culture area) with 10% (*v/v*) FBS at 37 °C in the incubator (humidified atmosphere with 5% CO₂). The cell cultures were well placed in a 96-well plate in case of MTT tests (10,000 cells per well), and 6-well plate in case of cell cycle analysis and apoptosis assay (100,000 cells per well).

3.4. MTT Cytotoxicity Assay

A total of 10,000 cells were placed into 96-well plates in 0.2 mL of medium 24 h before adding polymer systems. Controls were prepared in the first row and outer columns of wells. A series of dilutions of the inoculated compounds were prepared in the remaining wells (3125–100 µg/mL). The treated and untreated (control) cells were incubated for 72 h in standard conditions. Then, the solutions were removed, and 50 µL of MTT solution (0.5 mg/mL in RPMI 1640 without phenol red) were placed into each well. After incubation (1–2 h), the MTT solution was taken out of the wells. Created formazan crystals were dissolved in 75 µL of isopropanol/HCl mixture (*v/v* 1/0.04). The cytotoxicity was evaluated by measuring the absorbance of the formazan product at 570 nm with the use of a microplate reader. Readings were repeated three times (six technical repetitions for each concentration). The results were presented as the percentage fraction of the control. The cell density estimation, viability monitoring and confluence analysis were carried out with the use of a Live Cell Analyzer. After 72 h of incubation, the microscopic images were taken of treated and untreated cells.

3.5. Cytometric Analyses by Flow Cytometry

A total of 100,000 cells were placed into 6-well plates in 2 mL of medium for 24 h before treatment. Then, 2 mL of the polymer/conjugate sample was placed into each well and incubated for 72 h.

Part of the solutions from the wells was placed into sterile vials and centrifuged for 3 min (0.6 × *g*, RT). Then 50 µL of cold Annexin-V labeling buffer and 2.5 µL of FITC-labeled Annexin-V antibody were added to the pellet, and resuspended cells were incubated for 30 min in darkness. Next, the 250 µL of Annexin-V labeling buffer was added. An Annexin-V apoptosis assay was performed immediately using an Aria III flow cytometer.

For cell cycle analysis, the rest of the cell suspension collected from wells were centrifuged, and the supernatant was removed. Then, 250 µL of hypotonic buffer was added to the pellet (hypotonic buffer comprised PI 100 µg/mL in PBS; 5 mg/L of citric acid; 1:9 Triton-X solution; RNase 100 µg/mL in PBS from Sigma, Poznań, Poland) and the samples were incubated for 15 min in a cold and dark environment. The DNA levels were

assessed by fluorescence measurements via BD FACS Aria™ III sorter (Becton, Dickinson and Company, Franklin Lakes, NJ, USA) using PE configuration.

4. Conclusions

In vitro cytotoxicity evaluation of choline graft, polymer-carriers and their ionic PAS and CLV conjugates was based on MTT, apoptosis assay and cell cycle analysis. These tests indicated a strong correlation between biological action and carrier structure, including the type of attached pharmaceutical anions. Polymer systems with selective activity caused a negative effect on the tumor (A549) cell line, while they did not trigger significant changes in the normal (BEAS-2B) cell line. Moreover, the cytometric analyses proved the specific course of action. During studies on the type of cell death, it was found that in comparison to the control cells, a greater number of A549 cells died, mainly through necrosis. In turn, these compounds had no meaningful impact on BEAS-2B cells. Additional confirmation was achieved by cell cycle determination. Such findings suggest the potential usage of novel drugs for respiratory system diseases because of a wide application against cancer cells or pathogens (originated structures were reported as antimicrobial). For further findings, the specific test for antituberculosis therapy using standard assays should be performed [43].

The investigated ionic graft copolymers and their conjugates, previously tested for physicochemical evaluation, and evaluated cytotoxicity in this report, fulfilled the basic criteria for drug delivery systems. They are promising carriers of ionic drugs, especially those with a higher content of ionic units at lower graft density or lower content of ionic units at higher graft density, which can be used in the future for the treatment of lung diseases, such as tuberculosis, given the required specialized biomedical assessments.

Supplementary Materials: The following are available online at <https://www.mdpi.com/article/10.3390/ijms22147741/s1>, Figure S1. Microscopic images by Live Cell Analyzer of untreated control cells vs. treated A549 and BEAS-2B cells by polymer I and IV with Cl^- , PAS^- and CLV^- counterions; Tables S1 and S2. Results of Annexin V apoptosis assay in A549 and BEAS-2B cells for control probe, PIL carriers varying with content of TMAMA units (25% and 50%) and grafting degree (26% and 46%), and their conjugates with PAS and CLV; Figure S2. Plots of I and IV cell populations determined by flow cytometric analysis in A549 and BEAS-2B cell line; Tables S3 and S4. Results of cell cycle analysis for control probe, PIL carriers varying with TMAMA content (25% and 50%) and grafting degree (26% and 46%) and their conjugates with PAS and CLV, in treatment of A549 and BEAS-2B cells.

Author Contributions: K.N.: data curation, formal analysis, investigation, writing—original draft; W.L.: data curation; M.S.: biological evaluation and in vitro experiments supervision, data analysis, writing—original draft; D.N.: conceptualization, methodology, funding acquisition, project administration, writing—review and editing, supervision. All authors have read and agreed to the published version of the manuscript.

Funding: These studies were financially supported by the National Science Center, grant no. 2017/27/B/ST5/00960.

Institutional Review Board Statement: Not applicable.

Informed Consent Statement: Not applicable.

Data Availability Statement: Not applicable.

Conflicts of Interest: The authors declare no conflict of interest.

References

1. Amstad, E.; Reimhult, E. Nanoparticle actuated hollow drug delivery vehicles. *Nanomedicine* **2000**, *7*, 145–164. [[CrossRef](#)] [[PubMed](#)]
2. Neuse, E.W. Synthetic Polymers as Drug-Delivery Vehicles in Medicine. *Met. Based Drugs* **2008**, *2008*, 1–19. [[CrossRef](#)] [[PubMed](#)]

3. Deb, P.; Kokaz, S.; Abed, S.; Paradkar, A.; Tekade, R. Pharmaceutical and Biomedical Applications of Polymers. In *Advances in Pharmaceutical Product Development and Research, Basic Fundamentals of Drug Delivery*; Tekade, R.K., Ed.; Academic Press: Cambridge, MA, USA, 2019; pp. 203–267.
4. Liechty, W.B.; Kryscio, D.R.; Slaughter, B.V.; Peppas, N. Polymers for Drug Delivery Systems. *Annu. Rev. Chem. Biomol. Eng.* **2010**, *1*, 149–173. [[CrossRef](#)] [[PubMed](#)]
5. Kopeček, J. Polymer–drug conjugates: Origins, progress to date and future directions. *Adv. Drug Deliv. Rev.* **2013**, *65*, 49–59. [[CrossRef](#)]
6. Wilczewska, A.Z.; Niemirowicz, K.; Markiewicz, K.H.; Car, H. Nanoparticles as drug delivery systems. *Pharmacol. Rep.* **2012**, *64*, 1020–1037. [[CrossRef](#)]
7. Khandare, J.; Minko, T. Polymer–drug conjugates: Progress in polymeric prodrugs. *Prog. Polym. Sci.* **2006**, *31*, 359–397. [[CrossRef](#)]
8. Mamontova, N.V.; Chernyak, E.I.; Amosov, E.V.; Gatilov, Y.V.; Vinogradova, V.I.; Aripova, S.F.; Grigor'ev, I. First Ionic Conjugates of Dihydroquercetin Monosuccinate with Amines. *Chem. Nat. Compd.* **2017**, *53*, 1045–1051. [[CrossRef](#)]
9. Saraswat, J.; Wani, F.A.; Dar, K.I.; Rizvi, M.M.A.; Patel, R. Noncovalent Conjugates of Ionic Liquid with Antibacterial Peptide Melittin: An Efficient Combination against Bacterial Cells. *ACS Omega* **2020**, *5*, 6376–6388. [[CrossRef](#)]
10. He, D.; Liu, Z.; Huang, L. Progress in Ionic Liquids as Reaction Media, Monomers and Additives in High-Performance Polymers. In *Solvents, Ionic Liquids and Solvent Effects*; Glossman-Mitnik, D., Ed.; IntechOpen: London, UK, 2020; pp. 99–124.
11. Eftekhari, A.; Saito, T. Synthesis and properties of polymerized ionic liquids. *Eur. Polym. J.* **2017**, *90*, 245–272. [[CrossRef](#)]
12. Bielas, R.; Mielańczyk, A.; Skonieczna, M.; Mielańczyk, L.; Neugebauer, D. Choline supported poly(ionic liquid) graft copolymers as novel delivery systems of anionic pharmaceuticals for anti-inflammatory and anti-coagulant therapy. *Sci. Rep.* **2019**, *9*, 14410. [[CrossRef](#)]
13. Fedotova, M.V.; Kruchinin, S.E.; Chuev, G.N. Features of local ordering of biocompatible ionic liquids: The case of choline-based amino acid ionic liquids. *J. Mol. Liq.* **2019**, *296*, 112081. [[CrossRef](#)]
14. Lin, X.; Yang, Y.; Li, S.; Song, Y.; Ma, G.; Su, Z.; Zhang, S. Unique stabilizing mechanism provided by biocompatible choline-based ionic liquids for inhibiting dissociation of inactivated foot-and-mouth disease virus particles. *RSC Adv.* **2019**, *9*, 13933–13939. [[CrossRef](#)]
15. Petkovic, M.; Ferguson, J.L.; Gunaratne, H.Q.N.; Ferreira, R.; Leitão, M.C.; Seddon, K.R.; Rebelo, L.P.N.; Pereira, C.S. Novel biocompatible cholinium-based ionic liquids-toxicity and biodegradability. *Green Chem.* **2010**, *12*, 643–649. [[CrossRef](#)]
16. Noshadi, I.; Walker, B.W.; Portillo-Lara, R. Engineering Biodegradable and Biocompatible Bio-ionic Liquid Conjugated Hydrogels with Tunable Conductivity and Mechanical Properties. *Sci. Rep.* **2017**, *7*, 4345. [[CrossRef](#)] [[PubMed](#)]
17. Isik, M.; Gracia, R.; Kollnus, L.C.; Tomé, L.C.; Marrucho, I.M.; Mecerreyes, D. Cholinium-Based Poly(ionic liquid)s: Synthesis, Characterization, and Application as Biocompatible Ion Gels and Cellulose Coatings. *ACS Macro Lett.* **2013**, *2*, 975–979. [[CrossRef](#)]
18. Md Moshikur, R.; Chowdhury, M.R.; Moniruzzaman, M.; Goto, M. Biocompatible ionic liquids and their application in pharmaceuticals. *Green Chem.* **2020**, *22*, 8116–8139. [[CrossRef](#)]
19. Ibsen, K.N.; Ma, H.; Banerjee, A.; Tanner, E.E.L.; Nangia, S.; Mitragotri, S. Mechanism of Antibacterial Activity of Choline-Based Ionic Liquids (CAGE). *ACS Biomater. Sci. Eng.* **2018**, *4*, 2370–2379. [[CrossRef](#)]
20. Yuan, J.; Soll, S.; Drechsler, M.; Müller, A.; Antonietti, M. Self-Assembly of Poly(ionic liquid)s: Polymerization, Mesostructure Formation, and Directional Alignment in One Step. *J. Am. Chem. Soc.* **2011**, *133*, 17556–17559. [[CrossRef](#)]
21. Guo, J.; Zhou, Y.; Qiu, L.; Yuan, C.; Yan, F. Self-assembly of amphiphilic random co-poly(ionic liquid)s: The effect of anions, molecular weight, and molecular weight distribution. *Polym. Chem.* **2013**, *4*, 4004. [[CrossRef](#)]
22. Hosseinzadeh, F.; Mahkam, M.; Galehassadi, M. Synthesis and characterization of ionic liquid functionalized polymers for drug delivery of an anti-inflammatory drug. *Des. Monomers Polym.* **2012**, *15*, 279–388. [[CrossRef](#)]
23. Gao, Y.; Arritt, S.W.; Twamley, B.; Shreeve, J.M. Guanidinium-Based Ionic Liquids. *Inorg. Chem.* **2005**, *44*, 1704–1712. [[CrossRef](#)] [[PubMed](#)]
24. Stenzel, M.; Barner-Kowollik, C.; Davis, T.; Dalton, H.M. Amphiphilic Block Copolymers Based on Poly(2-acryloyloxyethyl phosphorylcholine) Prepared via RAFT Polymerisation as Biocompatible Nanocontainers. *Macromol. Biosci.* **2004**, *4*, 445–453. [[CrossRef](#)] [[PubMed](#)]
25. Yu, Y.; Yao, Y.; van Lin, S.; de Beer, S. Specific anion effects on the hydration and tribological properties of zwitterionic phosphorylcholine-based brushes. *Eur. Polym. J.* **2009**, *112*, 222–227. [[CrossRef](#)]
26. Joubert, F.; Yeo, R.; Sharples, G.; Musa, O.M.; Hodgson, D.; Cameron, N. Preparation of an Antibacterial Poly(ionic liquid) Graft Copolymer of Hydroxyethyl Cellulose. *Biomacromolecules* **2015**, *16*, 3970–3979. [[CrossRef](#)]
27. Niesyto, K.; Neugebauer, D. Synthesis and Characterization of Ionic Graft Copolymers: Introduction and In Vitro Release of Antibacterial Drug by Anion Exchange. *Polymers* **2020**, *12*, 2159. [[CrossRef](#)]
28. Niesyto, K.; Neugebauer, D. Linear Copolymers Based on Choline Ionic Liquid Carrying Anti-Tuberculosis Drugs: Influence of Anion Type on Physicochemical Properties and Drug Release. *Int. J. Mol. Sci.* **2021**, *22*, 284.
29. Gorbunova, M.; Lemkina, L.; Borisova, I. New guanidine-containing polyelectrolytes as advanced antibacterial materials. *Eur. Polym. J.* **2018**, *105*, 426–433. [[CrossRef](#)]
30. Shekaari, H.; Zafarani-Moattar, M.; Mirheydari, S.; Agha, E. The effect of pharmaceutically active ionic liquids, 1-methyl-(3-hexyl or octyl) imidazolium Ibuprofenate on the thermodynamic and transport properties of aqueous solutions of glycine at T = 298.2 K and p = 0.087 MPa. *J. Mol. Liq.* **2019**, *288*, 111009. [[CrossRef](#)]

31. Lu, B.; Zhou, G.; Xiao, F.; He, Q.; Zhang, J. Stimuli-Responsive Poly(ionic liquid) Nanoparticle for Controlled Drug Delivery. *J. Mater. Chem. B* **2020**, *8*, 7994–8001. [[CrossRef](#)]
32. Bielas, R.; Siewniak, A.; Skonieczna, M.; Adamiec, M.; Mielańczyk, Ł.; Neugebauer, D. Choline based polymethacrylate matrix with pharmaceutical cations as co-delivery system for antibacterial and anti-inflammatory combined therapy. *J. Mol. Liq.* **2019**, *285*, 114–122. [[CrossRef](#)]
33. De Jong, W.; Borm, P. Drug delivery and nanoparticles: Application and hazards. *Int. J. Nanomed.* **2008**, *3*, 133–149. [[CrossRef](#)]
34. Kumar, P.; Nagarajan, A.; Uchil, P.D. Analysis of Cell Viability by the MTT Assay. *Cold Spring Harb. Protoc.* **2018**, *2018*, 6. [[CrossRef](#)] [[PubMed](#)]
35. Bahuguna, A.; Khan, I.; Bajpai, V.K.; Kang, S.C. MTT assay to evaluate the cytotoxic potential of a drug. *Bangladesh. J. Pharmacol.* **2017**, *12*, 115–118. [[CrossRef](#)]
36. Bopp, S.K.; Lettieri, T. Comparison of four different colorimetric and fluorometric cytotoxicity assays in a zebrafish liver cell line. *BMC Pharmacol.* **2008**, *8*, 8. [[CrossRef](#)] [[PubMed](#)]
37. Präbst, K.; Engelhardt, H.; Ringgeler, S.; Hübner, H. Basic Colorimetric Proliferation Assays: MTT, WST, and Resazurin. *Methods Mol. Biol.* **2017**, *1601*, 1–17. [[PubMed](#)]
38. Mielańczyk, A.; Skonieczna, M.; Mielańczyk, Ł.; Neugebauer, D. In vitro evaluation of doxorubicin-conjugates based on sugar core non-linear polymethacrylates toward anticancer drug delivery. *Bioconjug. Chem.* **2016**, *27*, 893–904. [[CrossRef](#)] [[PubMed](#)]
39. Darzynkiewicz, Z.; Bedner, E.; Smolewski, P. Flow cytometry in analysis of cell cycle and apoptosis. *Semin Hematol.* **2001**, *38*, 179–193. [[CrossRef](#)]
40. Ormerod, M.G. Investigating the relationship between the cell cycle and apoptosis using flow cytometry. *J. Immunol. Methods* **2002**, *265*, 73–80. [[CrossRef](#)]
41. Koopman, G.; Reutelingsperger, C.P.M.; Kuijten, G.A.M.; Keehnen, R.M.J.; Pals, S.T.; Van Oers, M.H.J. Annexin V for Flow Cytometric Detection of Phosphatidylserine Expression on B Cells Undergoing Apoptosis. *Blood* **1994**, *84*, 1415–1420. [[CrossRef](#)]
42. Riccardi, C.; Nicoletti, I. Analysis of Apoptosis by Propidium Iodide Staining and Flow Cytometry. *Nat. Protoc.* **2006**, *1*, 1458–1461. [[CrossRef](#)]
43. Akcali, S.; Surucuoglu, S.; Cicek, C.; Ozbakkaloglu, B. In vitro activity of ciprofloxacin, ofloxacin and levofloxacin against *Mycobacterium tuberculosis*. *Ann. Saudi Med.* **2005**, *25*, 409–412. [[CrossRef](#)] [[PubMed](#)]

Biological In Vitro Evaluation of PIL Graft Conjugates: Cytotoxicity Characteristics

Katarzyna Niesyto¹, Wiktoria Łyżniak¹, Magdalena Skonieczna^{2,3,*} and Dorota Neugebauer^{1,*}

¹ Department of Physical Chemistry and Technology of Polymers, Faculty of Chemistry, Silesian University of Technology, 44-100 Gliwice, Poland; katarzyna.niesyto@polsl.pl

² Department of Systems Biology and Engineering, Silesian University of Technology, Akademicka 16, 44-100 Gliwice, Poland

³ Biotechnology Centre, Silesian University of Technology, Krzywoustego 8, 44-100 Gliwice, Poland

* Correspondence: Magdalena.Skonieczna@polsl.pl (M.S.); Dorota.Neugebauer@polsl.pl (D.N.)

Content:

Figure S1. Microscopic images by Live Cell Analyzer of untreated control cells vs treated (a) A549 and (b) BEAS-2B cells by polymer I and IV with Cl^- , PAS^- and CLV^- counterions;

Table S1. Results of Annexin V apoptosis assay in A549 cells for control probe, PIL carriers varying with content of TMAMA units (25% and 50%) and grafting degree (26% and 46%), and their conjugates with PAS and CLV;

Table S2. Results of Annexin V apoptosis assay in BEAS-2B cells for control probe, PIL carriers varying with content of TMAMA units (25% and 50%) and grafting degree (26% and 46%), and their conjugates with PAS and CLV;

Figure S2. Plots of I and IV cell populations determined by flow cytometric analysis in (a) A549 and (b) BEAS-2B cell line;

Table S3. Results of cell cycle analysis in A549 cells for control probe, PIL carriers varying with content of TMAMA units (25% and 50%) and grafting degree (26% and 46%), and their conjugates with PAS and CLV;

Table S4. Results of cell cycle analysis in BEAS-2B cells for control probe, PIL carriers varying with content of TMAMA units (25% and 50%) and grafting degree (26% and 46%), and their conjugates with PAS and CLV.

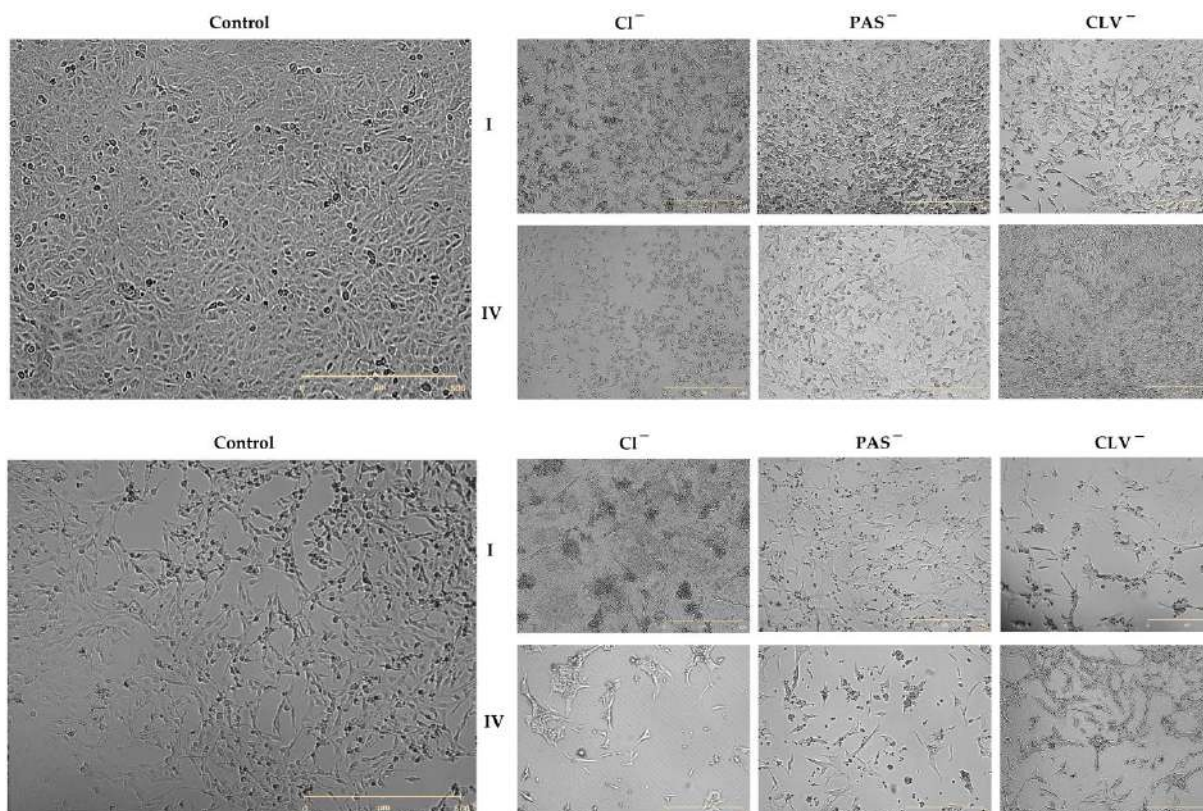


Figure S1. Microscopic images by Live Cell Analyzer of untreated control cells vs treated (a) A549 and (b) BEAS-2B cells by polymer I and IV with Cl^- , PAS^- and CLV^- counterions

Table S1. Results of Annexin V apoptosis assay in A549 cells for control probe, PIL carriers varying with content of TMAMA units (25% and 50%) and grafting degree (26% and 46%), and their conjugates with PAS and CLV

	Carrier				Conjugates with:							
					PAS				CLV			
	A- /PI- (%)	A+ /PI- (%)	A- /PI+ (%)	A+ /PI+ (%)	A- /PI- (%)	A+ /PI- (%)	A- /PI+ (%)	A+ /PI+ (%)	A- /PI- (%)	A+ /PI- (%)	A- /PI+ (%)	A+ /PI+ (%)
Control	78.7	0	21.3	0.04	78.7	0	21.3	0.04	78.7	0	21.3	0.04
I	42.2	0.8	48.8	8.3	65.3	1.8	21.9	11.0	92.3	0	7.6	0.03
II	32.9	1.7	48.1	17.3	69.5	0	30.5	0.03	82.9	0	17.1	0.03
III	32.4	1.9	53.0	12.7	82.0	0	17.9	0.01	72.6	0	27.4	0.01
IV	75.2	0.3	19.8	4.7	76.0	1	21.2	1.8	86.9	0	13.0	0.05

Table S2. Results of Annexin V apoptosis assay in BEAS-2B cells for control probe, PIL carriers varying with TMAMA content (25% and 50%) and grafting degree (26% and 46%), and their conjugates with PAS and CLV

	Carrier				Conjugates with:							
					PAS				CLV			
	A- /PI- (%)	A+ /PI- (%)	A- /PI+ (%)	A+ /PI+ (%)	A- /PI- (%)	A+ /PI- (%)	A- /PI+ (%)	A+ /PI+ (%)	A- /PI- (%)	A+ /PI- (%)	A- /PI+ (%)	A+ /PI+ (%)
Control	97.5	0.1	2.2	0.2	97.5	0.1	2.2	0.2	97.5	0.1	2.2	2.2
I	90.3	0.5	8.3	0.9	93.7	0.1	6.0	0.1	89.8	0.8	8.7	0.7
II	85.5	0.7	13.2	0.6	90.5	0.7	9.6	0.3	89.0	1.0	9.3	0.8
III	89.1	1.1	9.3	0.5	87.5	0.5	11.7	0.3	88.2	1.6	9.5	0.7
IV	93.4	1.0	5.2	0.4	92.8	0.7	6.2	0.3	90.1	0.8	8.7	0.5

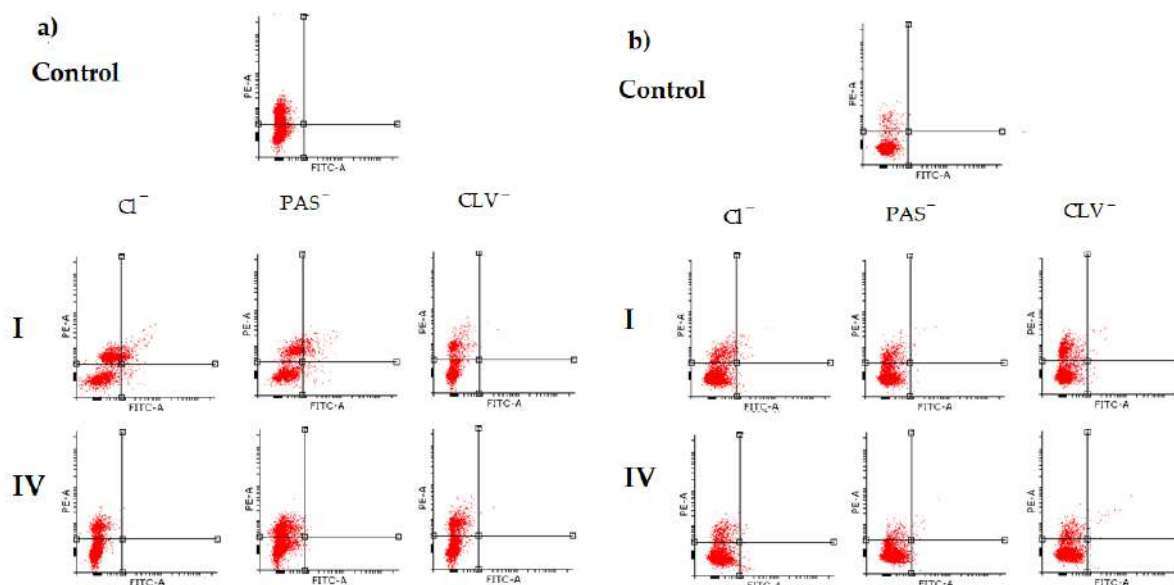


Figure S2. Plots of I and IV cell populations determined by flow cytometric analysis in (a) A549 and (b) BEAS-2B cell line.

Table S3. Results of cell cycle analysis in A549 cells for control probe, PIL carriers varying with content of TMAMA units (25% and 50%) and grafting degree (26% and 46%), and their conjugates with PAS and CLV.

	Carrier				Conjugates with:							
	Sub-G1 (%)	G0/G1 (%)	S (%)	G2/M (%)	PAS				CLV			
	Sub-G1 (%)	G0/G1 (%)	S (%)	G2/M (%)	Sub-G1 (%)	G0/G1 (%)	S (%)	G2/M (%)	Sub-G1 (%)	G0/G1 (%)	S (%)	G2/M (%)
Control	42.51	17.62	36.07	3.80	42.51	17.62	36.07	3.80	42.51	17.62	36.07	3.80
I	0.75	69.56	16.78	12.61	65.3	70.36	19.40	7.35	37.06	7.77	52.06	3.13
II	0.25	75.26	16.12	8.24	69.5	44.25	39.04	14.32	4.54	26.76	63.63	5.07
III	0.41	66.76	23.86	8.96	82.0	43.35	44.89	6.34	17.23	18.35	60.29	4.13
IV	2.82	68.40	18.95	9.82	76.0	68.40	18.95	9.82	2.95	43.04	48.75	5.24

Table S4. Results of cell cycle analysis in BEAS-2B cells for control probe, PIL carriers varying with content of TMAMA units (25% and 50%) and grafting degree (26% and 46%), and their conjugates with PAS and CLV.

	Carrier				Conjugates with:							
	Sub-G1 (%)	G0/G1 (%)	S (%)	G2/M (%)	PAS				CLV			
	Sub-G1 (%)	G0/G1 (%)	S (%)	G2/M (%)	Sub-G1 (%)	G0/G1 (%)	S (%)	G2/M (%)	Sub-G1 (%)	G0/G1 (%)	S (%)	G2/M (%)
Control	34.86	17.51	44.74	2.88	34.86	17.51	44.74	2.88	34.86	17.51	44.74	2.88
I	1.95	6.80	75.98	15.27	3.59	12.51	73.14	10.77	0.66	6.58	80.12	12.65
II	0.96	4.91	69.20	24.92	0.94	7.68	56.81	34.77	0.96	6.67	63.30	29.07
III	1.18	12.51	63.47	22.93	1.44	8.76	77.29	12.51	1.22	7.87	65.98	24.93
IV	2.12	13.52	75.78	8.57	1.92	15.48	75.13	7.47	3.92	16.06	71.56	8.46

PUBLIKACJA P.7





Toxicity evaluation of choline ionic liquid-based nanocarriers of pharmaceutical agents for lung treatment.

Niesyto, K., Skonieczna, M., Adamiec-Organisziok, M., Neugebauer, D.

Journal of Biomedical Materials Research Part B - Applied Biomaterials 2023,
7, 1374-1385

RESEARCH ARTICLE

Toxicity evaluation of choline ionic liquid-based nanocarriers of pharmaceutical agents for lung treatment

Katarzyna Niesyto¹  | Magdalena Skonieczna^{2,3}  |
Małgorzata Adamiec-Organisiok^{2,3}  | Dorota Neugebauer¹ 

¹Department of Physical Chemistry and Technology of Polymers, Faculty of Chemistry, Silesian University of Technology, Gliwice, Poland

²Department of Systems Biology and Engineering, Faculty of Automatic Control, Electronics and Computer Science, Silesian University of Technology, Gliwice, Poland

³Biotechnology Centre, Silesian University of Technology, Gliwice, Poland

Correspondence

Magdalena Skonieczna, Department of Systems Biology and Engineering, Faculty of Automatic Control, Electronics and Computer Science, Silesian University of Technology, 44-100 Gliwice, Poland.

Email: magdalena.skonieczna@polsl.pl

Dorota Neugebauer, Department of Physical Chemistry and Technology of Polymers, Faculty of Chemistry, Silesian University of Technology, Strzody 9, 44-100 Gliwice, Poland.

Email: dorota.neugebauer@polsl.pl

Funding information

Narodowe Centrum Nauki, Grant/Award Number: OPUS grant no. 2017/27/B/ST5/00960; Polish Budget Funds for Scientific Research, Grant/Award Numbers: 02/040/SDU/10-21-01, 04/040/BKM21/0176

Abstract

In vitro cytotoxicity evaluation of linear copolymer (LC) containing choline ionic liquid units and its conjugates with an antibacterial drug in anionic form, that is, *p*-aminosalicylate (LC_PAS), clavulanate (LC_CLV), or piperacillin (LC_PIP) was carried out. These systems were tested against normal: human bronchial epithelial cells (BEAS-2B), and cancers: adenocarcinoma human alveolar basal epithelial cells (A549), and human non-small cell lung carcinoma cell line (H1299). Cells viability, after linear copolymer LC and their conjugates addition for 72 h, was measured at concentration range of 3.125–100 µg/mL. The MTT test allowed the designation of IC₅₀ index, which was higher for BEAS-2B, and significantly lower in the case of cancer cell lines. The cytometric analyzes, that is, Annexin-V FITC apoptosis assay and cell cycle analysis as well as gene expression measurements for interleukins IL6 and IL8 were carried out, and showed pro-inflammatory activity of tested compounds toward cancer cells, while it was not observed against normal cell line.

KEYWORDS

cytotoxicity, drug delivery systems, ionic conjugates, polymer nanocarriers, trimethylammonium ionic liquids

1 | INTRODUCTION

Polymer-drug conjugates are a common form of drug delivery systems, which are designed to improve drug solubility, control, and targeting therapy.^{1,2} The other advantages have been reported for adjustment of drug release kinetics profile by the strength of chemical bonding as the conjugation sites and the type/length of the linker connecting drug with the polymer matrix. The presence of reactive carboxylic or hydroxyl and amine groups in polyelectrolytes is convenient for conjugation reactions.^{3,4} The specific type of conjugates are corresponding to the ionic polymers, which gain much consideration because of a variety of actions, for example, electrical conductivity,⁵ electrochemical,⁶ anti-electrostatic,⁷

energetic,⁸ and optical⁹ properties, as well as herbicidal,¹⁰ or biological activity.^{11,12} The last property can be generated by conjugation of the pharmaceutical compounds to provide drug delivery polymer systems. The main requirements for polymeric carriers are related to biocompatibility and non-toxicity. Therefore, among the vehicles, the ionic polymers as the representative group of polyelectrolytes can be especially distinguished, notably those based on ionic liquids (ILs), due to their unique benefits, including the concept of *green chemistry* and their ability to ion exchange, which is a strategic way for the introduction of the active pharmaceutical ingredients (API) as the counter-ions.^{12–14} ILs combining ionic structure and liquid phase are defined as molten salts in room temperature up to 100°C due to combination of bulky asymmetric cations

and weakly coordinating anions advantageous for destabilization of the crystal lattice and extraordinary flexibility. Their extraordinary potential to adjust solvation properties in water and biological fluids via ionic exchange provides a flexible approach for improvement of solubility and fine-tune hydrophobic/hydrophilic properties, tunable interactions at the molecular level, and formation of higher-ordered self-assembled nanostructures, bioavailability, and polymorphism limitations of conventional drugs.¹⁴ Some of ILs are the well-known antibiotics (ampicillin, penicillin G), anti-inflammatory (pravadoline, ibuprofen, naproxen, salicylate), antiviral (trifluoridine), or antifungal (clioquinol) compounds, whereas the others have been used to obtain pharmaceutical precursors, such as lactam, pyrazolone, thiazole, imidazole, and thiazolidine.¹⁵ Generally, API-ILs display enhanced solubility in water or dissolution rates of pharmaceuticals¹⁶ increasing their bioavailability¹⁷ when compared with the original APIs. For medical purposes, it is highly desirable when the IL polymer matrix offers biological activity, namely antioxidant, anti-tumoral and antimicrobial activity¹⁴ as it has been proved for tetrabutylammonium-, phosphonium-, imidazolium-, pyridinium-, piperidinium-, pyrrolidinium-, or choline-based cations.^{18–21} Especially, the polymerizable ILs, for example, 1-(4-vinylbenzyl)-3-methyl imidazolium and 1-(4-vinylbenzyl)-4-(dimethylamino)-pyridinium hexafluorophosphate,²² 2,2-diallyl-1,1,3,3-tetraethylguanidinium chloride,²³ vinyl benzyl trimethylammonium chloride,²⁴ [2-(methacryloyloxy)ethyl]trimethylammonium chloride known as choline methacrylate,^{25,26} seem to be attractive in the synthesis of polymers, which are named as the polymeric ILs in analogy to their monomeric constituents,²⁷ and can be applied for drug delivery. The latter one has been also applied to obtain the graft copolymers with IL units in the side chains carrying API anions with anti-inflammatory and anti-coagulant properties.^{28,29}

Depending on the type of IL or API, the obtained systems can be used in miscellaneous therapies. Due to the deterioration of the general immune system in the body as a result of a disease caused by various pathogens, the weakened organs are particularly vulnerable to cancer.^{30–32} For this reason, the drug delivery systems which do not promote the cancer cells are highly desirable. Recently, the ILs with ampicillin,¹⁷ taurine,³³ or *p*-aminosalicylate and clavulanate³⁴ have been investigated as potential delivery systems with additional antitumor activity. Hydrogel containing TMAMA units has been used as a carrier for fluorouracil delivery. The cytotoxicity tests against kidney cell lines proved that it was cell compatible and supported the cell proliferation.³⁵ Subsequent cytotoxicity studies against gastric epithelial cell line reported on TMAMA and *N*-(3-aminopropyl)methacrylamide hydrochlorid copolymer conjugated with hematoporphyrin as a tissue-adhesive marking agent demonstrated extremely low cytotoxicity.³⁶ The copolymers of TMAMA and methylenebisacrylamide as a drug carriers of cefuroxime have been tested in terms of blood compatibility and antioxidant activity showing the antimicrobial and antioxidant nature of polymer matrix.³⁷

We report the cytotoxicity evaluation against normal cell lines, namely human bronchial epithelial cells (BEAS-2B), and additionally cancer ones, that is, adenocarcinoma human alveolar basal epithelial cells (A549) and human non-small cell lung carcinoma cell line (H1299) of the ionic drug-polymer carrier. The previously synthesized

well-defined linear copolymers of (2-trimethylammonium)ethyl methacrylate and methyl methacrylate (LC) have been investigated successfully by their ability to self-assembling and anion exchange.³⁸ The biological activity of the ionic copolymers has been generated by the content of bioactive choline derivative units as important anti-inflammatory ingredient, as well as by the exchange with antibacterial drugs in anionic form (Scheme 1), that is, *p*-aminosalicylate, (PAS), clavulanate (CLV), piperacillin (PIP), which are used in the conventional treatment of lung diseases, especially tuberculosis. The selected drugs have been approved many years ago by the FDA and they are available as the commercial products, namely Paser (PAS), Augmentin, Clavulin, Amoclan (CLV combined with amoxicillin), and Zosyn (PIP combined with tazobactam). In this case the carrier toxicity is crucial issue due to its direct contact with the normal human cells and the potential risk of their damage. In the case of prolonged bacterial infections and/or reduced immunity, the beneficial effect of the polymer should not provoke the growth of the cancer cells. Satisfactory physicochemical properties of the nanocarriers and their drug release facility³⁸ require the extra characteristics with the cytotoxicity evaluation, including colorimetric tests with the use of 3-(4,5-dimethylthiazol-2-yl)-2,5-diphenyltetrazolium bromide (MTT) and cytometric analyses by flow cytometry, that is, apoptosis assay and cell cycle analysis, to confirm their beneficial application as drug delivery systems.

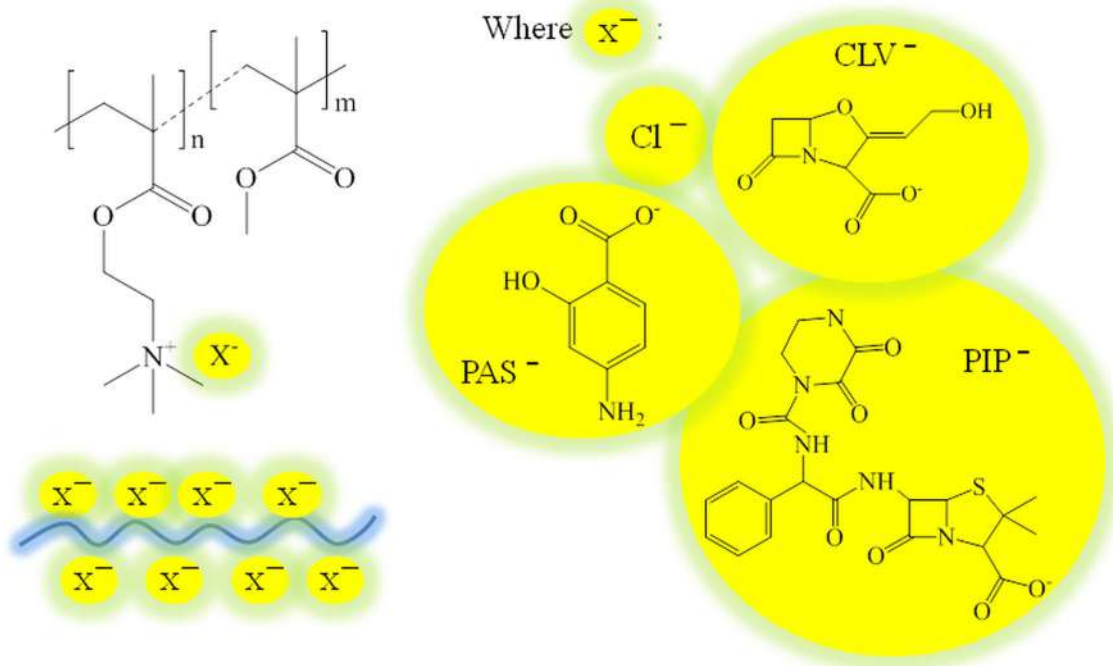
2 | MATERIALS AND METHODS

2.1 | Materials

DMEM-F12 medium, trypsin, sodium phosphate buffer saline (PBS, pH = 7.4) were bought from Aldrich (Poznań, Poland). Annexin-V apoptosis assay (BioLegend, San Diego, CA, United States). Propidium iodide solution (PI, BD Biosciences, San Jose, CA, United States). Fetal bovine serum (FBS, EURx, Gdańsk, Poland), physiological saline (PBS without Ca and Mg, PAN-Biotech GmbH, Aidenbach, Germany), and Annexin-V binding buffer (BD Biosciences) were used without earlier preparation. Human bronchial epithelial cells (BEAS-2B), adenocarcinoma human alveolar basal epithelial cells (A549), and human non-small cell lung carcinoma cell line (H1299) were received from ATCC (Cat# ATCC®CRL-9609; Manassas, VA, United States). LC with chloride counterions was synthesized by atom transfer radical polymerization (ATRP), whereas the anion exchange reaction was required to obtain conjugates with pharmaceutical anions, such as *p*-aminosalicylic (LC_PAS), clavulanic (LC_CLV), and piperacillin (LC_PIP), according to previously described procedures.³⁸

2.2 | Characterization

Differential scanning calorimetry (DSC) was performed using Mettler Toledo (DSC822e) apparatus for a temperature range from –60 to 200°C at heating rate of 10°C/min. The glass transition temperature (T_g) of LC was determined from the second run of heating.



SCHEME 1 Structure of linear polymers containing chloride (LC) or pharmaceutical anions.

Live Cell Analyzer (JuLI™ Br; NanoEnTek Inc., Seoul, Korea) was used to measure confluence, cell density, and viability monitoring analysis. Cell viability assay was performed by measuring the absorbance of the MTT reaction product (formazan) at 570 nm in a microplate reader (Epoch, BioTek, Winooski, VT, United States). The results of apoptosis and cell cycle analysis were obtained with the use of an Aria III flow cytometer (Becton Dickinson; Franklin Lakes, NJ, United States).

2.3 | Cell culture

The cells were grown in a DMEM-F12 medium in sterile culture bottles (75 cm² of culture area) with 10% (vol/vol) FBS addition and kept at 37°C in the incubator with humidified atmosphere with 5% CO₂. For the MTT tests, the cultures were plated in 96-well plates. For apoptosis and cell cycle assays the cell cultures were plated in 6-well plates.

2.4 | MTT cytotoxicity assay

Ten thousand cells were placed into 96-well plates in 0.2 mL of DMEM-F12 medium and incubated. After 24 h the polymer systems were added to each cell, whereas the first row and outer columns were prepared as control cells. The remaining wells were filled with prepared dilution series of the tested polymers (3.125–100 µg/mL). Treated cells were incubated for 72 h in standard conditions, then the solution was removed from wells. The 50 µL of MTT solution were placed into each well (0.5 mg/mL in RPMI 1640 without phenol red)

and incubated for 1–2 h. After the MTT solution removal, formed formazan crystals were dissolved in 75 µL of isopropanol/HCl mixture (vol/vol 1–0.04), and then used for measuring the absorbance at 570 nm. Readings were performed in triplicate (six technical readings for each concentration). The results were expressed as a percentage fraction of the control.

2.5 | Flow cytometry

One hundred thousand cells were placed into 6-well plates in 2 mL of medium for 24 h. After treatment, each well was filled with 2 mL of polymer or conjugate sample. The incubation was carried out for 72 h. After that, the solution from the wells was divided into three parts.

The first part was placed into sterile vials and centrifuged for 3 min (0.6 × g, RT). Cold Annexin-V labeling buffer (50 µL) and FITC-labeled Annexin-V antibody (2.5 µL) were added to the pellet. Suspended cells were incubated for 30 min in darkness. Then, 250 µL of Annexin-V labeling buffer was added. Samples were tested immediately after preparation using an Aria III flow cytometer.

The second part of the solution was centrifuged, and then the supernatant was removed. After the addition of 250 µL of hypotonic buffer (hypotonic buffer comprised from PI 100 µg/mL in PBS; 5 mg/L of citric acid; 1:9 Triton-X solution; RNase 100 µg/mL in PBS from Sigma, Poznań, Poland) the samples were incubated for 15 min in cold and dark area. The DNA states were determined by fluorescence measurements via BD FACS Aria™ III sorter (Becton, Dickinson and Company, Franklin Lakes, NJ, United States) using PE configuration.

2.6 | RT-qPCR genes expressions for pro-inflammatory interleukins IL6 and IL8

The third part of the cells solution was collected by trypsinization. From the pellet, RNA was extracted using a phenol-chloroform method, with the procedure from the Total RNA Isolation kit (A&A Biotechnology). The RNA concentration and quality were estimated by UV-Vis spectrophotometer (Nanodrop, Thermofisher). The commercial set of reagents (Real-Time 2xPCR Master Mix SYBR A; A&A Biotechnology) and following Genomed pairs: IL6 (AGATCACCTAGTCCACCC) and (GTTCTGCCAAACCAGCCTTG); IL8 (GGTGCAGTTTTGCCAAGGAG) and IL-8 reverse (ACCAAGGCACAGTGAACAA); reference RPL41 (ACGGTGAACAAGCTAGCGG) and (TCCTGCGTTGGGATTCCGTG) was used to gene expression assays for pro-inflammatory (IL6, IL8). The thermocycler CFX96 Touch™ Real-Time PCR Detection System (Bio-Rad) was used to accomplish the quantitative PCR reaction, preceded by execution a reverse transcription (NG dART RT kit, EURx). For qRT-PCR reaction the following thermal profile was used: (I) 50°C, 2 min, (II) 95°C, 4 min, (III) 54 cycles ended with fluorescence reading: 95°C, 45 s.; 52.3°C, 30 s.; (IV) 72°C, 5 min, (V) melting curve in the temperature range 52–92°C (every 0.5°C at 5 s), (VI) incubation carried at 4°C. The thermal profile of the reaction was described previously.³⁹ The standardized value calculation of relative gene expression level in an unknown sample was performed concerning control expression by the following formula $R = 2^{-\Delta\Delta C_T}$.⁴⁰

3 | RESULTS AND DISCUSSION

Amphiphilic linear copolymer (LC) based on [2-(methacryloyloxy)ethyl] trimethyl-ammonium chloride as the IL and methyl methacrylate as non-ionic component, that is, P(TMAMA-co-MMA) was received as a nanocarrier for delivery of ionic pharmaceutical compounds with antibacterial activity, that is, *p*-aminosalicylate (PAS), clavulanate (CLV) and piperacillin (PIP). The previous studies on their physicochemical characterization, as well as the drug introduction, and release process described in Niesyto and Neugebauer³⁸ have proved that the polymer obtained by ATRP at 40°C, where the ratio of TMAMA/MMA units was equal to 25/75, is a promising drug vehicle. The designed system was able to carry PAS, CLV or PIP anions by the exchange of chloride anions in 76%, 66%, 43%, respectively, and release 6%–33% of drug within 4 h (Figure S1). The polymer ability to self-organization was confirmed by critical micelle concentration (CMC = 0.055 mg/mL), whereas the formed nanoparticles including those with therapeutic counterions reached sizes ranging in 170–290 nm. The characteristics of ionic polymer systems varied with drug type and content are presented in Table 1.

The polymers containing chloride anions and its conjugates with PAS⁻, CLV⁻, and PIP⁻ were screened for their in vitro cytotoxic activity. The choline chloride as the main component of the polymer structure, apart from the properties of ILs, it also exhibits biological properties. The complex role of choline in living organisms includes synthesis of neurotransmitter, transformation to betaine for the

TABLE 1 Characteristics of linear TMAMA copolymer (LC) and its conjugates with PAS, CLV, and PIP anions.

Copolymer	$F_{\text{TMAMA/PHA}}$ (%)	D_h (nm) ³⁸	WCA (°) ³⁸
LC	-	239	46.1
LC_PAS	18	274	63.5
LC_CLV	16	169	47.4
LC_PIP	10	291	51.4

Note: LC: P(TMAMA-co-MMA) (Cl based TMAMA polymer obtained directly from ionic liquid TMAMA/Cl as the matrix for anion exchange) with the average molecular weight $M_n = 46,900$ g/mol, and dispersity index $\bar{D} = 1.74$; polymerization degree $DP_n = 370$; the content of TMAMA units $F_{\text{TMAMA}} = 0.24$; glass transition temperature $T_g = 73^\circ\text{C}$ (Figure S2); $F_{\text{TMAMA/PHA}}$ is the content of TMAMA units with pharmaceutical anions; D_h is hydrodynamic diameter by dynamic light scattering (DLS); WCA is water contact angle via goniometry using the sessile drop method; DC is drug content evaluated by UV-Vis.

methyl-group metabolism, synthesis of the cell membrane components and lipoproteins.^{41,42} Thanks to a wide spectrum of action the therapeutic effects of choline and its derivatives have been reported demonstrating their anti-inflammatory properties^{43,44} and the reduced risk of the cancer at the adequate choline level.^{45,46} PAS is an inhibitor of mycobactin biosynthesis and used as a second-line antituberculosis drug, usually applied to support other agents.⁴⁷ CLV is a compound that has a similar structure to penicillin and exhibits inhibitory properties of β -lactamase. It is usually used in combination with other drugs such as β -lactam antibiotics (amoxicillin). Penicillinase enzyme, which attacks the β -lactam antibiotic, is blocked by β -lactamase inhibitor, that is, CLV.⁴⁸ PIP is a β -lactam antibiotic with a high activity degree in comparison to other penicillin derivatives. It is a drug with a broad spectrum of action.⁴⁹ These agents (PAS, CLV, and PIP) are generally used in respiratory tract infections that are caused by various microorganisms, which may promote cancer. The drug delivery systems were tested against a human bronchial epithelial (BEAS-2B) to exclude the poisonous effect on normal cell lines. Additionally, these systems were studied in terms of excluding the promotion of cancer cells on a contrary panel of human cancer cell lines, namely adenocarcinoma human alveolar basal epithelial cells (A549) and human non-small cell lung carcinoma cell line (H1299).

The cells confluence was live-observed (from the MTT plates) and expressed as the percentage of the culture covered the bottom of the well (96-well plates) after 72 h of incubation with the compound (LC and its conjugates at a concentration of 100 $\mu\text{g/mL}$, presented as % of control [CTR], Figure 1). It was noticed that the polymer with Cl and CLV counterions caused an increase of the confluence in comparison to untreated CTR of normal and cancer cells. Especially in the case of BEAS-2B (LC: 171%; LC_CLV: 175% of the CTR). The conjugates with PAS⁻ and PIP⁻ induced the decrease of confluence, but these systems provoked a smaller decline in BEAS-2B cells confluence compared to the CTR (~60% decrease) than the cancer cells, where the confluence decreased up to 8%–30% of CTR. Microscopic images of cells treated by tested systems are shown in Figure 2.

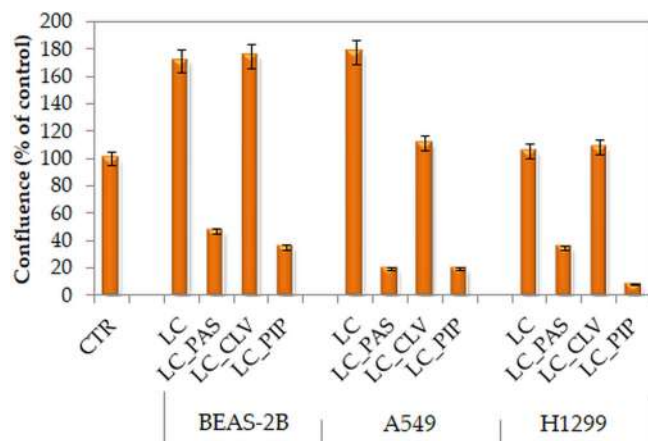


FIGURE 1 The confluence of cells treated for 72 h by chloride based LC or its conjugates at concentration of 100 $\mu\text{g}/\text{mL}$. Results presented as % in comparison to the untreated controls (CTR = 100%) of each cell line.

The colorimetric MTT test was carried out to evaluate the IC_{50} index as the value of a compound concentration corresponding to a 50% of growth inhibition. This parameter was determined only for compounds, for which a linear relationship between cell viability and the concentration was observed. The IC_{50} index was not determined in the case of chloride-based LC, which did not cause the proliferation of 50% of the normal or cancer cells population. However, it was confirmed for the conjugates with PAS, CLV, or PIP, which selectively affected cells (Table 2). In the case of BEAS-2B cells, the IC_{50} index was higher than 100 $\mu\text{g}/\text{mL}$, what means no toxicity at that concentration. A higher concentration of these compounds would have a toxic effect on normal cells, that suggest possible selectivity only against cancer cell line at IC_{50} dose. In turn, these systems have a higher toxic effect on cancerous cells, due to the lower IC_{50} values (49–73 $\mu\text{g}/\text{mL}$). The lowest IC_{50} was detected for LC_CLV in the treatment of A549 and H1299 cell lines, and the LC_PIP treated H1299 cell line, indicating the most toxic effect.

Cell viabilities were achieved at a series of concentrations (3.125–100 $\mu\text{g}/\text{mL}$) of nanocarrier LC and its conjugates with PAS^- , CLV^- , and PIP^- (Figure 3). The drug-free LC showed non-toxic activity against BEAS-2B cell line, where it was noticed, that higher concentration caused a significant increase of cell viability in comparison to the CTR (145% vs. 100%, respectively), and it was smaller at lower concentrations (50–3.125 $\mu\text{g}/\text{mL}$ = 135%–106%). A similar effect was observed in the treatment of A549 and H1299 cell lines by LC, but the cell viability was slightly reduced in comparison to CTR and the lower concentration evoked the cell death pathway (100–3.125 $\mu\text{g}/\text{mL}$ = 116%–96%). The introduction of pharmaceutical anions influenced the opposite cytotoxicity behavior of conjugates, which caused a decrease in BEAS-2B cell viabilities compared to untreated cells, although the toxic impact was not remarked in the lower concentrations (PAS: 53%–101%; CLV: 70%–102%; PIP: 56%–100% for 100–3.125 $\mu\text{g}/\text{mL}$). The conjugate systems, in a comparable way acted on the cancer cell lines, where the highest concentration

triggered the decrease up to 20% of cell viabilities of A549 and H1299, which did not show any significant response on the lowest portion of conjugates maintaining the cytotoxicity level like in CTR.

Further investigations focused on cell death were achieved by flow cytometry, where the Annexin V/PI assay allows distinguishing the variety of cell responses to compound treatment. If the cells survive and stay as living cells, they do not let any of the dyes—Annexin-V (A) or propidium iodide (PI), pass through (A–/PI–). If A or PI are detectable, they indicate through a stage of early (A+/PI–) or late apoptosis (A+/PI+), respectively. If the A is negative, and PI is positive, the cells die by necrosis (A–/PI+). The Annexin V/PI apoptosis assay was carried out by using normal (BEAS-2B) and cancer (A549 and H1299) cells. These lines were treated by the dose (50 $\mu\text{g}/\text{mL}$) of LC or conjugates with pharmaceutical ions, that is, LC_PAS, LC_CLV, and LC_PIP. The effects after treatment are presented on cell population plots in Figure 4.

The treatment of LC did not cause a large difference in comparison to CTR in normal BEAS-2B cells (A–/PI–_{CTR} = 55.6%; A–/PI–_{LC} = 49.5%) (Figure 5A). According to the literature, choline derivatives are characterized by biocompatibility and low cytotoxicity to normal cells.²² In turn, this compound provoked the increase of apoptotic state in cancer cells, thus, the number of viable cells decreased significantly, especially for the A549 cell line, parallel to untreated cells (A549: A–/PI–_{CTR} = 84.9%; A–/PI–_{LC} = 44.3%; H1299: A–/PI–_{CTR} = 80.2%; A–/PI–_{LC} = 65.7%) (Figure 5B,C).

The type of conjugated pharmaceutical anion had a meaningful influence on the type of cell death. LC_PAS adding induced the decrease of BEAS-2B live cells as compared to CTR up to 47% (A–/PI–_{LC_PAS} = 29.4%) (Figure 5A). In the case of tumor cells their decrease was higher, about 65% (A549: A–/PI–_{LC_PAS} = 32.1%; H1299: A–/PI–_{LC_PAS} = 27.4%) (Figure 5B,C). Similarly, LC_PIP activated the decrease in every cell line, but 91% of living H1299 cells died concerning CTR (A–/PI–_{LC_PIP} = 7.1%). Therefore these systems acted selectively on cells, due to the increase in death of cancer cells. LC_CLV system had a toxic activity for both normal and tumor cells, after treatment the cells survived only in 5%–10% (BEAS-2B: A–/PI–_{LC_CLV} = 2.9%; A549: A–/PI–_{LC_CLV} = 9.3%; H1299: A–/PI–_{LC_CLV} = 7.3%) (Figure 5).

Flow cytometry allowed to analyze the cell cycle. One of the dyes used is PI, which penetrates the cell membrane of permeabilized and dying cells and leads to DNA binding by intercalation between complementary bases.⁵⁰ It allows providing a piece of information about the PI reaction with DNA and individual phases of the cycle. The cell cycle goes through four phases, for which results are presented as the following parts: sub-G1, G0-G1, S, and G2/M (Figure 6). These measurements were performed both, on normal and cancer cell lines. The cell lines were treated by drug-free carrier LC or its conjugate systems with antibacterial ionic drugs in the dosage of 50 $\mu\text{g}/\text{mL}$ and incubated for 72 h. Typical cytometric histograms of the cell cycle are presented in Figures S3–S5.

In the case of BEAS-2B, the decrease of sub-G1 phase was observed comparing to the CTR (sub-G1_{CTR}: 57.0% vs. sub-G1_{LC}: 36.9%; sub-G1_{LC_PAS}: 7.5%; sub-G1_{LC_CLV}: 29.8%; sub-G1_{LC_PIP}:

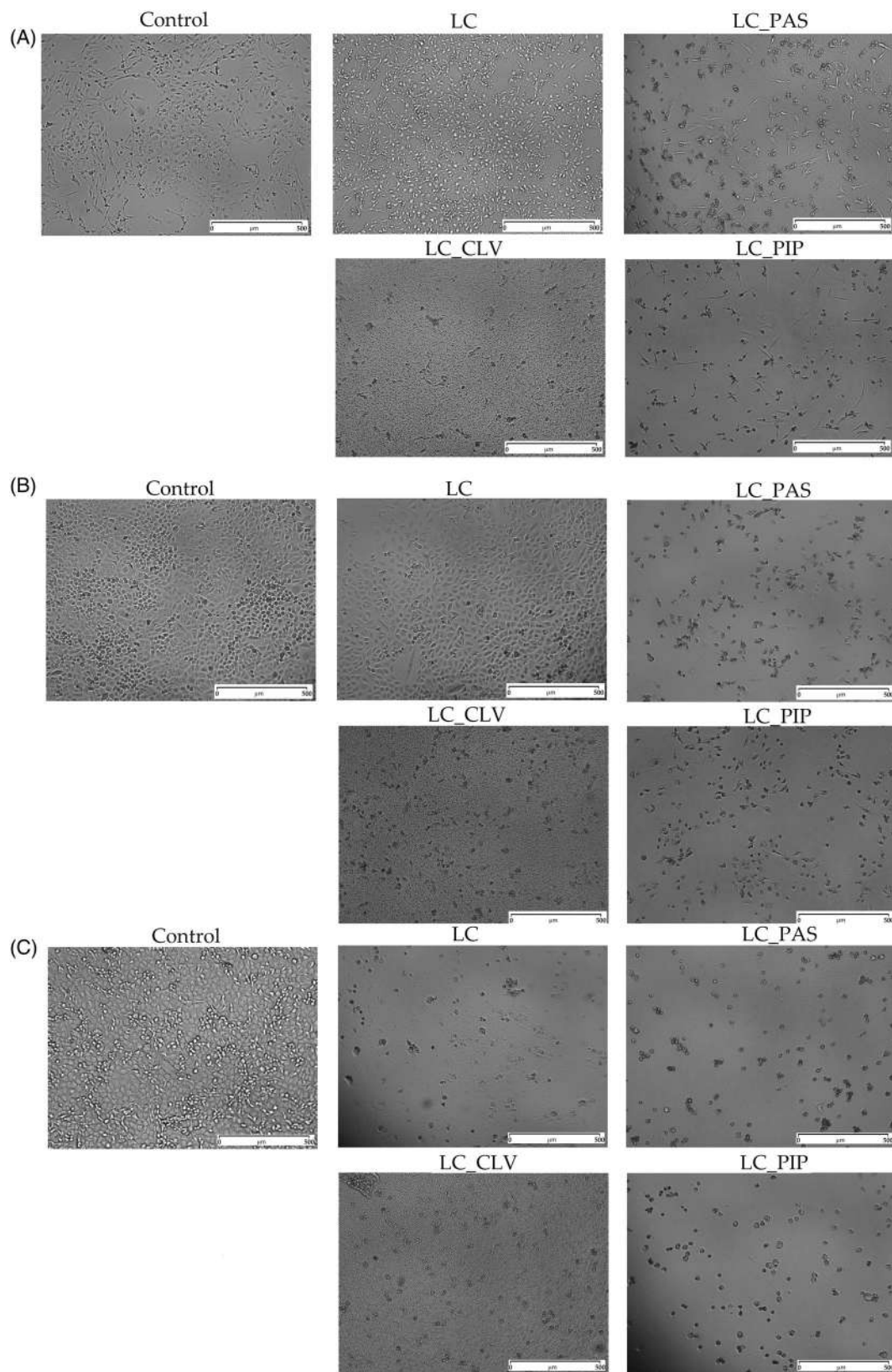


FIGURE 2 Microscopic images by Live Cell Analyzer for untreated control cells versus treated in: (A) BEAS-2B, (B) A549, and (C) H1299 cells by LC and its conjugates at concentration of 50 μg/mL. The scale bar represents 500 μm.

TABLE 2 IC₅₀ parameter for normal and cancer cell lines caused by the action of the linear copolymer and its conjugates.

Compound	IC ₅₀ (μg/mL)		
	Normal cells		Cancer cells
	BEAS-2B	A549	H1299
LC	-	-	-
LC_PAS	>100	69.6	60.7
LC_CLV	>100	57.8	53.2
LC_PIP	>100	73.4	49.2

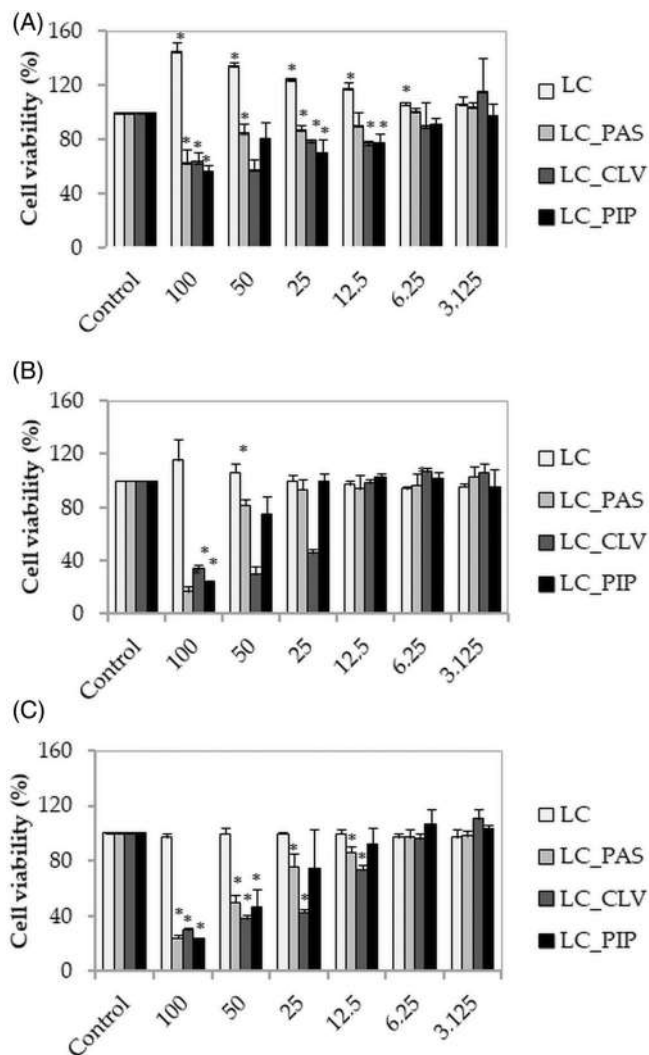


FIGURE 3 Cell viability of chloride based LC and its conjugates with PAS, CLV, and PIP at different concentrations for the treatment of (A) BEAS-2B, (B) A549, and (C) H1299 cell lines, after 72 h of incubation in comparison to the CTR (not treated) cells. Data are presented as mean \pm SD, from three experiments. Statistical significance was calculated with a *t* test and *p* value $<$.05 is indicated with the star.

9.0%). This phase represents the apoptotic state of cells. In the cancer cells, an increase of apoptotic cells was detected after the addition of

polymer systems, especially for the LC_CLV system (A549 sub-G1_{CTR}: 0.7% vs. sub-G1_{LC_CLV}:25.8% and H1299 sub-G1_{CTR}: 7.7% vs. sub-G1_{LC_CLV}: 76.8%), what means lethal effects and visible more dead cells. Significant changes were also noticed in G2/M phase, where the arrest of BEAS-2B cell lines, in comparison to the CTR, was observed (G2/M_{CTR}: 9.1% vs. G2/M_{LC}: 14.9%; G2/M_{LC_PAS}: 45.2%; G2/M_{LC_CLV}: 33.9%; G2/M_{LC_PIP}: 40.1%), whereas in A549 and H1299 the contrary dependency was remarked after drug treatment (A549 G2/M_{CTR}: 55.0% vs. G2/M_{LC}: 31.4%; G2/M_{LC_PAS}: 25.3%; G2/M_{LC_CLV}: 16.8%; G2/M_{LC_PIP}: 32.8%, H1299 G2/M_{CTR}: 32.5% vs. G2/M_{LC_PAS}: 25.9%; G2/M_{LC_CLV}: 4.8%; G2/M_{LC_PIP}: 21.7%). Those findings confirm the cytostatic effects of tested compounds on the G2/M phase of the cell cycle in normal and cancer cells.

Long-term incubation with LC_CLV showed the strongest proapoptotic and lethal effects in normal and cancer cells. The LC, LC_PAS, LC_CLV, and LC_PIP treated cells were also applied for the interleukins gene expression studies. The 72 h long-term treated cells with LC_CLV, responded with the worse condition for a gene of pro-inflammatory cytokines IL6 and IL8 expression evaluation. In normal BEAS-2B cells elevated level of IL6 was observed only after incubation with LC_CLV and LC_PIP, whereas nor LC nor LC_PAS could induce gene expression (Figure 7). The acute and late phase inflammation marker IL6 in BEAS-2B showed on the physiological feature of epithelial cells from the respiratory system—the protection through the inflammation process against damaging agents and pathogens.⁵¹ The IL8 gene expression in BEAS-2B cells was elevated above the control level, but similar for tested copolymers and relatively low (Figure 7).

In cancer A549 and H1299 cells after 72 h of incubation, the marker gene IL6 for the late phase of acute inflammation was not expressed (Figures 8 and 9), similar to the low control level. Although the IL8 gene was activated, the cancer cell lines responded with different elevated expression levels. The A549 cells were more sensitive to stimulation of inflammatory cytokines production observed on the transcriptional level. The expression level in A549 cells after 72 h of incubation with LC resulted in lowered level in comparison to the untreated control, whereas LC_PAS was almost four times higher (Figure 8). The LC_CLV and LC_PIP did not much influence the pro-inflammatory genes expression.

Modification of LC to conjugates with drugs in anionic form (LC_PAS, LC_CLV, and LC_PIP) showed increased potential in inflammatory pathway activation, especially in cancer cells. Both IL6 and IL8 cytokines are important chemokines for TNF α (tumor necrosis factor α) pathway regulation⁵² and tested copolymers overstimulated IL8 expression better than LC in H1299 cells (Figure 9). In the more aggressive type of lung cancers, such as adenocarcinoma H1299, IL8 activation promotes also inflammation burst accelerating cell death (pathway activated also in epithelial cells of the pulmonary system upon viral and microbial pathogen infection).⁵³ Considering possibilities to stimulation of such a mechanism of action, it could be a promising application for copolymers as antimicrobial and anticancer drugs in the future.

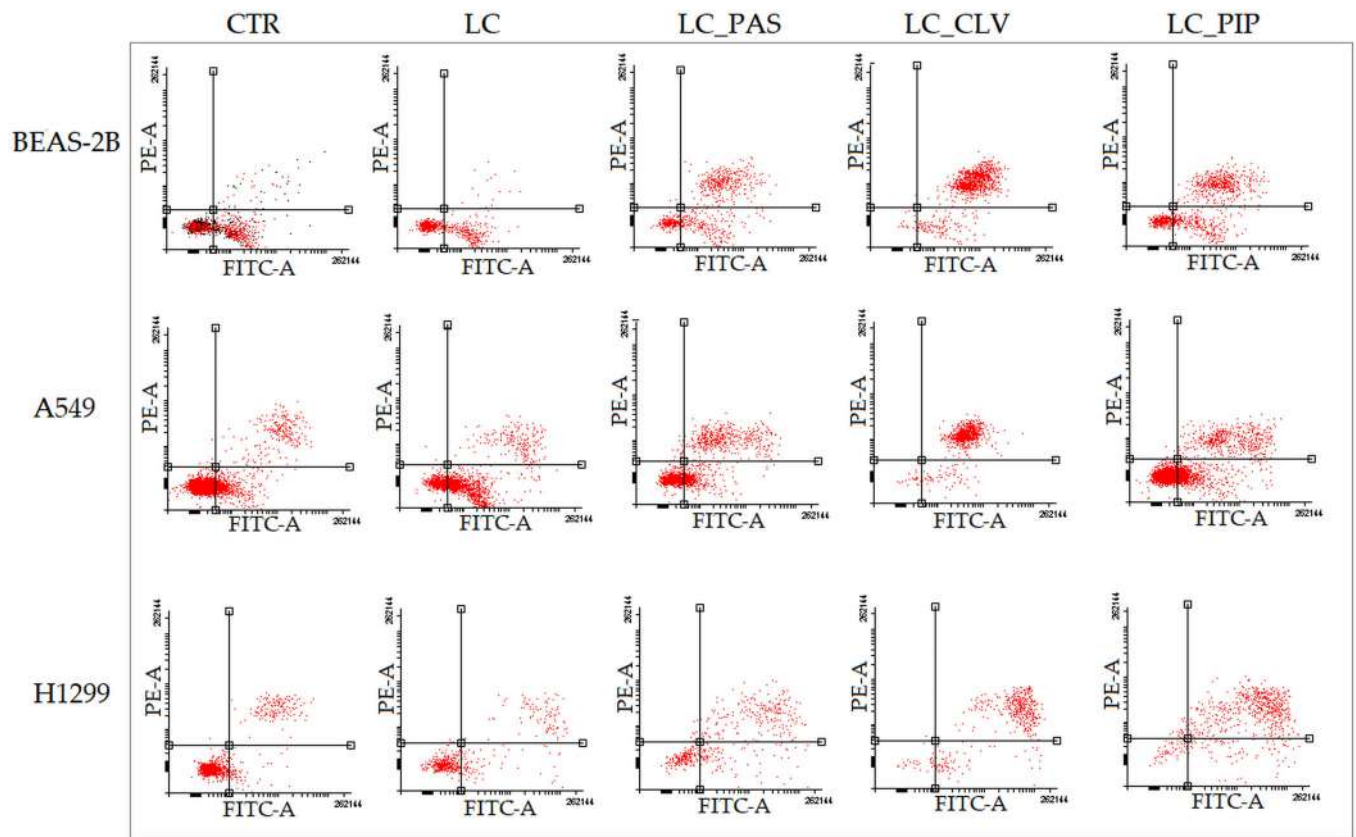


FIGURE 4 Typical dot plots of cell populations after treatment with LC, LC_PAS, LC_CLV, LC_PIP compared to control untreated cells by flow cytometry in BEAS-2B, A549, and H1299 cell lines.

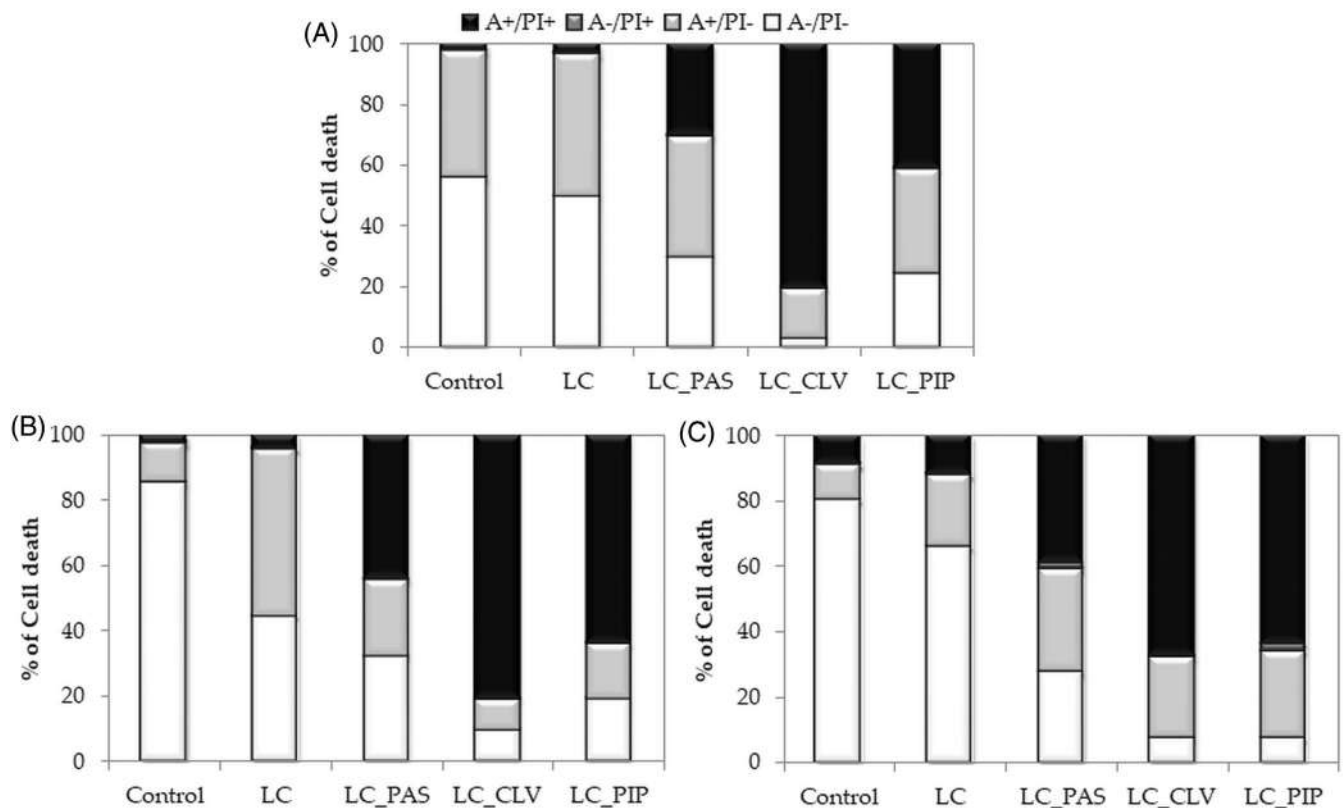


FIGURE 5 Annexin-V apoptosis results for normal (A) BEAS-2B, and cancer (B) A549 and (C) H1299 cell lines after 72 h of incubation.

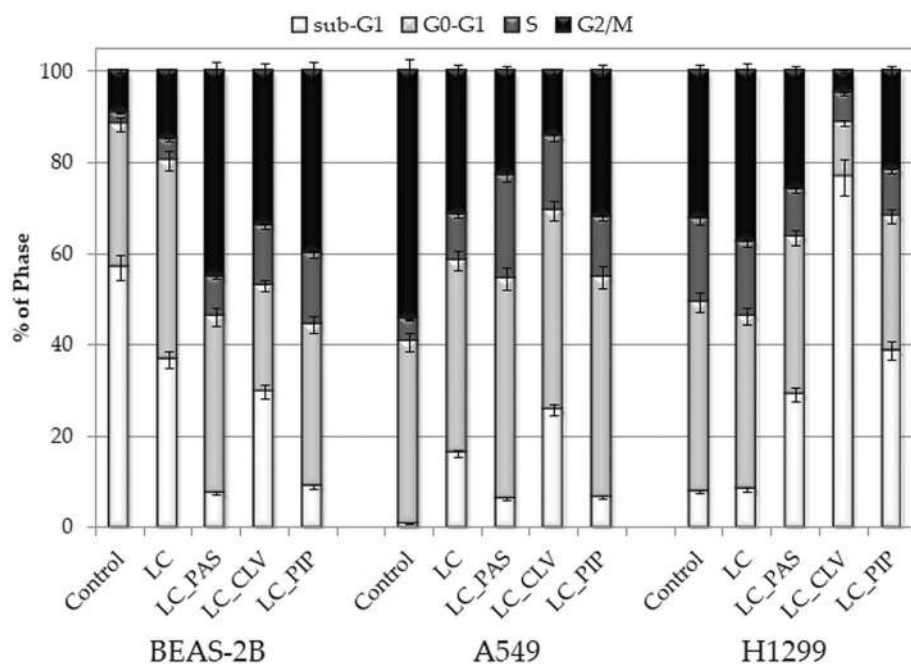


FIGURE 6 Cell cycle analysis of normal BEAS-2B, and tumor A549 and H1299 cell lines treated by carrier LC or its conjugates with PAS⁻, CLV⁻, or PIP⁻. Data are presented as mean \pm SD, from three experiments.

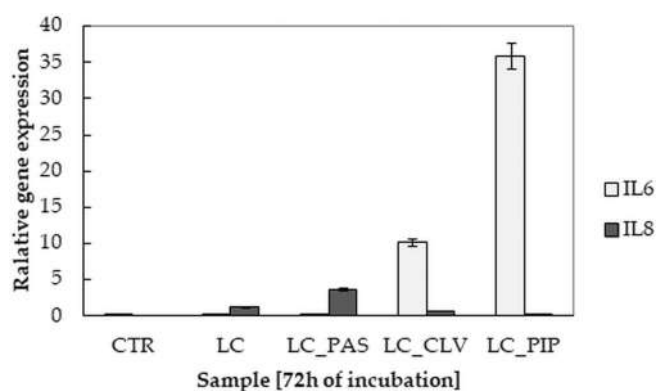


FIGURE 7 Relative gene expression level, for pro-inflammatory IL6 and IL8 cytokines in BEAS-2B cells after 72 h of incubation [$R = 2^{(-\Delta\Delta C_T)}$], results from three repeats with $\pm 5\%$ error bar. Cells were treated with a dose of 0 (CTR) or 50 $\mu\text{g}/\text{mL}$; LC-CLV—not analyzed. Data are presented as mean \pm SD, from three experiments.

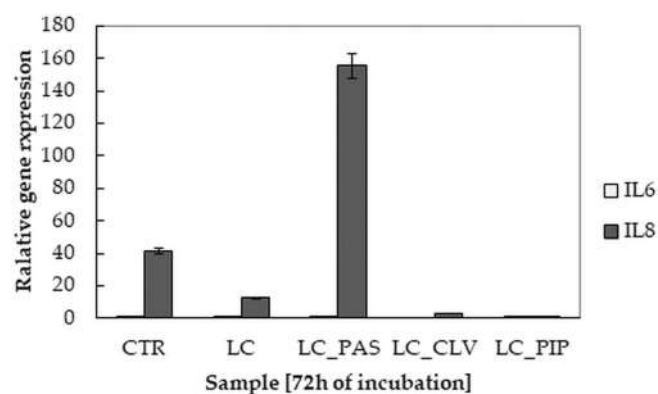


FIGURE 8 Relative gene expression level, for pro-inflammatory IL6 and IL8 cytokines in A549 cells after 72 h of incubation [$R = 2^{(-\Delta\Delta C_T)}$], results from three repeats with $\pm 5\%$ error bar. Cells were treated with a dose of 0 (CTR) or 50 $\mu\text{g}/\text{mL}$; LC-CLV—not analyzed. Data are presented as mean \pm SD, from three experiments.

The interesting conclusions arise from the cytotoxicity assays, where the BEAS-2B bronchial healthy cells presented rather resistant than sensitiveness against tested compounds. Focusing on the IC_{50} values (Table 2), the selectivity of LC derivatives is visible for cancer cells, and concentrations for all compounds (ca. 50 $\mu\text{g}/\text{mL}$) must be lower than used against BEAS-2B (more than 100 $\mu\text{g}/\text{mL}$) to inhibit proliferation or viability of cell lines. Such conclusions are promising, when the obtained results are compared also to the activation of pro-inflammatory genes expression IL6 and IL8 (Figures 7–9). Used gene IL6, known also as markers of proliferation, survival and migration process⁵⁴ are much elevated in healthy bronchial cells, BEAS-2B with even any expression in cancer A549 and H1299 cells (Figures 7–9). On the other side, the expression of pro-inflammatory marker IL8, especially in lung diseases⁵⁵ is

activated after LC derivative addition to the both cancer cell lines (Figures 8 and 9). Reassuring, the side effects after exposition of tested compounds in normal cells were reduced, whereas in cancer cells the selective action against cancer cell lines between A549 and H1299 was confirmed. The mode of action on cells, and cellular uptake of modified LC derivatives seemed to be different, however it need to be studied more carefully. Results from the cytometric analysis of cellular death, suggested of apoptosis induction as a signaling pathway, which was activated after exposition to the compounds (Figure 4). The pro-apoptotic, together with pro-inflammatory action, and microscopically visible cellular death, more advanced in cancer, then in healthy cells (Figure 2) confirmed eligible and anticancer potential of tested compounds.

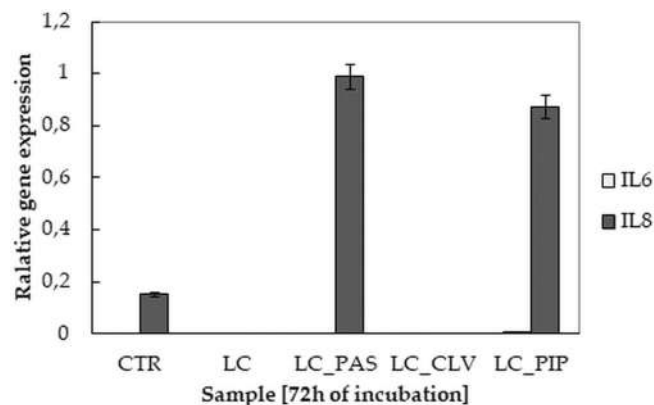


FIGURE 9 Relative gene expression level, for pro-inflammatory IL6 and IL8 cytokines in H1299 cells after 72 h of incubation [$R = 2^{\Delta\Delta C_T}$ ($-\Delta\Delta C_T$)], results from three repeats with $\pm 5\%$ error bar. Cells were treated with a dose of 0 (CTR) or 50 $\mu\text{g}/\text{mL}$; LC-CLV—not analyzed. Data are presented as mean \pm SD, from three experiments.

Similarly to the presented results, the biological research of analogous grafted copolymers, where the side chains composed of P(TMAMA-co-MMA) were transporting *p*-aminosalicylate, clavulanate and piperacillin anions, indicated a strong correlation between biological action and the type of counter anions. Moreover, the selective activity caused a negative effect on the lung tumor cell line, which was opposite action against BEAS-2B cell line.³⁴ Similar TMAMA-based systems bearing salicylate anions showed low toxic or even non-cytotoxic action against human normal cells, mainly Normal Human Dermal Fibroblasts and BEAS-2B cell lines. Moreover, in these studies the carrier biocompatibility was proved, as well as dose-dependent toxicity set the optimistic prognosis for antibacterial action.²⁸

4 | CONCLUSIONS

Cytotoxicity evaluation of nanocarriers based on linear choline based copolymer with chloride counterions (LC) and its ionic conjugates with PAS, CLV, and PIP (LC_PAS, LC_CLV, LC_PIP) as respiratory disease treatment systems, was carried. Due to the purpose of these agents, the studies were conducted against normal BEAS-2B cell lines. However the weakened immune system or often latent, early-stage form of tumor, is the cause of cancer promotion and development, so indifference to the cancer cells or extra antitumor activity of such systems is desirable. Therefore the toxicity against cancer cell lines, that is, A549 and H1299 were also indicated.

Test MTT, cytometric analyses (apoptosis assay and cell cycle analysis), and gene expression measurements for interleukins IL6 and IL8 demonstrated the selective action, wherein the system of LC, and conjugates with PAS and PIP, did not harm BEAS-2B cell line, while they induced the proliferation of cancer cells. The most cytotoxic activity was shown by the LC_CLV system. The result showed the anti-cancer properties of polymer carrier, which confirms the assumed

properties of choline, which derivative is included in the structure of carriers. Due to the biological activity of choline necessary for the functioning of the body, its biocompatibility, low cytotoxicity, and very good solubility in water, these features also characterize the obtained polymers.

The mechanism of action profile toward tested cell lines of investigated macromolecular compounds is desirable. The selective activity offers the possibility of future use of ionic copolymer-based carrier systems as antibacterial/antimicrobial drugs in lung diseases or upper respiratory tract treatment with the co-existing or developing cancer.

AUTHOR CONTRIBUTIONS

Katarzyna Niesyto and Dorota Neugebauer planned and designed the research. Katarzyna Niesyto synthesized copolymers and performed chemical and in vitro studies. Magdalena Skonieczna planned and designed biological evaluation; analyzed and interpreted results of the biological tests. Małgorzata Adamiec-Organisiok performed RT-PCR experiments and data analysis. Katarzyna Niesyto, Magdalena Skonieczna, and Dorota Neugebauer wrote the article. All authors reviewed the manuscript.

ACKNOWLEDGMENTS

This research was funded by the Polish Budget Funds for Scientific Research in 2021 as core funding for R&D activities in the Silesian University of Technology—funding for young scientists, grant no. 04/040/BKM21/0176 (Katarzyna Niesyto), and 02/040/SDU/10-21-01 (Magdalena Skonieczna), and by the National Science Center under the OPUS grant no. 2017/27/B/ST5/00960 (Dorota Neugebauer).

DATA AVAILABILITY STATEMENT

Data available in article supplementary material.

ORCID

Katarzyna Niesyto  <https://orcid.org/0000-0003-0313-9772>

Magdalena Skonieczna  <https://orcid.org/0000-0002-6263-9585>

Małgorzata Adamiec-Organisiok  <https://orcid.org/0000-0003-2403-0485>

Dorota Neugebauer  <https://orcid.org/0000-0002-3802-744X>

REFERENCES

- Larson N, Ghandehari H. Polymeric conjugates for drug delivery. *Chem Mater*. 2012;24:840-853. doi:10.1021/cm2031569
- Ren X, Wang N, Zhou Y, et al. An injectable hydrogel using an immunomodulating gelator for amplified tumor immunotherapy by blocking the arginase pathway. *Acta Biomater*. 2021;124:179-190. doi:10.1016/j.actbio.2021.01.041
- Mielańczyk A, Skonieczna M, Neugebauer D. Cellular response to star-shaped polyacids. Solution behavior and conjugation advantages. *Toxicol Lett*. 2017;274:42-50. doi:10.1016/j.toxlet.2017.03.022
- Mielańczyk A, Skonieczna M, Mielańczyk Ł, Neugebauer D. In vitro evaluation of doxorubicin conjugates based on sugar core nonlinear polymethacrylates toward anticancer drug delivery. *Bioconjug Chem*. 2016;27:893-904. doi:10.1021/acs.bioconjchem.5b00671

5. Diaz AF, Kanazawa KK, Gardini GP. Electrochemical polymerization of pyrrole. *J Chem Soc Chem Commun.* 1979;14:635-636. doi:10.1039/C39790000635
6. Yamaguchi I, Matsumoto Y, Miyoshi K, Wang A. Synthesis, properties and graft polymerization of ionic conjugated polymers with TCNQ anion radical. *Polymer.* 2021;219:123552. doi:10.1016/j.polymer.2021.123552
7. Pernak J, Czepukowicz A, Poźniak R. New ionic liquids and their anti-electrostatic properties. *Ind Eng Chem Res.* 2001;40:2379-2383. doi:10.1021/ie000689g
8. Smiglak M, Metlen A, Rogers RD. The second evolution of ionic liquids: from solvents and separations to advanced materials—energetic examples from the ionic liquid cookbook. *Acc Chem Res.* 2007;40:1182-1192. doi:10.1021/ar7001304
9. Gal Y, Jin S, Park J, et al. Synthesis and electro-optical properties of an ionic conjugated polymer: poly[N-(6-azidoethyl)-2-ethynylpyridinium iodide]. *Curr Appl Phys.* 2007;7:517-521. doi:10.1016/j.cap.2006.10.009
10. Pernak J, Syguda A, Janiszewska D, Materna K, Praczyk T. Ionic liquids with herbicidal anions. *Tetrahedron.* 2011;67:4838-4844. doi:10.1016/j.tet.2011.05.016
11. Mamontova N, Chernyak E, Gatilov Y, et al. First ionic conjugates of dihydroquercetin monosuccinate with amines. *Chem Nat Compd.* 2017;53:1045-1051. doi:10.1007/s10600-017-2198-6
12. Lebedyeva I, Oliferenko A, Oliferenko P, et al. Ionic conjugates of lidocaine and sweeteners as better tasting local anesthetics for dentistry. *J Mater Chem B.* 2015;3:8492-8498. doi:10.1039/C5TB00674K
13. Halayqa M, Zawadzki M, Domańska U, Plichta A. Polymer – Ionic liquid – Pharmaceutical conjugates as drug delivery systems. *J Mol Struct.* 2019;1180:573-584. doi:10.1016/j.molstruc.2018.12.023
14. Egorova KS, Gordeev EG, Ananikov VP. Biological activity of ionic liquids and their application in pharmaceuticals and medicine. *Chem Rev.* 2017;117:7132-7189. doi:10.1021/acs.chemrev.6b00562
15. Pedro SN, Freire CSR, Silvestre AJD, Freire MG. The role of ionic liquids in the pharmaceutical field: an overview of relevant applications. *Int J Mol Sci.* 2020;21:8298. doi:10.3390/ijms21218298
16. Stoimenovski J, MacFarlane DR, Bica K, Rogers RD. Crystalline vs ionic liquid salt forms of active pharmaceutical ingredients: a position paper. *Pharm Res.* 2010;27:521-526. doi:10.1007/s11095-009-0030-0
17. Ferraz R, Costa-Rodrigues J, Fernandes M, et al. Antitumor activity of ionic liquids based on ampicillin. *ChemMedChem.* 2015;10:1480-1483. doi:10.1002/cmcd.201500142
18. de Almeida TS, Julio A, Saraiva N, et al. Choline- versus imidazole-based ionic liquids as functional ingredients in topical delivery systems: cytotoxicity, solubility, and skin permeation studies. *Drug Dev Ind Pharm.* 2017;43:1858-1865. doi:10.1080/03639045.2017.1349788
19. Fujita K, MacFarlane DR, Forsyth M. Protein solubilising and stabilising ionic liquids. *Chem Commun.* 2005;38:4804-4806. doi:10.1039/B508238B
20. Noshadi I, Walker B, Portillo-Lara R, et al. Engineering biodegradable and biocompatible bio-ionic liquid conjugated hydrogels with tunable conductivity and mechanical properties. *Sci Rep.* 2017;7:4345. doi:10.1038/s41598-017-04280-w
21. Petkovic M, Ferguson JL, Gunaratne HQN, et al. Novel biocompatible cholinium-based ionic liquids—toxicity and biodegradability. *Green Chem.* 2010;12:643-649. doi:10.1039/B922247B
22. Hosseinzadeh F, Mahkam M, Galehassadi M. Synthesis and characterization of ionic liquid functionalized polymers for drug delivery of an anti-inflammatory drug. *Des Monomers Polym.* 2012;15:379-388. doi:10.1080/1385772X.2012.686689
23. Gorbunova M, Lemkina L, Borisova I. New guanidine-containing polyelectrolytes as advanced antibacterial materials. *Eur Polym J.* 2018;105:426-433. doi:10.1016/j.eurpolymj.2018.06.014
24. Haladjova E, Mountrichas G, Pispas S, Rangelov S. Poly(vinyl benzyl trimethylammonium chloride) homo and block copolymers complexation with DNA. *J Phys Chem B.* 2016;120:2586-2595. doi:10.1021/acs.jpcc.5b12477
25. Bielas R, Łukowiec D, Neugebauer D. Drug delivery via anion exchange of salicylate decorating poly(meth)acrylates based on a pharmaceutical ionic liquid. *New J Chem.* 2017;41:12801-12807. doi:10.1039/C7NJ02667F
26. Bielas R, Siewniak A, Skonieczna M, Adamiec M, Mielańczyk Ł, Neugebauer D. Choline based polymethacrylate matrix with pharmaceutical cations as co-delivery system for antibacterial and anti-inflammatory combined therapy. *J Mol Liq.* 2019;285:114-122. doi:10.1016/j.molliq.2019.04.082
27. Mecerreyes D. Polymeric ionic liquids: broadening the properties and applications of polyelectrolytes. *Prog Polym Sci.* 2011;36(12):1629-1648. doi:10.1016/j.progpolymsci.2011.05.007
28. Bielas R, Mielańczyk A, Skonieczna M, Mielańczyk Ł, Neugebauer D. Choline supported poly(ionic liquid) graft copolymers as novel delivery systems of anionic pharmaceuticals for anti-inflammatory and anti-coagulant therapy. *Sci Rep.* 2019;9:14410. doi:10.1038/s41598-019-50896-5
29. Niesyto K, Neugebauer D. Synthesis and characterization of ionic graft copolymers: introduction and in vitro release of antibacterial drug by anion exchange. *Polymers.* 2020;12:2159. doi:10.3390/polym12092159
30. Shephard RJ, Shek PN. Associations between physical activity and susceptibility to cancer: possible mechanisms. *Sports Med.* 1998;26:293-315. doi:10.2165/00007256-199826050-00002
31. Hakim FT, Flomerfelt FA, Boyiadzis M, Gress RE. Aging, immunity and cancer. *Curr Opin Immunol.* 2004;16:151-156. doi:10.1016/j.coi.2004.01.009
32. Derhovanessian E, Solana R, Larbi A, Pawelec G. Immunity, ageing and cancer. *Immun Ageing.* 2008;5:11. doi:10.1186/1742-4933-5-11
33. Lu B, Yi M, Hu S, et al. Taurine-based ionic liquids for transdermal protein delivery and enhanced anticancer activity. *ACS Sustain Chem Eng.* 2021;9:5991-6000. doi:10.1021/acssuschemeng.1c01064
34. Niesyto K, Łyżniak W, Skonieczna M, Neugebauer D. Biological in vitro evaluation of PIL graft conjugates: cytotoxicity characteristics. *Int J Mol Sci.* 2021;22:7741. doi:10.3390/ijms22147741
35. Qi X, Li J, Wei W, et al. Cationic Saiecan-based hydrogels for release of 5-fluorouracil. *RSC Adv.* 2017;7(24):14337-14347. doi:10.1039/C7RA01052D
36. Komatsu Y, Yoshitomi T, Furuya K, et al. Long-term fluorescent tissue marking using tissue-adhesive porphyrin with polycations consisting of quaternary ammonium salt groups. *Int J Mol Sci.* 2022;23(8):4218. doi:10.3390/ijms23084218
37. Singh B, Sharma V, Kumar R, Mohan M. Development of dietary fiber psyllium based hydrogel for use in drug delivery applications. *Food Hydrocoll Health.* 2022;2:100059. doi:10.1016/j.fhfh.2022.100059
38. Niesyto K, Neugebauer D. Linear copolymers based on choline ionic liquid carrying anti-tuberculosis drugs: influence of anion type on physicochemical properties and drug release. *Int J Mol Sci.* 2021;22:284. doi:10.3390/ijms22010284
39. Altmann S, Choroba K, Skonieczna M, et al. Platinum(II) coordination compounds with 4'-pyridyl functionalized 2,2':6',2''-terpyridines as an alternative to enhanced chemotherapy efficacy and reduced side-effects. *J Inorg Biochem.* 2019;201:110809. doi:10.1016/j.jinorgbio.2019.110809
40. Livak KJ, Schmittgen TD. Analysis of relative gene expression data using real-time quantitative PCR and the 2(-Delta Delta C(T)) method. *Methods.* 2001;25:402-408. doi:10.1006/meth.2001.1262

41. Awwad HM, Geisel J, Obeid R. The role of choline in prostate cancer. *Clin Biochem.* 2012;45(18):1548-1553. doi:[10.1016/j.clinbiochem.2012.08.012](https://doi.org/10.1016/j.clinbiochem.2012.08.012)
42. Zeisel SH, da Costa K-A. Choline: an essential nutrient for public health. *Nutr Rev.* 2009;67(11):615-623. doi:[10.1111/j.1753-4887.2009.00246.x](https://doi.org/10.1111/j.1753-4887.2009.00246.x)
43. Detopoulou P, Panagiotakos DB, Antonopoulou S, Pitsavos C, Stefanadis C. Dietary choline and betaine intakes in relation to concentrations of inflammatory markers in healthy adults: the ATTICA study. *Am J Clin Nutr.* 2008;87(2):424-430. doi:[10.1093/ajcn/87.2.424](https://doi.org/10.1093/ajcn/87.2.424)
44. Jonge WJ, Ulloa L. The alpha7 nicotinic acetylcholine receptor as a pharmacological target for inflammation. *Br J Pharmacol.* 2009;151(7):915-929. doi:[10.1038/sj.bjp.0707264](https://doi.org/10.1038/sj.bjp.0707264)
45. Xu X, Gammon MD, Zeisel SH, et al. Choline metabolism and risk of breast cancer in a population-based study. *FASEB J.* 2008;22(6):2045-2052. doi:[10.1096/fj.07-101279](https://doi.org/10.1096/fj.07-101279)
46. Glunde K, Jacobs MA, Bhujwalla ZM. Choline metabolism in cancer: implications for diagnosis and therapy. *Expert Rev Mol Diagn.* 2006;6(6):821-829. doi:[10.1586/14737159.6.6.821](https://doi.org/10.1586/14737159.6.6.821)
47. Ratledge C. Iron, mycobacteria and tuberculosis. *Tuberculosis (Edinb).* 2004;84:110-130. doi:[10.1016/j.tube.2003.08.012](https://doi.org/10.1016/j.tube.2003.08.012)
48. Cole M. Biochemistry and action of clavulanic acid. *Scott Med J.* 1982;27:10-16. doi:[10.1177/003693308202705103](https://doi.org/10.1177/003693308202705103)
49. Fortner CL, Finley RS, Schimpff SC. Piperacillin sodium: antibacterial spectrum, pharmacokinetics, clinical efficacy, and adverse reactions. *Pharmacotherapy.* 1982;2:287-299. doi:[10.1002/j.1875-9114.1982.tb03202.x](https://doi.org/10.1002/j.1875-9114.1982.tb03202.x)
50. Ormerod MG. Investigating the relationship between the cell cycle and apoptosis using flow cytometry. *J Immunol Methods.* 2002;265:73-80. doi:[10.1016/s0022-1759\(02\)00071-6](https://doi.org/10.1016/s0022-1759(02)00071-6)
51. Turner MD, Nedjai B, Hurst T, Pennington DJ. Cytokines and chemokines: at the crossroads of cell signalling and inflammatory disease. *Biochim Biophys Acta.* 1843;2014:2563-2582. doi:[10.1016/j.bbamcr.2014.05.014](https://doi.org/10.1016/j.bbamcr.2014.05.014)
52. Arnold R, König B, Galatti H, Werchau H, König W. Cytokine (IL-8, IL-6, TNF-alpha) and soluble TNF receptor-I release from human peripheral blood mononuclear cells after respiratory syncytial virus infection. *Immunology.* 1995;85(3):364-372.
53. Krupa A, Fol M, Dziadek B, et al. Binding of CXCL8/IL-8 to mycobacterium tuberculosis modulates the innate immune response. *Mediators Inflamm.* 2015;2015:124762. doi:[10.1155/2015/124762](https://doi.org/10.1155/2015/124762)
54. Srivastava A, Sharma H, Khanna S, et al. Interleukin-6 induced proliferation is attenuated by transforming growth factor-beta-induced signaling in human hepatocellular carcinoma cells. *Front Oncol.* 2022;11:811941. doi:[10.3389/fonc.2021.811941](https://doi.org/10.3389/fonc.2021.811941)
55. Goodman ER, Kleinstein E, Fusco AM, et al. Role of interleukin 8 in the genesis of acute respiratory distress syndrome through an effect on neutrophil apoptosis. *Arch Surg.* 1998;133(11):1234-1239. doi:[10.1001/archsurg.133.11.1234](https://doi.org/10.1001/archsurg.133.11.1234)

SUPPORTING INFORMATION

Additional supporting information can be found online in the Supporting Information section at the end of this article.

How to cite this article: Niesyto K, Skonieczna M, Adamiec-Organieciok M, Neugebauer D. Toxicity evaluation of choline ionic liquid-based nanocarriers of pharmaceutical agents for lung treatment. *J Biomed Mater Res.* 2023;111(7):1374-1385. doi:[10.1002/jbm.b.35241](https://doi.org/10.1002/jbm.b.35241)

Toxicity evaluation of choline ionic liquid-based nanocarriers of pharmaceutical agents for lung treatment

Katarzyna Niesyto¹, Magdalena Skonieczna^{*2,3}, Małgorzata Adamiec-Organiściok^{2,3}, Dorota Neugebauer^{*1}

¹ Department of Physical Chemistry and Technology of Polymers, Faculty of Chemistry, Silesian University of Technology, Strzody 9, 44-100, Gliwice, Poland

² Department of Systems Biology and Engineering, Faculty of Automatic Control, Electronics and Computer Science, Silesian University of Technology, 44-100 Gliwice, Poland

³ Biotechnology Centre, Silesian University of Technology, Krzywoustego 8, 44-100 Gliwice, Poland

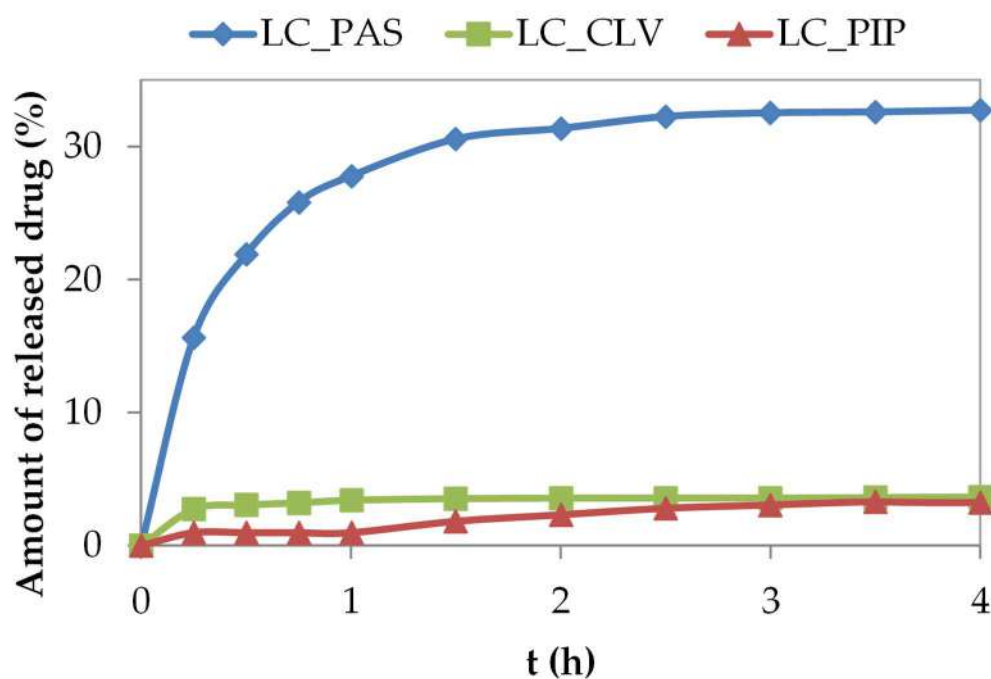


Figure S1. Kinetic profiles of drug release from TMAMA based LC via dialysis in PBS (pH = 7.4 in 37 °C) according to the data in ref. *Int. J. Mol. Sci.* 2021, 22: 284, DOI: 10.3390/ijms22010284.

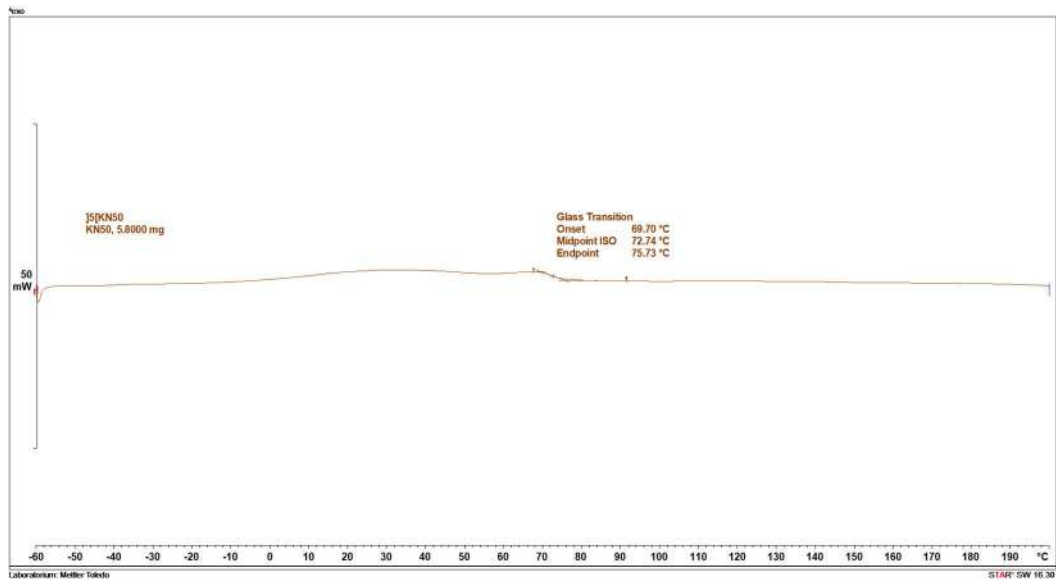


Figure S2. DSC termogram of LC.

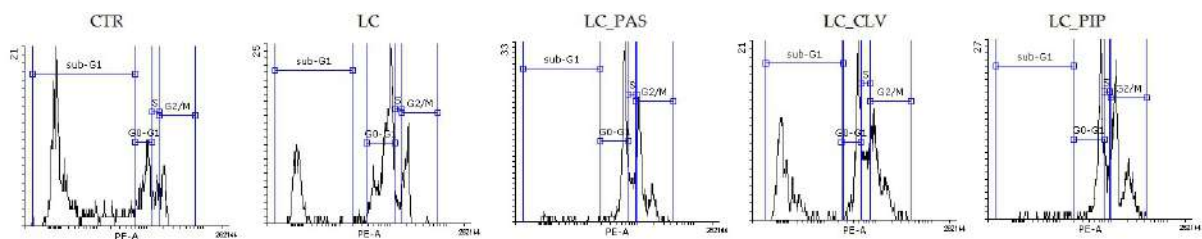


Figure S3. Representative flow cytometry histograms of cell cycle analysis of BEAS-2B cells after incubation with carrier LC or its conjugates with PAS⁻, CLV⁻ or PIP⁻.

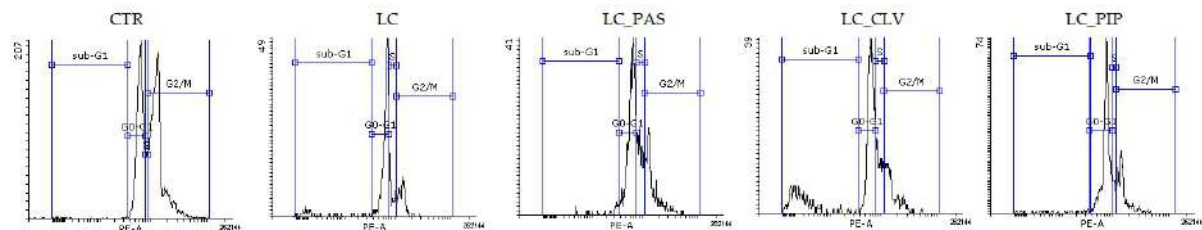


Figure S4. Representative flow cytometry histograms of cell cycle analysis of A549 cells after incubation with carrier LC or its conjugates with PAS⁻, CLV⁻ or PIP⁻.

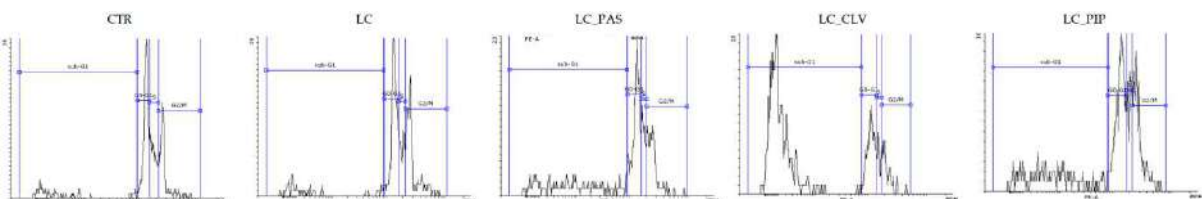



Figure S5. Representative flow cytometry histograms of cell cycle analysis of H1299 cells after incubation with carrier LC or its conjugates with PAS⁻, CLV⁻ or PIP⁻.

Oświadczenie współautorów publikacji

Niniejszym podaję procentowy wkład autorski w publikację pt.

Niesyto Katarzyna, Neugebauer Dorota; Synthesis and Characterization of Ionic Graft Copolymers: Introduction and In Vitro Release of Antibacterial Drug by Anion Exchange; Polymers; 2020; 12; 2159

(dane bibliograficzne publikacji)



Imię i nazwisko współautora	Procentowy wkład autorski	Data i podpis współautora
Niesyto Katarzyna	50%	16.05.2024 Niesyto
Neugebauer Dorota	50%	

Oświadczenie współautorów publikacji

Niniejszym podaję procentowy wkład autorski w publikację pt.

Niesyto Katarzyna, Neugebauer Dorota; Linear Copolymers Based on Choline Ionic Liquid Carrying Anti-Tuberculosis Drugs: Influence of Anion Type on Physicochemical Properties and Drug Release; International Journal of Molecular Sciences; 2021, 22, 284

(dane bibliograficzne publikacji)

Imię i nazwisko współautora	Procentowy wkład autorski	Data i podpis współautora
Niesyto Katarzyna	60%	16.05.2024 
Neugebauer Dorota	40%	

Oświadczenie współautorów publikacji

Niniejszym podaję procentowy wkład autorski w publikację pt.

Niesyto Katarzyna, Mazur Aleksy, Neugebauer Dorota; Dual-Drug Delivery via the Self-Assembled Conjugates of Choline-Functionalized Graft Copolymers; Materials; 2022, 15, 4457

(dane bibliograficzne publikacji)

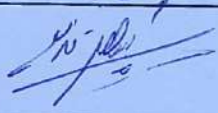


Imię i nazwisko współautora	Procentowy wkład autorski	Data i podpis współautora
Katarzyna Niesyto	40%	16.05.2024 niesyto
Aleksy Mazur	25%	Mazur
Dorota Neugebauer	35%	DN

Oświadczenie współautorów publikacji

Niniejszym podaję procentowy wkład autorski w publikację pt.

Niesyto Katarzyna, Keihankhadiv Shadi, Mazur Aleksy, Mielańczyk Anna, Neugebauer Dorota; Ionic Liquid-based Polymer Matrices for Single and Dual Drug Delivery: Impact of Structural Topology on Characteristics and In Vitro Delivery Efficiency; International Journal of Molecular Sciences; 2024, 25, 1292

(dane bibliograficzne publikacji)

Imię i nazwisko współautora	Procentowy wkład autorski	Data i podpis współautora
Katarzyna Niesyto	25%	16.05.2024 Cheryto
Shadi Keihankhadiv	20%	
Aleksy Mazur	20%	Mazur
Mielańczyk Anna	15%	
Dorota Neugebauer	20%	

Oświadczenie współautorów publikacji

Niniejszym podaję procentowy wkład autorski w publikację pt.

Niesyto Katarzyna, Mazur Aleksy, Neugebauer Dorota; Piperacillin/Tazobactam co-delivery by micellar ionic conjugate systems carrying pharmaceutical anions and encapsulated drug; *Pharmaceutics*; 2024, 16, 198

(dane bibliograficzne publikacji)

Imię i nazwisko współautora	Procentowy wkład autorski	Data i podpis współautora
Katarzyna Niesyto	40%	16.05.2024 Niesyto
Aleksy Mazur	30%	Mazur
Dorota Neugebauer	30%	DN

Oświadczenie współautorów publikacji

Niniejszym podaję procentowy wkład autorski w publikację pt.

Niesyto Katarzyna, Łyżniak Wiktoria, Skonieczna Magdalena, Neugebauer Dorota;
Biological in vitro evaluation of PIL graft conjugates: cytotoxicity characteristics;
International Journal of Molecular Sciences; 2021, 22, 7741

(dane bibliograficzne publikacji)

Imię i nazwisko współautora	Procentowy wkład autorski	Data i podpis współautora
Katarzyna Niesyto	40%	16.05.2024 <i>chnyto</i>
Wiktoria Łyżniak	10%	<i>dieyto</i>
Magdalena Skonieczna	15%	<i>Skonieczna</i>
Dorota Neugebauer	35%	<i>DN</i>

Oświadczenie współautorów publikacji

Niniejszym podaję procentowy wkład autorski w publikację pt.

Niesyto Katarzyna, Skonieczna Magdalena, Adamiec-Organisiok Małgorzata, Neugebauer Dorota; Toxicity evaluation of choline ionic liquid-based nanocarriers of pharmaceutical agents for lung treatment; Journal of Biomedical Materials Research Part B - Applied Biomaterials; 2023, 7, 1374-1385

(dane bibliograficzne publikacji)

Imię i nazwisko współautora	Procentowy wkład autorski	Data i podpis współautora
Katarzyna Niesyto	35%	16.05.2024 chwysto
Magdalena Skonieczna	15%	Phomin
Małgorzata Adamiec-Organisiok	15%	Adamiec-Organisiok
Dorota Neugebauer	35%	DN



Politechnika
Śląska



UCZELNIA
BADAWCZA
NCJATWA KOSZYKAŁECIO

Wydział Chemiczny
Katedra Fizykochemii i Technologii Polimerów

prof. dr hab. inż.
Dorota NEUGEBAUER

Gliwice, 06.05.2024 r.

Opinia

Pani mgr inż. Katarzyna Niesyto od października 2019 r. realizowała tematykę badawczą pod moim kierunkiem w ramach doktoratu. Wykonane badania mają charakter nowatorski, obejmują syntezę dobrze zdefiniowanych polimerów szczepionych i liniowych zawierających jednostki cholinowe jako nośników związków biologicznie aktywnych ukierunkowanych na działanie przeciwbakteryjne, a w szczególności o aktywności przeciwgruźliczej. Zastosowanie strategii wymiany jonowej umożliwiła wprowadzanie anionów farmaceutycznych i otrzymanie koniugatów jonowych polimer-lek, których właściwości mogą być regulowane poprzez parametry strukturalne nośnika polimerowego. Z kolei amfifilowy charakter polimerów pozwolił na wykorzystanie strategii enkapsulacji leku niejonowego i otrzymanie układów z dwoma lekami. Oprócz charakterystyki fizykochemicznej otrzymane układy polimerowe badano także pod kątem zdolności uwalniania leków i aktywności biologicznej, tj. cytotoksyczności. Tematyka ta wpisuje się w zakres zagadnień POB1.6 „Analiza i projektowanie leków” i POB3.4 „Nowoczesne materiały do zastosowań w medycynie” w ramach dyscypliny nauki chemiczne.

Na podstawie wykonanej pracy doświadczalnej popartej dorobkiem naukowym Doktorantka przygotowała rozprawę doktorską pt: „Zaprojektowanie szczepionych poli(cieczy jonowych) jako potencjalnych układów dostarczania leków w terapii przeciwbakteryjnej” w formie przewodnika po monotematycznym cyklu 7 publikacji. Natomiast, całkowity dorobek Doktorantki obejmuje 12 artykułów punktowanych, w tym 6 za 140 pkt oraz zgłoszenia patentowe i materiały w konferencjach naukowych. Dodatkowo była głównym wykonawcą projektu OPUS14 „Systemy współdostarczania leków na bazie jonowych polimerów szczepionych transportujących aniony farmaceutyczne o działaniu przeciwbakteryjnym do zastosowań w terapii skojarzonej” oraz sprawowała opiekę nad dyplomantami i studentami z Koła Naukowego.

Współpracę z Panią mgr Niesyto i efekty Jej pracy oceniam bardzo dobrze, w związku z czym rekomenduję wszczęcie postępowania doktorskiego.

Politechnika Śląska
Wydział Chemiczny
Biuro Dziekana

ul. Strzody 9, pok. 6, 44-100 Gliwice
+48 32 237 15 49
Krzysztof.Walczak@polsl.pl

NIP 631 020 07 36
ING Bank Śląski S.A. o/Gliwice 60 1050 1230 1000 0002 0211 3056



HR EXCELLENCE IN RESEARCH

75 lat
POLITECHNIKI
ŚLĄSKIEJ



WYKAZ DOROBKU NAUKOWEGO KANDYDATA DO STOPNIA DOKTORA

Katarzyna Niesyto.....
(imię i nazwisko kandydata)

Gliwice, 06.05.2024.....
(miejsce, data)

<https://orcid.org/0000-0003-0313-9772>
(nr ORCID)

Ul. Złoty Łan 13

43-220 Świerczyniec

(adres do korespondencji)

796872015; katarzyna.niesyto@polsl.pl
(nr telefonu i adres e-mail)

I. Artykuły naukowe opublikowane w czasopiśmie naukowym, które w roku opublikowania artykułu w ostatecznej formie było ujęte w ministerialnym wykazie czasopism naukowych i recenzowanych materiałów z konferencji międzynarodowych

Autor/autorzy; tytuł pracy; nazwa czasopisma; rok wydania; tom; strony od-do; punktacja MEiN, IF.

1. Neugebauer Dorota, Mielańczyk Anna, Bielas Rafał, Odrobińska Justyna, Kupczak Maria, Niesyto Katarzyna; Ionic polymethacrylate based delivery systems: effect of carrier topology and drug loading; *Pharmaceutics*; 2019, 11(7), 337-353; MEiN = 100 pkt; IF₂₀₁₉ = 4.773
2. Odrobińska Justyna, Niesyto Katarzyna, Erfurt Karol, Siewniak Agnieszka, Mielańczyk Anna, Neugebauer Dorota; Retinol-containing graft copolymers for delivery of skin-curing agents; *Pharmaceutics*; 2019, 11(8), 378-394; MEiN = 100 pkt; IF₂₀₁₉ = 4.773
3. Niesyto Katarzyna, Neugebauer Dorota; Synthesis and Characterization of Ionic Graft Copolymers: Introduction and In Vitro Release of Antibacterial Drug by Anion Exchange; *Polymers*; 2020, 12, 2159-2172; MEiN = 100 pkt; IF₂₀₂₀ = 4.329
4. Niesyto Katarzyna, Neugebauer Dorota; Linear Copolymers Based on Choline Ionic Liquid Carrying Anti-Tuberculosis Drugs: Influence of Anion Type on Physicochemical Properties and Drug Release; *International Journal of Molecular Sciences*; 2021, 22, 284-300; MEiN = 140 pkt; IF₂₀₂₁ = 6.208
5. Niesyto Katarzyna, Łyżniak Wiktoria, Skonieczna Magdalena, Neugebauer Dorota; Biological in vitro evaluation of PIL graft conjugates: cytotoxicity characteristics; *International Journal of Molecular Sciences*; 2021, 22, 7741-7753; MEiN = 140 pkt; IF₂₀₂₁ = 6.208
6. Niesyto Katarzyna, Mazur Aleksy, Neugebauer Dorota; Dual-Drug Delivery via the Self-Assembled Conjugates of Choline-Functionalized Graft Copolymers; *Materials*; 2022, 15, 4457-4468; MEiN = 140 pkt; IF₂₀₂₂ = 3.4
7. Mazur Aleksy, Niesyto Katarzyna, Neugebauer, Dorota; Pharmaceutical Functionalization of Monomeric Ionic Liquid for the Preparation of Ionic Graft Polymer Conjugates; *International Journal of Molecular Sciences*; 2022, 23, 14731-14745. MEiN = 140 pkt; IF₂₀₂₂ = 5.6
8. Niesyto Katarzyna, Skonieczna Magdalena, Adamiec-Organisćciok Małgorzata, Neugebauer Dorota; Toxicity evaluation of choline ionic liquid-based nanocarriers of pharmaceutical agents for lung treatment; *Journal of Biomedical Materials Research Part B - Applied Biomaterials*; 2023, 111(7), 1374-1385; MEiN = 140 pkt; IF₂₀₂₂ = 3.4
9. Niesyto Katarzyna, Keihankhadi Shadi, Mazur Aleksy, Mielańczyk Anna, Neugebauer Dorota; Ionic Liquid-based Polymer Matrices for Single and Dual Drug Delivery: Impact of Structural Topology on Characteristics and In Vitro Delivery Efficiency; *International Journal of Molecular Sciences*; 2024, 25, 1292-1310; MEiN=140 pkt; IF₂₀₂₂ = 5.6

10. Niesyto Katarzyna, Mazur Aleksy, Neugebauer Dorota; Piperacillin/Tazobactam co-delivery by micellar ionic conjugate systems carrying pharmaceutical anions and encapsulated drug; *Pharmaceutics*; 2024, 16, 198-211; MEiN = 100 pkt; IF₂₀₂₂ = 5.4

II. Publikacje w recenzowanych materiałach z międzynarodowych konferencji naukowych, które w roku opublikowania artykułu w ostatecznej formie były ujęte w ministerialnym wykazie czasopism naukowych i recenzowanych materiałów z konferencji naukowych

Autor/autorzy; tytuł pracy; nazwa konferencji; miejsce; rok; źródło publikacji; strony od-do.

1.
2.

III. Monografie naukowe wydane przez wydawnictwo, które w roku opublikowania monografii w ostatecznej formie było ujęte w ministerialnym wykazie wydawnictw

Autor/autorzy; tytuł książki; nazwa wydawnictwa; rok wydania; liczba stron; nr ISBN.

1.
2.

IV. Rozdziały w monografiach naukowych, które w roku opublikowania w ostatecznej formie były ujęte w ministerialnym wykazie wydawnictw

Autor/autorzy; tytuł rozdziału; redaktor/redaktorzy; tytuł monografii; nazwa wydawnictwa; rok wydania; strony od-do; nr ISBN.

1. Mielańczyk Anna, Odrobińska Justyna, Kupczak Maria, Niesyto Katarzyna, Neugebauer Dorota; Projektowanie innowacyjnych nanonośników polimerowych do transportu związków bioaktywnych; *Data Przemysław, Janas Dawid; Materiały przyszłości; Wydawnictwo Politechniki Śląskiej*; 2023; 125-130; ISBN 978-83-7880-932-6.....
2.

.....
(podpis kandydata)

**Oświadczenie o przebiegu wcześniejszego przewodu doktorskiego/postępowania
o nadanie stopnia doktora***

Katarzyna Niesyto.....
(imię i nazwisko kandydata)

Gliwice, 06.05.2024.....
(miejscowość, data)

ul. Złoty Łan 13

43-220 Świerczyniec

796872015; katarzyna.niesyto@polsl.pl
(nr telefonu i adres e-mail)

CZĘŚĆ A**

Oświadczam, że wcześniej nie ubiegałam się o wszczęcie przewodu doktorskiego w żadnej jednostce naukowej.

.....
(podpis kandydata)

CZĘŚĆ B**

Oświadczam, że nie zostałam dopuszczona/zostałam dopuszczony* do obrony rozprawy doktorskiej/została mi wydana decyzja o odmowie nadania stopnia doktora* we wcześniejszym postępowaniu/wcześniejszych postępowaniach* o nadanie stopnia doktora w dyscyplinie

W

(nazwa jednostki)

Tytuł rozprawy doktorskiej:

Data wszczęcia przewodu doktorskiego/postępowania o nadanie stopnia doktora*:

Data i nr uchwały o niedopuszczeniu do obrony/data i nr uchwały o odmowie nadania stopnia doktora/data i nr decyzji o odmowie nadania stopnia doktora*:

Przyczyna niedopuszczenia do obrony/odmowy nadania stopnia*:

Oświadczam, że wskazana rozprawa doktorska/wskazane rozprawy doktorskie*, wobec której/których* podjęto ww. uchwałę/uchwały/decyzję/decyzje* nie jest tożsama/nie są tożsame* z rozprawą doktorską, która stanowi podstawę o ubieganie się o nadanie stopnia doktora w niniejszym postępowaniu.

.....
(podpis kandydata)

* niewłaściwe skreślić

** należy wypełnić właściwą część – A albo B

Uwaga: jeżeli postępowań było więcej niż jedno, proszę podać informacje wymagane niniejszym załącznikiem dla każdego postępowania osobno.

Katarzyna Niesyto.....
(imię i nazwisko kandydata)

Gliwice, 06.05.2024.....
(miejscowość, data)

Ul. Złoty Jan 13

32-220 Świerczyniec

796872015; katarzyna.niesyto@polsl.pl
(nr telefonu i adres e-mail)

Oświadczenie kandydata o oryginalności rozprawy doktorskiej

Ja, niżej podpisana, oświadczam, że:

- a) rozprawa doktorska pt. Zaprojektowanie szczepionych poli(cieczy jonowych) jako potencjalnych układów dostarczania leków w terapii przeciwbakteryjnej
jest wynikiem mojej działalności twórczej i powstała bez niedozwolonego udziału osób trzecich,
- b) wszystkie wykorzystane przeze mnie materiały źródłowe i opracowania zostały w niej wymienione, a napisana przez mnie praca nie narusza praw autorskich osób trzecich,
- c) załączona wersja elektroniczna pracy jest tożsama z wydrukiem rozprawy.

.....
Niesyto
(podpis kandydata)

Oświadczenie kandydata o zgodności złożonej rozprawy doktorskiej

Ja, niżej podpisana, oświadczam, że rozprawa doktorska pt.

Zaprojektowanie szczepionych poli(cieczy jonowych) jako potencjalnych układów dostarczania leków w terapii przeciwbakteryjnej
jest zgodna z rozprawą doktorską przygotowaną i złożoną w ramach kształcenia w szkole doktorskiej prowadzonej przez Politechnikę Śląską.

.....
Niesyto
(podpis kandydata)

Oświadczenie kandydata o odpowiedzialności karnej

Ja, niżej podpisana, oświadczam, że jestem świadoma odpowiedzialności karnej za składanie fałszywych oświadczeń, wynikającej z art. 233 Kodeksu karnego.

.....
Niesyto
(podpis kandydata)